Flux Vacua and the Web of Type II Compactifications

Dissertation
zur
Erlangung des Doktorgrades (Dr. rer. nat.)
der
Mathematisch-Naturwissenschaftlichen Fakultät
der
Rheinischen Friedrich-Wilhelms-Universität Bonn

vorgelegt von
Julian Ferdinand Piribauer
aus
Heidelberg

Bonn, 2025

Angefertigt mit Genehmigung der Mathematisch-Naturwissenschaftlichen Fakultät
der Rheinischen Friedrich-Wilhelms-Universität Bonn

Gutachter/Betreuer: Prof. Dr. Albrecht Klemm
Gutachter: Priv.-Doz. Dr. Stefan Förste

Tag der Promotion: 16.12.2025
Erscheinungsjahr: 2026

Zusammenfassung

Diese Dissertation behandelt die Periodengeometrie in Kompaktifizierungen der Stringtheorie des Typs IIB im Kontext der supersymmetrischen Flussvakua und der Kondensation von Schwarzen Löchern. Als zentrale Fragestellung untersuchen wir, wie Übergänge zwischen Familien von Calabi–Yau Mannigfaltigkeiten die vielen a priori verschiedenen Kompaktifizierungen miteinander verknüpfen. Wir zeigen, dass Fixpunktloci im Modulraum der komplexen Struktur unter geeigneten diskreten Symmetrien eine rationale Aufspaltung der Perioden innehaben, welche erforderlich ist für Modulistabilisierungen auf symmetrischen Loci und des Weiteren eine Einbettung bekannter Flussvakua in Mehrparametermodelle bewirkt. Wir vereinfachen die Suche nach Flussvakua in vierdimensionalen Einparameter-Kompaktifizierungen zu Attraktorpunkten auf deren Yifan-Yang Rücktransport. Entlang singulären Komponenten des Modulraums identifizieren wir Einparametermodelle welche durch sogenannte „strong coupling"- bzw. „conifold"-Übergänge entstehen. Im zweiten Fall glättet eine Kondensation von Schwarzen Löchern die Singularität und führt zu einer gemischten Coulomb/Higgs-Phase mit einer induzierten integralen Periodenstruktur. Wir kategorisieren Übergänge in Genus-1-Faserungen über torische Basen welche durch reflexive Polygone beschrieben werden und identifizieren neue Verbindungen zwischen mehreren Familien. Ein Formalismus wird vorgeschlagen und unterstützt durch Beispielrechnungen, der mutmaßlich-integrale Periodenbasen für alle $(n > 3)$-dimensionale nicht-entartete Calabi–Yau Familien konstruiert.

Abstract

This dissertation investigates the period geometry in compactifications of type IIB string theory on restricted moduli spaces in the context of supersymmetric flux vacua and black hole condensations. The guiding question of this work is how transitions among families of Calabi–Yau manifolds connect the vast number of seemingly different compactifications. We show that fixed-point loci in the complex-structure moduli space under suitable discrete symmetries furnish a rational splitting of periods, which is necessary for symmetric moduli stabilisation and embeds known flux vacua into multi-parameter models. We reduce the search for flux vacua in compactifications on one-parameter Calabi–Yau four-folds to attractor points on their Yifan-Yang pullback. Along singular components of the moduli space, we identify one-parameter models arising in strong coupling and conifold transitions. In the latter case, black hole condensation smooths out the singularity and gives rise to a mixed Coulomb/Higgs branch with an induced integral period structure. We categorise the transitions in genus-one fibrations over toric bases described by reflexive polygons and identify new connections among several families. A formalism is proposed that constructs conjecturally integral period bases for $(n > 3)$-dimensional non-degenerate Calabi–Yau families, which is supported by exemplary computations.

Acknowledgements

I am deeply grateful to my supervisor Prof. Dr. Albrecht Klemm for giving me the opportunity to become part of his group and for mentorship throughout my PhD studies. I count myself fortunate to have learned from his intuition and expertise, which inspired this thesis from start to finish.

I thank my second referee Priv.-Doz. Dr. Stefan Förste and Prof. Dr. Klaus Desch together with Prof. Dr. Valentin Blomer for agreeing to be part of my PhD committee. It is a pleasure to acknowledge the guidance of Dr. Johannes Brödel, Lorenz Milla, Prof. Dr. Hartmut Monien, Prof. Dr. Lorenzo Tancredi and helpful discussions with Dr. Pyry Kuusela and Dr. Thorsten Schimannek. I am particularly grateful to my fellow group members and collaborators Paul Blesse and Janis Dücker for daily scientific discussions, unforgettable moments and for comments on the manuscript.

My thanks also go to the administration of the Bethe Center for everyday support, most notably Nadine Hassani, Priv.-Doz. Dr. Florian Löbbert, Lora Schindler, Dr. Andreas Wißkirchen and Patricia Zündorf.

Furthermore, I am thankful to all those who have accompanied me during this journey: Alexander Bocken, Dr. Ekta Chaubey, Dr. Maximilian Daschner, Till Dieminger, Dr. Dominik Köhler, Sara Maggio, Saurabh Natu, Oğuz Öner, Ronan Schwarz, Apoorva Shah, Eleni Soufis, Sven Stawinski and Justyna Stefaniak.

Writing this thesis would not have been possible without the support of my parents and grandparents, my sister Marlene and my godmother and aunt, Carolin Jung, and uncle, Tobias Jung.

Contents

List of Tables

List of Figures

Chapter 1

Introduction

One of the most profound questions in modern physics is about the existence of a theory unifying quantum theory with Einstein's theory of gravity. In the second half of the last century, a proposal was developed replacing point-like particles by strings, which are one-dimensional extended objects that trace out two-dimensional world-sheets in spacetime instead of single world-lines. The vibrational modes of the classical string are lifted to operators in the quantum theory that excite its ground state and characterise its physical properties such as spin and mass. In the origins of the bosonic string as a description of hadron interactions, the massive excitations matched the affine relation between total spin and mass squared of the Regge trajectory. Additionally, the closed string has a massless spin-two excitation, which was unexpected in hadron physics and only later identified as a graviton candidate. Order-by-order finiteness of string theory makes it a UV-complete theory of gravity, which is non-renormalisable as a point-particle theory. The UV divergences in quantum field theory come from short-distance interactions, which are absent in string theory due to finiteness of the string length l_{S}. Strings are not the only dynamical object in the spectrum: an open string ends on $(p+1)$-dimensional objects called Dp-branes, which themselves are dynamical objects.

In point-particle quantum field theories, one builds a Lagrangian from empirical evidence of experiments and tunes the parameters—such as couplings or masses—to fit the observations. This is in stark contrast to string theory, where the only free parameter is the string length. The string coupling $g_{\mathrm{S}} = \exp\langle\phi\rangle$, for example, is determined by the vacuum expectation value of the dilaton field ϕ. String scatterings replace the sum over Feynman integrals by smooth world-sheet integrals with vertex operators. The different channels are incorporated in a single expression, which was the motivating description for the dual resonance model of hadronic interactions.

The ground state of the bosonic string is a tachyon and it destabilises the vacuum. By introducing fermions as superpartners to the bosonic fields, one can remove the tachyon after a projection that furthermore renders the spectrum spacetime-supersymmetric. By 1985, five consistent supersymmetric string theories were developed that have either $N = 1$ or $N = 2$ supersymmetry. For them to incorporate Einstein's concept of relativity, one finds that they are consistent only in ten spacetime dimensions instead of the four we can observe. It follows that the six internal extra dimensions should be compact and small in relation to sizes accessible to us. The Kaluza–Klein momentum modes become massive with $M_{\mathrm{KK}} \sim 1/R$ and decouple in the effective theory as the characteristic length R shrinks. Strings can, however, also wind around the cycles. The masses of winding states scale as R/l_{S}^2. The large volume assumption $l_{\mathrm{S}} \ll R$ implies that both

momentum and winding states become increasingly heavy. The excitations of the string have masses $M_S \sim 1/l_\mathrm{S}$ and are then heavier than the momentum modes. In the low-energy approximation of supergravity $E \ll 1/R$, all these states can be integrated out and the spectrum consists only of the ground states. During the compactification on a flat manifold, e.g. a six-torus, a single Majorana–Weyl spinor with 16 real supercharges in ten dimensions decomposes into four Majorana spinors in four dimensions with four real supercharges each. It follows that superstring theories on T^6 yield $N = 4$ or $N = 8$ theories in four dimensions. Internal spaces with non-trivial holonomy group break part of the supersymmetry. Preserving supersymmetry in the four-dimensional theory restricts the internal manifold to possess covariantly constant spinors, which is equivalent to the holonomy group to be contained in $\mathrm{SU}(3)$. Spaces with this property were known to mathematicians under the name Calabi–Yau manifolds. We will reserve the name for manifolds whose holonomy group is precisely $\mathrm{SU}(3)$, which have a single pair of covariantly constant spinors of opposite chirality. Their existence imply that the manifold is furthermore Ricci-flat and thus a solution to the Einstein field equations in a vacuum. The compactified theory then has the same $N = 1$ or $N = 2$ symmetry as in ten dimensions. Supersymmetry can, for example, be halved by orientifold projections or broken completely by giving generic background values to the field strengths. In the years after 1985, dualities among the superstring theories were identified that relate, for example, the strongly coupled regime of one with the weak coupling region of another. For us the most important duality is mirror symmetry, linking type IIA compactifications on a Calabi–Yau X with type IIB on its mirror manifold $\hat{X}$. Before the turn of the century, all five were recognised as different limits of an eleven-dimensional theory called M-theory. In this work, we will mostly work with a theory called type IIB and its non-perturbative extension F-theory. Type IIB has an $\mathrm{SL}(2,\mathbb{Z})$ symmetry that connects its strongly and weakly coupled regime. This is manifested in F-theory by geometrising the responsible scalar as the complex-structure modulus of an elliptic curve, which is naturally invariant under the symmetry. F-theory compactifications to four dimensions demand complex four-dimensional Calabi–Yau manifolds with a genus-one fibration as internal spaces. The geometry of the compactification manifold describes a large part of the four-dimensional physics, such as spectrum and coupling strengths. The massless scalar fields parametrising the vacuum configuration are called moduli. Cycles of suitable dimensions yield fields in supersymmetry multiplets reduced from the ten-dimensional field content. The volume of such cycles determines the coupling of super Yang–Mills theory on D-branes wrapped around them. On D3-branes, the complexified coupling is given by $\tau = C_0 + \mathrm{i}\, e^{-\phi}$ and one identifies the expectation value of C_0 with a θ-angle.

The absence of massless scalar fields in the standard model requires a potential that assigns vacuum expectation values to the moduli and removes them from the effective theory by making them massive. For the moduli parametrising the complex structure, such a potential is obtained by fixing the cohomology classes of the field strengths F_3 and H_3 . The cohomology class is represented by a flux, which yields the integrals of the field strengths over internal cycles. Supersymmetry puts restrictions on the allowed choices of flux configurations and Calabi–Yau manifolds with a suitable Hodge structure furnishing a flux vacuum are special. For families of Calabi–Yau manifolds with a single complex structure modulus, the specific value of this modulus corresponding to a manifold with a supersymmetric flux configuration is an attractor point. This is because the equations governing the condition involve Calabi–Yau periods and are equivalent to that of the attractor mechanism, which dictate its value for the existence of a BPS black hole

in the four-dimensional theory. Attractor points are the analogue of points of complex multiplication on elliptic curves and feature interesting arithmetic properties. Similar identifications in multi-parameter families are more involved and all known loci of flux vacua on Minkowski backgrounds originate from symmetry properties of the moduli space.

Looking at the vast number of distinct Calabi–Yau three-folds, it might seem impossible to identify *the* internal space which explains the observations in experiments. Even before Calabi–Yau manifolds became of interest to string theorists, mathematicians were aware of transitions between two topologically different families. At so-called conifold points, the manifolds look like a cone with base $S^2 \times S^3$. At the singularity, one has two choices to regularise the space: either one glues in an S^2 or an S^3. These correspond to manifolds with different Hodge numbers and the two possibilities connect the moduli spaces of two distinct families. In type IIB theory, the topology determines the numbers of hyper- and vectormultiplets. At the singularity, hypermultiplets become massless and appear in the effective theory, which give mass to some of the vector multiplets via the Higgs mechanism. The hypermultiplets correspond to extremal black holes in the effective theory and the curing of the singularity is hence called black hole condensation. The resolution $S^3 \to S^2$ is called conifold transition, while the degeneration of $S^2 \to S^3$ is called strong-coupling transition, due to its identification with strongly coupled type IIA theory. One should note that these transitions here are schematic and that, in general, there are multiple cycles shrinking simultaneously subject to relations in homology. Several examples have been found that connect two moduli spaces in this way and it is an open conjecture that the ambiguity in the vacuum choice is resolved by an interconnectedness of all Calabi–Yau families.

We will study supersymmetric flux vacua and black hole condensations in type IIB compactifications. Both phenomena arise along special loci in the complex-structure moduli space, which are smooth in the first case and singular in the second. The thesis is partly based on the following joint work.

- [1] "Calabi–Yau Period Geometry and Restricted Moduli in Type II Compactifications" by J. Dücker, A. Klemm and J. F. Piribauer, JHEP 07 (2025), p. 225, doi: 10.1007/JHEP07(2025)225.
- [2] "Geometry and Arithmetic of Transitions in Type II String Theory" by P. Blesse, J. Dücker, A. Klemm and J. F. Piribauer, *In preparation.*

In [1], we studied the relations between symmetries of the moduli space and flux vacua on their fixed-point loci. Section 5.6 and Chapter 6 are based on this article. We identified the flux conditions of type IIB compactifications with those in F-theory on its antisymmetric-product lift. A construction for a cohomology basis was given that transforms under the Gauss–Manin connection in block-anti-diagonal form, which has further application in the computation of Feynman integrals in the form of iterated integrals. The article in preparation [2] gives an identification of strong coupling and conifold transitions as Hadamard products of the fibre and base of the fibration. We connect a variety of types of Calabi–Yau families and furthermore give a geometric realisation of an integral period structure on the Hadamard products. The results of chapter 7

will be part of this article. Unless otherwise indicated, the material reproduced in this work are the author's own work.

The quantities we compute and analyse are typically period integrals, i.e. pairings between the homology and cohomology. A holomorphic description of the complex structure is obtained by the integrals of the unique $(n,0)$-form $\Omega(\underline{z})$ over a fixed topological basis in homology. These periods are coordinates for the complex-structure moduli space. Due to Griffiths transversality, the derivative under the Gauss–Manin connection acts on the vector space of periods as a linear operator, which can be reduced to the scalar differential equation called Picard–Fuchs equation. This information is encoded in the generators of the Mori cone of the family. For Calabi–Yau families embedded in toric ambient spaces, we extracted them together with the topological data given by integrals of the Chern classes with SAGEMATH. All other computations were performed in MATHEMATICA. A SAGEMATH code for the computation of toric data and MATHEMATICA implementations for the integral basis construction of Chapter 5 and the decomposition of the middle cohomology under quotients in section 6.1 are available upon request. The Yukawa couplings in the Batyrev coordinates given in eq. (5.4.50) were obtained with a MATHEMATICA program written by Albrecht Klemm.

We begin with a brief review on Calabi–Yau manifolds in chapter 2, focusing on constructive methods for embeddings in toric ambient spaces. This is followed by a minimal introduction to string theory, its unification and flux vacua in chapter 3. The chapter ends with a discussion of black hole condensation as the string-theoretic realisation of strong coupling/conifold transitions. Chapter 4 reviews the period geometry for Calabi–Yau families of dimensions $n \leq 3$. The mathematical tools to describe periods in higher dimensions are collected in chapter 5. There, we also propose a novel formalism to construct integral bases in $n > 3$ and supplement it with examples. This will furthermore allow us to give a canonical splitting of the period matrix into a unipotent and semisimple part in the last section. The restriction to smooth loci in the moduli space in terms of supersymmetric flux vacua is the topic of chapter 6. We analyse the fixed-point loci of finite order symmetries and show that, there, the F-terms for orthogonal directions are satisfied automatically and explain how the rational splitting of the periods can be used to construct flux vacua. We derive the equivalence between vacua conditions on a four-fold compactification with that in type IIB on its Yifan-Yang pullback. The period structure of an F-theory flux vacuum found in [1] is identified as a Hadamard product. This general phenomenon of a shrinking cycle describing a transition to a fibre product is utilised in Chapter 7 to categorise strong coupling and conifold transitions in the context of black hole condensation in type IIB string theory.

We extend the study of Picard–Fuchs differential equations governing the local period structures to higher genus moduli spaces in Appendix A. The first genus-zero invariants of certain two-parameter $(n > 4)$-folds are listed in Appendix B, obtained with the formalism of Chapter 5.

Chapter 2

Families of Calabi–Yau manifolds

String theory introduces Calabi–Yau manifolds in a natural way by demanding supersymmetry after a compactification of extra dimensions. For reasons we will discuss in chapter 3, they are defined in a ten-dimensional spacetime, which must therefore include six small, compact dimensions that are invisible to us. It turns out that the geometry of these extra dimensions is tightly constrained by the requirement of supersymmetry in four dimensions. These conditions for the internal six-dimensional space precisely align with the definition of Calabi–Yau manifolds: Kähler manifolds with vanishing first Chern class. Although the definition involves some mathematical groundwork, their properties allowed mathematicians and physicists to develop immensely powerful techniques to discover their astonishingly rich structure. We will begin this section with a brief review of the formal definition of these manifolds in section 2.1 and continue with a practical introduction to their description as embeddings in toric ambient spaces in section 2.2. In section 2.3, we will end with a more detailed view on the special case of hypersurfaces in projective spaces and give the definition of quotient families used in later sections.

2.1 Preliminaries

Calabi–Yau n-folds are complex n-dimensional manifolds with further structure, which we will review here briefly. The lecture notes [3] serve as a good reference for further study. Given a complex manifold with complex structure $J : TX \to TX$, i.e. $J^2 = -\mathbb{1}$ with vanishing Nijenhuis tensor, it is called hermitian if it has a metric that is invariant under J in the sense that it satisfies $g(u, v) = g(Ju, Jv)$. The complex structure J splits the tangent bundle into eigenspaces, where $Je_i = \mathrm{i}\, e_i$ and $Je_{\bar{\jmath}} = -\mathrm{i}\, e_{\bar{\jmath}}$. In these coordinates, the hermitian metric can be written as $\mathrm{d}s = g_{\mu\bar{\nu}}\mathrm{d}z^\mu\mathrm{d}\bar{z}^{\bar{\nu}}$. In real coordinates, one defines $J_{mn} = J_m^a g_{an}$ with $J_{mn} = -J_{nm}$, giving the components of a two-form

$$\omega = \frac{1}{2} J_{mn}\mathrm{d}x^m \wedge \mathrm{d}x^n \,. \tag{2.1.1}$$

Such a complex manifold is called *Kähler*, if ω is closed, meaning $\mathrm{d}\omega = 0$. In this case, ω is called the *Kähler form*. Closedness implies that the metric components can be written in terms of a *Kähler potential* K as

$$g_{\mu\bar{\nu}} = \partial_\mu \partial_{\bar{\nu}} K \,. \tag{2.1.2}$$

The metric is independent under a shift of the Kähler potential with a holomorphic function $f(z)$ that maps

$$K(z, \bar{z}) \mapsto K(z, \bar{z}) - f(z) - \bar{f}(\bar{z}) \tag{2.1.3}$$

called Kähler-gauge transformation.

The complex structure splits the exterior derivative into a holomorphic and anti-holomorphic piece $\mathrm{d} = \partial + \bar{\partial}$ and thus the de Rahm cohomology groups

$$H^r(X, \mathbb{C}) = \bigoplus_{p+q=r} H^{p,q}(X)\,, \tag{2.1.4}$$

where $H^{p,q}(X)$ is part of the Dolbeault cohomology. Note that the Kähler form ω is part of $H^{1,1}(X)$. The complex dimensions of $H^i(X, \mathbb{C})$ is the i-th Betti number b^i and we write for the dimensions of the Dolbeault classes $h^{p,q} \coloneqq \dim H^{p,q}(X)$. Complex conjugation and the Hodge star operation act as symmetries and identify

$$\overline{H^{q,p}(X)} \cong H^{p,q}(X) \cong H^{n-p,n-p}(X). \tag{2.1.5}$$

While there are many equivalent definitions of Calabi–Yau manifolds building on the above, we define it as having *trivial first Chern class* $c_1(TX) = 0$ (we will comment on the other definitions further below). This path to Calabi–Yau geometry includes an instructive review of the adjunction formula used to obtain explicit geometric models.

The total Chern class of the tangent bundle is built from the Riemann curvature as

$$c(TX) = \det\left(1 + \frac{\mathrm{i}\,R}{2\pi}\right) \tag{2.1.6}$$

and yields invariants of the manifold under smooth deformations. For the tangent bundle, the Chern roots x_i are given by eigenvalues of $\mathrm{i}\,R/2\pi$ and allow for an expansion as

$$c(TX) = \prod_{i=1}^{n}(1 + x_i(TX)) = 1 + \sum_{i=1}^{n} c_i(TX), \tag{2.1.7}$$

where the Chern-classes $c_i(TX)$ are integral classes in $H^{i,i}(X)$ (due to R being a $(1,1)$-form) and are given by the i-th elementary symmetric polynomials in the Chern roots x_i . For smooth manifolds, the Chern classes integrate to integers and thus

$$c_i(TX) \in H^{2i}(X, \mathbb{Z}) \cap H^{i,i}(X)\,. \tag{2.1.8}$$

Since we will mostly deal with the Chern classes of the tangent bundle TX, we will sometimes omit their argument in these cases. More precisely, using the formula $\det(A) = \exp(\mathrm{tr}(\log A))$ on eq. (2.1.6) yields, for example, $2\pi c_1 = \mathrm{i}\,\mathrm{tr}R$ and $2(2\pi)^2 c_2 = \mathrm{tr}R^2 - (\mathrm{tr}R)^2$. For manifolds that are defined inside an ambient space as the zero locus of a single polynomial restriction (hypersurface) or several of such (complete intersection), the *adjunction formula* allows for a simple computation of these invariants using intersection theory on the ambient space. While the origins of this formula involve some technicalities, the end result boils down to a simple Taylor expansion. There, the normal bundle $\mathcal{N}_X = T\mathbb{P}|_X/TX$ is defined as the quotient of the tangent bundle of the ambient space $\mathbb{P}$ restricted to X by that of the hypersurface X. These bundles fit into the short exact sequence

$$0 \longrightarrow TX \longrightarrow T\mathbb{P}\big|_X \longrightarrow \mathcal{N}_X \longrightarrow 0\,, \tag{2.1.9}$$

which implies that the Chern class satisfies the relation

$$c(TX) = \frac{c(T\mathbb{P})}{c(\mathcal{N}_X)}\,. \tag{2.1.10}$$

For a hypersurface X being in the divisor-class $\mathfrak{D}$, the normal bundle is a line bundle with $\mathfrak{D}$ as its first Chern class and thus $c(\mathcal{N}_X) = 1 + \mathfrak{D}$, which generalises with eq. (2.1.10) to the complete intersection of r divisors $\mathfrak{D}_i$ to $c(\mathcal{N}_X) = \prod_{i=1}^{r}(1 + \mathfrak{D}_i)$. To apply eq. (2.1.10), one expresses $\mathfrak{D}_{(i)}$ in terms of the divisor classes of the ambient space. In the next subsection, we will see an example of how this works when the latter is toric. The numerator of eq. (2.1.10), i.e. the total Chern class of the toric ambient space, is then given by $c(T\mathbb{P}) = \prod_i(1+\mathcal{D}_i)$, where j enumerates all toric divisors $\mathcal{D}_i$. For the case when $\mathbb{P}$ is a weighted projective space with weights w_i, one finds $\mathcal{D}_i = w_i H$ for H the hyperplane class. The above is sufficient information to construct the simplest Calabi–Yau n-fold families: Consider the ambient spaces $\mathbb{P}^{n+1}$ with $\mathcal{D}_i = H$, $1 \leq i \leq n+2$. According to eq. (2.1.10), a hypersurface in $\mathbb{P}^{n+1}$ with H-degree k has total Chern class

$$c(TX_k) = \frac{(1+H)^{n+2}}{1+k\,H} = 1 + (n+2-k)\,H + \mathcal{O}\big(H^2\big)\,. \tag{2.1.11}$$

Such families have vanishing first Chern class if and only if $k = n+2$. For $n = 1, 2, 3$, these are the degree-three hypersurfaces in $\mathbb{P}^2$, degree-four in $\mathbb{P}^3$ and so forth. Possibly the most popular example is the family of quintic hypersurfaces in $\mathbb{P}^4$ used in the seminal work on mirror symmetry [4]. In this way, one also obtains the higher Chern classes as a degree-k polynomial in the toric divisors D_i.

One can extend the above in two ways: consider embeddings in products of spaces and generalise hypersurfaces to complete intersections. For the first, one uses that the Chern class is multiplicative and the numerator of eq. (2.1.10) generalises to the product of the individual Chern classes. By successive application of the adjunction formula, several restrictions are represented by the products of the normal bundle's Chern classes in the denominator. In this work, we will encounter complete intersections in products of (weighted) projective spaces $\mathbb{P}_{\underline{w}}$ with weights $\underline{w}$. One denotes them (or their mirror) by the configuration matrix

$$\left(\begin{array}{c|ccc} \mathbb{P}_{\underline{w}_1} & \omega_1^1 & \cdots & \omega_1^r \\ \vdots & \vdots & & \vdots \\ \mathbb{P}_{\underline{w}_k} & \omega_k^1 & \cdots & \omega_k^r \end{array}\right), \tag{2.1.12}$$

where each column $(\omega_j^i)_j$ corresponds to one hypersurface restriction. The adjunction formula then translates a vanishing first Chern class to

$$\sum_{i=1}^{r} \omega_j^i = \|w_j\|_1\,, \qquad \forall\, j\,. \tag{2.1.13}$$

In other words, the rows of the degrees w_i^j in eq. (2.1.12) must add up to the sum of weights of the projective space on the left. A common abbreviation for complete intersection Calabi–Yau is CICY.

While (i) $c_1 = 0$ is a sufficient Calabi–Yau condition for a Kähler manifold, there are five further equivalent conditions (see for example [5])

(ii) The canonical class K_X is trivial.

(iii) Each Kähler class of X has a unique Kähler metric with vanishing Ricci tensor $R_{i\bar{\jmath}} = 0$.

(iv) There exists a unique (up to normalisation), nowhere vanishing, holomorphic $(n,0)$-form called Ω.

(v) The holonomy group is contained in $\mathrm{SU}(n)$.

(vi) There exists a globally defined pair of covariantly constant spinors $(\varepsilon, \overline{\varepsilon})$, which are of the same/opposite chirality if n is even/odd.

As is common in the literature, we will furthermore restrict Calabi–Yau manifolds to be connected and to have the full $\mathrm{SU}(n)$ as their holonomy groups. As we will study only compact manifolds, the first condition implies $\dim H^{0,0}(X) = 1$ and the latter excludes products of lower-dimensional examples.

The original conjecture by Calabi [6] states that, for any Kähler manifold with vanishing first Chern class, there exists a Ricci-flat Kähler metric. This was proven by Yau in [7]. The physicist's interest in these manifolds was sparked by Candelas, Horowitz, Strominger and Witten [8] who showed such manifolds can be used in the compactification of ten-dimensional string theory to a four-dimensional theory with $N = 1$. Supersymmetry also demands the existence of covariantly constant spinors on the internal manifold. If the holonomy group is precisely $\mathrm{SU}(n)$, there is only a single pair of such spinors and each supersymmetry generator of the original theory yields one generator upon compactification. For product manifolds, additional constant spinors yield further supersymmetries. One can furthermore show that forms in $H^{0,p}(X)$ correspond to covariantly constant forms, which cannot exist for full holonomy as the only invariant representations of $\mathrm{SU}(n)$ are in the trivial $H^{0,0}(X)$ and antisymmetric $H^{n,0}(X)$ representation. With eq. (2.1.5), this implies, for example, that the Hodge diamond of a Calabi–Yau three-fold simplifies to

$$\begin{array}{ccccccc} & & & 1 & & & \\ & & 0 & & 0 & & \\ & 0 & & h^{1,1} & & 0 & \\ 1 & & h^{2,1} & & h^{2,1} & & 1 \\ & 0 & & h^{1,1} & & 0 & \\ & & 0 & & 0 & & \\ & & & 1 & & & \end{array} \,. \tag{2.1.14}$$

The description of $H^{n-1,1}(X)$ as the complex-structure moduli space's tangent space goes back to Kodaira and Spencer [9]. As we saw in the beginning of the subsection, the complex structure J tells us which directions on the Calabi–Yau are holomorphic and which are anti-holomorphic. Changes in the complex structure correspond to elements $A \in H^{0,1}(X, TX)$, where A rotates one holomorphic index of J into an anti-holomorphic one. Contracting A with the $(n,0)$-form Ω corresponds to an isomorphism $H^{0,1}(X, TX) \cong H^{n-1,1}(X)$. These deformations in $H^{n-1,1}(X)$ correspond to infinitesimal deformations and, a priori, *could* be corrected by higher order terms. Due to Tian [10] and Todorov [11], one knows that the complex-structure moduli space for Calabi–Yau manifolds is unobstructed, i.e. that these deformations can be integrated to give complex structures.

The other important moduli space of Calabi–Yau manifolds is that of the Kähler structure. Deformation to the Kähler form (2.1.1) are given by real forms in $H^{1,1}(X, \mathbb{R})$, whose real dimension

is given by $h^{1,1}$. Positivity of the metric furthermore restricts ω to lie in the $h^{1,1}$-dimensional Kähler cone, as we will see in the next section. In string theory, one complexifies this cone to account for the R-R B-field, cf. section 4.3.

In section 3.1, we will identify these moduli spaces with the vector- and hypermultiplet moduli spaces of type II compactifications on Calabi–Yau three-folds. The mirror conjecture states that each Calabi–Yau X comes with a mirror partner $\hat{X}$ where the complex-structure moduli space of X is locally isomorphic to the complexified Kähler moduli space of $\hat{X}$ and vice versa. We will return to this identification in later sections.

2.2 Compact Calabi–Yau manifolds in toric varieties

Many families of Calabi–Yau n-folds can be described in terms of reflexive $(n+1)$-dimensional reflexive lattice polytopes. In fact, all these polytopes together with their polar duals correspond to mirror pairs of such families. The toric ambient space constructed from such a polytope has a natural anti-canonical divisor class $-\mathcal{K}$ and a generic global section P of the associated line bundle $\mathcal{O}_X(-\mathcal{K})$ has Calabi–Yau manifolds as its zero locus. Here, we will briefly repeat the results of Batyrev [12] most useful for us and give two examples illustrating the methods of this formalism. We will also review the extension to complete intersection Calabi–Yau families (CICY) due to Batyrev and Borisov [13, 14].

Let Δ be a convex lattice polytope in the integral lattice $\mathbb{Z}^{n+1}$ containing the origin. The polar dual is defined as the subset in the real dual space as

$$\Delta^\circ = \left\{ x \in \mathbb{Z}^{n+1} \otimes \mathbb{R} \,\middle|\, \langle x|y\rangle \geq -1 \;\forall y \in \Delta \right\}. \tag{2.2.1}$$

One calls Δ reflexive if Δ° is again integral, i.e. if all its vertices are in $\mathbb{Z}^{n+1}$. Due to $(\Delta^\circ)^\circ = \Delta$, these then constitute a pair of reflexive polytopes. As a simple example, consider the polytope sketched in Figure 2.1a

$$\Delta = \text{convex hull}\big\{(1,0),(0,1),(-1,-1),(0,-1)\big\}. \tag{2.2.2}$$

With equation eq. (2.2.1), we find the conditions for the dual polytope

$$x \geq -1\,,\; y \geq -1\,,\; x+y \leq 1\,,\; y \leq 1\,, \tag{2.2.3}$$

leading immediately to the polytope in Figure 2.1b. Since its vertices are integral, (Δ, Δ°) is a pair of reflexive polytopes.

The ambient space $\mathbb{P}_\Delta$ is constructed from a reflexive polytope Δ equipped with a triangulation that is fine, star and regular. Explicitly, this means the triangulation includes all points of Δ (except for those in facets, see below), every maximal simplex contains the interior point, and all resulting cones have unit simplicial volume. We denote the fan constructed from this triangulation by $\Sigma(\Delta)$. The generators $\{\nu_i \,|\, i \in \{1,\ldots,s\}\}$ of this fan correspond to the coordinates x_i of $\mathbb{P}_\Delta$. As will be demonstrated later in this section, one can safely disregard generators terminating at points located within codimension-one faces (facets) of $\mathbb{P}_\Delta$. This is because their divisor $\{\rho = 0\}$ does not intersect the Calabi–Yau manifolds and we can consider the patch $\rho \neq 0$ and set

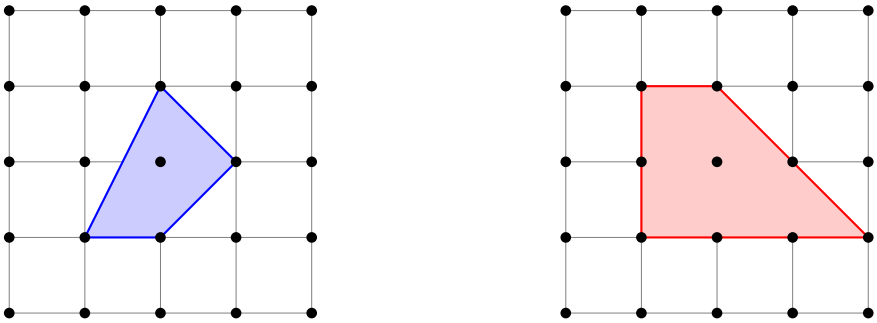

(a) Original polytope Δ (b) Dual polytope Δ°

Figure 2.1: A pair of reflexive polytopes corresponding to families of elliptic curves.

$\rho = 1$. We denote these one-dimensional cones generating the fan by $\Sigma(1)$. The Stanley–Reisner ideal $Z(\Sigma)$ is generated by the divisors

$$x_{i_1} = \ldots = x_{i_k} = 0 \tag{2.2.4}$$

for index sets $I = \{i_1, \ldots, i_k\}$ where $\{\nu_i\}_{i\in I}$ does not generate a cone in $\Sigma(\Delta)$. Let us assume that there are m relations among the generators ν_i given by

$$0 = \sum_{i=1}^{s} Q_{ij}\nu_i, \quad Q \in \mathrm{Mat}_{s\times m}(\mathbb{Z})\,. \tag{2.2.5}$$

Then, the coordinates x_i obey the scaling relations

$$Q_{*,j}(\lambda):\ (x_1, \ldots, x_s) \mapsto \left(\lambda^{Q_{1,j}} x_1, \ldots, \lambda^{Q_{s,j}} x_s\right), \quad \lambda \in \mathbb{C}^*. \tag{2.2.6}$$

The matrix Q is also called charge matrix and gives the continuous part of the toric group. For non-regular fans, it contains a discrete subgroup given by $\mathbb{Z}^{n+1}/N$, where N is the sub-lattice $N \subset \mathbb{Z}^{n+1}$ spanned by the generators ν_i over $\mathbb{Z}$. For the regular triangulations considered here, we may write the toric variety corresponding to the fan $\Sigma(\Delta)$ as

$$\mathbb{P}_\Delta = \frac{\mathbb{C}^s \setminus Z(\Sigma)}{Q}\,. \tag{2.2.7}$$

In general, the ambient space depends strongly on the fan $\Sigma(\Delta)$, which is left implicit in our notation.

We return to the example polytope Δ in Figure 2.1a. The space $\mathbb{P}_\Delta$ is described by four coordinates x_i, with the two scaling relations coming from linear dependencies of the vertices

$$Q_{*,1}(\lambda) : (x_1, x_2, x_3, x_4) \mapsto (\lambda\, x_1, \lambda\, x_2, \lambda\, x_3, x_4)\,, \tag{2.2.8}$$

$$Q_{*,2}(\lambda) : (x_1, x_2, x_3, x_4) \mapsto (x_1, \lambda\, x_2, x_3, \lambda\, x_4)\,. \tag{2.2.9}$$

There is only one regular, fine, star triangulation consisting of the zero-dimensional cone given by the origin, the rays towards the vertices as the one-dimensional cones and the top-dimensional

cones are the four triangles separated by the one-dimensional cones[1]. The Stanley–Reisner ideal is generated by

$$x_1 = x_3 = 0 \quad \text{and} \quad x_2 = x_4 = 0\,. \tag{2.2.10}$$

The toric variety $\mathbb{P}_{\Delta^\circ}$ is generated by eight coordinates with $8 - 2 = 6$ scaling relations. As four of them lie in facets of Δ°, we can ignore them for the construction of a fan and, for the patch we are interested in, again obtain four variables with two scaling relations.

An important ingredient for the period geometry of a Calabi–Yau manifold is the Kähler form $\omega \in H^{1,1}(X, \mathbb{R})$. By mirror symmetry, the complex-structure moduli space $\mathcal{M}_{\text{c.s.}}$ (in which we are interested the most) is identified with the complexified Kähler moduli space of the mirror $H^{1,1}(\hat{X}, \mathbb{C})$. A Kähler form ω of X is defined by the conditions

$$\int_{S_k} \omega^k > 0 \tag{2.2.11}$$

for all homologically non-trivial k-dimensional subvarieties $S_k \subseteq X$, $1 \leq k \leq n$. More precisely, one speaks of the Kähler cone generated by $h^{1,1}$ forms $J_i \in H^{1,1}(X, \mathbb{R})$, where $\omega = \sum_{i=1}^{h^{1,1}} t_i J_i$ with Kähler moduli $t_i \in \mathbb{R}_{>0}$. We will explain the construction of this cone as the dual to the Mori cone. For a more rigorous treatment, see the original derivation in [15] or, for the application to Calabi–Yau manifolds, [16].

As an example, we consider the polytope Δ corresponding to the weighted projective space $\mathbb{P}_{6,2,2,1,1}$ with vertices

$$\begin{aligned} &\nu_1 = (1,0,0,0)\,, && \nu_2 = (0,1,0,0)\,, \\ &\nu_3 = (0,0,1,0)\,, && \nu_4 = (0,0,0,1)\,, \\ &\nu_5 = (-6,-2,-2,-1)\,. \end{aligned} \tag{2.2.12}$$

Computing the scaling relations eq. (2.2.6), one readily verifies that the space is indeed $\mathbb{P}_{6,2,2,1,1}$. This space contains a singular curve at $x_4 = x_5 = 0$ and to construct a fan describing a resolved ambient space $\mathbb{P}_\Delta$, we need to subdivide the polytope which, besides the vertices and the origin, also contains the two points

$$\nu_6 = (-3,-1,-1,0)\,, \quad \nu_7^* = (-1,0,0,0)\,. \tag{2.2.13}$$

The vertex $\nu_6 = (\nu_4 + \nu_5)/2$ lies on a two-dimensional cone and comes from the resolution of the singular curve [17]. On the other hand, $\nu_7^* = (2\nu_2 + 2\nu_3 + \nu_4 + \nu_5)/6$ is contained in the facet spanned by these four vertices and can be ignored. The Mori cone consists of all curves in the ambient space and is generated by the irreducible curves $\mathcal{C}_i$. The latter are represented by vectors

$$l^{(i)} = \left(-l_0^{(i)};\, l_1^{(i)}, \ldots, l_n^{(i)}\right). \tag{2.2.14}$$

The integers $l_j^{(i)}$ are the intersection of $\mathcal{C}_i \cdot \mathcal{D}_i$, where $\mathcal{D}_i$ is the divisor class of $\{x_i = 0\}$ and $l_0^{(i)} = \mathcal{C}_i \cdot \mathcal{K}$ with $\mathcal{K} = -\sum_i \mathcal{D}_i$ the canonical divisor class. To find these intersection numbers, one

[1] For more complicated (also higher-dimensional) polytopes, the following SAGEMATH commands can be used

```
pc=PointConfiguration([(0,0),(1,0),(0,1),(-1,-1),(0,-1)])
pc.restrict_to_star_triangulations((0,0)).restrict_to_fine_triangulations().triangulations_list()
```

identifies them as *strictly convex, piecewise linear (SCPL) functions* $u(v)$ on the extended polytope $\bar{\Delta} = \{(1,\nu) \,|\, \nu \in \Delta\}$ with the following property: For each $(n+1)$-dimensional simplex $\sigma \subset \Delta$, we assign variables u_i to each of the vertices $\bar{\nu}_0 = (1,\underline{0}), \bar{\nu}_1, \ldots, \bar{\nu}_n$ and denote an element in σ by $v = c_0\bar{\nu}_0 + \ldots + c_n\bar{\nu}_n$. Then, in each simplex, an SCPL function $u(v) = c_0u_0 + \ldots + c_nu_n$ is described by a vector $\underline{w}_\sigma$ with

$$u(v) = \langle \underline{w}_\sigma, v\rangle\,, \quad \text{if } v \in \sigma\,, \tag{2.2.15}$$

$$u(v) > \langle \underline{w}_\sigma, v\rangle\,, \quad \text{else.} \tag{2.2.16}$$

We return to the example polytope of eq. (2.2.12) to see how these inequalities give rise to the Mori cone. The polytope $\bar{\Delta}$ has the vertices

$$\begin{aligned} &\bar{\nu}_0 = (1,0,0,0,0)\,, && \bar{\nu}_1 = (1,1,0,0,0)\,,\\ &\bar{\nu}_2 = (1,0,1,0,0)\,, && \bar{\nu}_3 = (1,0,0,1,0)\,,\\ &\bar{\nu}_4 = (1,0,0,0,1)\,, && \bar{\nu}_5 = (1,-6,-2,-2,-1)\,,\\ &\bar{\nu}_6 = (1,-3,-1,-1,0)\,. \end{aligned} \tag{2.2.17}$$

Let us first consider the simplex with vertices $\bar{\nu}_0, \ldots, \bar{\nu}_4$. Inverting the conditions $u_i = \langle \underline{w}_\sigma, \bar{\nu}_i\rangle$, $1 \le i \le 4$, implies that

$$\underline{w}_\sigma = (u_0,\ -u_0+u_1,\ -u_0+u_2,\ -u_0+u_3,\ -u_0+u_4). \tag{2.2.18}$$

Then, the inequalities $u_i > \langle \underline{w}_\sigma, \bar{\nu}_i\rangle$, $5 \le i \le 6$, read in terms of the variables u_i

$$0 < -12u_0 + 6u_1 + 2u_2 + 2u_3 + u_4 + u_5\,, \tag{2.2.19}$$

$$0 < -6u_0 + 3u_1 + u_2 + u_3 + u_6\,. \tag{2.2.20}$$

Choosing the simplex with vertices $\bar{\nu}_0, \bar{\nu}_1, \bar{\nu}_2, \bar{\nu}_5, \bar{\nu}_6$, we find the more stringent condition

$$0 < -2u_6 + u_4 + u_5\,, \tag{2.2.21}$$

$$0 < -6u_0 + 3u_1 + u_2 + u_3 + u_6\,. \tag{2.2.22}$$

Note that eq. (2.2.19) is a consequence of eqs. (2.2.21) and (2.2.22). To obtain the Mori cone, we write the restrictions as $0 < \langle \underline{w}_\sigma, l^{(i)}_\sigma\rangle$. For each simplex σ, these integral vectors $l^{(i)}_\sigma$ span a cone. The Mori cone contains those vectors that satisfy the positivity bound globally and thus consists of the union of all these simplices. Here, we find that the other simplices do not extend the cone described by eqs. (2.2.21) and (2.2.22) and we conclude

$$l^{(1)} = (-6;3,1,1,0,0,1)\,, \tag{2.2.23}$$

$$l^{(2)} = (0;0,0,0,1,1,-2)\,. \tag{2.2.24}$$

To find the dual basis in $H^{1,1}(X,\mathbb{R})$, i.e. the Kähler cone, we pick two independent divisor classes, say[2] $\mathcal{D}_1$ and $\mathcal{D}_6$. The Kähler divisors D_1 and D_2 are defined implicitly by

$$\begin{pmatrix} D_1 \\ D_2 \end{pmatrix} = \mathbf{A} \begin{pmatrix} \mathcal{D}_1 \\ \mathcal{D}_6 \end{pmatrix}, \qquad \mathbf{A} \in M_{2\times 2}(\mathbb{Q})\,, \tag{2.2.25}$$

[2] In this example, $\mathcal{D}_1$ and $\mathcal{D}_4$ would of course be orthonormal to $l^{(1)}$ and $l^{(2)}$. To exemplify the methods we purposely make a poor choice.

where duality means

$$\mathbb{1} = \begin{pmatrix} 3 & 1 \\ 0 & -2 \end{pmatrix}^T \cdot \mathbf{A} \quad \longrightarrow \mathbf{A} = \frac{1}{6} \begin{pmatrix} 2 & 0 \\ 1 & -3 \end{pmatrix}. \tag{2.2.26}$$

Before computing the intersection numbers of the divisors D_i, we want to give some relations among the toric divisors $\mathcal{D}_i$ obtained from the polytope[3] Δ. Writing $\underline{D} = \sum_i \mathcal{D}_i \nu_i$, we have $0 = \langle \underline{D}, v \rangle$, $\forall v \in \mathbb{R}^n$. This gives us the relations

$$\frac{1}{3}\mathcal{D}_1 = \mathcal{D}_2 = \mathcal{D}_3 = 2\mathcal{D}_5 + \mathcal{D}_6 \equiv D_1\,, \tag{2.2.27}$$

$$\mathcal{D}_4 = \mathcal{D}_5 \equiv D_2\,. \tag{2.2.28}$$

The intersection number of n divisors $D_{i_1}, \ldots, D_{i_n}$ is given by $|\nu_{i_1}^T, \ldots, \nu_{i_n}^T|$. Thus, we have

$$D_1^4 = \big(2|\nu_1^T, \nu_2^T, \nu_3^T, \nu_5^T| + \underbrace{|\nu_1^T, \nu_2^T, \nu_3^T, \nu_6^T|}_{=0}\big)/3 = \frac{2}{3}\,, \tag{2.2.29}$$

$$D_1^3 D_2 = \big(|\nu_1^T, \nu_2^T, \nu_3^T, \nu_4^T|\big)/3 = \frac{1}{3}\,, \tag{2.2.30}$$

$$D_1^2 D_2^2 = D_1 D_2^3 = D_2^4 = 0\,. \tag{2.2.31}$$

To obtain the intersection numbers on the Calabi–Yau manifold, we must intersect the three-fold intersection with the anti-canonical class (also called hypersurface class) $-\mathcal{K}$, which, in this example, is given by $6D_1$. Here, we have $(D_1^3)_{\mathrm{CY}} \equiv D_1^3(6D_1) = 4$ and, equivalently, $(D_1^2 D_2)_{\mathrm{CY}} = 2$ while the other two vanish. We will omit the subscript "CY", since it should be clear by dimensionality which intersection is meant.

We mentioned above that the Calabi–Yau hypersurfaces are given by the zero loci of sections of the anti-canonical bundle. We note that the entries l_i^k, $i > 0$, reflect the relations eq. (2.2.6) of the vertices. So for P_Δ to be a well-defined function of $\mathbb{P}_\Delta$, it transforms homogeneously under a scaling $x_i \mapsto \lambda^{l_i^{(k)}} x_i$ for all k, where $l_0^{(k)}$ gives the weight. Then, in the example above, for P_Δ to be a section of the anti-canonical bundle, it must obtain a factor λ^6 under the scalings

$$Q_{-\mathcal{K}}(\lambda, \mu) :\ (x_1, \ldots, x_6) \mapsto (\lambda^3 x_1, \lambda x_2, \lambda x_3, \mu x_4, \mu x_5, \lambda \mu^{-2} x_6), \tag{2.2.32}$$

where we used eq. (2.2.27) to express $\mathcal{D}_6$ as $D_1 - 2D_2$. To find an explicit expression of these sections, we turn to specific coordinates of the space. All $(n+1)$-dimensional toric varieties $\mathbb{P}_\Delta$ contain an open subset that is isomorphic to the algebraic torus $(\mathbb{C}\backslash\{0\})^n$. We denote these affine coordinates by[4] $t_1, \ldots, t_{n+1}$. For any Weil divisor $D = \sum_{\rho \in \Sigma(1)} a_\rho D_\rho$, its sections are given by characters from lattice points of the polytope [18]

$$\Delta_D = \big\{ x \in \mathbb{Z}^{n+1} \otimes \mathbb{R} \,\big|\, \langle x | y \rangle \geq -a_\rho \ \forall \rho \in \Sigma(1) \big\}\,. \tag{2.2.33}$$

For the anti-canonical divisor $-\mathcal{K}$, we have $a_i = 1$, $\forall\, i$, and therefore

$$\Delta_{-\mathcal{K}} = \Delta^\circ\,. \tag{2.2.34}$$

[3] Note that, by considering the extension $\bar{\Delta}$ instead, one additionally obtains an equation $D_0 \equiv \mathcal{K} = -\sum_{i=1}^n D_i$.

[4] These are not to be confused with the mirror maps of section 4.3.

In the torus patch of $\mathbb{P}_\Delta$, the sections of the anti-canonical bundle are given by the Laurent polynomials

$$P_\Delta(\underline{a},\underline{t}) = \sum_{\nu^\circ\in\Delta^\circ} a_{\nu^\circ}\underline{t}^{\nu^\circ}\,, \quad a_{\nu^\circ}\in\mathbb{C}\,, \tag{2.2.35}$$

where the above characters are given by $\underline{t}^{\nu^\circ} \equiv t_1^{\nu_1^\circ}\dots t_n^{\nu_{n+1}^\circ}$. In the toric coordinates x_i, these polynomials take the form

$$P_\Delta(\underline{a},\underline{x}) = \sum_{\nu^\circ\in\Delta^\circ} a_{\nu^\circ}\prod_{\rho\in\Sigma(1)} x_\rho^{\langle\rho|\nu^\circ\rangle+1}\,. \tag{2.2.36}$$

All Calabi–Yau manifolds obtained by tuning a_{ν° in $\mathbb{P}_\Delta$ together form a *family*, which we sometimes denote by a calligraphic letter $\mathcal{X}$. Hypersurfaces in weighted projective spaces are oftentimes written as $\mathcal{X} = \mathbb{P}_{\underline{w}}[d]$, where $d = \sum_i w_i$ for a trivial canonical bundle.

To see why we were allowed to omit in $\Sigma(1)$ rays ρ' ending in facets, let $\rho'\in\Sigma(1)$. The unique vertex $\nu^\circ_{\rho'}\in\Delta^\circ$ with the property $\langle\rho'|\nu^\circ_{\rho'}\rangle = -1$ for all points in the facet of ρ' will then give rise to the only term in (2.2.36) with $x_{\rho'}$-exponent zero. This means that the divisor $x_{\rho'}=0$ intersects the hypersurface for

$$0 = P_{\mathcal{X}_\Delta}\Big|_{x_{\rho'}=0} = c_{\nu^\circ_{\rho'}}\prod_{\rho\in\Sigma(1)\setminus\{\rho'\}} x_\rho^{\langle\rho|\nu^\circ_{\rho'}\rangle+1}\,. \tag{2.2.37}$$

The inner product of $\nu^\circ_{\rho'}$ with any element in the face dual to $\nu^\circ_{\rho'}$ is also -1. Denoting the vertex opposite to this face by ρ^*, the condition simplifies to $0 = x_{\rho^*}$. But since vertices cannot share a simplex with points in their opposite face in a regular triangulation, the Stanley–Reisner ideal contains the set $\{x_{\rho^*} = x_{\rho'} = 0\}$ and the intersection is not part of the ambient space. If there are several vertices not part of the facet of ρ', still, one of them needs to be zero for the monomial to vanish. Also in this case, the Stanley–Reisner ideal excludes these loci from the ambient space. Therefore, the entire hypersurface can be described in a patch with $x_{\rho'}=1$. This argument for a single point inside a facet extends to multiple such points.

Instead of hypersurfaces, one can also consider complete intersections of r polynomials in an $n+r$ dimensional ambient space. The idea is to decompose the anti-canonical bundle into a tensor product of line bundles $\mathcal{L}_i$. The joint zero locus of their sections P_{Δ_i} is called a complete intersection. It follows from the adjunction formula and the fact that the first Chern class of the tensor product is the sum of the line bundle's divisor classes that the complete intersection is indeed Calabi–Yau. From the point of view of the polytope, it was shown in [14] how to obtain a suitable decomposition of the anti-canonical bundle: For two polytopes Δ_1 and Δ_2 in $\mathbb{R}^d$, their Minkowski sum is given by

$$\Delta_1+\Delta_2 = \{v+w \mid v\in\Delta_1,\ w\in\Delta_2\}\subset\mathbb{R}^d\,. \tag{2.2.38}$$

If an $(n+r)$-dimensional reflexive polytope has a Minkowski decomposition into r lattice polytopes Δ_r containing the origin,

$$\Delta = \Delta_1+\ldots+\Delta_r, \tag{2.2.39}$$

then the sections P_{Δ_i} give rise to Calabi–Yau manifolds on their intersection

$$\{P_{\Delta_1} = \ldots = P_{\Delta_r} = 0\}\,. \tag{2.2.40}$$

This decomposition is also called a *NEF (numerically effective) partition*, due to the divisors of the corresponding line bundles being NEF. Since the polytopes Δ_i are not reflexive, we cannot simply take their polar duals to obtain the mirror family. Instead, the mirror construction by Borisov [13] proposes a mirror polytope

$$\nabla = \nabla_1 + \ldots + \nabla_r \,, \tag{2.2.41}$$

where the summands in this Minkowski decomposition are defined by

$$\nabla_i = \{x \in \mathbb{R}^d \mid \langle x, y\rangle \geq -1 \,\forall\, y \in \Delta_i \;\; \langle x, z\rangle \geq 0 \,\forall\, z \in \Delta_j \,, j \neq i\} \,. \tag{2.2.42}$$

For an approachable review with an example pair of such partitions, see [19]. In this work, we will restrict ourselves to CICYs in products of (weighted) projective spaces $\mathbb{P}_\Delta = \bigoplus_{i=1}^k \mathbb{P}_{\underline{w}_i}$ [16] with $\underline{w}_i$ the projective weights. We denote the dimension of $\mathbb{P}_{\underline{w}_i}$ by d_i and assume that $w_{d_i+1} = 1$. Then, the (mirror) polytope is given by

$$\Delta = \Delta_1 \times \ldots \times \Delta_k \subset \mathbb{R}^{d_1} \times \ldots \times \mathbb{R}^{d_k} \,, \tag{2.2.43}$$

where Δ_r is the convex hull of the $d_i + 1$ vertices e_j, $1 \leq j \leq d_i$, and $(-w_{i,1}, \ldots, -w_{i,d_i})$. To obtain a NEF partition, one decomposes the set of vertices $\nu_{i,j}$, $1 \leq i \leq r$, $1 \leq j \leq d_i$, into sets $\bigcup_{i=1}^r E_i$, where the total weight $\omega_j^{(i)}$ of vertices in Δ_j in the set E_i is subject to the Calabi–Yau condition given in section 2.1. As an example, let us consider the K3-family given by the mirror of

$$\left(\begin{array}{c|cc} \mathbb{P}^2 & 2 & 0 \\ \mathbb{P}_{2,1^3} & 1 & 4 \end{array}\right) . \tag{2.2.44}$$

The polytope Δ has the vertices

$$\begin{aligned} &\nu_1 = (1,0,0,0) \,, \quad \nu_2 = (-1,0,0,0) \,, \\ &\nu_3 = (0,1,0,0) \,, \quad \nu_4 = (0,0,1,0) \,, \\ &\nu_5 = (0,0,0,1) \,, \quad \nu_6 = (0,-2,-1,-1) \,, \end{aligned} \tag{2.2.45}$$

where ν_1 and ν_2 describe the $\mathbb{P}^1$ and the remaining four $\mathbb{P}_{2,1^3}$. Noticing that x_3 is the coordinate with weight two, we obtain the NEF partition given by

$$\{\nu_1 \,,\, \nu_2 \,,\, \nu_4\} \cup \{\nu_3 \,,\, \nu_5 \,,\, \nu_6\} \,, \tag{2.2.46}$$

where the first set describes the polynomial $(2\;1)^T$ and the second one $(0\;4)^T$. To obtain the Mori cone, we proceed similarly to the hypersurface case above. We consider a simplex σ in the polytope Δ, say the one with vertices ν_1, ν_3, ν_4 and ν_5. Then, we consider the extended polytope $\bar{\Delta}$ with vertices (e_i, ν_j), where $i = 1, 2$ depending on in which set of eq. (2.2.46) the vertex lies, and $(e_i, \underline{0})$ for $i = 1, 2$. In contrast to the case before, we now have two "origins" $(e_i, \underline{0})$, which are parametrised by the variables u_{0i}. The condition for piecewise linearity implies

$$z_\sigma = (u_{01}, u_{02}, u_1 - u_{01}, u_2 - u_{02}, u_3 - u_{02}, u_4 - u_{02}) \,. \tag{2.2.47}$$

Then, the conditions for $\nu_2, \nu_6 \neq \sigma$ imply

$$0 < -2u_{01} + u_1 + u_2 \,, \tag{2.2.48}$$

$$0 < -u_{01} - 4u_{02} + 2u_3 + u_4 + u_5 + u_6 \,. \tag{2.2.49}$$

More generally, CICYs of the form eq. (2.1.12) with coprime[5] weights always have a Mori cone generated by

$$l^{(i)} = (-\omega_i^1, \ldots, -\omega_i^r \,;\, 0, \ldots, 0, w_{i,1}, \ldots, w_{i,d_i+1}, 0, \ldots, 0)\,, \tag{2.2.50}$$

where the parts to the right of the semicolon have disjoint supports; that is, none of the other l-vectors have non-zero entries at positions where $l^{(i)}$ does. Note that the Calabi–Yau property is again reflected in the vanishing of the sum over all components of each $l^{(i)}$. The defining (Laurent) polynomials $\mathbb{P}_{\Delta_i}$ are constructed as for the hypersurface case. An example can be found in section 4.4, where we will use the explicit form of the sections to compute the so-called fundamental period of the above CICY.

There are several equivalent definitions of a hypersurface becoming singular. For example, singularities are given by points in the moduli space where the Jacobian $\partial_i P_{\Delta_j}$ drops in rank. For a hypersurface, this happens at

$$0 = P_\Delta = \partial_{x_\rho} P_\Delta\,, \quad \forall\, \rho \in \Sigma(1)\,. \tag{2.2.51}$$

This is equivalent to saying that the tangent space is of larger dimension than the Calabi–Yau itself, corresponding to a point where the tangent space is ill-defined. The singular locus can be obtained from the polytope $\bar{\Delta}$ [20] (see also [21]): For each face of $\bar{\Delta}$ (this includes $\bar{\Delta}$ itself) whose points are linearly dependent, we denote the entries of the kernel matrix by s_{ij}, where $1 \leq j \leq |\bar{\Sigma}|$. Note that, as in the above, points inside facets will be ignored in this analysis. In a suitable basis, this matrix gives rise to Batyrev coordinates (defined later in eq. (4.4.8))

$$z^i = \sum_{j=1}^{|\bar{\Sigma}|} a_j^{s_{ij}}\,, \tag{2.2.52}$$

where the a_j correspond to the deformations $a_{\nu_j^\circ}$ of P_Δ. Then, the singular locus is parametrised by $(\lambda_1 : \ldots : \lambda_r) \in \mathbb{P}^{r-1}$ subject to

$$z^i = \sum_{j=1}^{|\bar{\Sigma}|} \left(\sum_{k=1}^{r} s_{kj} \lambda_k \right)^{s_{ij}}\,. \tag{2.2.53}$$

One finds the discriminant locus as the vanishing of a polynomial in the Batyrev coordinates by eliminating the variables λ_i from eq. (2.2.53). Let us consider the example CICY K3 family with polytope and NEF partition as in eqs. (2.2.45) and (2.2.46). Extending the polytope Δ with the NEF partition to $\bar{\Delta}$ as explained above, we obtain the two Mori cone (cf. eq. (2.2.50)) generators

$$l^{(1)} = (-2, 0; 1, 1, 0, 0, 0, 0)\,, \tag{2.2.54}$$

$$l^{(2)} = (-1, -4; 0, 0, 2, 1, 1, 1)\,. \tag{2.2.55}$$

From the whole polytope, we obtain from eq. (2.2.53) the relations

$$z^1 = \frac{\lambda_1^2}{(2\lambda_1 + \lambda_2)^2}\,, \quad z^2 = -\frac{\lambda_2}{64\,(2\lambda_1 + \lambda_2)}, \tag{2.2.56}$$

[5] If the weights are not coprime one might need to desingularise the space first, which introduces exceptional divisors. Each of these divisors will give rise to another l-vector and Batyrev coordinate. This is also the origin of the two Mori cone generators in eqs. (2.2.23) and (2.2.24), where one desingularises the space by including ν_6.

where we eliminate λ_1 and λ_2 to obtain the discriminant factor

$$\Delta_1 = 4z^1 - (1 + 64z^2)^2 \,. \tag{2.2.57}$$

The three points related by $l^{(1)}$ are also contained in lower dimensional faces of $\bar{\Delta}$, which is not true for those of $l^{(2)}$. From these faces, the coordinate λ_1 in eq. (2.2.53) cancels automatically and we immediately obtain the second and last factor

$$\Delta_2 = 1 - 4z^1 \,. \tag{2.2.58}$$

2.3 Hypersurfaces in weighted projective spaces and their quotients

In section 2.2, we showed how to obtain hypersurfaces and CICYs as the vanishing loci of certain sections from reflexive polytopes. The complex-structure moduli space consist of the deformations P_Δ (cf. eqs. (2.2.35) and (2.2.36)) parametrised by the a_{ν°. The Calabi–Yau does not change, when we perform a change of variables in the ambient space. It follows that there is a redundancy in the description of the moduli space in terms of the a_{ν°, which we will account for in this subsection. Here, we will restrict ourselves to hypersurfaces in weighted projective space. This allows us to describe the complex structure moduli space in more detail and, furthermore, to introduce the notion of a quotient family. The latter acts as a framework to compute the mirror family as first done in [22].

Let $\mathcal{X}$ be a family of Calabi–Yau manifolds given by the zero locus of a section P_Δ of the anti-canonical bundle of a toric variety $\mathbb{P}_\Delta$ as introduced in section 2.2. The moduli space[6] $\mathcal{M}_\mathcal{X}$ is given by the polynomial deformations a_ν of the defining polynomials P_{Δ_i} modulo the automorphisms of the ambient space $\mathbb{P}_\Delta$

$$\mathcal{M}_{\mathcal{X}_\Delta} = \frac{\bigoplus_{i=1}^r \mathrm{Def}(\{P_{\Delta_i} = 0\})}{\mathrm{Aut}(\mathbb{P}_\Delta)} \,. \tag{2.3.1}$$

The identity component of the automorphism group of $\mathbb{P}_\Delta$ consists of coordinate scalings and so-called roots [23]. The other components are obtained via suitable coordinate permutations. By the definition of $\mathbb{P}_\Delta$ in eq. (2.2.7), the automorphisms are given by those of $\mathbb{C}^s \setminus Z(\Delta)$ which commute with the action of Q. This implies that coordinate scalings are part of $\mathrm{Aut}(\mathbb{P}_\Delta)$. Roots deform the coordinates by suitable monomials of the others, preserving homogeneity under the scalings. This follows from commutativity with Q and thus they are given by

$$x_i \mapsto x_i + \mu x^D, \;\; \text{for } \deg_Q(x^D) = \deg_Q(x_i), \quad \mu \in \mathbb{C} \,. \tag{2.3.2}$$

For example, let us consider the family of degree-six hypersurfaces $\mathcal{X} = \mathbb{P}_{2,1,1,1,1}[6]$. The torus action is given by

$$Q : \, (x_1, x_2, x_3, x_4, x_5) \mapsto (\lambda^2 x_1, \lambda x_2, \lambda x_3, \lambda x_4, \lambda x_5) \,, \quad \lambda \in \mathbb{C}^* . \tag{2.3.3}$$

[6] From now on, we will always refer to the complex-structure moduli space when writing about "the moduli space". Consequently, we drop the subscript "c.s." and indicate the correspondong family instead.

Besides the five rescalings, we have the roots

$$x_1 \mapsto x_1 + \sum_{j,k=2}^{5} A^{(1)}_{jk} x_j x_k \,, \tag{2.3.4}$$

$$x_i \mapsto x_i + \sum_{j=2, j\neq i}^{5} A^{(i)}_{j} x_j \,, \quad i \in \{2,3,4,5\} \,. \tag{2.3.5}$$

Since $A^{(1)}_{jk}$ is symmetric, it has ten degrees of freedom. Adding these to the $3 \cdot 4 = 12$ parameters of $A^{(i)}_j$ and the five scaling relations, we have

$$\dim(\mathrm{Aut}(\mathbb{P}_\Delta)) = 22 + 5 = 27 \,. \tag{2.3.6}$$

A simple counting of monomials with Q-degree six tells us that there are 130 deformations of $\mathcal{X}$. In this way, we find

$$h^{2,1}(\mathcal{X}) = \dim(\mathcal{M}_\mathcal{X}) = 130 - 27 = 103 \,. \tag{2.3.7}$$

In practise, the automorphisms of the ambient space allow us to transform $\underline{x}$ in a way such that the defining polynomial becomes of the form

$$P_\Delta(\underline{a}, \underline{x}) = P_0(\underline{x}) + \sum_j a_j \mathrm{def}_j(\underline{x}) \tag{2.3.8}$$

with $\dim \mathcal{M}_\mathcal{X}$ monomials $\mathrm{def}_j(\underline{x})$. The infinitesimal coordinate transformations give equivalences among monomials of lower degree, generated by $\{\partial_{x_i} P_\Delta(\underline{a}, \underline{x})\}_i$. These elements span the *Jacobian ideal* $\mathrm{Jac}_{\underline{a}}(P_\Delta)$ of P_Δ. In eq. (2.3.8), all monomials of $P_{\mathcal{X}_\Delta}$ are inequivalent over the Jacobian ideal, which, for a generic hypersurface with all deformations present, generates the same equivalences as $\mathrm{Aut}(\mathbb{P}_\Delta)$.

Another way of taking into account the reparametrisations of the ambient space is the removal of monomials in (2.2.36) that correspond to points inside codimension one faces of Δ°. A point $\tilde{\nu}^\circ$ inside a facet yields a relation $0 = \partial_{x_\rho} P_\Delta$ with ρ the vertex with $\langle \rho, \nu^\circ \rangle = -1$ for all ν° in that face. This relation allows us to set the monomial parametrised by $a_{\tilde{\nu}^\circ}$ to zero. Besides these polynomial deformations, there are also non-polynomial deformations. Denoting the points in the interior of a face θ by $\hat{l}(\theta)$ and the total points of the polytope by $l(\Delta)$, Batyrev derived the following formula for the number of complex-structure moduli

$$h^{n-1,1}(\mathcal{X}_\Delta) = l(\Delta) - (n+2) - \sum_{\mathrm{codim}(\theta)=1} \hat{l}(\theta) + \sum_{\mathrm{codim}(\theta)=2} \hat{l}(\theta) \cdot \hat{l}(\theta^*) \,, \tag{2.3.9}$$

where the number of Kähler parameters is obtained by applying eq. (2.3.9) to its mirror

$$h^{1,1}(\mathcal{X}_\Delta) = h^{n-1,1}(\mathcal{X}_{\Delta^\circ}) \,. \tag{2.3.10}$$

A similar combinatorical formula for the number of moduli $h^{n-1,1}$ in CICYs can be found in [14]. One can consider the Calabi–Yau family in a patch where coordinates not corresponding to vertices are non-zero and use the scaling relations to set them equal to one. For hypersurfaces in weighted projective space, this implies that the defining polynomial in eq. (2.2.36) becomes

a function of $n+2$ variables x_i. For the degree-twelve hypersurfaces in $\mathbb{P}_{6,2,2,1,1}$, we needed to introduce the coordinate x_6 to regularise the ambient space. There, the dual polytope Δ° gives rise to the restriction

$$P_\Delta = a_1\, x_1^4 + a_2\, x_1^3 x_2 + a_3\, x_1^3 x_4^2 x_6 + \dots \,. \tag{2.3.11}$$

In the patch $x_6 \neq 0$, we can use eq. (2.2.32) with $\mu = \sqrt{\lambda}\, x_6$ to set $x_6 = 1$ and recover the degree-twelve hypersurfaces in $\mathbb{P}_{6,2,2,1,1}$. This model is discussed in much detail in [17]. We will compute the periods of its mirror $\mathcal{X}_{\Delta^\circ}$ in section 4.4.

For the rest of the subsection, we will restrict ourselves to hypersurfaces $\mathbb{P}_{w_1,\dots,w_{n+2}}[d]$ in weighted projective spaces with weights w_i and $w_{n+1} = 1$ where the moduli independent term of the defining polynomial is Fermat, i.e. given by

$$P_0(\underline{x}) = \sum_{i=1}^{n+2} x_i^{d/w_i} \quad \text{with} \quad d = \sum_{i=1}^{n+2} w_i \,. \tag{2.3.12}$$

After dividing out the automorphism group of the ambient space, the family $\mathcal{X}_\Delta$ still has a residual symmetry group G consisting of discrete phase symmetries that act on the variables $\underline{x}$. We will consider the extension $\hat{G}$, which also acts on the moduli $\underline{a}$ such that the defining polynomial is invariant under its action. This allows us to see $\hat{G}$ as an automorphism of $\mathcal{M}_{\text{c.s.}}$. We denote an element g in G (or $\hat{g}$ in $\hat{G}$) by $\mathbb{Z}_p : (\beta_1, \dots, \beta_{n+2})$, which then acts with $\alpha = e^{2\pi \mathrm{i}/p}$ as

$$\hat{g} : \begin{array}{l} x_i \mapsto g(x_i) = \alpha^{\beta_i} x_i \,, \quad \beta_i \in \{0, \dots, d-1\} \,, \\ a_j \mapsto a_j \frac{\mathrm{def}_j(\underline{x})}{g(\mathrm{def}_j(\underline{x}))} \,, \end{array} \tag{2.3.13}$$

where g acts on the deformation monomials multiplicatively. The action of $\hat{G}$ on the moduli is such that it cancels the phase obtained by $\mathrm{def}_i(\underline{x})$ and renders the defining polynomial $\mathbb{P}_\Delta$ invariant. Since these symmetries identify points in the moduli space corresponding to equivalent hypersurfaces, it is natural to study the moduli space modulo these symmetries. Elements of this quotient then represent closed paths in the moduli space, which, owing to the flatness of the Gauss–Manin connection (cf. section 4.2), yield monodromy actions dependent only on the cycles' homotopy class. We will revisit this topic in section 6.1.

With this residual symmetry group, we can construct new Calabi–Yau families over fixed-point loci of a subgroup $\hat{S} \subset \hat{G}$: We refer to the part of the moduli space that is invariant under the induced action of $\hat{S}$ as $\mathrm{Inv}_{\hat{S}}(\mathcal{M}_\mathcal{X})$. Then, we define the quotient of $\mathcal{X}_\Delta$ by $\hat{S}$ as

$$\frac{\mathcal{X}}{\hat{S}} \coloneqq \pi^{-1}\left(\mathrm{Inv}_{\hat{S}}(\mathcal{M}_\mathcal{X})\right). \tag{2.3.14}$$

The invariant slice $\mathrm{Inv}_{\hat{S}}(\mathcal{M}_{\mathcal{X}_\Delta})$ is nothing more than $\mathcal{M}_\mathcal{X}$ with $a_i = 0$ for all moduli a_i that transform non-trivially under $\hat{S}$. For the defining polynomial in (2.3.8), this means that only the invariant deformations appear in the defining polynomial of $\mathcal{X}_\Delta/\hat{S}$.

To make this more explicit and draw the connection to the mirror construction by Greene and Plesser [22], we consider a hypersurface in a weighted projective space. The abelian symmetry group $\hat{G}$ is isomorphic to

$$\hat{G} \cong \mathbb{Z}_{d/w_1} \times \dots \times \mathbb{Z}_{d/w_{n+2}} \,. \tag{2.3.15}$$

There is one factor coming from the projective scaling of the ambient space, which is called the quantum symmetry $\hat{Q}$. The mirror group $\hat{H}$ used in the mirror construction is given by the elements in $\hat{G}/\hat{Q}$ which leave the symmetric deformation a_0 (coming from $\nu^\circ = \underline{0}$ and belonging to $\prod_{i=1}^{n+2} x_i$) invariant.

As an example, consider the family $\mathcal{X} = \mathbb{P}_{4,1,1,1,1}[8]$. The defining polynomial has phase symmetries $\hat{G} \cong \mathbb{Z}_2 \times \mathbb{Z}_8^4$ generated, for example, by

$$\left.\begin{array}{l} \mathbb{Z}_2 : (1,0,0,0,1) \\ \mathbb{Z}_8 : (0,1,0,0,7) \\ \mathbb{Z}_8 : (0,0,1,0,7) \end{array}\right\} \hat{H} \Bigg\} \hat{G}/\hat{Q}\,, \qquad \begin{array}{l} \mathbb{Z}_8 : (0,0,0,-1,0) \\ \mathbb{Z}_8 : (4,1,1,1,1) \end{array} \Big\} \hat{Q}\,.$$

The last generator corresponds to the scaling symmetry of the ambient space while the second to last $\mathbb{Z}_8$ does not act trivially on $\prod_i x_i$. Its action on the modulus ψ is given by $\psi \mapsto \exp(2\pi\mathrm{i}/8)\,\psi$. The quotient family $\mathcal{X}/\hat{H}$ is described by the polynomial

$$P_{\mathcal{X}/\hat{H}}(\psi, \underline{x}) = x_1^2 + x_2^8 + x_3^8 + x_4^8 + x_5^8 - 8\psi \prod_{i=1}^{5} x_i\,, \tag{2.3.16}$$

where we ignored the monomial $x_2^2 x_3^2 x_4^2 x_5^2$ that can be removed with the element in the Jacobian ideal $0 = \partial_{x_1} P_{\mathcal{X}/\hat{H}}(\psi, \underline{x})$. Coming from the mirror side directly, this monomial comes from a point inside a facet: Due to eq. (2.2.34), the polynomial defining the mirror is given by the polytope defining $\mathbb{P}_{4,1,1,1,1}$, which has vertices $e_1, \ldots, e_4$ and $(-4,-1,-1,-1)$. One easily shows that above monomial comes from the point $(-1,0,0,0)$ inside the facet generated by the last four vertices.

While we will ignore deformations coming from points inside facets in the rest of this work, it is interesting to see how the machinery eliminates the redundancy when they are included. In section 4.4, we will introduce the Picard–Fuchs differential equations giving a local basis for the periods. At the so-called MUM point, the solution structure to this differential ideal is highly restricted. The holomorphic and single-logarithmic periods are homogeneous coordinates for the complex-structure moduli space and there should be $h^{n-1,1}$ of the latter. Omitting points inside facets, for $n > 1$, we get exactly $h^{n-1,1}$ Batyrev coordinates and $h^{n-1,1}$ solutions that are of the form $\log z^i + \mathcal{O}(\underline{z})$. No restriction of the Frobenius structure is necessary at the single-logarithmic order and the differential ideal is generated by operators of order greater than one. The structure for including points inside facets is very similar to the case of elliptic curves. In the latter case, $h^{0,1} = 1$ and multiple Batyrev coordinates should give rise to only a single single-logarithmic period. It follows that operators of order one exist that restrict the solution space to a single holomorphic and one single-logarithmic period. If we were to include the point $(-1,0,0,0)$ in the toric description of the model above, we would, besides the operator of order four, also find an operator of order one. While the number of solutions remains the same, the Batyrev coordinates give a redundant parametrisation of the moduli space. However, the periods still act as proper coordinates and are not affected by this toric aspect.

Chapter 3

String theories, M-theory and F-theory

String theory originated in the 1970s in the context of strong interactions: The force field between a quark-antiquark pair subject to colour confinement can be described as a quantised bosonic string, whose excitations reproduce the potential between them. Shortly after the four-point scattering amplitudes due to Veneziano [24], Virasoro [25] and Shapiro [26] in the late 1960s, a stringy interpretation was given independently by Nambu [27], Susskind [28] and Nielsen [29]. A precise description of the quantised bosonic string was given in 1973 [30], which is consistent only in 26 spacetime dimensions and whose groundstate is tachyonic. The removal of the latter went hand in hand with the introduction of the supersymmetric string due to Ramond [31], Neveu and Schwarz [32] after performing the GSO-projection onto a supersymmetric spectrum named after the authors of [33]. The first time string theory was proposed to be a unifying theory including the graviton as its massless spin-two excitation was in 1974 [34]. The rest of the century was shaped by two superstring revolutions: The discovery of gauge and gravity anomaly cancellation for ten-dimensional supergravity with gauge group SO(32) or $E_8 \times E_8$ due to Greene and Schwarz in 1984 [35] initiated the construction of the two heterotic superstring theories [36]. Shortly after, supersymmetric theories in ten dimensions were found to allow for supersymmetry in four dimensions when compactified on Calabi–Yau manifolds [8]. After some years of extensive research in the field and the discovery of mirror symmetry in 1990 [4], unification of the five superstring theories as different limits of M-theory sparked the second superstring revolution. U-duality as a unification of S- and T-duality between the string theories was proposed [37] which lead to the construction of M-theory [38] (see also [39]) by Witten in 1995. Polchinski [40] showed that D-branes are fundamental objects that source the R–R fields and are half-BPS, meaning that they satisfy the BPS bound and that the effective world-volume theory on the brane has half the supercharges of the bulk theory. Further evidence for M-theory was provided with the duality between its decompactification on $S^1/\mathbb{Z}_2$ and the strongly coupled $E_8 \times E_8$ superstring [41]. In 1996, Vafa furthermore manifested the SL$(2,\mathbb{Z})$-symmetry of type IIB theory in the geometric construction of its non-perturbative extension called F-theory [42].

This chapter sets the stage for the findings on supersymmetric flux vacua and conifold transitions in chapters 6 and 7. We begin with a minimal introduction to the five superstring theories together with M- and F-theory in sections 3.1 and 3.2, followed by a review on effective $N = 1$ four-dimensional theories from type II orientifold compactifications. The moduli of the internal manifold can be stabilised by giving background values to the n-form fields (fluxes) with $n = 3, 4$ its complex dimension. For the study of flux vacua, we review the conditions for unbroken supersymmetry in both type IIB and F-theory in section 3.4. Families of Calabi–Yau

manifolds are connected by transitions at singular points of their moduli space. Mathematically, this corresponds to two topologically different desingularisations, which was identified with the condensation of extremal black holes in type IIB compactifications [43]. Section 3.5 gives a brief mathematical and physical account of these transitions.

3.1 Superstring theories

Bosonic string theory as a conformal field theory on the world-sheet has critical number of dimensions $D = 26$, where it becomes anomaly-free and negative-norm states are absent. In its classical description, the D bosonic fields are coordinates for the string in spacetime. The world-sheet theory can be supplemented with fermions to realise world-sheet supersymmetry. In superconformal gauge, the resulting CFT is given by [44]

$$S = -\frac{1}{8\pi}\int \mathrm{d}^2\sigma \left(\frac{2}{\alpha'}\partial_\alpha X^\mu \partial^\alpha X_\mu + 2\mathrm{i}\overline{\psi}^\mu \rho^\alpha \partial_\alpha \psi_\mu\right). \tag{3.1.1}$$

The superstring has critical dimension $D = 10$, which follows from the central charge of the ghost CFT with central charge $c = -15$: The Weyl anomaly can only be cancelled by the D bosons with their D fermionic superpartners, which contribute $\frac{1}{2}$ and 1 to the central charge, respectively, demanding $D = 10$. During the derivation of the equations of motions for the fermionic fields ψ^μ with NN boundary conditions, the vanishing of the boundary term allows for two sectors. Without loss of generality, we can redefine the fields such that both sectors have $\psi^\mu_+(0) = \psi^\mu_-(0)$ and the difference lies at the other string end. The Ramond sector (R) is described by a positive sign in $\psi^\mu_+(l) = \pm\psi^\mu_-(l)$, while a negative sign yields the Neveu–Schwarz (NS) sector. The spectra of these sectors differ: The ground state in (NS) is a tachyon and the first excited level consists of a massless SO(8) vector representation ($\mathbf{8}_\mathrm{v}$), whereas the ground state of (R) is massless and contains one SO(8) spinor and co-spinor representation ($\mathbf{8}_\mathrm{s}\oplus\mathbf{8}_\mathrm{c}$). The Gliozzi–Scherk–Olive (GSO) projection [45] assigns to each state the eigenvalue of $(-1)^F$ with the fermion number F and singles out those with either $(-1)^F = 1$ or $(-1)^F = -1$. For (NS), one demands $(-1)^F = 1$ to remove the tachyon from its spectrum leaving two choices for (R). Besides removing the tachyon, this projection furthermore renders the surviving spectrum spacetime supersymmetric and restores invariance of the one-loop partition function under $\mathrm{SL}(2,\mathbb{Z})$. The closed string spectrum is given by the tensor product of two open strings' spectra. The above translates to two inequivalent theories called type IIA and type IIB, where the difference lies in the relative sign between the GSO projections in the two (R) sectors. Denoting the fermion numbers of the left- and right-moving sectors by F and $\overline{F}$, respectively, type IIA corresponds to the choice $(-1)^F = -(-1)^{\overline{F}}$ and IIB to $(-1)^F = +(-1)^{\overline{F}}$. Before listing the massless spectrum of these two theories, we list the tensor product decompositions that appear here

$$\mathbf{8}_\mathrm{v} \otimes \mathbf{8}_\mathrm{v} = \mathbf{1} \oplus \mathbf{28} \oplus \mathbf{35}_\mathrm{v}\,, \tag{3.1.2}$$

$$\mathbf{8}_\mathrm{s/c} \otimes \mathbf{8}_\mathrm{s/c} = \mathbf{1} \oplus \mathbf{28} \oplus \mathbf{35}_{+/-}\,, \tag{3.1.3}$$

$$\mathbf{8}_\mathrm{s} \otimes \mathbf{8}_\mathrm{c} = \mathbf{8}_\mathrm{v} \oplus \mathbf{56}_\mathrm{v}\,, \tag{3.1.4}$$

$$\mathbf{8}_\mathrm{v} \otimes \mathbf{8}_\mathrm{s/c} = \mathbf{8}_\mathrm{c/s} \oplus \mathbf{56}_\mathrm{c/s}\,. \tag{3.1.5}$$

Equation (3.1.2) produces a scalar (dilaton), an antisymmetric rank-two tensor and a symmetric traceless tensor (graviton). The ($\mathbf{35}_{+/-}$) in eq. (3.1.3) are rank-four selfdual/anti-selfdual antisymmetric tensors and ($\mathbf{56}_\mathrm{v}$) is an antisymmetric rank-three tensor. Lastly, the representations

($\mathbf{56}_{c/s}$) include the gravitini of given chirality. It then follows that the massless states of **type IIA** are collected in

$$\begin{aligned} \text{bosonic:} \quad & [\mathbf{1} \oplus \mathbf{28} \oplus \mathbf{35}_v]_{(NS,NS)} \oplus [\mathbf{8}_v \oplus \mathbf{56}_v]_{(R,R)} \,, \\ \text{fermionic:} \quad & [\mathbf{8}_c \oplus \mathbf{56}_c]_{(NS,R)} \oplus [\mathbf{8}_s \oplus \mathbf{56}_s]_{(R,NS)} \,, \end{aligned} \tag{3.1.6}$$

where the subscripts denote the sectors the representations originate from. Here, it is important to note that the chiralities of the gravitini (and dilatinos) are *opposed* and the theory is thus *non-chiral*. The bosonic spectrum consists of the dilaton, the metric and the B-field in the NS-NS sector together with a one- and three-form C_1 and C_3 in the R-R sector. This is in contrast to the massless spectrum of **type IIB**:

$$\begin{aligned} \text{bosonic:} \quad & [\mathbf{1} \oplus \mathbf{28} \oplus \mathbf{35}_v]_{(NS,NS)} \oplus [\mathbf{1} \oplus \mathbf{28} \oplus \mathbf{35}_+]_{(R,R)} \,, \\ \text{fermionic:} \quad & [\mathbf{8}_c \oplus \mathbf{56}_c]_{(NS,R)} \oplus [\mathbf{8}_c \oplus \mathbf{56}_c]_{(R,NS)} \,. \end{aligned} \tag{3.1.7}$$

Due to equal chirality of the gravitini, this theory is *chiral*. While the NS-NS sector has the same field content as type IIA, the R-R sector now contributes a scalar (axion) C_0, a two form C_2 and a self-dual four-form C_4. The choice $(-1)^F = (-1)^{\overline{F}}$ in type IIB treats the left- and right-moving sectors symmetrically. The open string theory arising from the quotient of type IIB by this symmetry is called **type I**, due to its $N = 1$ supersymmetry. The surviving spectrum is

$$\begin{aligned} \text{bosonic:} \quad & [\mathbf{1} \oplus \mathbf{35}_v]_{(NS,NS)} \oplus [\mathbf{28}]_{(R,R)} \,, \\ \text{fermionic:} \quad & [\mathbf{8}_c \oplus \mathbf{56}_c]_{(NS,R),(R,NS)} \,, \end{aligned} \tag{3.1.8}$$

which is supplemented by massless gauge bosons of an SO(32) gauge symmetry coming from the inclusion of 32 D9-branes that cancel the R–R charge of the O9-plane. In section 3.3, we will review the orientifold projections for the compactified theories to realise $N = 1$ four-dimensional vacua from type IIB theory. There are two further string theories that are heterotic, meaning that they treat the right moving sector as the 10D superstring and the left-movers as the 26D bosonic string. The difference in dimensions is accounted for by compactifying the 16 extra-dimensions in the left sector on a 16-torus T^{16}. The internal momenta of the latter need to lie on an even self-dual lattice for modularity of the torus partition function. In 16 dimensions, these are given by the root lattices of $E_8 \times E_8$ and $\text{Spin}(32)/\mathbb{Z}_2$. Depending on the choice of the lattice, the resulting theory has gauge symmetry $E_8 \times E_8$ or SO(32).

The reappearance of the gauge group SO(32) leads us to dualities between these five superstring theories. In fact, type I has been shown to be dual to heterotic SO(32) with inverse coupling strengths [46, 47, 48]. These kind of relations between weakly and strongly coupled regimes are known as non-perturbative dualities. Further example are given by self-duality of type IIB (S-duality) [49] and the duality between type IIA on a K3 and heterotic on T^4, where the gauge group of the heterotic theory is reflected on the IIA-side by $H_2(X, \mathbb{Z})$ of the K3 [38]. Compactifying the latter duality further leads to a strong-weak relation between type IIA on K3-fibred three-folds and heterotic on T^6 [50], where the singular locus in the three-fold's vector moduli space mapping to the weak-coupling limit is thus called strong-coupling discriminant [51]. These perturbative dualities are in contrast to those that relate theories by their order-by-order expansion in the string coupling, which exchange, for example, the two heterotic theories [52] and connect type IIA with type IIB [53] by compactifying both theories on circles with inverted

radii (T-duality). In the latter case, circle inversion flips the chirality of the ground state in (R), which exchanges their spectra. Above connections among the five string theories led Witten to formulate an eleven-dimensional unification called M-theory [38], which has $N = 1$ supergravity as its low-energy limit. We will introduce this theory in section 3.2 as a decompactification of strongly coupled type IIA. Furthermore, we will give a brief review of the non-perturbative extension of Type IIB, which is described elegantly by F-theory [42] created by Vafa. For the rest of this section, we will return to the type II theories and review their description of supergravity in ten dimensions.

In the low-energy limit where the mass scale $1/\sqrt{\alpha'}$ becomes large, the type II theories reduce to ten-dimensional $N = 2$ supergravity theories with 32 supercharges. The field content is described purely by the massless sector, while all other excitations decouple. As we discussed above, both theories feature a dilaton ϕ, a B-field and the metric $g_{\mu\nu}$ from the NS-NS sector. The field strength of the B-field is denoted by $H_3 = \mathrm{d}B_2$ and for the fields in the R-R sector we write $F_{p+1} = \mathrm{d}C_p$. Up to normalisations, their interactions are fixed by supersymmetry. The bosonic action is given by summands from the NS-NS and R-R sectors together with a Chern–Simons term

$$S = S_{\text{NS-NS}} + S_{\text{R-R}} + S_{\text{CS}}. \tag{3.1.9}$$

The NS-NS sectors for IIA and IIB are the same and their contribution to the action is given by

$$S_{\text{NS-NS}} = \frac{1}{2\kappa_{10}^2} \int \mathrm{d}x^{10} \sqrt{-g}\, e^{2\phi} \left(R + 4\partial_\mu \phi\, \partial^\mu \phi - \frac{1}{2}|H_3|^2 \right) \tag{3.1.10}$$

with R the scalar curvature and the gravitational constant relates to the string parameters as $2\kappa_{10}^2 = (2\pi)^7 \alpha'^4 g_{\text{S}}^2$. The dilaton parametrises the string coupling as $g_{\text{S}} = e^{\phi}$. In type IIA supergravity, the remaining two terms are given by

$$S_{\text{R-R}}^{(\text{IIA})} = -\frac{1}{4\kappa_{10}^2} \int \mathrm{d}x^{10} \sqrt{-g} \left(|F_2|^2 + |\tilde{F}_4|^2 \right), \tag{3.1.11}$$

$$S_{\text{CS}}^{(\text{IIA})} = -\frac{1}{4\kappa_{10}^2} \int B_2 \wedge F_4 \wedge F_4 \tag{3.1.12}$$

with $\tilde{F}_4 \coloneqq F_4 - C_1 \wedge H_3$. The self-duality of the five-form field-strength in type IIB cannot be enforced by a covariant action and give an additional constaint. The two remaining terms in the action are given by

$$S_{\text{R-R}}^{(\text{IIB})} = -\frac{1}{4\kappa_{10}^2} \int \mathrm{d}x^{10} \sqrt{-g} \left(|F_1|^2 + |\tilde{F}_3|^2 + \frac{1}{2}|\tilde{F}_5|^2 \right), \tag{3.1.13}$$

$$S_{\text{CS}}^{(\text{IIB})} = -\frac{1}{4\kappa_{10}^2} \int C_4 \wedge H_3 \wedge F_3\,, \tag{3.1.14}$$

where the R-R term uses $\tilde{F}_3 = F_3 - C_0 \wedge H_3$ and $\tilde{F}_5 = F_5 - \frac{1}{2} C_2 \wedge H_3 + \frac{1}{2} B_2 \wedge F_3$. The equations of motion for the latter are given by

$$\mathrm{d}\tilde{F}_5 = H_3 \wedge F_3 \tag{3.1.15}$$

with the additional self-duality constraint $\tilde{F}_5 = *\tilde{F}_5$. In the Einstein frame, the action of type IIB supergravity becomes manifestly $\mathrm{SL}(2,\mathbb{R})$ invariant, where $\left(\begin{smallmatrix} a & b \\ c & d \end{smallmatrix}\right) \in \mathrm{SL}(2,\mathbb{R})$ acts on the axio-dilaton

$$\tau = C_0 + \mathrm{i}\, e^{-\phi} \tag{3.1.16}$$

as a Möbius transformation while (F_3, H_3) behaves as a vector. In the full string theory, the mixing of F_3 and H_3 supplements the fundamental string by (p, q)-strings with p units of B_2-charge and q units of C_2-charge, where the charges $(1, 0)$ correspond to the fundamental one. These BPS objects exist for all coprime integers (p, q), where non-coprime charges represent stacks of them. Charge quantisation implies the breaking of the symmetry group to $\mathrm{SL}(2, \mathbb{Z})$[1].

The $(p + 1)$-form fields are sourced by Dp-branes, which are extended objects in p spatial dimensions on which open strings end. These branes are non-perturbative, as their tension

$$\tau_{\mathrm{D}p} = \frac{1}{g_{\mathrm{S}}(2\pi)^p \alpha'^{(p+1)/2}} \tag{3.1.17}$$

is anti-proportional to the string coupling and they are infinitely heavy at weak coupling. The field content of the two supergravity theories implies the existence of Dp-branes for p even (odd) in type IIA (IIB). The string coupling can also be given as $g_{\mathrm{S}} = \tau_{\mathrm{F1}}/\tau_{\mathrm{D1}}$ and the strong-weak duality of the $\mathrm{SL}(2, \mathbb{Z})$ duality in type IIB exchanges the fundamental string with the D1-brane coupling to C_2 instead of B_2. The latter is also called "D-string" and corresponds to the $(0, 1)$-string above. The D0-brane will play an important role in the introduction of M-theory in the next section.

3.2 M- and F-theory

The dualities among the five superstring theories discussed in the previous section motivated Witten to formulate M-theory [38] with eleven-dimensional supergravity as its low-energy limit. Of the five superstring theories, the two heterotic and type I posses $N = 1$ supersymmetry whereas type II has $N = 2$. In ten dimensions, these correspond to 16 and 32 supercharges, respectively, where 16 is the number of components of the smallest Majorana-Weyl spinor. Theories with more than 32 supercharges include particles whose spins exceed two, which leads to inconsistencies [54, 55]. As the smallest Majorana spinor in $D = 11$ has 32 components, M-theory with $N = 1$ has maximal supersymmetry. A spinor in four-dimensions has at least four real degrees of freedom and reducing M-theory (or type II) to four dimensions without breaking any supersymmetry would lead to $N = 8$.

Starting from strongly coupled type IIA, a state with N units of D0-brane charge and mass $N/g_{\mathrm{S}}\alpha^{1/2}$ can be seen as a Kaluza–Klein excitation of the supergraviton in eleven dimensions compactified on a circle with radius $R = g_{\mathrm{S}}\alpha^{1/2}$. The strong-coupling limit of type IIA theory can therefore be seen as a decompactification to eleven dimensions, called M-theory. The bosonic field content of the low-energy theory is given by the metric and a three-form potential A_3 with field strength $G_4 = \mathrm{d}A_3$. The fermionic counterpart is formed by the single gravitino. The bosonic part of the supergravity action reads

$$\mathcal{S} = \frac{1}{2\kappa_{11}^2} \int \mathrm{d}x^{11} \sqrt{-g} \left(R - \frac{1}{2}|G_4|^2 \right) - \frac{1}{12\kappa_{11}^2} \int A_3 \wedge G_4 \wedge G_4 \tag{3.2.1}$$

with κ_{11} the eleven-dimensional gravity constant. After the above Kaluza–Klein reduction on the circle, the metric yields the ten-dimensional metric, the dilaton and C_1, while A_3 reduces

[1] Another indication for the breaking to $\mathrm{SL}(2, \mathbb{Z})$ is invariance of the contribution of D(-1)-branes to the path integral of the form $e^{2\pi \mathrm{i} \tau}$.

to C_3 and B_2. The electric and magnetic sources for A_3 are formed by M2 and M5 branes, respectively. Upon reduction, the wrapped and unwrapped branes give the brane content of type IIA (except for D0, which comes from KK-modes). Furthermore, the fundamental string arises as an M2 brane wrapping the circle.

The strong-coupling extension of type IIB is called F-theory [42] and builds on the transformation properties of the axio-dilaton (3.1.16) to interpret it as the complex-structure parameter of an elliptic curve. We refer to [56] for a review on the matter. The two extra dimension are however fictitious and their sole purpose is to allow for a non-perturbative description. Starting with M-theory on a $T^2 = S^1_A \times S^1_B$ where the radius of the first circle is $R_A = g_S \alpha^{1/2}$ (see above), this theory is T-dual to type IIB theory on a circle with radius $R'_B = \alpha'/R_B$. As the elliptic curve degenerates to zero volume with $R_B \to 0$, type IIB decompactifies to ten dimensions. This description is generalised by considering instead elliptic fibrations over bases B, where the axio-dilaton becomes a function of the coordinates of B. Elliptic fibrations over complex d-dimensional compact bases allow for a compactification to a $(10-2d)$-dimensional theory. For a compactification on an elliptically fibred compact K3 ($d = 1$), the points of degeneration, i.e. the zeros of the elliptic curve's discriminant, mark the positions of 7-branes in the uncompactified dimensions. The fibration can be brought into Weierstraß-form $y^2 = x^3 + x\, f(\underline{u})\, x + g(\underline{u})$ with discriminant $\Delta = 27 f^3 - 4 g^2$. For the base to be a $\mathbb{P}^1$, one shows that 24 7-branes are required and that Δ must be of degree 24. The axio-dilaton is subject to a monodromy transformation during transportation around a 7-brane and its conjugacy class determines the type of the so-called (p,q)-brane and the Kodaira fibre type. Resolving the singularities introduces intersecting $\mathbb{P}^1$s whose intersecting graph is a Dynkin diagram determining the gauge group. Intersections of such loci in the base, i.e. singular loci in co-dimensions two and three yield matter and Yukawa coupling, respectively. The properties of singularities in such fibrations are used for model building with realistic gauge sectors. F-theory relates to type IIB in the Sen limit [57, 58] in the following way. One starts from the coefficients of the Weierstraß-equation in the form

$$f = C\eta - 3h^2\,, \qquad g = h\,(C\,\eta - 2h^2) + C^2\chi \tag{3.2.2}$$

with h, η and χ functions of the base coordinates $\underline{u}$. It follows that $C \to 0$ describes weak coupling in which the discriminant is given by

$$\Delta = -C^2 h^2\,(\eta^2 + 12 h\,\chi) + \mathcal{O}\big(C^3\big)\ . \tag{3.2.3}$$

The locus $(\eta^2 + 12 h\,\chi) = 0$ describes the positions of D7-branes and $h = 0$ that of O7-planes. This limit is also reached from compactification of type IIB on the double covering of the base

$$h - \xi^2 = 0 \tag{3.2.4}$$

with an orientifold projection acting on the internal manifold as $\xi \mapsto -\xi$. We note that not all F-theory models exhibit a weak coupling limit [59]. While hypersurface three-folds of the form (3.2.4) can be described naturally as a Sen limit, the range of possible upflifts was enlarged by the articles [60, 61].

3.3 Effective theories from Calabi–Yau compactification

To obtain theories describing our four-dimensional spacetime, the ten-dimensional superstring theories discussed in the previous sections need to be compactified on a six-dimensional man-

ifold. In the seminal article [8], the authors provided a description of this internal space and showed that ten-dimensional $N = 1$ is reduced to four-dimensional $N = 1$ precisely when it is given by a Calabi–Yau three-fold, i.e. a complex three-dimensional Kähler manifold with vanishing first Chern class (cf. section 2.1). In terms of supercharges, compactification on Calabi–Yau n-folds reduces their count by $1/2^{n-1}$. The 32 or 16 supercharges in ten dimensions thus become 8 and 4 in $D = 4$, which again corresponds to $N = 2$ and $N = 1$. Note that F-theory has the same amount of supercharges as type IIB (32), which reduces to four supercharges or $N = 1$ in compactifications on elliptically fibred four-folds.

The spectrum of type II theories on Calabi–Yau three-folds is given by one gravity multiplet together with both vector- and hypermultiplets whose count is determined by the geometry of the Calabi–Yau. More precisely, type IIA has $(h^{2,1} + 1)$ hypermultiplets, where the "+1" refers to the universal one, and $h^{1,1}$ vectormultiplets. Type IIB has $(h^{1,1} + 1)$ hypermultiplets and $h^{2,1}$ vectormultiplets. Supersymmetry implies that the scalars of both types of multiplets do not mix and that the moduli space is a direct product. Denoting the number of hyper-/vectormultiplets by $n_{\mathrm{h/v}}$, the moduli space of vectormultiplets is so-called[2] special Kähler and of complex dimension n_{v} and the four real scalar degrees of freedom in the hypermultiplet yield an n_{h}-dimensional quaternionic space. In type IIB, the vectormultiplet moduli space is described by the complex-structure moduli, whereas the scalars in hypermultiplets descend from ϕ, C_0, C_2 and C_4 and are supplemented by the complexified Kähler parameters of the metric and B-field. Below, we will consider an orientifold projection that removes the two-forms B_2 and C_2 from the spectrum and breaks half of the supersymmetry. The scalars of the chiral multiplets in $N = 1$ are then given by the axio-dilaton and $h^{2,1}$ complex-structure moduli together with $h^{1,1}$ real Kähler moduli from the metric and $h^{1,1}$ real scalars coming from C_4, combining to $h^{1,1}$ complex moduli.

It is conjectured that each Calabi–Yau X comes with a *mirror partner* $\hat{X}$, where the vectormultiplet moduli spaces of type IIA on $\hat{X}$ and type IIB on X are locally isomorphic. While, at the time of this writing, mirror symmetry has not been proven, strong evidence for it was established and it has been verified in special cases such as hypersurfaces in toric ambient spaces [62].

One important aim is to reduce the number of free moduli by giving background values to the field strengths H_3 and F_3 (fluxes), which turns the theory into gauged supergravity [63] and yields a scalar potential [64, 65]:

$$V = e^{K_{\mathrm{tot}}} \left(\sum_{A,\overline{B}} g^{A\overline{B}} D_A W D_{\overline{B}} \overline{W} - 3|W|^2 \right) \tag{3.3.1}$$

with the Gukov–Vafa–Witten superpotential

$$W = \int_X G_3 \wedge \Omega \,, \tag{3.3.2}$$

where we defined $G_3 \coloneqq F_3 - \tau H_3$ and the sum runs over all scalars z^A . In M/F-theory, where we already have $N = 1$ supersymmetry, the scalar potential V is built from the four-fold equivalent

[2] The term "special" refers to special geometry, cf. section 4.6.

of eq. (3.3.2)

$$W = \int_Y G_4 \wedge \Omega \tag{3.3.3}$$

with Y the Calabi–Yau fourfold and G_4 the field strength for A_3. This results in a similar scalar potential as in eq. (3.3.1) where the 3 is exchanged with a 4. The total Kähler potential K_{tot} is defined below (3.3.6) and depends on the axio-dilaton and both vector- and hypermultiplets. As discussed in section 2.1, it yields the Kähler metric

$$g_{A\overline{B}} \coloneqq \frac{\partial}{\partial z_A} \frac{\partial}{\partial \overline{z}_{\overline{B}}} K_{\text{tot}} \tag{3.3.4}$$

and furthermore the covariant derivative $D_A = \partial_A + \partial_A K_{\text{tot}}$. Fluxes either break $N = 2$ completely or leave it untouched [66] and a breaking to $N = 1$ presupposes an orientifold projection [67], see [1] for a more careful review of the following. We consider an O3/O7 orientifold projection (inverting an even number of complex coordinates on X) and demand $h^{2,1} = h^{2,1}_-$, $h^{1,1} = h^{1,1}_+$ under the induced action on the cohomology. In this way one obtains $h^{2,1}$ complex-structure moduli fields and the axio-dilaton, while B_2 and C_2 are removed from the theory and the Kähler moduli now describe $h^{1,1}$ scalars in the chiral multiplet. At tree level, they are given by

$$T_\alpha = -h_\alpha + \frac{\mathrm{i}}{2} c_{\alpha\beta\gamma} v^\beta v^\gamma, \tag{3.3.5}$$

where the real moduli v_α and h_α come from the metric and C_4, respectively. The Kähler potential is then given by

$$K_{\text{tot}} \coloneqq K_{\text{cs}} + K_\tau + K_{\text{Ks}}\,. \tag{3.3.6}$$

At zeroth order in α' and g_{S}, the contribution of the axio-dilaton reads

$$K_\tau = -\log\left(-\mathrm{i}(\tau - \overline{\tau})\right) \tag{3.3.7}$$

and, seeing v_α as functions of T_α and h_α, one writes for the Kähler moduli term

$$K_{\text{Ks}} = -2\log\left(c_{\alpha\beta\gamma} v^\alpha v^\beta v^\gamma\right), \tag{3.3.8}$$

This form of the total Kähler potential allows one to derive a "no-scale property" effectively cancelling the contributions of the Kähler moduli with the term $-3|W|^2$ in eq. (3.3.1). This simplification is however broken by corrections in α' and g_{S}. The complex-structure Kähler potential K_{cs} is a function of the complex-structure moduli and will be given in eq. (4.1.14).

The action for type IIB supergravity implies a no-go theorem, which follows from the ten-dimensional Einstein equations for a compactification on a warped background and prohibits non-zero values for G_3. To still generate a scalar potential in the above way, one needs to introduce brane sources to the action [68]. For a Dp-brane filling the uncompactified dimensions and wrapping a $(p-3)$-cycle Ξ in the internal Calabi–Yau manifold, this additional term is of the form

$$S_{\text{loc}} = -T_{\text{D}p} \int_{\mathbb{R}^4 \times \Xi} \mathrm{d}\xi^{p+1} \sqrt{-g} + \tau_{\text{D}p} \int_{\mathbb{R}^4 \times \Xi} C_{p+1} \tag{3.3.9}$$

with the Einstein-frame tension $T_{\text{D}p}$ given by

$$T_{\text{D}p} = |\tau_{\text{D}p}| e^{(p-3)\phi/4} \tag{3.3.10}$$

for positive-tension objects. This introduces another term in the equation of motion for the self-dual field strength $\tilde{F}_5$ (3.1.15)

$$\mathrm{d}\tilde{F}_5 = H_3 \wedge F_3 + 2\kappa_{10}^2 T_{\mathrm{D3}} \rho_3 \tag{3.3.11}$$

with ρ_3 the density of O3-planes and D3- and D7-branes. The coupling of the latter to C_4 comes from a world-volume flux F_2 on the D7-brane and is described by $\int_\Sigma C_4 \wedge F_2 \wedge F_2$. By integrating eq. (3.3.11) over the internal Calabi–Yau, we find the tadpole constraint

$$\int_X H_3 \wedge F_3 = -2\kappa_{10}^2 T_{\mathrm{D3}} Q_3 \tag{3.3.12}$$

with the total D3-brane charge $Q_3 = \int_X \rho_3$. We will not be concerned with specific brane configurations and simply demand a non-zero l.h.s. to avoid the no-go theorem above.

The eleven-dimensional low-energy limit of M-theory is described by the action in eq. (3.2.1). It obtains quantum corrections of the form

$$\delta S = -T_{\mathrm{M2}} \int A_3 \wedge X_8 \,, \tag{3.3.13}$$

with an eight-form X_8 given in terms of the curvature two-form

$$X_8 = \frac{1}{(2\pi)^4} \left(\frac{1}{192} \mathrm{tr} R^4 - \frac{1}{768} \left(\mathrm{tr} R^2 \right)^2 \right). \tag{3.3.14}$$

As in the case of type IIB, one introduces source terms for M2 and M5 branes to allow for non-zero G_4. The equations of motion for its field A_3 then read

$$\mathrm{d} \star G_4 = -\frac{1}{2} G_4 \wedge G_4 - 2\kappa_{11}^2 T_{\mathrm{M2}} \left(X_8 + \sum_i Q^i_{\mathrm{M2}} \delta_i^{(8)} + \sum_i Q^i_{\mathrm{M5}} \delta_i^{(5)} \wedge A_3 \right). \tag{3.3.15}$$

To derive a tadpole restriction for four-fold compactifications, we need to integrate eq. (3.3.15) over the four-fold Y. The X_8-form can be expressed in Pontryagin classes which translate for a Calabi–Yau geometry with Chern classes c_i to

$$X_8 = \frac{1}{192} \left(c_1^4 - 4c_1^2 c_2 + 8 c_1 c_3 - 8 c_4 \right), \tag{3.3.16}$$

Since $c_1(Y) = 0$ and its Euler number is defined as $\chi = \int_Y c_4$, one derives the tadpole restriction

$$N_{\mathrm{M2}} + \frac{1}{4\kappa_{11}^2 T_{\mathrm{M2}}} \int_X G_4 \wedge G_4 = \frac{\chi}{24} \,. \tag{3.3.17}$$

Here, our searches for fluxes are restricted to $\frac{1}{4\kappa_{11}^2 T_{\mathrm{M2}}} \int_X G_4 \wedge G_4 \leq \frac{\chi}{24}$, which allows to reconstruct the number of M2 branes.

3.4 Flux vacua criteria

In the previous subsection, we mentioned that background values for F_3 and H_3 give an $N = 1$ superpotential V (3.3.1) in the four-dimensional effective theory. Generically, these fluxes break $N = 1$ supersymmetry obtained from $N = 2$ after the orientifold projection. For a general metric

background, the vacuum expectation values of the supersymmetry variations for the gravitino ψ_μ and the chiral multiplet superpartners χ^A to the scalars z_A read (cf. [69], section 18.2)

$$\langle \delta\chi^A \rangle = -\frac{1}{\sqrt{2}} e^{K_{\text{tot}}/2} g^{A\overline{B}} D_{\overline{B}} \overline{W} P_L \varepsilon = 0\,, \tag{3.4.1}$$

$$\langle \delta P_L \psi_\mu \rangle = D_\mu \left(P_L \varepsilon\right) + \frac{1}{2} e^{K_{\text{tot}}/2} W \gamma_\mu P_R \varepsilon = 0\,. \tag{3.4.2}$$

The first equation yields directly the F-term equations for the moduli fields

$$e^{K_{\text{tot}}/2} D_A W = 0\,. \tag{3.4.3}$$

In the case of a Minkowski background, the covariant derivative in eq. (3.4.2) of the supersymmetry parameter ε vanishes if its is chosen to be constant and one is left with

$$e^{K_{\text{tot}}/2} W = 0 \qquad \text{(Minkowski)}\,. \tag{3.4.4}$$

Generally, however, this leads to a Killing spinor equation for ϵ with the gravitino mass

$$m_{3/2} = e^{K_{\text{tot}}/2} W\,. \tag{3.4.5}$$

A solution to this equation exists only for a cosmological constant given by[70]

$$\Lambda = -3 m_{3/2}^2 = -3 e^{K_{\text{tot}}} |W|^2\,, \tag{3.4.6}$$

in which case the gravitino is shown to have two polarisations (physically massless) and supersymmetry is unbroken. In the string picture, negative cosmological constants arise, for example, due to D3-branes wrapping euclidean four-cycles and thus introduce terms in the superpotential that are dependent on Kähler moduli. A proposal to lift an AdS vacuum constructed that way via anti-D3-branes to a dS vacuum is known as KKLT mechanism [71]. While configurations with $W \neq 0$ can lead to AdS vacua, in this work, we will consider only Minkowski vacua with eq. (3.4.4).

To translate these conditions to properties of the Calabi–Yau geometry, we express the flux G in a homology basis Γ_i

$$W = \int G \wedge \Omega = g^T \Sigma \underline{\Pi}\,, \qquad \Pi_i = \int_{\Gamma_i} \Omega\,, \tag{3.4.7}$$

with dual-intersection form Σ and periods $\underline{\Pi}$, cf. section 4.1. Equation (3.4.7) holds for both three- and four-dimensional compactifications, where $g_3 = f_3 - \tau h_3$ in the former case. The fluxes must satisfy a Dirac–Zwanziger [72] quantisation condition which requires the entries of f_3 and h_3 to be integral. In M-theory, Witten's flux quantisation condition [73]

$$G_4 + \frac{c_2(Y)}{2} \in H^4(Y, \mathbb{Z}) \tag{3.4.8}$$

requires special attention for four-folds with odd c_2-integrals. Returning to the vacuum conditions in eqs. (3.4.3) and (3.4.4), we consider ranges of the moduli fields where K_τ and K_{Ks} are regular. While varying the complex structure, when necessary, we perform a Kähler gauge transformation (2.1.3) such that the prefactor $e^{-K_{\text{tot}}}$ is regular and can be omitted. The vacua conditions then translate into a splitting of the integral Hodge structure as we will see in the following.

We begin by considering compactifications on three-folds X. The F-term condition for the axio-dilaton τ requires

$$\begin{aligned} 0 = D_\tau W &= \partial_\tau W + (\partial_\tau K_\tau) W \\ &= -\int_X H_3 \wedge \Omega \,, \end{aligned} \tag{3.4.9}$$

where we used $W = 0$ for the second equality. Inserting this back into the definition of the superpotential (3.3.2) also yields

$$0 = \int_X F_3 \wedge \Omega \,. \tag{3.4.10}$$

In terms of cohomology classes, these equations imply that both F_3 and H_3 are orthogonal to $H^{0,3}(X)$. Since these are real fields, the same is true for $H^{3,0}(X)$. The tadpole condition in eq. (3.3.12) requires that $h^T \Sigma f \neq 0$ and antisymmetry of Σ thus implies that h and f must be linearly independent and span a rank-two lattice Λ in the middle cohomology $H^3(X, \mathbb{Z})$. More precisely, the latter splits as

$$H^3(X, \mathbb{Z}) = \Lambda \oplus \Lambda^\perp \tag{3.4.11}$$

with $\Lambda \subset H^3(X, \mathbb{Z}) \cap (H^{2,1}(X, \mathbb{C}) \oplus H^{1,2}(X, \mathbb{C}))$. Schematically, this splits the Hodge structure into $(0, 1, 1, 0) \oplus (1, h^{2,1} - 1, h^{2,1} - 1, 1)$. The flux vacua we study in this work lie along codimension one loci in the moduli space. If one finds two fluxes f and h along $z^{\text{vac}} = 0$, the F-terms for the remaining vector moduli z^A, $A \neq \text{vac}$, are satisfied automatically as W is flat in these directions. The only further restriction follows from $D_{z^{\text{vac}}} W = 0$, which puts a restriction on the axio-dilaton

$$\tau(z^A, z^{\text{vac}} = 0) = \left. \frac{\int_X F_3 \wedge D_{z^{\text{vac}}} \Omega}{\int_X H_3 \wedge D_{z^{\text{vac}}} \Omega} \right|_{z^{\text{vac}}=0} . \tag{3.4.12}$$

For $h^{2,1} = 1$, type IIB flux vacua are also called attractor points due to their appearance in the description of extremal black hole solutions in supergravity [74].

For four-fold compactifications, supersymmetry implies additionally that G_4 must be self-dual, which can be enforced by an additional superpotential for the Kähler moduli in terms of the Kähler form J

$$W^{1,1} = \int_Y J \wedge J \wedge G_4 \,. \tag{3.4.13}$$

The Kähler F-terms $0 = \partial_i W^{1,1}$ then guarantee $J \wedge G_4 = 0$, i.e. that G_4 is primitive. The same flux conditions of eqs. (3.4.3) and (3.4.4) translate to a similar yet different Hodge splitting on four-folds. Together with reality of the flux, they restrict the configurations to $G_4 \in H^{2,2}_{\text{prim}}(Y)$ and we are left with a decomposition of the primitive middle cohomology

$$(0, 0, 1, 0, 0) \oplus (1, h^{3,1}, h^{2,2}_{\text{prim}} - 1, h^{3,1}, 1) \,. \tag{3.4.14}$$

3.5 Black hole condensation

There exist connections between the moduli spaces of (some) families of Calabi–Yau manifolds in the sense that one can shrink cycles and resolve the singularity by gluing in a cycle of different dimension. Such transitions between two families change the Hodge numbers and have been known to Mathematicians since the 1980s [75, 76]. Reid's conjecture [77] that all families are

connected in this way is still open and, so far, has only been shown for CICYs in products of projective spaces [78]. Locally, such transitions can be understood as two different resolutions of a conic singularity. Following [79], a conifold fibre of a three-fold family looks like the zero locus

$$\sum_{i=1}^{4} w_i^2 = 0\,. \tag{3.5.1}$$

The obvious regularisation deforms this cone to contain an S^3

$$\sum_{i=1}^{4} w_i^2 = \epsilon \tag{3.5.2}$$

with a parameter $\epsilon > 0$. Instead, one can perform a change of variables to express (3.5.1) as

$$X\,Y - U\,V = \det \begin{pmatrix} X & U \\ V & Y \end{pmatrix} = 0\,. \tag{3.5.3}$$

One can perform a small resolution/blow-up by including a $\mathbb{P}^1 \cong S^2$ parametrised by $(\lambda_1 : \lambda_2)$ at the singularity

$$\begin{pmatrix} X & U \\ V & Y \end{pmatrix} \begin{pmatrix} \lambda_1 \\ \lambda_2 \end{pmatrix} = 0\,. \tag{3.5.4}$$

Note that eq. (3.5.4) reduces to eq. (3.5.3) away from the singularity. Looking at a conifold fibre, there are two ways of desingularisation that lead to different families of manifolds. In other words, the singularity allows us to travel from one family to another.

In the seminal work [43], Greene, Morrison and Strominger found a physical realisation of such transitions in type IIB string vacua with D3-branes wrapping vanishing three-cycles, relating compactifications on different Calabi–Yau families X. The article was built upon Strominger's description [80] of three-branes wrapping vanishing cycles and producing massless black holes curing their singularities. While the vast number of possible compactifications made the search for realistic vacua seem intractable, these findings gave new hope that all such vacua are in fact connected. The results were extended to type IIA vacua on mirrors $\hat{X}$, where D2-branes wrapping vanishing two-cycles can give rise to non-abelian gauge-symmetries and localised matter [81, 82, 83, 84].

In the type IIB picture, the number of vectormultiplets is given by $h^{2,1}$ and the hypermultiplets are counted by $h^{1,1}$ (plus the universal one). Due to [80], three-cycles wrapped by D3-branes correspond to BPS hypermultiplets, whose masses are thus proportional to their Ω-volume. Approaching a conifold, there is an S^3 shrinking to zero size. At this singularity, one finds that the BPS hypermultiplet from the D3-brane appears in the effective theory. Importantly, the hypermultiplet is charged under the U(1) vector V^I coming from reducing C_4 on the dual cycle to the vanishing Γ. Reducing the four-form in a cohomology basis (α_I, β^I), $C_4 = V^I \wedge \alpha_I + V_I \wedge \beta^I$ yields the coupling

$$\mu_3 \int_{\Gamma\times\gamma} C_4 = \mu_3 \underbrace{\Gamma \cap \Gamma_I}_{=q_I} \int_\gamma V^I. \tag{3.5.5}$$

One can resolve the singularity in the Coulomb branch[3] by giving a vev to the hypermultiplet. Via the Higgs effect, the vectormultiplet becomes massive by absorbing the hypermultiplet. In general, there are several, say k, vanishing three-cycles that satify r relations in homology. Still, for each of the k vanishing cycles, there will appear one massless hypermultiplets in the effective theory. After giving vevs to the hypermultiplet scalars, $k - r$ (then massive) vectormultiplets disappear and r additional massless hypermultiplets remain in the spectrum. Turning on these vevs leads one from the Coulomb branch to a mixed branch with a Higgs-branch direction. In [43], the authors identified such a transition for the quintic hypersurfaces where 16 S^3's subject to one relation in homology vanish. The dual model with $h^{2,1} = 101 - 15 = 86$ and $h^{1,1} = 1 + 1$ was identified with the octic hypersurfaces in $\mathbb{P}_{2,2,2,1,1}$. In section 7.2, we will study the period geometry of these transitions in detail and catalogue those arising in genus-one fibrations over bases described by reflexive polygons.

After this discovery, similar results were found in type IIA compactified on Calabi–Yau three-folds, where D2-branes wrap vanishing two-cycles. Ignoring the graviphoton, the gauge group $U(1)^{h^{1,1}}$ coming from reducing C_3 on $H^{1,1}(X)$ is enhanced to $U(1)^{h^{1,1}-r} \times G$, where r is the rank of G, whose Cartan matrix is given by the negative of vanishing cycles' intersection numbers [81]. The group G is of the same Dynkin type as an ADE surface singularity over a curve C in the three-fold that is resolved by the intersecting two-cyles. If their intersection is of type A_{N-1} over a genus g curve C, there are additionally g hypermultiplets in the adjoint representation [82]. Similarly to the findings in F-theory (cf. section 3.2), at points on C where the gauge-symmetry enhances due to another two-cycle that shrinks to zero size, localised fundamental matter appears [85, 84]. Mirror symmetry allows one to study these gauge enhancements in type IIB on the mirror family. In this language, the loci of shrinking of the two-cycles translates into vanishing periods representing the associated Kähler parameter t^i under the mirror map. The locus of enhanced gauge symmetry is then again described by a Calabi–Yau families whose topological data follow from the prepotential at $t^i = 0$. It is gratifying to observe that this transition is exact, in the sense that the instanton corrections re-sum to that of the gauge-enhanced theory on the mirror family. We will review these transitions and their period geometry in section 7.1.

[3]The Coulomb branch describes the moduli space for vanishing vevs of the *charged* hypermultiplets. Note that the $h^{1,1} + 1$ hypermultiplets from the closed string spectrum are neutral.

Chapter 4

Period geometry for elliptic curves, K3 surfaces and CY three-folds

4.1 Periods and the middle homology

In string theory compactifications, understanding how Calabi–Yau manifolds vary as one moves in moduli space is essential, both mathematically and physically. Crucially, each point in this moduli space represents a different geometry and transitioning between these points reveals how physical quantities, like D-brane charges or coupling constants, change continuously. To track these changes systematically, one uses periods, integrals of the unique holomorphic form over topological cycles on the Calabi–Yau manifold. These periods encode physical data, such as central charges of D-branes or couplings in the effective theory, and evolve smoothly across the moduli space according to special differential equations known as Picard–Fuchs equations. From this perspective, the Gauss–Manin connection emerges naturally as the tool that captures how the middle cohomology, including brane charges and fluxes, transform as the geometry varies.

First, let us consider a specific Calabi–Yau manifold X. There are two important pairings for the description of the complex structure and with it the middle (co-)homology: There is an *intersection form*[1] in homology between cycles

$$\hat{\Sigma}: H_n(X,\mathbb{Z}) \times H_n(X,\mathbb{Z}) \to \mathbb{Z}\,, \tag{4.1.1}$$

which represents how two of them intersect or are linked, and a pairing between the homology and cohomology, whose components give the so-called *period matrix*

$$\mathbf{\Pi}: H_n(X,\mathbb{Z}) \times H^n(X,\mathbb{Q}) \to \mathbb{C}\,. \tag{4.1.2}$$

To give the components of these two forms, we introduce a topological basis for $H_n(X,\mathbb{Z})$ consisting of cycles Γ_i, $1 \leq i \leq b_n$. The term topological means that these cycles are invariant under small[2] deformations of the complex structure, which will be of importance when considering variations of the Hodge structure. In components, we have $\hat{\Sigma}_{ij} = \Gamma_i \cap \Gamma_j$. Let us denote the dual basis to $\{\Gamma_i\}_i$ in cohomology by $\{\gamma^j\}_j$, satisfying $\int_{\Gamma_i} \gamma^j = \delta_i^j$. We note that this is not the Poincaré-dual basis denoted by $\eta_i \in H^n(X,\mathbb{C})$ where

$$\int_{\Gamma_i} \gamma = \int_X \gamma \wedge \eta_i\,, \quad \forall\, \gamma \in H^n(X,\mathbb{C})\,. \tag{4.1.3}$$

[1] We will use the term intersection form for both Σ and $\hat{\Sigma}$. It should be clear from the context whether it relates to homology or cohomology.

[2] Globally, the cycles are subject to monodromy transformations.

These have the same intersection form as the cycles

$$\int_X \eta_i \wedge \eta_j = \hat{\Sigma}_{ij} \,, \tag{4.1.4}$$

while the dual basis $\gamma^i = \Sigma^{ik}\eta_k$ we will mostly use yields an intersection form in cohomology given by the inverse of this matrix. First, note that

$$\delta^i_j = \int_{\Gamma_j} \gamma^i = \int_X \gamma^i \wedge \eta_j = \Sigma^{ik} \int_X \eta_k \wedge \eta_j = \Sigma^{ik}\hat{\Sigma}_{kj} \,, \tag{4.1.5}$$

implying $\Sigma = \hat{\Sigma}^{-1}$. Furthermore, the dual pairing is given by

$$\int_X \gamma^i \wedge \gamma^j = \Sigma^{ik}\Sigma^{jl} \int_X \eta_k \wedge \eta_l = \Sigma^{ij} \,. \tag{4.1.6}$$

Some authors choose to use the Poincaré-dual basis, which for three-folds give an expansion of the $(3,0)$-form with a negative sign between the A- and B-periods. In this work, we only use the basis γ^i with expansion of Ω given by

$$\Omega = \gamma^i \int_{\Gamma_i} \Omega \,. \tag{4.1.7}$$

We conclude that the intersection form in homology $\hat{\Sigma}$ induces a pairing in the middle cohomology as

$$\begin{aligned} &\Sigma : \; H^n(X,\mathbb{Q}) \times H^n(X,\mathbb{Q}) \to \mathbb{Q} \,, \\ &\Sigma^{ij} = \int_X \gamma^i \wedge \gamma^j = (\hat{\Sigma}^{-1})^{ij} \,. \end{aligned} \tag{4.1.8}$$

In (odd) even dimensions, the non-degenerate pairings Σ and $\hat{\Sigma}$ are (anti-)symmetric. In section 5.3, we will construct bases for the homology that bring $\hat{\Sigma}$ into a particular simple form (cf. eq. (5.3.14)). In this basis, the second pairing $\mathbf{\Pi}$ is trivially given by $\mathbf{\Pi}_i{}^j = \int_{\Gamma_i} \gamma^j = \delta^j_i$. To extract data about the complex structure of the manifold, it is useful to use a different basis for the cohomology. From section 2.1, we know that there exists a unique holomorphic $(n,0)$-form Ω. We call *periods* the integrals of this form over the cycles Γ_i, which we collect in the *period vector*

$$\underline{\Pi} = \int_{\underline{\Gamma}} \Omega \,. \tag{4.1.9}$$

Having discussed the intersection form and period integrals for a single Calabi–Yau manifold X, we now consider what happens as the manifold itself varies smoothly in a *family* $\mathcal{X}$. These have been introduced in section 2.2 and we recall that they are defined over their complex-structure moduli space $\mathcal{M}_{\text{c.s.}}$ by the map

$$\pi : \; \mathcal{X} \longrightarrow \mathcal{M}_{\text{c.s.}} \,. \tag{4.1.10}$$

Let z^i, $1 \leq i \leq h^{n-1,1}$, be local coordinates on $\mathcal{M}_{\text{c.s.}}$. The Calabi–Yau manifolds are given by fibres of π, which we denote by $X_{\underline{z}} = \pi^{-1}(\underline{z})$. As we move continuously through the moduli space, the holomorphic top form $\Omega(z)$ changes smoothly, causing its period integrals to vary as well. This leads directly to the concept of variations of Hodge structures [86, 87], where one studies precisely how the decomposition of the middle cohomology changes as we vary moduli. In this broader picture, the intersection form Σ remains constant (since it is topological), while the periods evolve, governed by differential equations known as Picard–Fuchs equations. Before we get to the latter, we must introduce some more structure.

The moduli space $\mathcal{M}_{\text{c.s.}}$ is typically not smooth but contains singular points or loci, where the fibre $X_{\underline{z}_0}$ becomes a singular manifold[3]. From the point of view of the periods, singularities are characterised by cycles growing or shrinking to infinite size. A typical example is the conifold, where an S^n shrinks to a point. One must then resolve these singular loci (e.g. by so-called blow-ups) to ensure that the proper transforms $\hat{\Delta}_k$ of all discriminant components together with the exceptional divisors introduced to resolve the singularities have normal crossings. The periods $\underline{\Pi}$ are multivalued functions on the resolved moduli space, as becomes apparent seeing them as solutions to a *Picard–Fuchs system* of differential equations, which we will discuss in more detail in section 4.4. There, we describe methods obtaining local solutions and patching these together to a global basis of periods. Moving along a closed path around a singular locus, this branch structure is reflected in a non-trivial monodromy action $\underline{\Pi} \mapsto M\,\underline{\Pi}$ for M a $b_n \times b_n$ matrix. For a general basis of the periods, these matrices are complex. However, for many applications, one needs a basis that has only rational or even integral monodromy matrices. For an arithmetic discussion and computation of a local ζ-function, for example, one needs rationality of the basis, while for applications in physical theories, the Dirac–Zwanziger quantisation condition demands integrality of the basis. We will continue using the notion of 'rationality/integrality of a period basis', meaning that all monodromy matrices have rational/integer entries. The whole purpose of section 5.3 is to give a description of obtaining integral periods for families in any dimension. Since the matrix Σ represents the intersection of a topological basis, it is not affected by monodromy actions

$$M^T \Sigma\, M = \Sigma\,. \tag{4.1.11}$$

For odd dimensions, the monodromy group of an integral basis is a subgroup of $\mathrm{Sp}(b_n, \mathbb{Z})$[4]. For even dimensions, we call the integral matrix group with relation eq. (4.1.11) $\mathcal{O}(\Sigma, \mathbb{Z})$. The moduli space is Kähler (cf. section 2.1) and its so-called Weil–Petersson metric[5] is given by

$$g_{i\bar{\jmath}} = \partial_{z^i}\partial_{z^{\bar{\jmath}}} K(\underline{z}, \bar{\underline{z}})\,, \tag{4.1.13}$$

where the Kähler potential K is defined implicitly by

$$e^{-K} = \mathrm{i}^n \int_X \overline{\Omega} \wedge \Omega = \mathrm{i}^n \underline{\Pi}^\dagger \Sigma\, \underline{\Pi} > 0\,. \tag{4.1.14}$$

Due to the additional special geometry structure in $n = 3$, there, the moduli space is called special Kähler. Positivity of the above is the special case $p = n$, $q = 0$ of the Hodge–Riemann bilinear relations

$$\mathrm{i}^{p-q} \int_X \overline{\alpha} \wedge \alpha > 0\,, \qquad \alpha \in H^{p,q}(X) \tag{4.1.15}$$

[3] It is important to note that singularities of the differential equations describing the periods may also come from poor choices of coordinates for a patch of the moduli space. An example are the (smooth) Fermat hypersurfaces, where the differential equations obtain an orbifold singularity.

[4] In appendix A.1, starting from a specific modular congruence sub-group, we derive a Picard–Fuchs system with this monodromy group over the fundamental domain with genus one.

[5] With the covariant derivative introduced in eq. (4.2.18), we find

$$\begin{aligned} g_{i\bar{\jmath}} &= -\mathrm{i}^n \partial_i \left(e^K \int_X \partial_{\bar{\jmath}} \overline{\Omega} \wedge \Omega \right) = -\mathrm{i}^n e^K \left(\partial_i K \int_X \partial_{\bar{\jmath}} \overline{\Omega} \wedge \Omega + \int_X \partial_{\bar{\jmath}} \overline{\Omega} \wedge \partial_i \Omega \right) \\ &= -\mathrm{i}^n e^K \int_X \partial_{\bar{\jmath}} \overline{\Omega} \wedge \chi_i = -\mathrm{i}^n e^K \int_X \overline{\chi}_{\bar{\jmath}} \wedge \chi_i . \end{aligned} \tag{4.1.12}$$

Due to the Hodge–Riemann relations (eq. (4.1.15)), independence of the choice of basis for the tangential space implies that $g_{i\bar{\jmath}}$ is positive definite.

The overall sign in eq. (4.1.14) is a matter of convention. Here, it suits the choice of Σ in eq. (5.3.15). The expression for $g_{i\bar{\jmath}}$ in eq. (4.1.13) presumes a connection—called Gauss–Manin connection—on the vector space of periods. We will introduce it in section 4.2 and show that eq. (4.1.13) indeed defines a metric by defining a covariant derivative D_i on the moduli space.

The Kähler-gauge freedom of eq. (2.1.3) corresponds to a moduli-dependent re-scaling of the holomorphic form $\Omega(\underline{z}) \mapsto e^{f(\underline{z})}\Omega(\underline{z})$. To preserve holomorphicity of Ω in the moduli, f must itself be holomorphic. Another way of phrasing this is that $\Omega(z)$ is a section of a holomorphic line bundle $\mathcal{L}$ over the moduli space $\mathcal{M}_{\text{c.s.}}$ and e^{-K} is a section of $\mathcal{L} \otimes \overline{\mathcal{L}}$.

4.2 Rational middle cohomology and Gauss–Manin connection

In [88], Griffiths showed that, for Calabi–Yau manifolds $X_{\underline{z}}$ embedded in toric ambient spaces $\mathbb{P}_\Delta$, one can obtain their rational middle cohomology from rational forms defined on $\mathbb{P}_\Delta \setminus X_{\underline{z}}$. While this result has been generalised to complete intersections [89] (see also [90]), we will restrict the review to hypersurfaces. This will hopefully suffice to convey the idea and spare the reader from technicalities. We will follow the discussion of [91].

We denote rational p-forms on $\mathbb{P}_\Delta \setminus X_{\underline{z}}$ by $\mathcal{A}^p(X_{\underline{z}})$. Given an n-cycle Γ on $X_{\underline{z}}$, the elements in $\mathcal{A}^{n+1}(X_{\underline{z}})$ yield differential forms under the residue map and we have

$$\frac{1}{2\pi\mathrm{i}} \int_{T(\Gamma)} \phi = \int_\Gamma \mathrm{Res}(\phi)\,, \tag{4.2.1}$$

where $T(\Gamma)$ is a tubular neighbourhood of Γ in $\mathbb{P}_\Delta \setminus X_{\underline{z}}$. It turns out that this constitutes a map from the cohomology group $\mathcal{H}(X_{\underline{z}}) = \frac{\mathcal{A}^{n+1}(X_{\underline{z}})}{\mathrm{d}\mathcal{A}^n(X_{\underline{z}})}$ to the primitive middle cohomology group of the hypersurface

$$\mathrm{Res}: \ \mathcal{H}(X_{\underline{z}}) \to H^n(X_{\underline{z}}, \mathbb{C})\,. \tag{4.2.2}$$

Here and in the following, we consider the complexified middle cohomology. Splitting the cohomology class above into those of forms with poles of order k along $X_{\underline{z}}$

$$\mathcal{H}_k(X_{\underline{z}}) = \frac{\mathcal{A}^{n+1}_k(X_{\underline{z}})}{\mathrm{d}\mathcal{A}^n_{k-1}(X_{\underline{z}})}\,, \tag{4.2.3}$$

one obtains a filtration

$$\mathcal{H}_1(X_{\underline{z}}) \subset \ldots \subset \mathcal{H}_{n+1}(X_{\underline{z}}) = \mathcal{H}(X_{\underline{z}})\,. \tag{4.2.4}$$

The result of Griffiths' theorem is that eq. (4.2.2) maps the filtrant $\mathcal{H}_{k+1}$ into the k-th Hodge filtrant F^k in

$$F^0(X_{\underline{z}}) \subset \ldots \subset F^n(X_{\underline{z}}) \equiv H^n(X_{\underline{z}}, \mathbb{C})\,, \tag{4.2.5}$$

with

$$F^i(X_{\underline{z}}) = \bigoplus_{j=0}^{i} H^{n-j,j}(X_{\underline{z}})\,. \tag{4.2.6}$$

The differential forms are invariant under the scaling relations of the ambient weighted projective space. It follows that, under the residue map, homogeneous polynomials of degree kd correspond to an element in $F^k(X_{\underline{z}}, \mathbb{C})$. The kernel of this map is given by the Jacobian ideal, spanned by

the derivatives of the defining polynomial w.r.t. the coordinates of the ambient space. To obtain a one-to-one map, we consider the ring

$$\mathcal{R}_{\underline{z}} = \bigoplus_{k=0}^{n} \frac{\mathbb{C}\left[x_1, \ldots, x_{n+2}\right]_{kd}}{\mathrm{Jac}_{\underline{z}}(P)}\,, \tag{4.2.7}$$

where $\mathbb{C}\left[x_1, \ldots, x_{n+2}\right]_{kd}$ denotes the polynomial ring of weighted degree kd. From the filtration structure one deduces that each summand is generated by $h^{n-k,k}$ monomials. We end up with the map

$$\begin{aligned} \mathrm{Res}: \ \frac{\mathbb{C}\left[x_1, \ldots, x_{n+2}\right]_{kd}}{\mathrm{Jac}(P, \underline{z})} &\to H^{n-k,k}(X_{\underline{z}})\,, \\ Q &\mapsto \ \mathcal{P}^{n-k,k}\,\mathrm{Res}\left[\frac{Q\mu}{P^{k+1}}\right], \end{aligned} \tag{4.2.8}$$

where we use the projection $\mathcal{P}^{n-k,k}$ into $H^{n-k,k}(X_{\underline{z}})$ and the volume form

$$\mu := \sum_{i=1}^{n+2} (-1)^i w_i x_i \,\mathrm{d}x_1 \wedge \ldots \wedge \widehat{\mathrm{d}x_i} \wedge \ldots \wedge \mathrm{d}x_{n+2}\,, \quad \text{omit } \hat{k}\,. \tag{4.2.9}$$

As a special case, we find that the holomorphic $(n,0)$-form on a hypersurface can be constructed as

$$\Omega = \mathrm{Res}\left[\frac{\mu}{P}\right] = \frac{1}{2\pi \mathrm{i}} \oint_T \frac{\mu}{P} \tag{4.2.10}$$

with T encircling the hypersurface. The derivatives of Ω with respect to the complex-structure moduli generate the *horizontal* middle cohomology. For three-folds, all forms in the middle cohomology are primitive since $h^{1,0} = 0$. In higher dimensions, the horizontal cohomology is just a subset of the primitive cohomology, which itself is only a subset of the middle cohomology. The derivative has the effect of increasing the exponent of P and consequently maps the residue into the next filtrant. So, for example, we have

$$\partial_i \Omega(\underline{z}) \in H^{n,0}(X_{\underline{z}}, \mathbb{C}) \oplus H^{n-1,1}(X_{\underline{z}}, \mathbb{C})\,. \tag{4.2.11}$$

Since the cohomology is finitely generated, we obtain an expression for the variation of Hodge structure on the Calabi–Yau family

$$\left(\partial_{z^i} - A_i\right) \alpha = 0, \quad \alpha \in H^n(X, \mathbb{Q})\,, \tag{4.2.12}$$

called the *Gauss–Manin connection*. In mathematical terms , the filtrants $F^p(X_{\underline{z}})$ of eq. (4.2.5) fit into locally free constant sheaves $\mathcal{F}^p$ over the moduli space [92]

$$\mathcal{F}^0 \subset \ldots \subset \mathcal{F}^n\,, \tag{4.2.13}$$

where $\mathcal{F}^n$ is the holomorphic vector bundle $R^n\pi_*(\mathbb{C}) \otimes_{\mathbb{C}} \mathcal{O}_{\mathcal{M}_{\text{c.s.}}}$ with $R^n\pi_*(\mathbb{C})$ the n-th derived functor of π_* capturing the middle cohomology. The periods are flat sections of this connection

$$\nabla: \ \mathcal{F}^n \longrightarrow \mathcal{F}^n \otimes \Omega^1_{\mathcal{M}_{\text{c.s.}}} \tag{4.2.14}$$

with $\Omega^1_{\mathcal{M}_{\text{c.s.}}}$ the bundle of one-forms on $\mathcal{M}_{\text{c.s.}}$. Following a path in the moduli space, the periods are transported parallelly w.r.t. ∇. The statement that derivatives map into the next filtrant is called *Griffiths transversality* and reads in this language

$$\nabla \mathcal{F}^p \subset \mathcal{F}^{p+1} \otimes \Omega^1_{\mathcal{M}_{\text{c.s.}}}\,. \tag{4.2.15}$$

In fact, the periods can be calculated by solving the system of differential equation eq. (4.2.12). Oftentimes, it is easier to transform this system to a higher order but scalar system of equations. These so-called *Picard–Fuchs differential equations* have been studied extensively and we will review some techniques for solving them in section 4.4.

Returning to eq. (4.2.11), we want to express the derivatives of Ω as

$$\partial_i \Omega(\underline{z}) = \alpha_i(\underline{z})\Omega(\underline{z}) + \chi_i(\underline{z}), \quad \text{with } \chi_i(\underline{z}) \in H^{n-1,1}(X_{\underline{z}}, \mathbb{C})\,. \tag{4.2.16}$$

By using orthogonality of the $H^{n-p,p}$ and $H^{p,n-p}$ for $p \neq q$, we derive an expression for α_i

$$-\partial_i K\, e^{-K} = \partial_i \int_X \overline{\Omega} \wedge \Omega = \int_X \overline{\Omega} \wedge \partial_i \Omega = \alpha_i\, e^{-K}. \tag{4.2.17}$$

Since $e^{-K} > 0$ (4.1.14), we can define the *covariant derivatives*

$$\begin{aligned} D_i :\ H^{n-k,k}(X,\mathbb{C}) &\to H^{n-k-1,k+1}(X,\mathbb{C})\,, \\ \gamma &\mapsto \partial_i \gamma + (\partial_i K)\gamma\,. \end{aligned} \tag{4.2.18}$$

The generators of $H^{n-1,1}(X,\mathbb{C})$ are denoted by $\chi_i \coloneqq D_i\Omega$, $1 \leq i \leq h^{n-1,1}$. The term covariant is meant w.r.t. the Kähler gauge symmetry $\Omega \mapsto e^f\Omega$ for holomorphic functions f, cf. section 4.1. We recall that, under this symmetry, the Kähler potential transforms as $K \mapsto K - f - \bar{f}$, which implies that the classes χ_i transform covariantly:

$$\chi \mapsto (\partial_i + \partial_i K - \partial_i f) e^f \Omega = e^f \chi\,. \tag{4.2.19}$$

With the same argument, we can let $H^{1,n-1}(X,\mathbb{C})$ be generated by $\overline{\chi}_{\bar{\jmath}} \coloneqq \overline{D}_{\bar{\jmath}}\overline{\Omega}$, where the complex-conjugated derivative reads $\overline{D}_{\bar{\jmath}} = \partial_{\bar{\jmath}} + \partial_{\bar{\jmath}} K$.

Griffiths transversality (4.2.15) implies that derivatives of $\Omega(z)$ of order less than n have no contributions of $H^{0,n}(X)$. Consequently, these forms wedged with Ω cannot give a form in $H^{n,n}$ and their integrals over X vanish. At order n, however, the integral produces non-trivial functions in the moduli:

$$\int_X \partial_{\mathcal{I}}\Omega \wedge \Omega = \begin{cases} 0 & \text{if } |\mathcal{I}| < n\,, \\ C_{i_1,\ldots,i_n}(\underline{z}) & \text{if } |\mathcal{I}| = n\,. \end{cases} \tag{4.2.20}$$

These so-called n-point or Yukawa couplings $C_{i_1,\ldots,i_n}$ are sections of $\mathcal{L}^{\otimes 2} \otimes \mathrm{Sym}^3(T^*\mathcal{M}_{\text{c.s.}})$ with $T^*\mathcal{M}_{\text{c.s.}}$ the holomorphic cotangent bundle of $\mathcal{M}_{\text{c.s.}}$. We will introduce them from a physical standpoint in section 4.5. Importantly, in the Batyrev coordinates we usually express the Picard–Fuchs system in, these couplings are *rational* functions. For any dimension n, they can always be written as products of three-point functions, as one might expect seeing these couplings as correlators in a conformal field theory. This decomposition is dictated by the Frobenius algebra structure, which we will discuss in section 5.1.

4.3 Periods as moduli space coordinates and mirror symmetry

So far, this section was concerned with the geometry of a single family of Calabi–Yau manifolds. In chapter 2, we discussed the observation that many such families come in mirror pairs. The astonishing connection between the mirror partners is that the complex-structure moduli space of one is locally isomorphic to the complexified Kähler moduli space of the other. The complexification of the latter is a stringy effect and we will comment on it below.

In section 2.2, we first introduced the Kähler cone with generators J_i as being dual to the irreducible curves $\mathcal{C}_i$. These parametrise the deformations of the metric $\delta g_{i\bar{\jmath}}$ while the deformations of mixed index entries δg_{ij} are described by $H^{0,1}(X, TX) \cong H^{2,1}(X)$. In closed string theories, there are further massless scalar degrees of freedom coming from NS–NS sector, more precisely, from the antisymmetric rank-two tensor. These are the components of the B-field (also called Kalb–Ramond field). We can encode both the deformation $\delta B_{i\bar{\jmath}}$ and $\delta g_{i\bar{\jmath}}$ in the real and imaginary parts of the complexified Kähler parameters t^i. The volume of a two cycle $\mathcal{C}^{(k)}$ is given by

$$v^k \propto \int_{\mathcal{C}^{(k)}} \omega \,. \tag{4.3.1}$$

Note that one might call v^k the un-complexified Kähler parameters, as $\omega = v^i J_i$. We define the complexified Kähler form by

$$\omega_{\mathbb{C}} = B - \mathrm{i}\,\omega \,, \tag{4.3.2}$$

where, again by duality of J_i and $\mathcal{C}^{(i)}$, the complexified Kähler parameters are given by

$$t^k = \frac{1}{(2\pi\mathrm{i})^2\alpha'} \int_{\mathcal{C}^{(k)}} \omega_{\mathbb{C}} = \frac{1}{(2\pi\mathrm{i})^2\alpha'} \left(b^k - \mathrm{i}\, v^k\right) . \tag{4.3.3}$$

We choose a normalisation such that the coupling of the B-field to the world-sheet appears in the string theory's path integral as a factor[6] [93]

$$\exp\left(\frac{1}{2\pi\alpha'} \int_\Sigma \omega_C\right) = \exp\left(2\pi\mathrm{i}\, t^i n_i\right) , \tag{4.3.4}$$

where the integers n_i give the expansion of Σ in $\mathcal{C}^{(i)}$. From eq. (4.3.4), we deduce the B-field shift symmetry

$$t \longmapsto t + 1 \,. \tag{4.3.5}$$

The volume v^k of the cycle $\mathcal{C}^{(k)}$ w.r.t. the Kähler form ω is encoded in the complexified Kähler parameter t^k as

$$v^k = \frac{1}{4\pi^2\alpha'} \mathrm{Im} t^k \,. \tag{4.3.6}$$

As we will see shortly, the volumes t^k are the coordinates that mirror symmetry relates to the complex-structure moduli of the mirror manifold. The above defined the complexified Kähler cone for three-folds motivated by string compactifications to four dimensions. In the following, we will give coordinates for the complex structure that are mapped to the t^i under mirror symmetry. This identification works for all Calabi–Yau mirror pairs and is not limited to three (complex) dimensions. For $n \geq 3$, the periods and the couplings obtain corrections of the form eq. (4.3.4) which vanish in the large volume limit $v^k \to \infty$.

This limit is of particular interest to us, since, there, the identification between the Kähler moduli space of X and the complex-structure moduli space on the mirror $\hat{X}$ becomes exact. This limit corresponds to the MUM point of the B-side and we will see below how the logarithmic period structure gives rise to the *mirror map* between these two moduli spaces. The periods of the unique $(n, 0)$ form Ω over the topological basis γ^i have, at the MUM point, one regular solution and $h^{n-1,1}$ ones with single-logarithmic divergences. These cycles are called A-cycles and we

[6] The coordinates T^A of [93] is related to our t^i by $t^i = \frac{\mathrm{i}T^i}{4\pi^2\alpha'}$.

index this set A^I by uppercase Roman letters $I, J, \ldots \in \{0, \ldots, h^{n-1,1}\}$, whereas lowercase letters are reserved for the indices in $\{1, \ldots, h^{n-1,1}\}$. By a local Torelli theorem, the periods of Ω over the cycles A^I give coordinates on the complex-structure moduli space which we define as

$$X^I(\underline{z}) \coloneqq \int_{A^I} \Omega(\underline{z})\,. \tag{4.3.7}$$

We emphasise that the cycles A^I are topological and independent of the moduli $\underline{z}$. The coordinates X^I are homogeneous due to the Kähler gauge freedom $\Omega \mapsto e^f\Omega$. Inhomogeneous coordinates are obtained by normalising the functions X^I by the fundamental period X^0. In section 4.4, we will see that (in a suitable Kähler gauge) the fundamental period is of the form $X^0(z) = 1+\mathcal{O}(z)$. Due to the work of Deligne [87], one identifies X^i with the single-logarithmic solutions of the form $X^i(z) = \log(z^i)X^0(z)/(2\pi\mathrm{i}) + \mathcal{O}(z)$. We note that the absence of a constant term makes this choice unique. It follows that the inhomogeneous coordinates are of the form

$$t^i(\underline{z}) = \frac{X^i(\underline{z})}{X^0(\underline{z})} = \frac{\log(z)}{2\pi\mathrm{i}} + \mathcal{O}(z)\,. \tag{4.3.8}$$

The conventions are such that the coordinates t^i are exactly those we introduced for the Kähler moduli space. We verify that $z^i \to 0$ yields $\mathrm{Im}t_i \to \infty$. Locally, eq. (4.3.8) is invertible, allowing us to express the Batyrev coordinate as $z^i = q^i + \mathcal{O}(q)$ with $q^i = \exp 2\pi\mathrm{i}\, t^i$.

The mirror maps t^i have the important property that they are flat coordinates on the moduli space and that the covariant derivative D_i we introduced in section 4.2 becomes the ordinary derivative ∂_i in these coordinates. This will be an elementary ingredient for the analysis of the CY-Frobenius algebra in section 5.1 and the construction of a canonical cohomology basis in section 5.6.

4.4 Picard–Fuchs differential equations and their global solutions

In this section, we give an account of the computation of the complex vector space of periods of $\Omega(\underline{z})$. We reserve the symbol $\underline{\Pi}$ for the periods over the integral basis $\underline{\Gamma}$ introduced in section 4.1 and use $\underline{\varpi}$ for an arbitrary set of generators over $\mathbb{C}$. It will be the topic of section 5.3 to find linear combinations of $\underline{\varpi}$ that yield $\underline{\Pi}$. While one can, in principle, solve the Gauss–Manin differential equation eq. (4.2.12) to obtain periods $\underline{\varpi}(\underline{z})$, it is usually easier to solve the equivalent (higher-order) scalar differential system called Picard–Fuchs system. The information of the matrices $\{A_i\}_i$ can be packaged into a differential ideal generated by operators $\left\{\mathcal{L}_j^{(k)}(\underline{z})\right\}_j$. As these are rational in the moduli, we can always normalise them such that they are polynomials in the logarithmic derivatives $\theta_i = z^i\partial_{z^i}$ of order k

$$\mathcal{L}_i^{(k)}(\underline{z}) = \sum_{|\underline{r}|=0}^{k} \sum_{|\underline{s}|=0}^{o} a_{i,\underline{r},\underline{s}}(\underline{z})\, \underline{z}^{\underline{s}}\, \underline{\theta}^{\underline{r}} \tag{4.4.1}$$

with $\underline{z}^{\underline{s}} = \prod_{i\in\underline{s}} z^i$ and $\underline{\theta}^{\underline{r}} = \prod_{i\in\underline{r}} \theta^i$ for some degree $o \in \mathbb{N}$. The ideal has the property that the solution space is precisely the vector space of periods. A crucial piece of information is that if a period is annihilated by a differential operator, then so are all the other periods. Having an expression for one period, we can therefore obtain elements in the ideal systematically by starting

at $k = o = 1$ and working ourselves up in the k-o-grid. A set of operators generates the ideal if the solution space is exactly b_n^{hor}-dimensional. There is a useful approximation of how many operators one typically expects at each order k. Before explaining this, we should discuss the general solution structure given by the Frobenius method.

Given a Picard–Fuchs system, we are now interested in computing solutions, i.e. a local basis for the periods, to this ideal. At any point $\underline{z} = 0$ in the resolved moduli space, there always exists at least one solution of the form

$$\varpi_{\underline{\alpha}}^{(0)}(\underline{z}) = \prod_{i=1}^{h^{2,1}} (z^i)^{\alpha_i} \, f(\underline{z}) \tag{4.4.2}$$

with $f(\underline{z}) = (1 + \mathcal{O}(\underline{z}))$ a power series in the moduli. Applying $\mathcal{L}_i^{(k)}(\underline{z})$ on this solution, we obtain the *indicial equations* by demanding that the coefficient to lowest order in $\underline{z}$ vanishes for all operators

$$\sum_{|\underline{r}|=0}^{k} a_{i,\underline{r},\underline{0}} \, \alpha_{\underline{r}} = 0 \, . \tag{4.4.3}$$

The solutions α_i are then called indicials at this point $\underline{z} = 0$. In models with more than one modulus, these equations typically do not restrict the possible set sufficiently to fix the leading order behaviour of the periods completely. In any case, the indicial equation helps us forming an ansatz of the form eq. (4.4.2) where we solve for the coefficients of $f(z)$. If an indicial $\underline{\alpha}$ is degenerate, i.e. it is a higher-order zero of the indicial equation, the Frobenius method tells us that there exist solutions

$$\varpi_{\underline{\alpha}}^{(k)} = \sum_{i=0}^{k} P^{(k-i)}(\log(\underline{z})) \, \sigma_{\underline{\alpha}}^{(i)}, \tag{4.4.4}$$

where $P^{(k-i)}$ are rational polynomials of order $k - i$ and $\sigma_{\underline{\alpha}}^{(0)} = \varpi_{\underline{\alpha}}^{(0)}$. At generic (non-singular) points in the moduli space, there exist b_n^{hor} power series solution to the differential ideal. The monodromy representation around a divisor $z^i = 0$ is obtained by considering the leading order behaviour of the local solutions $\underline{\varpi}$ and mapping

$$\log(z^i) \mapsto \log(z^i) + 2\pi\mathrm{i} \text{ and } (z^i)^{\alpha_i} \mapsto e^{2\pi\mathrm{i}\alpha_i} (z^i)^{\alpha_i} \, . \tag{4.4.5}$$

The monodromy matrices M_i express the transformed periods in terms of the original ones $\widetilde{\underline{\varpi}} = M_i \underline{\varpi}$. Clearly, the monodromy around non-singular points is trivial and its matrix representation is the identity. The families of Calabi–Yau manifolds that we study always have a point of *maximal unipotent monodromy*, also called MUM-point, with

$$(M_i - \mathbb{1})^k \neq 0 \, , \quad k \leq n \, , \tag{4.4.6}$$

$$\text{but } (M_i - \mathbb{1})^{n+1} = 0 \, . \tag{4.4.7}$$

The indicials at this point are all zero and there are $h^{n-k,k}$ solutions with a k-fold logarithmic pole for $0 \leq k \leq n$.

From now on, the coordinates $\underline{z}$ will always be defined to have the MUM point at their origin $\underline{z} = 0$. Given a geometric realisation of the underlying Calabi–Yau family as a hypersurface or CICY in a toric ambient space, it is known how to obtain such coordinates in terms of the

deformation parameter of the defining polynomial(s). In section 2.2, we reviewed these kinds of families and found generators of the Mori cone $l^{(i)}$. These tell us, how to construct the Batyrev coordinates $\underline{z}$ in terms of the parameters a_ν of the sections, cf. eq. (2.2.36),

$$z^i = \frac{\prod_{j=1}^{|\Delta|} a_j^{l_j^{(i)}}}{\prod_{k=1}^{r}(-a_{0k})^{l_{0k}^{(i)}}} \,. \tag{4.4.8}$$

As in section 2.2, r is the codimension of the Calabi–Yau in the ambient space and subscripts $0*$ refer to the points $(e_j, \underline{0})$ of Δ and to the entries of $l^{(i)}$ left of the semicolon, respectively.

The rule of thumb for the expected number of operators generating the ideal mentioned above works as follows: The Frobenius method creates $\binom{m+k-1}{k}$ solutions in m variables of logarithmic order k. In many—but not all—cases, an operator of order k' yields one restriction at logarithmic order k'. Furthermore, one can multiply the operator from the left with a logarithmic derivative to obtain further restrictions at higher logarithmic order. With the knowledge of the Hodge structure, one can then make an estimate of how many operators at which order one needs. We stress that, in general, this estimate is neither sufficient nor necessary. Instead of trusting the predicted set of operators, one should always verify that no further solutions to the PFDI exist, see for example [16]. Even then, a smaller set of operators might generate the PFDI, see the PFDI of $\mathcal{X}_{10}^{(3)}$ in [1].

By construction, each $(n+r)$-dimensional toric space contains an open set that is isomorphic to the algebraic torus $(\mathbb{C}\{0\})^{n+r}$. We expressed the defining sections $\mathbb{P}_{\Delta_i}$ in coordinates for this patch in section 2.2. The torus contains the real $(n+r)$-cycle $T^{n+r} = |t_i| = \epsilon$, which, for suitable values of the parameters a_i, is a tubular neighbourhood of the complete intersection. The generalisation of section 4.2 to CICYs implies that we have a period given by

$$\varpi_0(\underline{z}) = \int_{T^{n+r}} \prod_{i=1}^{r} \frac{1}{P_{\Delta_r}(\underline{z}, \underline{t})} \prod_{j=1}^{n+r} \frac{\mathrm{d}t_i}{t_i} \,. \tag{4.4.9}$$

This period can be evaluated via an expansion for small parameters $\underline{z}$ and the residue formula. It is commonly referred to as the *fundamental period*. We present two example computations: one for a hypersurface and one for a CICY.

Let us first consider the hypersurface in $\mathbb{P}_{\Delta^{(1)}}$ with $\Delta^{(1)}$ the convex hull of the points in eq. (2.2.12). With eq. (2.2.35), the defining polynomials are given by

$$P_{\Delta_1}(\underline{a}, \underline{t}) = a_0 + a_1 t_1 + a_2 t_2 + a_3 t_3 + a_4 t_4 + \frac{a_5}{t_1^2 t_2^2 t_3^2 t_4} + \frac{a_6}{t_1 t_2 t_3} \,. \tag{4.4.10}$$

We use the freedom to re-scale the variables t_i and $P_{\Delta^{(1)}}$ itself to set $a_i = 1$, $0 \leq i \leq 4$. From the l-vectors in eqs. (2.2.23) and (2.2.24) and eq. (4.4.8), we obtain the relation

$$a_5 = (z^1)^2 z^2 \qquad \text{and} \qquad a_6 = z^1 \,. \tag{4.4.11}$$

Finally, we expand

$$\frac{1}{P_{\Delta_1}} = \frac{1}{1 - \left(-t_1 - \ldots - \frac{z^1}{t_1 t_2 t_3}\right)} = \sum_{k=0}^{\infty} \left(-t_1 - \ldots - \frac{z^1}{t_1 t_2 t_3}\right)^k \,. \tag{4.4.12}$$

Equation (4.4.9) tells us that an expansion of $\varpi_0(\underline{z})$ is given by the terms in eq. (4.4.12) independent of any t_i

$$\varpi_0^{(1)}(\underline{z}) = 1 + 24z^1 + 2520(z^1)^2 + 5040(z^1)^2z^2 + 369600(z^1)^3 + \mathcal{O}\big(\underline{z}^4\big)\,. \tag{4.4.13}$$

For a CICY example, we return to the polytope $\Delta^{(2)}$ of eq. (2.2.45). The NEF partition eq. (2.2.46) implies that the two restrictions are given by

$$P_{\Delta_1^{(2)}} = a_{01} + a_1t_1 + \frac{a_2}{t_1} + a_4t_3\,, \tag{4.4.14}$$

$$P_{\Delta_2^{(2)}} = a_{02} + a_3t_2 + a_5t_4 + \frac{a_6}{t_2^2t_3t_4}\,. \tag{4.4.15}$$

Re-scalings as for $P_{\Delta^{(1)}}$ leave a_2 and a_6 as independent moduli, which are related to the Batyrev coordinates via the l-vectors

$$a_2 = z^1 \qquad \text{and} \qquad a_6 = z^2\,. \tag{4.4.16}$$

The product of the restrictions has the expansion

$$\frac{1}{P_{\Delta_1^{(2)}}P_{\Delta_2^{(2)}}} = \sum_{k_1,k_2=0}^{\infty}\left(-t_1 - \frac{z^1}{t_1} - t_3\right)^{k_1}\left(-t_2 - t_4 - \frac{z^2}{t_2^2t_3t_4}\right)^{k_2} \tag{4.4.17}$$

and the terms independent of $\underline{t}$ give the fundamental period (up to factors of $2\pi\mathrm{i}$)

$$\varpi_0^{(2)}(\underline{z}) = 1 + 2z^1 + 12z^2 + 6(z^1)^2 + 72z^1z^2 + 420(z^2)^2 + \mathcal{O}\left(\underline{z}^3\right). \tag{4.4.18}$$

As mentioned above, the fundamental period can be used to compute differential operators in the Picard–Fuchs ideal.

The period $\varpi_0(\underline{z})$ can be given directly in terms of the Mori cone generators. By solving the general integral eq. (4.4.9), one finds the fundamental period in an $m = h^{n-1,1}$ parameter model in codimension r with $|\Delta| = \delta$

$$\varpi_0(\underline{z}) = \sum_{\underline{n}\in\mathbb{N}_0^m}\frac{\prod_{i=1}^{r}\Gamma(1+\sum_{j=1}^{m}l_{0i}^{(j)}n_j)}{\prod_{i=1}^{\delta}\Gamma(1+\sum_{j=1}^{m}l_i^{(j)}n_j)}\prod_{j=1}^{m}(z^j)^{n_j}. \tag{4.4.19}$$

The differential ideal annihilating this period is a special case of a Gel'fand–Kapranov–Zelevinskii system [94], which is determined by the generators of the Mori cone. However, the operators coming from this description do not yield the generators of the Picard–Fuchs system and one needs to factorise them first. While this by itself can be computationally expensive, these factorised operators do not even need to generate the Picard–Fuchs system, as was discussed, for example, in [16]. In our experience, it is much easier to expand the period eq. (4.4.9) to a sufficient order and search for differential operators with an ansatz of the form eq. (4.4.1) directly. The explicit form of the GKZ differential operators allows to give the solution $\varpi_0(\underline{z},\underline{\alpha})$ with open indicials $\underline{\alpha}$. While the indicial equation demands all of them to be zero, this structure allows to construct the whole solution space via the Frobenius method by taking derivatives w.r.t. these indicials before setting them to zero. To obtain the $h^{n-p,p}$ periods with logarithmic order p, one must take linear combinations of the solutions similar to the restriction of sheaves we will discuss

in section 5.3. We again experienced that a direct computation of the periods by first computing the PFDI and then solving for the solutions by making an ansatz of the form eq. (4.4.4) is in general significantly faster than computing derivatives of the Γ-functions appearing in $\varpi_0(\underline{z}, \underline{\alpha})$. For this reason, we will not discuss the GKZ system in more detail and refer the reader to the two references mentioned above instead.

Having obtained the PFDI and a local basis for the periods $\underline{\varpi}$ at the MUM point, we need to perform an analytical continuation of this basis throughout the moduli space. While this seems unnecessary for the local basis $\underline{\varpi}$, it will be of importance for the integral basis $\underline{\Pi}$ we will construct in section 5.3, since the known methods allow only for its construction at the MUM point. To find local solutions at a different point $\underline{u} = 0$ in the moduli space, one expresses the operators in the PFDI in terms of the coordinates $\underline{u}$ and solves for solutions satisfying the indicial equations of the transformed PFDI. Oftentimes, one considers solutions in a neighbourhood of the intersection of $m = h^{n-1,1} = \dim \mathcal{M}_{\text{c.s.}}$ discriminant factors Δ_i. As discussed in section 4.1, one must ensure that these singular loci have normal intersection, since, otherwise, one might not be able to express all solutions in terms of (logarithmic) power series as in eq. (4.4.4). If the regions of convergence of two solutions do not intersect, one must choose points between them to form a chain of such regions that intersect. Assuming that solutions $\underline{\varpi}$ and $\underline{\widetilde{\varpi}}$ at the points $\underline{z} = 0$ and $\underline{u} = 0$ have overlapping regions of convergence, there are two ways to obtain the *transition matrix* $T_{\underline{z},\underline{u}}$ satisfying

$$\underline{\widetilde{\varpi}} = T_{\underline{z},\underline{u}}\underline{\varpi} \tag{4.4.20}$$

at points where both solutions converge: one can either evaluate the period matrices[7] of the solutions at a single point in the intersection or demand that eq. (4.4.20) holds at b_n points in the intersection. We note that, away from the MUM point, there does not exist a prescription of the local period matrix and one needs to carefully choose linear independent derivatives of the solution vector. For this reason, we used exclusively the latter method of evaluating the solutions at different points. Due to the finite precision of the solutions, it is important to pick points that are sufficiently close to each other. For an application to two-parameter three-folds, see [17, 95], and for a similar study of a four-fold, see [1].

The computation of periods and the description of the complex-structure moduli space simplify immensely in the one-parameter case with $h_{n-1,1} = 1$. There, the Picard–Fuchs ideal is generated by a single operator in the modulus z. For dimensions $n > 3$, it is possible that not all classes in the middle homology are one-dimensional. In the terminology we will introduce in section 5.1, these are said to have degenerate Frobenius algebra. In contrast to the non-degenerate case with $h_{n-p,p} = 1$, $0 \leq p \leq n$, where the differential operator is always of order $n + 1$, the degenerate cases have higher-order operators. Besides the $n + 1$ solutions of the indicial equation at $\alpha = 0$, there are further solutions with different indicials. In [96], the authors constructed four-fold families with Hodge structure $(1, 1, 2, 1, 1)$ and showed that the Picard–Fuchs operator is of order six (instead of five). Next to the five periods with indicial zero, there is another power series solution with indicial one. We expect that similar families exist in higher dimensions.

[7] These period matrices for a local solution $\underline{\varpi}$ are generalisations of the Wronskian of the one-parameter case. To obtain b_n independent solutions, in general, one must let specific linear combinations of derivatives act on the solution vector. We will discuss this further in section 5.6.

Non-degenerate one-parameter families are a vast field of study by themselves. For three-folds, the term Calabi–Yau operator was coined in the article [97], which allows for a natural generalisation to higher dimensions. The defining properties are motivated by those that are known to have a geometric realisation. An irreducible operator

$$\mathcal{L}^{(n+1)}(z) = \sum_{r=0}^{n+1} p_r(z)\partial_z^r \in \mathbb{Z}[z, \partial_z]\,, \tag{4.4.21}$$

is a Calabi–Yau operator, if it

- is of Fuchian type,
- is essentially self-adjoint,
- has at least one MUM point,
- has integral coefficients in the fundamental period $\varpi(z) = 1 + \mathcal{O}(z)$ and the coordinate $q(z) = e^{2\pi\mathrm{i}\,t(z)}$
- and has integral instanton numbers.

Let us explain what each of these points means: the singularities of the operator are the zeros of p_{n+1}. An operator is Fuchsian [98], if all singularities z_0 are regular, meaning that the orders of the poles satisfy $\mathrm{ord}_{z_0}(p_r/p_{n+1}) \leq n + 1 - r$. The adjoint of an operator is w.r.t. the standard inner product $\langle f, g\rangle = \int fg\,\mathrm{d}z$ and given by

$$\mathcal{L}^{(n+1)\vee}(z) = \sum_{i=0}^{n+1}(-\partial_z)^i a_i(z)\,. \tag{4.4.22}$$

An operator is essentially self-adjoint, if there exists a function $\alpha(z)$ with which

$$\mathcal{L}^{(n+1)}\alpha f(z) = (-1)^{n+1}\alpha\mathcal{L}^{(n+1)\vee} f(z) \tag{4.4.23}$$

holds for all sufficiently differentiable functions $f(z)$. Let us normalise the operator such that $p_{n+1} = 1$. Then, we can compare the coefficients of $\partial_z^n f(z)$ on both sides of eq. (4.4.23), yielding

$$\alpha'(z) = -\frac{2}{n+1}p_n(z)\,\alpha(z)\,. \tag{4.4.24}$$

In general, the solution $\alpha(z)$ is an algebraic function. Oftentimes, roots indicate an unsuitable Kähler gauge or that the differential system is defined over a branched cover of $\mathbb{P}^1$. In section 4.5, we will see that the Yukawa couplings of one-parameter families satisfy the same differential equation and we can therefore identify $\alpha(z)$ (up to a constant normalisation) with the n-point coupling $C_{z\ldots z}$. Above integrality conditions concern the coefficients of $\varpi_0(z)$ and the exponentiated mirror map $q = \exp 2\pi\mathrm{i}t$ (see (4.3.8)) as a power series around $z = 0$ and the instanton numbers. We postpone a discussion of the latter to section 4.5. In short, the coupling $C_{z\ldots z}$ expressed in terms of the mirror coordinate t (or q) obtains exponential (or power series) corrections, whose coefficients (after a re-summation) are identified with curve-counting invariants, called instanton numbers. Integrality of $\varpi(z)$ and the instanton numbers presume a suitable normalisation of z and of α, respectively.

A prominent database for Calabi–Yau three-fold operators was created by the authors of [99, 100, 101] and can currently be accessed at [102]. It is customary to express the operator in logarithmic derivatives $\theta = z\partial_z$ and normalise to be of the form $\mathcal{L}^{(n+1)}(z) = \theta^{n+1} + \mathcal{O}(z)$. The singularities z_i are given by the poles of $\alpha(z)$ together with a possible singularity at infinity. These, together with their indicials, are summarised in the Riemann symbol, which we write as

$$\mathcal{P}_{\mathcal{L}^{(n+1)}} \left\{ \begin{array}{cccc} 0 & z_1 & \cdots & \infty \\ \hline 0 & \alpha_1 & \cdots & \cdots \\ \vdots & \vdots & \cdots & \cdots \\ 0 & \alpha_{n+1} & \cdots & \cdots \end{array} , \; z \right\} . \tag{4.4.25}$$

Much of the local structure can be read off from this expression. The indicials indicate special points such as MUM-, conifold-, K- and orbifold points. While the first three all have logarithmic divergences and thus infinite order monodromies, orbifold points are characterised by having finite order monodromies, whose exact order can be read off from the indicials.

4.5 Yukawa couplings

In the analysis of Calabi–Yau operators in section 4.4, we encountered a function $\alpha(z)$ which we claimed is related to an n-point coupling $C_{z\ldots z}$. There are in fact four different couplings that, in the context of heterotic string theory, correspond to the Yukawa couplings between massless fields transforming in certain representations of the gauge group. For a review on heterotic string theory and its effective theory, see e.g. [44, 93]. When compactifying heterotic $E_8 \times E_8$ string theory on a Calabi–Yau three-fold, one needs to embed the spin connection SU(3) in this gauge group. In this process, one of the E_8 is broken to

$$E_8 \longrightarrow \mathrm{SU}(3) \times E_6 \,, \tag{4.5.1}$$

where E_6 is the commutant with SU(3) inside E_8. The matter content in the four-dimensional theory descends from the adjoint representation **248** of E_8, which splits under the symmetry breaking (4.5.1) as

$$\mathbf{248} \longrightarrow (\mathbf{3}, \mathbf{27}) + (\overline{\mathbf{3}}, \overline{\mathbf{27}}) + (\mathbf{1}, \mathbf{78}) + (\mathbf{8}, \mathbf{1}) \,. \tag{4.5.2}$$

The four-dimensional field content arranges itself—among others—into $h^{2,1}$ and $h^{1,1}$ charged chiral multiplets transforming in the **27** and $\overline{\mathbf{27}}$ representation, respectively. There are also $b^1(X, \mathrm{End}(TX))$ neutral chiral multiplets in the singlet **1** of the E_6 part of the gauge group. These fields can interact via four E_6-invariant triple couplings, also called *Yukawa couplings*, given by $\langle \mathbf{27^3} \rangle$, $\langle \overline{\mathbf{27}}^{\mathbf{3}} \rangle$, $\langle \mathbf{1^3} \rangle$ and $\langle \mathbf{27}\, \overline{\mathbf{27}}\, \mathbf{1} \rangle$, where the first two utilise the fully symmetric invariant χ_{ijk} of E_6. In this work we will only be concerned with these first two.

The $h^{2,1}$ chiral superfields in the effective theory transforming in **27** are described by the cohomology classes $u^{(i)} \in H^1(X, TX) \cong H^{2,1}(X)$. To express their Yukawa couplings $\langle \mathbf{27^3} \rangle$ explicitly, recall that

$$H^{n-1,p}(X) \cong H^{0,p}(X, TX) \tag{4.5.3}$$

and, with $p = 1$ for $n = 3$, we write $u^{(i)} = u^{(i)}_{\bar{l}} \partial_i \mathrm{d}\bar{x}^{\bar{l}}$. The isomorphism eq. (4.5.3) consists of contracting these elements with $\Omega \in H^{3,0}(X)$ to obtain $u^{(i)}_{\bar{l}} \Omega_{ist} \mathrm{d}\bar{x}^{\bar{l}} \wedge \mathrm{d}x^s \wedge \mathrm{d}x^t \in H^{2,1}(X)$. Their

Yukawa coupling is thus given by

$$\langle \mathcal{O}_i \mathcal{O}_j \mathcal{O}_k \rangle_{\langle \mathbf{27^3} \rangle} = \int_X u_{\bar{l}}^{(i)} u_{\bar{p}}^{(j)} u_{\bar{q}}^{(k)} \Omega_{ijk} \Omega_{rst} \mathrm{d}x^r \wedge \mathrm{d}x^s \wedge \mathrm{d}x^t \wedge \mathrm{d}\bar{x}^{\bar{l}} \wedge \mathrm{d}\bar{x}^{\bar{p}} \wedge \mathrm{d}\bar{x}^{\bar{q}}, \tag{4.5.4}$$

which one can rewrite using the Kodaira–Spencer map as

$$\langle \mathcal{O}_i \mathcal{O}_j \mathcal{O}_k \rangle_{\langle \mathbf{27^3} \rangle} = \int_X \partial_i \partial_j \partial_k \Omega \wedge \Omega \,. \tag{4.5.5}$$

Importantly, this coupling is exact and can be computed explicitly.

The $h^{1,1}$ chiral multiplets in the $\overline{\mathbf{27}}$ representation correspond, on the other hand, to the elements $J^{(i)} \in H^1(X, T^*X) \cong H^{1,1}(X)$ and give rise to couplings

$$\langle \mathcal{O}_i \mathcal{O}_j \mathcal{O}_k \rangle_{\langle \overline{\mathbf{27}}^{\mathbf{3}} \rangle} = \int_X J^{(i)} \wedge J^{(j)} \wedge J^{(k)} + \text{ instanton corrections}\,, \tag{4.5.6}$$

where the constant term is given by the classical intersection numbers c_{ijk} and the instanton corrections are of the form $\mathcal{O}(e^{2\pi \mathrm{i}\, \underline{t}})$ in the complexified Kähler parameters $\underline{t}$. The computation of the instanton corrections is extremely involved—unless one exploits mirror symmetry, which, in the context of heterotic compactifications exchanges the representations $\overline{\mathbf{27}}$ and $\mathbf{27}$. If we make the compactification explicit in the notation for the couplings, this implies

$$\langle \mathcal{O}_i \mathcal{O}_j \mathcal{O}_k \rangle^{(X)}_{\langle \overline{\mathbf{27}}^{\mathbf{3}} \rangle} = \langle \mathcal{O}_i \mathcal{O}_j \mathcal{O}_k \rangle^{(\hat{X})}_{\langle \mathbf{27^3} \rangle}. \tag{4.5.7}$$

As a first computational confirmation of mirror symmetry, the authors of [4] considered the heterotic string on the quintic three-fold $X \subset \mathbb{P}^4$. Recall that this family has one Kähler modulus and 101 complex-structure moduli. They computed the instanton corrections for the Yukawa coupling $\langle \mathcal{O}_i \mathcal{O}_j \mathcal{O}_k \rangle_{\langle \overline{\mathbf{27}}^{\mathbf{3}} \rangle}$ by evaluating eq. (4.5.5) on the mirror $\hat{X}$ as a function of the one complex-structure modulus z and expressing it in the mirror coordinate $t \sim \log z$, see eq. (4.3.8). To see how this works, we will first derive the aforementioned equality between $\alpha(z)$ and $\langle \mathbf{27^3} \rangle$ on the mirror quintic. As the most prominent Calabi–Yau families have few Kähler moduli and many complex-structure moduli, one usually considers only the sector $\overline{\mathbf{27}}$ on X, which is equivalent under mirror symmetry to $\mathbf{27}$ on $\hat{X}$. We therefore introduce the notation

$$C_{z^i z^j z^k} = \int_{\hat{X}} \partial_{z^i} \partial_{z^j} \partial_{z^k} \Omega \wedge \Omega \,. \tag{4.5.8}$$

The quintic mirror has a PFDI generated by the operator

$$\mathcal{L}^{(4)}(z) = \theta^4 - 5z \prod_{i=1}^{4} (5\theta + i) \,. \tag{4.5.9}$$

Following section 4.4, we normalise this operator such that its fourth derivative has coefficient one

$$\widetilde{\mathcal{L}}^{(4)}(z) = \partial_z^4 + p_3(z) \partial^3 + \dots \,, \tag{4.5.10}$$

where, here, $p_3(z) = \frac{6 - 8 \cdot 5^5 z}{z(1 - 5^5 z)}$. As we can expand Ω in terms of the periods, which are annihiliated by this differential operator, we deduce

$$0 = \int_{\hat{X}} \widetilde{\mathcal{L}}^{(4)} \Omega \wedge \Omega = \int_{\hat{X}} \partial_z^4 \Omega \wedge \Omega + p_3 C_{zzz} = 2 \partial_z C_{zzz} + p_3 C_{zzz} \,, \tag{4.5.11}$$

where we used the identity (cf. Appendix A.2 of [1])

$$\partial_{(i_0} C_{i_1 \dots i_n)} = \frac{2}{n+1} C_{i_0 i_1, \dots i_n} \,. \tag{4.5.12}$$

Equation (4.5.11) is the same differential equation we obtained in eq. (4.4.24), showing that $\alpha(z)$ from section 4.4 is, up to a constant factor, identical to the coupling C_{zzz}. Here, this fixes the Yukawa coupling up to a constant number c to

$$C_{zzz} = \frac{c}{z^3(1-5^5 z)} \,. \tag{4.5.13}$$

Computing the holomorphic and single-logarithmic solution to $\mathcal{L}^{(4)}$, one obtains the mirror map

$$2\pi \mathrm{i} t = \log z + 770 z + 717825 z^2 + \frac{3225308000}{3} z^3 + \mathcal{O}\big(z^4\big) \,, \tag{4.5.14}$$

$$z = q - 770 q^2 + 171525 q^3 - 81623000 q^4 + \mathcal{O}\big(q^5\big) \,, \quad q = e^{2\pi \mathrm{i} t}. \tag{4.5.15}$$

For the identification of the couplings, it is important to note that both $\langle \overline{\mathbf{27}}^{\mathbf{3}} \rangle$ and $\langle \mathbf{27}^{\mathbf{3}} \rangle$ transform as components of a symmetric rank-three tensor. Furthermore, Ω is expanded in homogeneous coordinates for the moduli space, while the coupling $\langle \overline{\mathbf{27}}^{\mathbf{3}} \rangle$ is expressed in the inhomogeneous Kähler coordinates $\underline{t}$. It follows that we must divide the coupling $C_{z^i z^j z^k}$ by the square of the fundamental period. Writing

$$C_{ijk} \equiv C_{t_i t_j t_k} = \int_X J_i \wedge J_j \wedge J_k + \text{ instanton corrections} \tag{4.5.16}$$

with J_i the Kähler cone generators, the Yukawa coupling $\langle \overline{\mathbf{27}}^{\mathbf{3}} \rangle$ is obtained via

$$C_{ijk} = \frac{1}{\varpi_0^2} \frac{\partial z^r}{\partial t^i} \frac{\partial z^s}{\partial t^j} \frac{\partial z^t}{\partial t^k} C_{z^r z^s z^t} \,. \tag{4.5.17}$$

In the case of the quintic, one obtains the expression

$$C_{111} = 5 + 2875 q + 4876875 q^2 + 8564575000 q^3 + 15517926796875 q^4 + \mathcal{O}\big(q^5\big) \,, \tag{4.5.18}$$

where we used $c = 5$ in eq. (4.5.13) to identify the leading order term with the classical intersection number $\int_X H^3 = 5$ on the quintic. The instanton corrections stem from rational curve classes and we can express the couplings as [103]

$$C_{ijk} = c_{ijk} + \sum_{\underline{l} > 0} \frac{n_{\underline{l}} l_i l_j l_k}{1 - \underline{q}^{\underline{l}}} \underline{q}^{\underline{l}} \,, \tag{4.5.19}$$

where $n_{\underline{l}}$ are called the genus-zero instanton numbers of degree $\underline{l}$, which count the number of holomorphic curves of degree $\underline{l}$ in X. While only conjectured and not proven at the time, the numbers of such curves on the quintic three-fold, where computed in [4] to be

$$n_1 = 2875 \,, \quad n_2 = 609250 \,, \quad n_3 = 317206375 \,, \dots \,. \tag{4.5.20}$$

By considering the higher genus amplitudes, one can also compute the analogues of $n_{\underline{l}}$, which then count holomorphic maps from genus g surfaces into X.

For multi-parameter models, the computation of the couplings $C_{z^i z^j z^k}$ is done by solving a system of differential equations similar to the one-parameter case we saw in section 4.4 [16]. Writing the generators of the PFDI as

$$\mathcal{L}_i(\underline{z}) = \sum_{\underline{r}} p_i^{(\underline{r})}(\underline{z})\partial^{\underline{r}}\,, \tag{4.5.21}$$

one obtains the following linear relations among the couplings

$$0 = \sum_{\underline{r}} p_i^{(\underline{r})}(\underline{z}) C_{\underline{z}_{\underline{r}}}(\underline{z})\,. \tag{4.5.22}$$

Together with eq. (4.5.12) and further relations from operators of the form $\partial_z \mathcal{L}_i$, one can solve this system of equations for the triple couplings $C_{z_i z_j z_k}$. If one has already computed an integral basis for the periods at the MUM point—using e.g. the topological data from the mirror (cf. section 5.3)—the series expansion of C_{ijk} in terms of the mirror coordinates $\underline{t}$ can be obtained directly by using $\underline{t}$ as coordinates for the complex-structure moduli space in eq. (4.5.8). Expanding Ω in terms of the periods $\underline{\Pi}(t)$ (where we now divided $\underline{\Pi}$ by ϖ_0 to obtain inhomogeneous coordinates), one finds

$$C_{ijk} = \partial_{t^i}\partial_{t^j}\partial_{t^k}\underline{\Pi}^T \Sigma\, \underline{\Pi}\,. \tag{4.5.23}$$

Except for the re-summation and identification in terms of instanton numbers, all these methods carry over to n-point couplings in higher-dimensional mirror pairs [104], where the above generalises to

$$C_{i_1 \dots i_n} = \partial_{i_1} \dots \partial_{i_n} \underline{\Pi}^T \Sigma\, \underline{\Pi}\,. \tag{4.5.24}$$

As expected from results of conformal field theory, all higher couplings can be expressed in terms of triple couplings. The three-point couplings on compactifications in dimensions $n > 3$ are more subtle and require us to introduce the CY-Frobenius algebra (cf. section 5.1).

In section 4.1, we explained that the family has singular fibres that lie over certain loci in the complex-structure moduli space. The singular points are given by the vanishing locus of the discriminant Δ (not to be confused with the polytope in the toric construction). The factors Δ_i in Δ correspond to different components of the set of singularities. In section 4.4, we identified the singular points of the differential system as the poles of the Yukawa coupling $\alpha(z) = C_{zzz}$. In the multi-parameter cases, the Yukawa couplings $C_{z^i z^j z^k}$ again become singular along these loci.

4.6 Conventional period geometry for ($n \leq 3$)-folds

Before discussing more involved methods necessary for the description of the period geometry of Calabi–Yau manifolds of dimension $n \geq 4$, this section reviews the known methods for the analysis of elliptic curves, K3 surfaces and Calabi–Yau three-folds.

Elliptic curves

The simplest example of compact Calabi–Yau manifolds is given by elliptic curves, which are complex one-dimensional and therefore have the following Hodge diamond

$$\begin{array}{ccc} & 1 & \\ 1 & & 1 \\ & 1 & \end{array} \tag{4.6.1}$$

They are useful to introduce the concepts of complex-structure variations, periods and Hodge decomposition, which we will extend to higher-dimensional manifolds with a richer structure in the following subsections.

For the middle homology of rank two, we introduce a symplectic basis (A, B) with intersection form[8]

$$\Sigma = -\hat{\Sigma} = \begin{pmatrix} 0 & -1 \\ 1 & 0 \end{pmatrix}, \tag{4.6.2}$$

meaning $A \cap B = -B \cap A = 1$. The dual basis (α, β) satisfies $\int_A \alpha = \int_B \beta = 1$ while the other pairings vanish. The holomorphic $(1,0)$-form Ω then yields the periods $\underline{\Pi} = (\int_A \Omega, \int_B \Omega)$. To find an explicit expression for these periods in terms of the complex-structure moduli, let us return to the example of the hypersurface in the toric space described by the polytope Δ in section 2.2 with

$$\Delta = \text{convex hull}\big((1,0),(0,1),(-1,-1),(0,-1)\big)\,, \tag{2.2.2}$$

$$\Delta^\circ = \text{convex hull}\big((0,1),(2,-1),(-1,-1),(-1,1)\big)\,. \tag{4.6.3}$$

The sections of the anti-canonical bundle are given by the points of the dual polytope Δ° that are not in the interior of facets

$$\begin{aligned} P_\Delta &= a_0 + a_1 t_2 + a_2 \frac{t_1^2}{t_2} + a_3 \frac{1}{t_1 t_2} + a_4 \frac{t_2}{t_1} \\ &= a_0 x_1 x_2 x_3 x_4 + a_1 x_1 x_2^2 + a_2 x_1^3 x_4^2 + a_3 x_3^3 x_4^2 + a_4 x_2^2 x_3\,, \end{aligned} \tag{4.6.4}$$

where we expressed P_Δ first in the affine and then in homogeneous coordinates of $\mathbb{P}_\Delta$. With the techniques of section 2.2 and the help of SAGEMATH, we obtain the Mori cone generators

$$l^{(1)} = (-2; -1, 1, 0, 2)\,, \tag{4.6.5}$$

$$l^{(2)} = (-2; 2, 0, 1, -1)\,. \tag{4.6.6}$$

To compute the fundamental period (4.4.9) in terms of the Batyrev coordinates (4.4.8), we can either perform the integral directly (as we have done in section 4.4) or use the closed form given in eq. (4.4.19)

$$\varpi_0 = 1 + 24 z^1 z^2 + 60 z^1 (z^2)^2 + 60 (z^1)^2 z^2 + 2520 (z^1)^2 (z^2)^2 + \mathcal{O}(\underline{z}^5)\,. \tag{4.6.7}$$

As expected from the l-vectors, the solutions are symmetric in the Batyrev coordinates. With this period, we can search for operators in the PFDI.

In section 4.4, we mentioned a rule of thumb for the numbers of operators we expect at each order; this seems like a good place to give an example: As shown in Table 4.1, the Frobenius structure of a two-parameter system has $k+1$ solutions at order k. To obtain a Hodge structure of $(1,1)$, we expect one operator of order one and one of order two.

[8] This intersection form is the negative of the general formula we propose in section 5.3. This is because two conditions are contradicting for elliptic curves: Either one can have that the asymptotic period vector is of the form $(1, t)$, or that the sign of the intersection form is as in eq. (5.3.15). The convention used here is more prominent in the literature.

logarithmic order	0	1	2
n.o. solution	1	2	3
$\mathcal{L}^{(1)}$	–	-1	-2
$\mathcal{L}^{(2)}$	–	–	-1
Hodge numbers	1	1	0

Table 4.1: Estimate for the PFDI of a two-parameter elliptic curve family. One concludes that one operator of order one and one of order two generically restrict the solution space to the Hodge structure of the elliptic curve.

In this specific example, we indeed find the operators

$$\begin{aligned}\mathcal{L}^{(1)}(\underline{z}) &= \theta_1 - \theta_2 + \left(z^1 + 2z^2\right)\theta_1 - \left(2z^1 + z^2\right)\theta_2 + 54 z^1 z^2 \left(\theta_2 - \theta_1\right) \\ &\quad - 36 z^1 z^2 \left(z^1 - z^2\right)\left(2\theta_1 + 2\theta_2 + 1\right), \end{aligned} \tag{4.6.8}$$

$$\begin{aligned}\mathcal{L}^{(2)}(\underline{z}) &= \left(\theta_1 - \theta_2\right)\left(\theta_1 + \theta_2 - 1\right) \\ &\quad + z^1\left(\theta_1 + 4\theta_2\right)\left(\theta_1 - 2\theta_2\right) + z^2\left(2\theta_1 - \theta_2\right)\left(4\theta_1 + \theta_2\right). \end{aligned} \tag{4.6.9}$$

There is only one logarithmic solution (and especially no higher logarithmic solution) given by

$$\varpi_1 = \left(\log z^1 + \log z^2\right)\varpi_0 + z^1 + z^2 - \frac{(z^1)^2}{2} + 104 z^1 z^2 - \frac{(z^2)^2}{2} + \mathcal{O}\left(\underline{z}^3\right). \tag{4.6.10}$$

We note that, while there exist two Batyrev coordinates, there is only one complex-structure modulus $t = \int_B \Omega / \int_A \Omega$, which is parametrised redundantly by z^1 and z^2. The integral basis of an elliptic curve family has leading order

$$\underline{\Pi}(t) = \varpi_0(t) \begin{pmatrix} 1 \\ t \end{pmatrix}. \tag{4.6.11}$$

In the limit $z^i \to 0$, one identifies $2\pi\mathrm{i}\, t$ with the expression $\log z^1 + \log z^2$ multiplying the fundamental period, yielding

$$\underline{\Pi} = \begin{pmatrix} \int_B \Omega \\ \int_A \Omega \end{pmatrix} = \begin{pmatrix} \varpi_0 \\ \frac{\varpi_1}{2\pi\mathrm{i}} \end{pmatrix}. \tag{4.6.12}$$

This allows us to express the complex-structure parameter in terms of Batyrev coordinates

$$t = \log z^1 + \log z^2 + z^1 + z^2 - \frac{(z^1)^2}{2} + 104 z^2 z^1 - \frac{(z^2)^2}{2} + \mathcal{O}\left(\underline{z}^3\right). \tag{4.6.13}$$

In the conventions we use, the Hodge–Riemann bilinear (4.1.15) and the non-trivial Griffiths transversality condition (4.2.15) take the form

$$0 < \mathrm{i}\underline{\Pi}^\dagger \Sigma\, \underline{\Pi} = 2\mathrm{Im} t\,, \tag{4.6.14}$$

$$1 = \partial_t \underline{\Pi}^T \Sigma\, \underline{\Pi}\,. \tag{4.6.15}$$

For Griffiths transversality, we used/concluded that $C_t = 1$. We emphasise that the identification of the mirror coordinate t is fundamentally different in the higher-dimensional cases. There, all single-logarithmic solutions (divided by the fundamental period) give independent coordinates

t_i for the complexified Kähler moduli space of the mirror. It is only for the elliptic curve[9] that the space of single-logarithmic solutions is restricted and a special linear combination is identified with the mirror coordinate.

K3 surfaces

Going one dimension higher, we reach the complex two-dimensional K3 surfaces. The three K represent the mathematicians Kummer, Kähler and Kodaira and the name is a reference to the mountain K2. The Hodge diamond for these manifolds is given by

$$\begin{array}{ccccc} & & 1 & & \\ & 0 & & 0 & \\ 1 & & 20 & & 1 \\ & 0 & & 0 & \\ & & 1 & & \end{array} \tag{4.6.16}$$

and the dimension of the middle homology is $b_2 = 22$. An important concept in the study of K3 surfaces is the Picard lattice given by the elements in the integral cohomology that are purely of Hodge-type $(1,1)$

$$\text{Pic}(X) = H^{1,1}(X) \cap H^2(X,\mathbb{Z})\,. \tag{4.6.17}$$

The rank of this lattice is called the Picard number $\rho(X) := \text{rk}(\text{Pic}(X))$. It gives the dimension of the vector space in which the Kähler cone is embedded. The orthogonal complement in $H^2(X,\mathbb{Z})$ is called the transcendental lattice

$$T(X) = \text{Pic}(X)^\perp\,. \tag{4.6.18}$$

For us, the most important thing is that, by Poincaré duality, the classes in the Picard lattice give rise to vanishing periods, as the wedge product with Ω gives a form in $H^{3,1}(X)$ which is zero for a K3. The Picard lattice and thus its rank depends on the specific manifold of the family. As we move around in the moduli space, integral linear combinations of the periods may vanish, indicating an increment of the Picard number. This is the same mechanism that we will study for three- and four-folds to identify flux vacua in type II string theory and F-theory, respectively. Mirror symmetry for K3 families exchanges the Picard lattice with with its orthogonal complement in $H^{1,1}(X)$. It follows that the Picard number of the mirror is $\rho(\hat{X}) = 20 - \rho(X)$.

Let us consider an example: One of the most prominent families is given by the quartic hypersurfaces in $\mathbb{P}^3$. This ambient space is described by the polytope with vertices e_i, $1 \leq 1 \leq 3$ and $(-1,-1,-1)$. By the methods of section 2.2, we find a single Mori cone generator

$$l^{(1)} = (-4;1,1,1,1) \tag{4.6.19}$$

and thus deduce that, generically, $\rho(X) = 1$. For the mirror, this implies that the transcendental lattice has the Hodge structure $(1,1,1)$ and we expect three independent periods of $\Omega(z)$. Following section 4.4, we obtain the fundamental period in the Batyrev coordinate

$$\varpi_0(z) = 1 + 24z + 2520z^2 + 369600z^3 + 63063000z^4 + \mathcal{O}(z^5)\,. \tag{4.6.20}$$

[9]This assumes that the coordinates z^i parametrise the moduli space faithfully. If e.g. points inside facets are included in the toric description of the anti-canonical bundle, such a restriction is also necessary for higher-dimensional families, see the paragraph at the end of section 2.3.

This period restricts the Picard–Fuchs ideal to be generated by the third-order operator

$$\mathcal{L}^{(3)}(z) = \theta^3 - 4z\prod_{i=1}^{3}(4\theta + i)\,. \tag{4.6.21}$$

The full local solution consists also of a single- and a double-logarithmic solution. A period basis over an integral lattice in homology is obtained by identifying $\log(z^i) \sim 2\pi\mathrm{i}\, t_i$ in the limit $z^i \to 0$ and the leading order behaviour

$$\underline{\Pi}(\underline{t}) = \varpi_0(\underline{t}) \begin{pmatrix} 1 \\ \underline{t} \\ \frac{1}{2}c_{ij}t^i t^j \end{pmatrix}, \tag{4.6.22}$$

where $c_{ij} = \int_X J_i \wedge J_j$ are the classical intersection numbers of the Kähler cone generators J_i. An important difference between elliptic curves and K3 surfaces on one side and the higher-dimensional families on the other is that the expression in eqs. (4.6.11) and (4.6.22) are exact, i.e. they do not obtain corrections in $\mathcal{O}\left(e^{2\pi\mathrm{i}\underline{t}}\right)$. This basis in homology implies the intersection form in cohomology[10]

$$\Sigma = \begin{pmatrix} & & 1 \\ & -c_{ij} & \\ 1 & & \end{pmatrix}. \tag{4.6.23}$$

The Hodge–Riemann bilinear relation restricts the moduli $\underline{t}$ to satisfy

$$0 < \underline{\Pi}^\dagger \Sigma\, \underline{\Pi} = 2c_{ij}\mathrm{Im}t^i\, \mathrm{Im}t^j\,. \tag{4.6.24}$$

The first two relations from Griffiths transversality (4.2.15) are satisfied trivially with eqs. (4.6.22) and (4.6.23). Due to the exactness of eq. (4.6.22), the third relation

$$\partial_{t^i}\partial_{t^j}\underline{\Pi}^T \Sigma\, \underline{\Pi} = C_{ij} = c_{ij}\,, \tag{4.6.25}$$

holds without corrections, which we expressed by $C_{ij} = c_{ij}$. Recall from section 4.5 that the couplings without a reference to the variables are in the mirror coordinates $\underline{t}$ and that c denote the classical intersection numbers and thus the constant term in the n-point couplings C.

In the example of the quartic, there is only one Kähler cone generator and, following section 2.2, we find $c_{11} = 4$. This allows us to express the period vector in the Batyrev coordinate

$$\underline{\Pi}(z) = \begin{pmatrix} 1 & 0 & 0 \\ 0 & -\frac{\mathrm{i}}{2\pi} & 0 \\ 0 & 0 & -\frac{1}{\pi^2} \end{pmatrix} \begin{pmatrix} \varpi_0(z) \\ \log(z)\varpi_0(z) + \sigma_1(z) \\ \frac{1}{2}\log(z)^2\varpi_0(z) + \log(z)\sigma_1(z) + \sigma_2(z) \end{pmatrix}, \tag{4.6.26}$$

where the vector is our local solution to $\mathcal{L}^{(4)}(z)$ and the matrix was obtained by the above identification. Such a matrix transforming a local basis into an integral one is called *transition matrix*. Here, $\sigma_i(z)$ are formal power series given by

$$\sigma_1(z) = 104z + 12276z^2 + \frac{5632160}{3}z^3 + 327270650z^4 + \mathcal{O}\left(z^5\right), \tag{4.6.27}$$

$$\sigma_2(z) = 5408z^2 + 1146912z^3 + \frac{688332760}{3}z^4 + \mathcal{O}\left(z^5\right). \tag{4.6.28}$$

[10] As for the elliptic curve, the conventions of section 5.3 are incompatible with this intersection form. To guarantee the period structure of eq. (4.6.22), we must use a basis of sheaves that generally has non-integer HRR pairing Σ^{-1}.

To describe the periods globally, we deduce its singular points from the denominator of the Yukawa coupling given by the solution to the differential equation (4.5.11)

$$C_{zz}(z) = \frac{4}{z^2(1-256z)}\,. \tag{4.6.29}$$

The normalisation (which is irrelevant for the following) can be obtained by demanding that the coupling in the mirror coordinate has the classical intersection number as the constant term $C_{tt}(t) = 4 + \mathcal{O}(q)$. Here, we are only interested in the poles of this function, i.e. $z_0 = 0$ and $z_1 = 1/256$. We express the differential operator in the coordinate $u_1 = z - z_1$ to solve for the indicials at z_1. The function C_{zz} does not give us any information about the behaviour at infinity. Therefore, we must always express the operator in the variable $u_\infty = 1/z$ (where $\theta_\infty = -\theta$)) and verify whether the indicials make it a singular point. In general, a point is singular point if and only if it has indicials that are not integral and/or not all different. Both conditions imply that the monodromy transformation is non-trivial. Here, the Riemann symbol reads

$$\mathcal{P}_{\mathcal{L}^{(3)}}\left\{\begin{array}{cccc} 0 & 1/256 & \infty & \\ \hline 0 & 0 & \frac{1}{4} & \\ 0 & \frac{1}{2} & \frac{1}{2} & , \; z \\ 0 & 1 & \frac{3}{4} & \end{array}\right\}. \tag{4.6.30}$$

As explained in section 4.4, we express the operator $\mathcal{L}^{(4)}(z)$ in coordinates around the other two singularities and obtain local solutions with the indicials as in eq. (4.6.30). Then, we perform an analytical continuation of $\underline{\Pi}(z)$ to these points. The monodromy transformations are computed to be

$$M_0 = \begin{pmatrix} 1 & 0 & 0 \\ 1 & 1 & 0 \\ 2 & 4 & 1 \end{pmatrix},\; M_{1/256} = \begin{pmatrix} 0 & 0 & -1 \\ 0 & 1 & 0 \\ -1 & 0 & 0 \end{pmatrix},\; M_\infty = \begin{pmatrix} -2 & 4 & -1 \\ -1 & 1 & 0 \\ -1 & 0 & 0 \end{pmatrix}. \tag{4.6.31}$$

These obey $M_0 M_{1/256} M_\infty = \mathbb{1}$, which is expected since a path encircling all singularities contains, when seen from the other "hemisphere" of the $\mathbb{P}^1$, no singularities at all and is thus trivial.

At the beginning of this subsection, we mentioned that the Picard number can increase for special fibres of the family. Furthermore, smooth fibres with $\rho = 20$ are called attractive. The K3 surfaces over the two singularities $z_1 = 1/256$ and $z_2 = \infty$ are examples of this phenomenon. Importantly, the fibre at z_1 is singular and technically not attractive by definition. It reflects, however, the structure of integral linear combinations of period values and we therefore mention it on an equal footing. The singularity of the differential operator at infinity is due to a quartic covering in the Batyrev coordinate and corresponds to a smooth fibre instead. Either by the methods of section 6.1 or the explicit expression of $\Pi(z_i)$, $1 \leq i \leq 2$, we find that there exist integral vectors f_i with $f_i \,\Sigma\, \Pi(z_i) = 0$. The former tells us that the monodromy representations both contains a one-dimensional representation with eigenvalue -1. These periods then must vanish at the singularity. From the explicit monodromy representations in eq. (4.6.31) or from the kernel of $\Sigma\,\Pi(z_i)$, we identify

$$f_1 = \begin{pmatrix} 1 & 0 & 1 \end{pmatrix}, \quad f_2 = \begin{pmatrix} 2 & 1 & 2 \end{pmatrix}. \tag{4.6.32}$$

We conclude that these special fibres have Picard numbers $\rho(X_{1/256}) = \rho(X_\infty) = 20$. The term attractive is derived from attractor points of three-fold families, which we will discuss in more detail later.

One-parameter K3 families have another interesting property: Their period geometry can be described by the symmetric square of the solutions to a second order Calabi–Yau operator. Denoting the two solution of the second order operator $\mathcal{L}^{(2)}(z)$ by $\varpi^{(2)}(z)$, we find that the three solutions of the K3 operator $\mathcal{L}^{(3)}(z)$ are given by

$$\left(\varpi_0^{(2)}\right)^2, \quad \varpi_0^{(2)}\varpi_1^{(2)}, \quad \left(\varpi_1^{(2)}\right)^2. \tag{4.6.33}$$

One calls $\mathcal{L}^{(3)}(z)$ the symmetric square of $\mathcal{L}^{(2)}(z)$ and writes

$$\mathcal{L}^{(3)} = \mathrm{Sym}^2\left(\mathcal{L}^{(2)}\right). \tag{4.6.34}$$

The origin for this description is the decomposition of the fundamental representation of

$$\mathrm{SO}(2,1)_0 \cong \frac{\mathrm{SL}(2,\mathbb{R})}{\pm\mathbb{1}} \tag{4.6.35}$$

into the symmetric square of the fundamental of $\mathrm{SL}(2,\mathbb{R})$, see e.g. [105]. As not all monodromy transformations of the K3 family are necessarily in the identity component of $\mathrm{SO}(2,1)$, the monodromy transformations of the second order operator are not guaranteed to be real. In general, they lie in a imaginary quadratic field extension of $\mathbb{Q}$.

Let us again consider the degree-four hypersurfaces in $\mathbb{P}^3$. We find that the functions $\varpi_i^{(2)}(z)$ obtained by inverting eq. (4.6.33) are solutions to the Calabi–Yau operator

$$\mathcal{L}^{(2)}(z) = \theta^2 - 4z(1+8\theta)(3+8\theta)\,. \tag{4.6.36}$$

with Riemann symbol

$$\mathcal{P}_{\mathcal{L}^{(2)}}\left\{\begin{array}{ccc|c} 0 & 1/256 & \infty & \\ \hline 0 & 0 & \frac{1}{8} & z \\ 0 & \frac{1}{2} & \frac{3}{8} & \end{array}\right\}. \tag{4.6.37}$$

It follows from the leading order of the K3 periods (4.6.22) that the *integral* basis, in general, cannot be written as a symmetric square of two solutions of a second order operator. However, the local solutions can always be expressed in this way. Treating the operator of eq. (4.6.36) with the methods of the previous subsection, the monodromies are matrices valued in $\mathbb{Q}[\sqrt{-2}]$.

Calabi–Yau Threefold

From many perspectives, three-dimensional families are the most intriguing embodiment of Calabi–Yau manifolds. On one side, this is of course due to their application in the compactification of ten-dimensional string theories to four-dimensional theories. On the other, the increasing complexity—arising from instanton corrections in the periods and the couplings—is balanced out by a rich structure coming from mirror symmetry and Griffiths transversality. As we will discuss in more detail below, the latter ensures the existence of a *prepotential* containing much of the information of the period geometry. The moduli space is said to be *special* Kähler.

Due to complex conjugation and Hodge star duality, the only independent Hodge numbers are $h^{2,1}$ and $h^{1,1}$ and the Hodge diamond has the form

$$\begin{array}{ccccccc} & & & 1 & & & \\ & & 0 & & 0 & & \\ & 0 & & h^{1,1} & & 0 & \\ 1 & & h^{2,1} & & h^{2,1} & & 1 \\ & 0 & & h^{1,1} & & 0 & \\ & & 0 & & 0 & & \\ & & & 1 & & & \end{array} \tag{2.1.14}$$

We have seen in chapter 2 that these two numbers count the number of complex-structure moduli and Kähler moduli in type II compactifications. As in section 4.3, uppercase indices $I, J, K, \ldots \in \{0, \ldots, h^{2,1}\}$ and lowercase indices $i, j, k, \ldots \in \{1, \ldots, h^{2,1}\}$ represent homogeneous and inhomogeneous coordinates for the complex-structure moduli space, respectively. Since the intersection form $\hat{\Sigma}$ is antisymmetric for odd n, one introduces a symplectic basis in the middle homology $\{A^I, B_I\}_I \subset H_3(X, \mathbb{Z})$ and a dual basis $\{\alpha_I, \beta^I\}_I \subset H^3(X, \mathbb{Z})$, satisfying $A^I \cap B_{b_3+1-J} = -B_{b_3+1-J} \cap A^I = -\delta^I_J$ and $\int_{A^I} \alpha_J = \int_{B_J} \beta^I = \delta^I_J$ where all other pairings vanish. In matrix form, the pairing in cohomology is then given by

$$\Sigma = \begin{pmatrix} & & & & & & 1 \\ & & & & & \iddots & \\ & & & & 1 & & \\ & & & -1 & & & \\ & & \iddots & & & & \\ & -1 & & & & & \end{pmatrix}, \tag{4.6.38}$$

The periods consist of so-called A- and B-periods $X^I = \int_{A^I} \Omega$ and $F_I = \int_{B_I} \Omega$ with which the period vector takes the form

$$\underline{\Pi} = \left(X^0, \ldots, X^{h^{2,1}}, F_{h^{2,1}}, \ldots, F_0\right)^T . \tag{4.6.39}$$

In turn, we can express Ω in terms of the periods in the basis dual basis in cohomology

$$\Omega = X^I \alpha_I + F_I \beta^I . \tag{4.6.40}$$

As explained in section 4.3, the periods X^I serve as homogeneous coordinates on the complex-structure moduli space and give rise to the mirror maps t^i. Comparing to the period structure of elliptic curves (4.6.11) and K3 surfaces (4.6.22), the B-periods F_I contain corrections in the form of formal power series in $q = \exp 2\pi \mathrm{i}\, t$. Nevertheless, the asymptotic structure, i.e. the part polynomial in $\underline{t}$, can be obtained from a prepotential. The instanton corrections can then be obtained by matching the asymptotic period vector with the solutions to the Picard–Fuchs differential ideal.

To derive the existence of a prepotential, one considers the relation coming from Griffiths transversality (4.2.15) with $\partial_I = \partial_{X^I}$

$$0 = \langle \Omega | \partial_I \Omega \rangle = \underline{\Pi}^T \Sigma\, \partial_{X^I} \underline{\Pi} = X^J \partial_J F_I - F_J = \partial_I (X^J F_J) - 2F_J . \tag{4.6.41}$$

It follows that the B-periods are given by $F_I = \partial_I F$ with the prepotential

$$F = \frac{1}{2} X^I F_I \,, \tag{4.6.42}$$

which is thus a function of the homogeneous coordinates X^I. To get an expression for the asymptotic behaviour of the periods in terms of the mirror maps, we define the inhomogeneous prepotential

$$\mathcal{F}(\underline{t}) = \frac{F(\underline{X})}{(X^0)^2} \,. \tag{4.6.43}$$

This function allows us to write the period vector as

$$\underline{\Pi} = X^0 \left(1, t^1, \ldots, t^{h^{2,1}}, \partial_{t^{h^{2,1}}}\mathcal{F}, \ldots, \partial_{t^1}\mathcal{F}, 2\mathcal{F} - t^i \partial_i \mathcal{F}\right) . \tag{4.6.44}$$

Homological mirror symmetry gives a prescription of the asymptotic behaviour of the periods (the polynomial structure in $\underline{t}$) via the $\hat{\Gamma}$-class formalism. We will review it in section 5.2 as it is part of a more complex mechanism to describe the integral periods in higher dimensions. Here, the only necessary result is that an integral basis can be given in terms of the topological data of *the mirror* $\hat{X}$:

$$\mathcal{F} = \frac{c_{ijk}}{3!} t^i t^j t^k - \frac{A_{ij}}{2!} t^i t^j - \frac{c_2 \cdot D_i}{24} t^i - \frac{\chi\, \zeta_3}{2(2\pi\mathrm{i})^3} + \mathcal{F}_{\text{inst}}(\underline{q}) \,. \tag{4.6.45}$$

Let us explain what each of these terms means: c_{ijk} are again the classical intersection numbers, the quadratic coefficients are given by

$$A_{ij} = \frac{1}{2} \int_{\hat{X}} i_* c_1(D_i) \wedge J_j = -\frac{1}{2} \int_{\hat{X}} J_i \wedge J_i \wedge J_j \,, \tag{4.6.46}$$

where integer shifts in these numbers correspond to $\mathrm{Sp}(4, \mathbb{Z})$ transformations on the periods. The linear term includes the integers $c_2 \cdot D_i \equiv \int_{\hat{X}} c_2 \wedge J_i$ and χ is the Euler number (again of the mirror $\hat{X}$). We also included a term $\mathcal{F}_{\text{inst}}$ containing the instanton corrections

$$\mathcal{F}_{\text{inst}}(\underline{q}) = \frac{1}{(2\pi\mathrm{i})^3} \sum_{\underline{l} > 0} n_{\underline{l}}\, \mathrm{Li}_3\left(\underline{q}^{\underline{l}}\right) . \tag{4.6.47}$$

In section 4.5, we introduced the triple coupling on a three-fold as the pairing of Ω and the third derivative of it. In the $\underline{t}$ coordinates, we obtain with eq. (4.6.44)

$$C_{ijk} = \frac{1}{(X^0)^2} \partial_i \partial_j \partial_k \underline{\Pi}^T \Sigma\, \underline{\Pi} = \partial_i \partial_j \partial_k \mathcal{F} \,. \tag{4.6.48}$$

Note that the form of the prepotential together with eq. (4.6.48) implies the formula for the instanton-corrected triple coupling formula we gave in eq. (4.5.19).

Since we already encountered an explicit example for the three-fold structure in section 4.5, we will refrain from discussing another example for the classical treatment at this dimension. In subsection 5.4.1, we will describe their period structure using the $\hat{\Gamma}$-class formalism. As three-folds are well-understood due to the special geometry property, it is a suitable dimension to introduce these more technical concepts.

Chapter 5

Integral structures in higher dimensions

We saw in the previous chapter how the solutions to the Picard–Fuchs differential ideal combine to an integral period basis for $n \leq 3$. For elliptic curves and K3 surfaces, the period vector is given by polynomials in the mirror coordinates $\underline{t}$. In the latter case, the classical intersection numbers appear in the highest-logarithmic period F_0. Importantly, these expressions for $\underline{\Pi}$ are exact and no non-perturbative corrections appear. This changes for Calabi–Yau three-folds, where both the periods and the Yukawa coupling is instanton-corrected. However, the prepotential dictates the behaviour of the B-periods and the period geometry requires no further structure. For higher dimensions, we need more elaborate techniques to obtain an integral structure for the period geometry. A crucial role is played by the Frobenius algebra we introduce in section 5.1. The leading order of the periods, i.e. the polynomial part in $\underline{t}$, is described by central charges of B-branes, which correspond to structure sheaves on certain divisors on the mirror manifold. We will review the necessary structure in section 5.2. This will allow us to introduce our method to obtain the asymptotic period vector in section 5.3. We will supplement this subsection with examples in section 5.4. This integral structure is not only necessary for the compactification to lower dimensions, but also yields a canonical splitting of the period matrix into a unipotent and semisimple part. It follows that the periods can be written as an iterated integral, which is used in the computation of Feynman integrals.

5.1 Frobenius algebra

We review the Frobenius algebra structure [106] following [107], see also [104]. A mathematical review can be found in [108]. The idea is to identify the cohomology groups $H^{n-p,p}(X)$ with vector spaces $\mathcal{A}^{(p)}$ for $0 \leq p \leq n$. The whole middle cohomology is then represented by the graded vector space $\mathcal{A} = \bigoplus_{p=0}^{n} \mathcal{A}^{(p)}$. The Yukawa coupling introduced in section 4.5 is a special case of the more general map

$$C^{(a,b,c)} : \mathcal{A}^{(a)} \times \mathcal{A}^{(b)} \times \mathcal{A}^{(c)} \longrightarrow \mathbb{C} . \tag{5.1.1}$$

The three indicials in the Yukawa couplings C_{ijk} all belonged to the cohomology group $H^{2,1}$ or $p = 1$. For three-folds, the Yukawa couplings are therefore represented by $C_{ijk}^{(1,1,1)}$. The indices i, j and k represent a choice of basis, which, for any of the $\mathcal{A}^{(p)}$, we denote by $\{e_i^{(p)}\}_i$. The (non-degenerate) bilinear Frobenius form is given by a map

$$\Sigma : \mathcal{A} \times \mathcal{A} \longrightarrow \mathbb{Q} , \tag{5.1.2}$$

whose matrix representation in the above basis are denoted by Σ^{ij} with inverse $\hat{\Sigma}_{ij}$. In chapter 4, we always chose bases for the middle homology with block-anti-diagonal intersection forms, see eqs. (4.6.2), (4.6.23) and (4.6.38). This is crucial for the grading of the Frobenius algebra—it will be assumed in the following and ensured in the explicit construction of a homology basis in section 5.3. We denote the blocks on the anti-diagonal of Σ and $\hat{\Sigma}$ by $\sigma_{(a)}$ and $\hat{\sigma}^{(a)}$, respectively. Note that this implies

$$\sigma^{ik}_{(a)}\hat{\sigma}^{(n-a)}_{kj} = \delta^i_j\,. \tag{5.1.3}$$

By the properties of a CY-Frobenius algebra, we mean, in particular, the following identities for the functions $C^{(a,b,c)}$.

(i) Permutation symmetry: $C^{(a,b,c)}_{ijk} = C^{\sigma(a,b,c)}_{\sigma(ijk)}$, $\forall\,\sigma \in S_3$.

(ii) Griffiths transversality: $C^{(a,b,c)} = 0$ if $a+b+c < n$.

Due to property (ii), it is customary to abbreviate the couplings as $C^{(a,b)} := C^{(a,b,n-a-b)}$. For better readability, we will thus omit the third degree whenever the dimensionality n is clear from context.

(iii) Unit: $\mathcal{A}^{(0)} = \mathbb{C}\cdot 1$ and $C^{(0,a)}_{1,i,j} = \hat{\sigma}^{(a)}_{ij}$.

(iv) Associativity: $C^{(a,b)}_{ijp}\sigma^{pq}_{(n-a-b)}C^{(a+b,c)}_{qkl} = C^{(a,c)}_{ikr}\sigma^{rs}_{(n-a-c)}C^{(a+c,b)}_{sjl}$.

(v) Fusion rule: $e^{(a)}_i \cdot e^{(b)}_j = C^{(a,b)}_{ijk}\sigma^{kl}_{(n-a-b)}e^{(a+b)}_l$.

We mentioned above that one should think of the $\mathcal{A}^{(p)}$ as the cohomology group $H^{n-p,p}(X)$. The origin of these elements lies, however, in the mirror partner's cohomology group

$$H^p\left(\hat{X}, \wedge^p T\hat{X}\right) \cong H^{p,p}(\hat{X}) \cong H^{n-p,p}(X)\,, \tag{5.1.4}$$

where the first relation comes from Dolbeault's theorem and the second one assumes mirror symmetry between X and $\hat{X}$. As an example, we can use the above rules (i), (iii) and (v) to obtain the triple coupling of a three-fold via

$$e^{(1)}_i \cdot e^{(1)}_j \cdot e^{(1)}_k = C^{(1,1)}_{ijl}\sigma^{ls}_{(1)}e^{(2)}_s \cdot e^{(1)}_k = C^{(1,1)}_{ijl}\sigma^{ls}_{(1)}\underbrace{C^{(2,1)}_{sk1}}_{\hat{\sigma}^{(2)}_{sk}} = C^{(1,1)}_{ijk}, \tag{5.1.5}$$

where we used eq. (5.1.3) in the last equality. More interestingly, the rules also give the decomposition of n-point couplings (cf. eq. (4.5.24)) into triple couplings for $n > 3$. This phenomenon is expected from a conformal field theoretic point of view. The n-point couplings for four- and five-folds decompose as

$$\begin{aligned} n=4:\qquad e^{(1)}_i \cdot e^{(1)}_j \cdot e^{(1)}_k \cdot e^{(1)}_l &= C^{(1,1)}_{ijr}\sigma^{rs}_{(2)}e^{(2)}_s \cdot e^{(1)}_k \cdot e^{(1)}_l \\ &= C^{(1,1)}_{ijr}\sigma^{rs}_{(2)}C^{(2,1)}_{skt}\sigma^{tu}_{(1)}\hat{\sigma}^{(3)}_{ul} = C^{(1,1)}_{ijl}\sigma^{ls}_{(2)}C^{(1,1)}_{kls}\,, \end{aligned} \tag{5.1.6}$$

$$\begin{aligned} n=5:\ e^{(1)}_i \cdot e^{(1)}_j \cdot e^{(1)}_k \cdot e^{(1)}_l \cdot e^{(1)}_m &= C^{(1,1)}_{ijr}\sigma^{rs}_{(3)}e^{(2)}_s \cdot e^{(1)}_k \cdot e^{(1)}_l \cdot e^{(1)}_m \\ &= C^{(1,1)}_{ijr}\sigma^{rs}_{(3)}C^{(2,1)}_{skt}\sigma^{tu}_{(2)}e^{(3)}_u \cdot e^{(1)}_l \cdot e^{(1)}_m \\ &= C^{(1,1)}_{ijr}\sigma^{rs}_{(3)}C^{(2,1)}_{skt}\sigma^{tu}_{(2)}C^{(3,1)}_{ulv}\sigma^{vw}_{(1)}e^{(4)}_w \cdot e^{(1)}_m \\ &= C^{(1,1)}_{ijr}\sigma^{rs}_{(3)}C^{(1,2)}_{kst}\sigma^{tu}_{(2)}C^{(1,1)}_{lmu}\,. \end{aligned} \tag{5.1.7}$$

In section 5.6, we will see how this pattern fits together nicely with the general form of the Gauss–Manin connection in the corresponding period basis and eq. (4.5.24).

In this work, we discuss only families with Frobenius algebras that are generated by $\mathcal{A}^{(1)}$. This means that the fusion rule (v) for $a = 1$ can be inverted, i.e. each element $e_i^{(b+1)}$ is a linear combination of the elements $e_j^{(1)} \cdot e_k^{(b)}$. This inversion will play a central role in the construction of an integral basis in section 5.3. This condition is typically phrased in the literature as

(vi) Non-degeneracy: $\mathcal{A}$ is generated by $\mathcal{A}^{(1)}$.

It was observed in [96] that this is not guaranteed in dimensions $n > 3$. There, one-parameter four-fold families given by complete intersections in Grassmanian varieties were analysed. The Hodge structure of these models is $(1, 1, 2, 1, 1)$, in contrast to the $(1, 1, 1, 1, 1)$ structure of a non-degenerate one-parameter four-fold. Non-degenerate one-parameter models furthermore have a Picard–Fuchs operator of order $n + 1$. For the four-folds in [96], the degeneracy is reflected in a order-six Picard–Fuchs operator with indicials $(0^5, 1)$. The additional holomorphic solution mixes with the others to form a second second-order logarithmic period.

Similar to the instanton expansion of the couplings for three-folds in eq. (4.5.19), the expansions of the triple-couplings of higher-dimensional families also give rise to genus-zero invariants. For $n > 3$, the couplings have either one or two indices in $\mathcal{A}^{(1)}$. The single couplings with two such indices enjoy the expansion

$$C_{ij}{}^{\alpha} = c_{ij}{}^{\alpha} + \sum_{\underline{l}>0} n_{\underline{l}}^{\alpha}\, l_i l_j \frac{\underline{q}^{\underline{l}}}{1-\underline{q}^{\underline{l}}}\,, \tag{5.1.8}$$

while the remaining couplings can be written as

$$C_{i\alpha}{}^{\beta} = c_{i\alpha}{}^{\beta} + \sum_{\underline{l}>0} n_{\underline{l}\alpha}{}^{\beta}\, l_i \frac{\underline{q}^{\underline{l}}}{1-\underline{q}^{\underline{l}}}\,. \tag{5.1.9}$$

The invariants $n_{\underline{l}}^{\alpha}$ and $n_{\underline{l}\alpha}{}^{\beta}$ are conjectured to be integral. In appendix B, we list the first such invariants for Calabi–Yau families of dimension five, six and seven.

As done in section 4.1, one can express Ω in a basis γ^i dual to the topological homology basis Γ_i, where the coefficients are given by the periods over these cycles. This basis allows us to supplement $\Omega \in \mathcal{A}^{(0)}$ with *pure* elements of the Frobenius algebra to obtain a basis for the (horizontal) middle cohomology. An element in called pure, if it is contained in one of the vector spaces $\mathcal{A}^{(i)}$. Multiplication with $e_i^{(1)}$ is represented by the derivative ∂_i w.r.t. the mirror coordinate t^i. As shown in [104], the mirror maps t^i are flat coordinates on the moduli space for which the covariant derivative D_i (cf. section 4.2) reduces to the ordinary derivative ∂_i. Then, the fusion rule (v) implies that the Gauss–Manin connection—the matrix representation of ∂_{t^i} on the cohomology basis—is of a particular canonical form, which we will discuss further in section 5.6.

5.2 $\hat{\Gamma}$-class and central charges of B-branes

To obtain an integral period basis, one identifies the solutions to the Picard–Fuchs equations with the asymptotic period vector, which is polynomial in the mirror coordinates $\underline{t}$. For dimensions $n > 3$, one needs to use the fact that the asymptotic behaviour is given by central charges of branes, see below. The key takeaways of this section are eqs. (5.2.5) and (5.2.8) computing the asymptotic period vector and the intersection form in terms of topological data of the mirror.

We begin with some mathematical preliminaries. Given a rank-r vector bundle E, the Chern roots x_i are formal roots of the total Chern class

$$c(E) \coloneqq 1 + \sum_{i=1}^{r} c_r(E) = \prod_{i=1}^{r} (1 + x_i(E)) \,.$$

The r.h.s. allows us to view the bundle as the sum of r line bundles and write it as $E = \bigoplus_{i=1}^{r} L_i$ with $c_1(L_i) = x_i$. This is known as the *splitting principle* and can be used to reduce many statements for rank-r bundles down to line bundles. We will encounter it again further below to describe the dual bundle. The $\hat{\Gamma}$-class is defined in terms of the Chern roots as [109]

$$\hat{\Gamma}(E) = \prod_{i=1}^{r} \Gamma\left(1 - \frac{x_i(E)}{2\pi\mathrm{i}}\right) = \exp\left(-\gamma c_1(TX) + \sum_{k\geq 2} (-1)^k (k-1)! \zeta_k \mathrm{ch}_k(TX)\right),$$

with γ being the Euler constant and $\mathrm{ch}_k = \frac{1}{k!} \sum_{i=1}^{r} \left(-\frac{c_i}{2\pi\mathrm{i}}\right)^k$. For a Calabi–Yau manifold with $c_1(TX) = 0$, this results in the series expansion

$$\hat{\Gamma}(TX) = 1 + \frac{c_2}{24} + \frac{c_3\zeta_3}{(2\pi\mathrm{i})^3} + \frac{\left(7c_2^2 - 4c_4\right)}{5760} + \frac{\left(c_5 - c_2c_3\right)\zeta_5 - c_2c_3\zeta_2\zeta_3}{(2\pi i)^5} + \mathcal{O}\left(6\right),$$

where we wrote $c_i = c_i(TX)$. The Todd class is given by

$$\mathrm{Td}(E) = \prod_{i=1}^{r} \frac{x_i}{1 - e^{-x_i}} \,.$$

To give a simple relation between the Todd class and the $\hat{\Gamma}$ class for Calabi–Yau manifolds, we introduce the dual bundle $E^\vee$ of E, where each fibre of $E^\vee$ consists of the linear maps from the corresponding fibre of E to $\mathbb{C}$:

$$E^\vee = \mathrm{Hom}(E, \mathbb{C}) \,.$$

For a line bundle L, the bundle $L \otimes L^\vee = \mathrm{Hom}(L, L)$ has the identity as a nowhere vanishing section and its first Chern class is therefore zero. It follows that $0 = c_1(L \otimes L^\vee) = c_1(L) + c_1(L^\vee)$. Using the splitting principle as introduced above, one finds for the Chern roots $x_i(E^\vee) = -x_i(E)$, which implies $c_k(E^\vee) = (-1)^k c_k(E)$. With Euler's reflection formula $\Gamma(z)\Gamma(1-z) = \pi/\sin(\pi z)$ and $\Gamma(z+1) = z\Gamma(z)$, one obtains

$$\Gamma\left(1 + \frac{x}{2\pi\mathrm{i}}\right)\Gamma\left(1 - \frac{x}{2\pi\mathrm{i}}\right) = \frac{x}{2\mathrm{i}\sin\frac{x}{2\mathrm{i}}} = e^{-x/2}\frac{x}{1-e^{-x}}.$$

Using $\sum_{i=1}^{r} x_i = c_1$, one gets for Calabi–Yau manifolds

$$\mathrm{Td}(TX) = \hat{\Gamma}(TX)\,\hat{\Gamma}(TX^\vee) \,.$$

We will now show how the $\hat{\Gamma}$- and Td-class give rise to the leading order of an integral basis of periods.

A-branes and B-branes are described using the language of sheaves and derived categories. On the A-model side, A-branes correspond to special Lagrangian cycles within a Calabi–Yau manifold, which are submanifolds that minimise volume in their homology class and satisfy certain calibration conditions related to the manifold's geometry. On the B-model side, B-branes are described purely algebraically as coherent sheaves (or, more precisely, objects in the derived category of coherent sheaves on the mirror Calabi–Yau manifold). Mirror symmetry relates these two pictures by mapping A-branes on a Calabi–Yau manifold X to B-branes on its mirror $\hat{X}$, and vice versa. This equivalence, famously conjectured by Kontsevich as the homological mirror symmetry conjecture [110], asserts that the category of A-branes, described by special Lagrangian cycles, is equivalent to the derived category of coherent sheaves on the mirror manifold.

The identification uses the map [111]

$$\begin{aligned} \mu : K(X) &\to H^*(X,\mathbb{Z})\,, \\ \mathcal{E} &\mapsto \mathrm{ch}(\mathcal{E})\hat{\Gamma}(TX)\,, \end{aligned} \tag{5.2.1}$$

where we will let the K-theory group $K(X)$ be generated by rational linear combinations of the structure sheaf on X, on divisors generating the Kähler cone D_i, $1 \leq i \leq h^{1,1}(X)$, and on successive intersections thereof. The highest-dimensional D-brane on the A-side is the D$(2n)$-brane and the corresponding sheaf is the structure sheaf on the whole manifold $\mathcal{O}_X$ with $\mathrm{ch}(\mathcal{O}_X) = 1$. The D$(2n-2)$-branes are described by the structure sheaves on divisors D_i and lower-dimensional branes by the structure sheaves on their intersections. Let $\mathcal{I} \subset \{1,\ldots,h^{1,1}\}$ be an index set. The Chern character of the structure sheaf on $S = \bigcap_{i\in\mathcal{I}} D_i$ can be obtained by the long exact sequence

$$\begin{aligned} 0 \longrightarrow \mathcal{O}_X(-\sum_{i\in\mathcal{I}} D_i) \longrightarrow \bigoplus_{j\in\mathcal{I}} \mathcal{O}_X(-\sum_{i\in\mathcal{I}\setminus j} D_i) \longrightarrow \ldots \\ \ldots \longrightarrow \bigoplus_{i\in\mathcal{I}} \mathcal{O}_X(-D_i) \longrightarrow \mathcal{O}_X \longrightarrow \mathcal{O}_S \longrightarrow 0 \end{aligned} \tag{5.2.2}$$

combined with the fact that the alternating sum over the elements' Chern characters vanishes. In this sequence, we use that the Chern character of a line bundle $\mathcal{O}_X(D)$ associated with a divisor D is given by e^J, where J is the first Chern class of the line bundle or equivalently the Poincaré-dual form in $H^{1,1}(X)$. For example, for D$(2n-2)$-branes, we choose $S = D_i$ and find

$$\mathrm{ch}(\mathcal{O}_{D_i}) = \mathrm{ch}(\mathcal{O}_X) - \mathrm{ch}(\mathcal{O}_X(-D_i)) = 1 - e^{-J_i}. \tag{5.2.3}$$

and, for D$(2n-4)$-branes, we use $S = D_1 \cap D_2$ and obtain

$$\begin{aligned} \mathrm{ch}(\mathcal{O}_{D_i\cdot D_j}) &= \mathrm{ch}(\mathcal{O}_X) - (\mathrm{ch}(\mathcal{O}_X(-D_i)) + \mathrm{ch}(\mathcal{O}_X(-D_j))) + \mathrm{ch}(\mathcal{O}_X(-D_i-D_j)) \\ &= 1 - e^{-J_i} - e^{-J_j} + e^{-J_i-J_j}. \end{aligned} \tag{5.2.4}$$

The central charges of these sheaves can then be computed via

$$\Pi_{\mathcal{E}} = Z(\mathcal{E}) = \int_X e^{\sum_i t^i\cdot J_i} \wedge \mu(\mathcal{E}^\vee)\,. \tag{5.2.5}$$

In other works [96], the D2 and D0 branes were described by twisted structure sheaves on curves dual to the Kähler divisors and the skyscraper sheaf, respectively. In our conventions, their central

charges are always given by

$$\Pi_{\mathcal{E}^i_{D2}} = t_i \,, \tag{5.2.6}$$

$$\Pi_{\mathcal{E}_{D0}} = 1 \,. \tag{5.2.7}$$

The Hirzebruch–Riemann–Roch (HRR) pairing is defined as

$$\chi(\mathcal{E},\mathcal{F}) = \int_X \mu(\mathcal{E}) \wedge \mu(\mathcal{F}^\vee) = \int_X \mathrm{Td}(TX) \wedge \mathrm{ch}(\mathcal{E}) \wedge \mathrm{ch}(\mathcal{F}^\vee) \,. \tag{5.2.8}$$

Evaluated in the basis corresponding to the period basis, we have $\chi = \hat{\Sigma}$ and its inverse is giving rise to the intersection form $(\chi)^{-1} = \Sigma$ for the periods.

In section 5.3, we will construct integral period bases for Calabi–Yau n-folds. There, we will use certain rational linear combinations of structure sheaves on intersections of Kähler divisors, where μ and thus eq. (5.2.5) extend linearly to other sheaves. In $n \leq 4$, the above yields a sufficient set of sheaves to obtain the leading order of a rational basis of periods of the mirror[1]. For higher dimensions, however, it is a priori unclear how to obtain an independent set of sheaves for, for example, sheaves in dimension two. Another problem is finding a basis that has an intersection form of block-anti-diagonal form. This is crucial for the simplification of many identities such as the Griffiths transversality conditions and will also allows us to construct a basis for the cohomology in which the Gauss–Manin connection is of a particular simple and canonical form. We will show that the classical part of the (inverse) couplings naturally give rise to such a basis.

5.3 Integral period bases

In the previous section, we reviewed how homological mirror symmetry identifies the leading order structure of the periods to the central charges of B-branes. Much of the period structure of a Calabi–Yau family is revealed only in a K-theory basis with block-anti-diagonal HRR pairing χ. We note that this pairing is also given by the cup product $\hat{\Sigma} = \chi$ of the cycles that support the sheaves. Here, we will propose a formalism that yields a period basis that has block-anti-diagonal intersection form Σ and *conjecturally* integral monodromies. We will support the latter with explicit analytical continuations and the integrality of genus-zero invariants of several models.

The proposed basis consists of two different sets of periods, which we will call A- and B-periods. These names are chosen by analogy to the three-dimensional case (section 4.6)). However, this should not mislead one to assume that the structures carry over to higher dimensions. The B-periods are central charges of structure sheaves on divisors of X and intersections thereof. For a Calabi–Yau three-fold, F_0 corresponds to the structure sheaf on X while F_i to those on divisors D_i. In n dimensions, there are B-periods coming from zero up to $\lceil n/2 \rceil - 1$ intersections of divisors. In the Hodge structure of the middle cohomology at the MUM point, these elements correspond to the groups that are strictly on the right side $H^{p,n-p}(X)$, $p < \lceil n/2 \rceil$. The rest of the middle cohomology is represented by A-periods, which are defined as being dual to the B-periods in the sense that the intersection form resembles that of for the three-fold (4.6.38), see

[1] For $n = 4$, one must restrict to an independent basis of sheaves for dimension two, see subsection 5.4.2. Furthermore, integrality demands that this choice generates the whole space integrally.

eq. (5.3.15). To obtain their leading order behaviour, we need to define inverses $\mathfrak{c}$ to the classical intersection numbers c.

To each vector space $\mathcal{A}^{(n-k)}$ in the Frobenius algebra, we want to assign a basis represented by tuples of length k. The tuples give the support of the structure sheaves, where the entries correspond to the divisors we intersect. We thus define index sets $\mathcal{N}_k$ for the Frobenius algebra with m generators in $\mathcal{A}^{(1)}$

$$\mathcal{N}_k := \Big([i_1, \ldots, i_k] \mid 1 \leq i_l \leq m\,, \bigcap_{l=1}^{k} D_{i_l} \neq 0\Big)\,, \quad 1 \leq k \leq n\,. \tag{5.3.1}$$

As the index sets shall represent intersections of divisors, we demand that the their intersection is non-vanishing. First of all, these intersections are not necessarily independent in homology. The number of independent elements, which is equivalent to the Betti number, is given by the rank of the pairing

$$c_k := c_{i_1,\ldots,i_k,j_1,\ldots,j_{n-k}}\,, \quad i \in \mathcal{N}_k,\ j \in \mathcal{N}_{n-k}\,, \tag{5.3.2}$$

where c denotes the classical intersection numbers. The c_k should be seen as a two-by-two matrix for computing the rank. It follows that $c_{n-k} = c_k^T$. We furthermore demand that the following inverses $\mathfrak{c}$ to the classical intersection numbers exist

$$\delta_i^j = \sum_{l_1,\ldots,l_{n-k}} c_{i_1,\ldots,i_k,l_1,\ldots,l_{n-k}} \mathfrak{c}^{l_1,\ldots,l_{n-k},j_1,\ldots,j_k}\,. \tag{5.3.3}$$

We will call the subsets of $\mathcal{N}_k$ that allow for such an inverse N_k. Before we start identifying these sets with sheaves, we must restrict the set further.

There is another subtlety that is crucial for integrality of the monodromies: As we will see in subsection 5.4.2, the brane charge $\Pi_{\mathcal{O}_{D_i}}$ obtains a contribution of $\pm\Pi_{\mathcal{O}_{D_i \cap D_j}}$ under a monodromy around $z^j = 0$. When projecting onto an independent basis, it is important that $\Pi_{\mathcal{O}_{D_i \cap D_j}}$ is given by an integer combination of the generators. As we will explain in detail below, the preliminary (with intersection form in general not block-anti-diagonal) basis of sheaves we propose consists of two parts: The B-periods of logarithmic order $p > \lceil \frac{n-1}{2} \rceil$ correspond directly to periods $\Pi_{\mathcal{O}_S}$ with $S = \bigcap_{i \in n} D_i$ for some $n \in N_k$, while the A-periods will be contracted with the inverse couplings $\mathfrak{c}$. For the latter set, the resulting sheaf is independent of the restriction to independent elements in N_k due to the multiplication with $\mathfrak{c}$—they are defined to be dual to their opposing period. However, in the first set we must pay attention to select generators that generate all sheaves at this level integrally.

To find such generators, we consider the matrices c_k^T and focus on the kernel. We write a set of generators of the kernel as rows into a matrix and perform a Gaussian elimination. We then divide each row by its greatest common divisor. If there exist at least $\dim(\ker(c_k^T))$ basis elements for which there exists a generator with a ± 1 in that element's position, we may omit these elements to obtain an independent basis for this level. This sufficient but not necessary condition then naturally preserves integrality of the monodromies. Let us give an example.

We consider the four-fold hypersurface family $\mathbb{P}_{18,12,3,1^3}[36]$ with intersection ring

$$72J_3^4 + 12J_1J_3^3 + 36J_2J_3^3 + 2J_1^2J_3^2 + 18J_2^2J_3^2 + 6J_1J_2J_3^2 + 9J_2^3J_3 + 3J_1J_2^2J_3 + J_1^2J_2J_3\,.$$

Sorting the set of indices for this level as[2]

$$\mathcal{N}_2 = ([1,1],[1,2],[1,3],[2,2],[2,3],[3,3])\,, \tag{5.3.4}$$

the intersection matrix has rank $b^{\text{hor}}_{2,2} = 4$ and reads

$$c_2^T = c_2 = \begin{pmatrix} 0 & 0 & 0 & 0 & 1 & 2 \\ 0 & 0 & 1 & 0 & 3 & 6 \\ 0 & 1 & 2 & 3 & 6 & 12 \\ 0 & 0 & 3 & 0 & 9 & 18 \\ 1 & 3 & 6 & 9 & 18 & 36 \\ 2 & 6 & 12 & 18 & 36 & 72 \end{pmatrix}. \tag{5.3.5}$$

We find that the four-point coupling is invertible as in eq. (5.3.3) for

$$N_2 = (\{1,2,3,5\},\{1,2,3,6\},\{1,3,4,5\},\{1,3,4,6\})\,, \tag{5.3.6}$$

where the numbers represent the elements in $\mathcal{N}_2$ as in eq. (5.3.4). Performing a Gaussian elimination on the kernel generators of c_2^T, these read

$$\underline{k} = \begin{pmatrix} 0 & 3 & 0 & -1 & 0 & 0 \\ 0 & 0 & 0 & 0 & 2 & -1 \end{pmatrix}. \tag{5.3.7}$$

From the above we conclude that integrality is guaranteed, if we omit the fourth and sixth element, i.e. if we generate level two by

$$\{[1,1],[1,2],[1,3],[2,3]\} \equiv \{1,2,3,5\}\,.$$

Choosing another one of the four possible bases, one obtains non-integral monodromies around the MUM point. Nevertheless, if one divides the sheaves $\mathcal{O}_{D_2\cap D_2}$ and $\mathcal{O}_{D_3\cap D_3}$ by a factor of three and two (coming from the relations of the kernel generators) one gets the same central charge lattice for any of the four sets (up to permutations). This example shows the importance of a proper choice for a basis for the B-periods already at $n = 4$.

Finally, we demand that the tuples are horizontal, i.e. that each tuple at level k comes from a tuple of level $k-1$ extended by one index. Let us call the final index set at each level $\underline{s}_k = (s_k^1, s_k^2, \ldots)$, which has length $h^{n-k,k}_{\text{hor}}$. The inverse couplings $\mathfrak{c}_k$ from before are then defined by

$$\delta_i^j = \sum_{l\in\underline{s}_{n-k}} c_{i,l}\mathfrak{c}_k^{l,j}\,, \tag{5.3.8}$$

where we shortened the indices for better readability. For each level, one obtains a vector of sheaves

$$\underline{\widetilde{\mathcal{O}}}_k \coloneqq \left(\mathcal{O}_{S_k^i}\,\middle|\, S_k^i = D_{s_k^{i,1}}\cap\ldots\cap D_{s_k^{i,k}}\ 1\le i\le b^{\text{hor}}_{n-k,k}\right). \tag{5.3.9}$$

[2] At level one, $\mathcal{N}_1 = ([1],[2],[3])$ and c_1^T is a 9×3 matrix with nullity zero. Therefore, we omit none of the elements in $N_1 = (\{1,2,3\})$.

We can then define a K-theory basis consisting of two parts (corresponding to A- and B-periods)

$$\begin{aligned}\underline{\widetilde{\mathcal{O}}} = &\left(\sum_{l\in \underline{s}_k} \mathfrak{c}_k^{i,l} \underline{\widetilde{\mathcal{O}}}_{k,l} \,\middle|\, i \in \underline{s}_{n-k}\,,\ n \geq k \geq \left\lceil \frac{n+1}{2} \right\rceil \right) \\ &\cup \left((-1)^{k+n} \underline{\widetilde{\mathcal{O}}}_{k,i} \,\middle|\, i \in \underline{s}_k\,,\ \left\lceil \frac{n-1}{2} \right\rceil \geq k \geq 0 \right).\end{aligned} \tag{5.3.10}$$

The awkward range for k in both tuples is such that $\underline{\widetilde{\mathcal{O}}}$ is sorted in ascending order by dimension of the sheaves' support, i.e. the skyscraper sheaf given by a linear combination of $\underline{\widetilde{\mathcal{O}}}_n$ is the first entry while the structure sheaf $\underline{\widetilde{\mathcal{O}}}_{0,1} = \mathcal{O}_X$ comes last. This will lead to a period vector that is in ascending logarithmic order. The HRR pairing of this set is not in block-anti-diagonal form. To achieve this, we perform for each level $k < \lfloor \frac{n+1}{2} \rfloor$ a basis transformation R_k with coefficients

$$(R_k)_{i,j} = \begin{cases} 1\,, & \text{if } i = j\,, \\ -\langle \widetilde{\mathcal{O}}_{b_n+1-j}, \widetilde{\mathcal{O}}_i \rangle\,, & \text{if } i > j \ \ \&\ \ i+j < b_n+1 \ \ \&\ \ j \in B(k)\,, \\ -\frac{1}{2}\langle \widetilde{\mathcal{O}}_i, \widetilde{\mathcal{O}}_i \rangle\,, & \text{if } i > j \ \ \&\ \ i+j = b_n+1 \ \ \&\ \ j \in B(k)\,, \\ 0\,, & \text{else,} \end{cases} \tag{5.3.11}$$

where we transform $\underline{\widetilde{\mathcal{O}}} \mapsto R_k \underline{\widetilde{\mathcal{O}}}$ for the computation of R_{k+1}. We denoted the index range in $\{1, \dots, b_n\}$ corresponding to level k by $B(k)$. In the above example for $\mathbb{P}_{18,12,3,1^3}[36]$, there are two matrices

$$R_1 = \begin{pmatrix} 1 & 0 & 0 & 0 & 0 & 0 & 0 & 0 & 0 & 0 & 0 & 0 \\ 2 & 1 & 0 & 0 & 0 & 0 & 0 & 0 & 0 & 0 & 0 & 0 \\ 1 & 0 & 1 & 0 & 0 & 0 & 0 & 0 & 0 & 0 & 0 & 0 \\ 0 & 0 & 0 & 1 & 0 & 0 & 0 & 0 & 0 & 0 & 0 & 0 \\ -46 & 0 & 0 & 0 & 1 & 0 & 0 & 0 & 0 & 0 & 0 & 0 \\ -14 & 0 & 0 & 0 & 0 & 1 & 0 & 0 & 0 & 0 & 0 & 0 \\ -6 & 0 & 0 & 0 & 0 & 0 & 1 & 0 & 0 & 0 & 0 & 0 \\ -2 & 0 & 0 & 0 & 0 & 0 & 0 & 1 & 0 & 0 & 0 & 0 \\ -37 & 0 & 0 & 0 & 0 & 0 & 0 & 0 & 1 & 0 & 0 & 0 \\ -9 & 0 & 0 & 0 & 0 & 0 & 0 & 0 & 0 & 1 & 0 & 0 \\ -1 & 0 & 0 & 0 & 0 & 0 & 0 & 0 & 0 & 0 & 1 & 0 \\ -1 & 0 & 0 & 0 & 0 & 0 & 0 & 0 & 0 & 0 & 0 & 1 \end{pmatrix},\ R_2 = \begin{pmatrix} 1 & 0 & 0 & 0 & 0 & 0 & 0 & 0 & 0 & 0 & 0 & 0 \\ 0 & 1 & 0 & 0 & 0 & 0 & 0 & 0 & 0 & 0 & 0 & 0 \\ 0 & 0 & 1 & 0 & 0 & 0 & 0 & 0 & 0 & 0 & 0 & 0 \\ 0 & 0 & 0 & 1 & 0 & 0 & 0 & 0 & 0 & 0 & 0 & 0 \\ 0 & 4 & 9 & 9 & 1 & 0 & 0 & 0 & 0 & 0 & 0 & 0 \\ 0 & 1 & 2 & 1 & 0 & 1 & 0 & 0 & 0 & 0 & 0 & 0 \\ 0 & 0 & 0 & -1 & 0 & 0 & 1 & 0 & 0 & 0 & 0 & 0 \\ 0 & 0 & 0 & -1 & 0 & 0 & 0 & 1 & 0 & 0 & 0 & 0 \\ 0 & 13 & 37 & 37 & 0 & 0 & 0 & 0 & 1 & 0 & 0 & 0 \\ 0 & 6 & 9 & 0 & 0 & 0 & 0 & 0 & 0 & 1 & 0 & 0 \\ 0 & 1 & 0 & 0 & 0 & 0 & 0 & 0 & 0 & 0 & 1 & 0 \\ 0 & 0 & 0 & 0 & 0 & 0 & 0 & 0 & 0 & 0 & 0 & 1 \end{pmatrix}. \tag{5.3.12}$$

Note that, for $n > 4$, this basis change is generally not integral due to the rational factors we included in the linear combinations of the A-periods' sheaves in eq. (5.3.10). Finally, we obtain our K-theory basis

$$\underline{\mathcal{O}} = \cdots R_2 \cdot R_1 \cdot \underline{\widetilde{\mathcal{O}}}\,, \tag{5.3.13}$$

which has, depending on the dimension, the HRR pairing

$$\hat{\Sigma}_{\text{even}} = \begin{pmatrix} & & & & & & & & 1 \\ & & & & & & & \iddots & \\ & & & & & & 1 & & \\ & & & & & \hat{\sigma}^{(n/2)} & & & \\ & & & & 1 & & & & \\ & & & \iddots & & & & & \\ & & 1 & & & & & & \end{pmatrix},\quad \hat{\Sigma}_{\text{odd}} = \begin{pmatrix} & & & & & & & & -1 \\ & & & & & & & \iddots & \\ & & & & & & -1 & & \\ & & & & & 1 & & & \\ & & & & \iddots & & & & \\ & & & 1 & & & & & \\ & & & & & & & & \end{pmatrix}, \tag{5.3.14}$$

where $\hat{\sigma}^{(n/2)}$ denotes the pairing of the elements in $H^{n,n}$, which is positive/negative if $n/2$ is even/odd. It follows that the intersection form $\Sigma = (\hat{\Sigma})^{-1}$ in cohomology is of the form

$$\Sigma_{\text{even}} = \begin{pmatrix} & & & & & & 1 \\ & & & & & \iddots & \\ & & & & 1 & & \\ & & & \sigma_{(n/2)} & & & \\ & & 1 & & & & \\ & \iddots & & & & & \\ 1 & & & & & & \end{pmatrix}, \quad \Sigma_{\text{odd}} = \begin{pmatrix} & & & & & & 1 \\ & & & & & \iddots & \\ & & & & 1 & & \\ & & & -1 & & & \\ & & \iddots & & & & \\ -1 & & & & & & \end{pmatrix}. \tag{5.3.15}$$

Since, in this period basis, there is only one bilinear form of the Frobenius algebra that appears non-trivially, we will sometimes omit the index $n/2$ of $\sigma_{(n/2)}$ and $\hat{\sigma}^{(n/2)}$. In the following subsection, we will give examples to this construction, starting from $n = 3$, where we will emphasise the advantage of this formalism over the prepotential approach of section 4.6. Afterwards, we will describe the asymptotic period vector for four-folds used, for example, in F-theory compactifications to four-dimensions and extend the discussion to higher dimensions.

5.4 Three- and four-folds using $\hat{\Gamma}$-class

The techniques of the previous sections are first exemplified on the already discussed case of three-folds (cf. section 4.6) and then applied on four-folds in subsection 5.4.2, where the absence of a prepotential requires homological mirror symmetry for the construction of an integral period basis. The three-fold example includes a suitable description of the integral structure on symmetric quotient families. The example four-fold is the popular elliptic X_6-fibration over $\mathbb{P}^2$, which we will encounter again in the study of supersymmetric F-theory flux vacua in section 6.3, see also [1].

5.4.1 Three-folds revisited

The model we will consider was already discussed in the context of flux compactifications in [1]

$$\mathcal{X}^{(3)}_{\text{sym}} = \left(\begin{array}{c|ccc} \mathbb{P}^2 & 1 & 1 & 1 \\ \mathbb{P}^2 & 1 & 1 & 1 \\ \mathbb{P}^2 & 1 & 1 & 1 \end{array} \right)^{3,48}_{-90}. \tag{5.4.1}$$

Using the toric methods discussed in section 2.2, one readily obtains the classical intersection numbers

$$R = 3J_1^2J_2 + 3J_1^2J_3 + 3J_1J_2^2 + 3J_1J_3^2 + 6J_1J_2J_3 + 3J_2J_3^2 + 3J_2^2J_3 \tag{5.4.2}$$

and integrals of the Chern classes

$$\chi = -90\,, \quad c_2 \cdot J_i = 36\,,\ i \in \{1,2,3\}\,. \tag{5.4.3}$$

For the $\hat{\Gamma}$-class formalism, we actually need the full forms of the Chern classes, which are given by

$$c_2 = 3\left(J_1J_2 + J_1J_3 + J_2J_3\right), \tag{5.4.4}$$
$$c_3 = -3\left(J_1 + J_2\right)\left(J_1 + J_3\right)\left(J_2 + J_3\right). \tag{5.4.5}$$

Following section 5.3, we have $\mathcal{N}_0 = ([])$, $\mathcal{N}_1 = ([1],[2],[3])$. There is only a single choice to match the Betti numbers $h^{3,0} = 1$ and $h^{2,1} = 3$ and we have $N_0 = (\{1\})$ and $N_1 = (\{1,2,3\})$. For the B-periods, $\mathcal{N}_2$ and $\mathcal{N}_3$ have cardinality six and seven

$$\mathcal{N}_2 = ([1,1],[1,2],[1,3],[2,2],[2,3],[3,3]), \tag{5.4.6}$$
$$\mathcal{N}_3 = ([1,1,2],[1,1,3],[1,2,2],[1,2,3],[1,3,3],[2,2,3],[2,3,3]). \tag{5.4.7}$$

Note that we omitted the index tuples representing the vanishing intersections $D_i \cap D_i \cap D_i$ for $1 \leq i \leq 3$. There are 17 possible ways to choose $h^{1,2} = 3$ elements in $\mathcal{N}_2$ with invertible couplings, which are collected in N_2. We will choose the element

$$\underline{s}_2 = (2,4,5) \equiv ([1,2],[2,2],[2,3]). \tag{5.4.8}$$

Horizontality implies that we cannot take the generators $[1,1,3]$ or $[1,3,3]$ for $\underline{s}_3 = (s_3^1)$ and we thus choose $s_3^1 = [1,1,2]$. As the B-periods follow directly from eq. (5.3.10) and the computation of the Chern characters via the Koszul complex we discussed in section 5.2, we focus on the A-periods. Let us start with the skyscraper sheaf at $k = n = 3$: The inverse coupling(s) defined by eq. (5.3.8) must satisfy

$$\delta_i^j = \sum_{l \in N_0} c_{i,l}\mathfrak{c}^{l,i} \Longrightarrow 1 = c_{211}\mathfrak{c}^{211} \Longrightarrow \mathfrak{c}^{211} = \frac{1}{3}. \tag{5.4.9}$$

Then, we obtain immediately

$$\widetilde{\mathcal{O}}_{n,1} = \frac{1}{3}\mathcal{O}_{D_1\cap D_2\cap D_2}. \tag{5.4.10}$$

For the remaining A-periods, we have $k = n - 1 = 2$ and obtain the relevant couplings in eq. (5.3.8)

$$c_{i,l} = \begin{pmatrix} c_{121} & c_{122} & c_{123} \\ c_{221} & c_{222} & c_{223} \\ c_{231} & c_{232} & c_{233} \end{pmatrix} = \begin{pmatrix} 3 & 3 & 6 \\ 3 & 0 & 3 \\ 6 & 3 & 3 \end{pmatrix}. \tag{5.4.11}$$

The row index i runs through N_2 while l is in N_1. Then, the inverse couplings are obtained by

$$\mathfrak{c}^{l,j} = \begin{pmatrix} \mathfrak{c}^{112} & \mathfrak{c}^{122} & \mathfrak{c}^{123} \\ \mathfrak{c}^{212} & \mathfrak{c}^{222} & \mathfrak{c}^{223} \\ \mathfrak{c}^{312} & \mathfrak{c}^{322} & \mathfrak{c}^{323} \end{pmatrix} = \begin{pmatrix} 3 & 3 & 6 \\ 3 & 0 & 3 \\ 6 & 3 & 3 \end{pmatrix}^{-1} = \frac{1}{6}\begin{pmatrix} -1 & 1 & 1 \\ 1 & -3 & 1 \\ 1 & 1 & -1 \end{pmatrix}. \tag{5.4.12}$$

It follows that the sheaves in $\underline{\widetilde{\mathcal{O}}}_2$ are given by

$$\underline{\widetilde{\mathcal{O}}}_2 = \frac{1}{6}\begin{pmatrix} -1 & 1 & 1 \\ 1 & -3 & 1 \\ 1 & 1 & -1 \end{pmatrix}\begin{pmatrix} \mathcal{O}_{D_1\cap D_2} \\ \mathcal{O}_{D_2\cap D_2} \\ \mathcal{O}_{D_2\cap D_3} \end{pmatrix}. \tag{5.4.13}$$

Together with

$$\underline{\widetilde{\mathcal{O}}}_1 = \begin{pmatrix} \mathcal{O}_{D_1} \\ \mathcal{O}_{D_2} \\ \mathcal{O}_{D_3} \end{pmatrix} \quad \text{and} \quad \underline{\widetilde{\mathcal{O}}}_0 = \begin{pmatrix} \mathcal{O}_X \end{pmatrix}, \tag{5.4.14}$$

these central charges give an integral basis of the periods. The Chern characters of these sheaves $\widetilde{\mathcal{O}}$ are given by

$$\mathrm{ch}(\widetilde{\mathcal{O}}) = \begin{pmatrix} \frac{1}{3}J_1^2 J_2 \\ -\frac{J_2^3}{6} + \frac{1}{12}J_1 J_2^2 - \frac{1}{12}J_3 J_2^2 + \frac{J_2^2}{6} + \frac{1}{12}J_1^2 J_2 - \frac{1}{12}J_3^2 J_2 - \frac{J_1 J_2}{6} + \frac{J_3 J_2}{6} \\ \frac{J_2^3}{2} - \frac{1}{12}J_1 J_2^2 - \frac{1}{12}J_3 J_2^2 - \frac{J_2^2}{2} - \frac{1}{12}J_1^2 J_2 - \frac{1}{12}J_3^2 J_2 + \frac{J_1 J_2}{6} + \frac{J_3 J_2}{6} \\ -\frac{J_2^3}{6} - \frac{1}{12}J_1 J_2^2 + \frac{1}{12}J_3 J_2^2 + \frac{J_2^2}{6} - \frac{1}{12}J_1^2 J_2 + \frac{1}{12}J_3^2 J_2 + \frac{J_1 J_2}{6} - \frac{J_3 J_2}{6} \\ \frac{J_3^3}{6} - \frac{J_3^2}{2} + J_3 \\ \frac{J_2^3}{6} - \frac{J_2^2}{2} + J_2 \\ \frac{J_1^3}{6} - \frac{J_1^2}{2} + J_1 \\ -1 \end{pmatrix}. \tag{5.4.15}$$

However, their intersection form is not in block-anti-diagonal form and we need to perform a basis change as in eq. (5.3.13). Here, the only non-trivial matrix is given by

$$R_1 = \begin{pmatrix} 1 & 0 & 0 & 0 & 0 & 0 & 0 & 0 \\ 0 & 1 & 0 & 0 & 0 & 0 & 0 & 0 \\ 1 & 0 & 1 & 0 & 0 & 0 & 0 & 0 \\ 0 & 0 & 0 & 1 & 0 & 0 & 0 & 0 \\ -3 & 0 & 0 & 0 & 1 & 0 & 0 & 0 \\ -3 & 0 & 0 & 0 & 0 & 1 & 0 & 0 \\ -3 & 0 & 0 & 0 & 0 & 0 & 1 & 0 \\ 0 & 0 & 0 & 0 & 0 & 0 & 0 & 1 \end{pmatrix}. \tag{5.4.16}$$

In the new basis $\underline{\mathcal{O}}$, the corresponding periods are subject to the intersection form eq. (4.6.38). We compute the central charges of these branes with eq. (5.2.5), yielding

$$\underline{\Pi}(\underline{t}) \sim \begin{pmatrix} 1 \\ t_1 \\ t_2 \\ t_3 \\ \frac{3}{2}\left(t_1^2 + (4t_2 + 2t_3 - 1)\,t_1 + t_2\,(t_2 + 2t_3 - 1) - 1\right) \\ \frac{3}{2}\left(t_1^2 + (2t_2 + 4t_3 - 1)\,t_1 + t_3\,(2t_2 + t_3 - 1) - 1\right) \\ \frac{3}{2}\left(t_2^2 + (2t_1 + 4t_3 - 1)\,t_2 + t_3\,(2t_1 + t_3 - 1) - 1\right) \\ -\frac{3}{2}\left((t_2 + t_3)\,t_1^2 + \left(t_2^2 + 4t_2 t_3 + t_3^2 + 1\right)t_1 + (t_2 + t_3)\,(t_2 t_3 + 1)\right) - \frac{90\zeta(3)}{(2\pi\mathrm{i})^3} \end{pmatrix}. \tag{5.4.17}$$

Note that entries six and seven are obtained from entry five by the replacements $t_2 \leftrightarrow t_3$ and $t_1 \leftrightarrow t_3$, respectively, and that the last entry is completely symmetric in the three coordinates. This information is sufficient to compute the monodromies M_i around the Batyrev coordinate axes $z_i = 0$, $1 \leq i \leq 3$. As the coordinates are permutation symmetric, M_2 and M_3 can be

logarithmic order	0	1	2	3	4
n.o. solution	1	3	6	10	15
$\mathcal{L}^{(2)}$	–	–	-3	-9	-15
Hodge numbers	1	3	3	1	0

Table 5.1: Estimate for the PFDI of a three-parameter three-fold family. Generically, three second-order operators should restrict the solution space sufficiently.

obtained from symmetry considerations and

$$M_1 = \begin{pmatrix} 1 & 0 & 0 & 0 & 0 & 0 & 0 & 0 \\ 1 & 1 & 0 & 0 & 0 & 0 & 0 & 0 \\ 0 & 0 & 1 & 0 & 0 & 0 & 0 & 0 \\ 0 & 0 & 0 & 1 & 0 & 0 & 0 & 0 \\ 0 & 3 & 6 & 3 & 1 & 0 & 0 & 0 \\ 0 & 3 & 3 & 6 & 0 & 1 & 0 & 0 \\ 0 & 0 & 3 & 3 & 0 & 0 & 1 & 0 \\ -3 & 0 & -3 & -3 & 0 & 0 & -1 & 1 \end{pmatrix}. \tag{5.4.18}$$

The Mori cone is generated by (see eq. (2.2.50))

$$l^{(1)} = (-1,-1,-1;1,1,1,0,0,0,0,0,0)\,, \tag{5.4.19}$$
$$l^{(2)} = (-1,-1,-1;0,0,0,1,1,1,0,0,0)\,, \tag{5.4.20}$$
$$l^{(3)} = (-1,-1,-1;0,0,0,0,0,0,1,1,1)\,. \tag{5.4.21}$$

For three-folds with three-parameters, we usually expect to have three operators of order two generating the PFDI, see Table 5.1. Here, we indeed find three operators

$$\begin{aligned} \mathcal{L}_1^{(2)}(\underline{z}) = &-2\theta_1^2 + \theta_2\theta_1 + (\theta_1-\theta_2)\,\theta_3 \\ &+ z_1\left(2\theta_1^2 + (5\theta_2+5\theta_3+4)\,\theta_1 + 3\theta_2^2 + (\theta_3+1)\,(3\theta_3+2) + \theta_2\,(7\theta_3+5)\right) \\ &+ z_2\left(-\theta_1^2 - (\theta_2+\theta_3+1)\,\theta_1 + \theta_3\,(\theta_2+3\theta_3+1)\right) \\ &+ z_3\left(-\theta_1^2 - (\theta_2+\theta_3+1)\,\theta_1 + \theta_2\,(3\theta_2+\theta_3+1)\right), \end{aligned} \tag{5.4.22}$$

where $\mathcal{L}_2^{(2)}$ and $\mathcal{L}_3^{(2)}$ are obtained by coordinate permutations $z_1 \leftrightarrow z_2$ and $z_1 \leftrightarrow z_3$, respectively.

The $\mathbb{Z}_2$ symmetries between the Batyrev coordinates give rise to supersymmetric flux vacua along the two-dimensional fixed-point loci in the complex-structure moduli space. We will discuss this further in section 6.2. There, we will also see that the symmetry between the three permutations symmetries guarantees that the intersection of the fixed-point loci yields a supersymmetric vacuum. This one-dimensional locus is parametrised by $z \equiv z_1 = z_2 = z_3$ and the periods are given by solutions to the operator [97]

$$\begin{aligned} \mathcal{L}^{(4)}_{\text{AESZ17}}(z) = &\,25\theta^4 - 15z_1\,(51\theta^4 + 84\theta^3 + 72\theta^2 + 30\theta + 5) \\ &+ 6z_1^2\,(531\theta^4 + 828\theta^3 + 541\theta^2 + 155\theta + 15) \\ &- 54z_1^3\,(423\theta^4 + 2160\theta^3 + 4399\theta^2 + 3795\theta + 1170) \\ &+ 243z_1^4\,(279\theta^4 + 1368\theta^3 + 2270\theta^2 + 1586\theta + 402) \\ &- 59049z_1^5\,(1+\theta)^4\,. \end{aligned} \tag{5.4.23}$$

We focus on the asymptotic structure at the MUM point of the family over the symmetric locus inherited from the three-parameter model. First, we give the Riemann symbol of this operator:

$$\mathcal{P}_{\mathcal{L}^{(4)}_{\text{AESZ17}}}\left\{\begin{array}{cccccc|c} 0 & \frac{i}{3\sqrt{3}} & -\frac{i}{3\sqrt{3}} & \frac{1}{27} & \frac{5}{9} & \infty & \\ \hline 0 & 0 & 0 & 0 & 0 & 1 & \\ 0 & 1 & 1 & 1 & 1 & 1 & , z \\ 0 & 1 & 1 & 1 & 3 & 1 & \\ 0 & 2 & 2 & 2 & 4 & 1 & \end{array}\right\}. \tag{5.4.24}$$

The point $z = 5/9$ is a so-called apparent singularity and does not affect the operator's regions of convergence. The local solutions are linear combinations of formal power series and the monodromy around this point is thus trivial. Such points correspond to zeros of the Yukawa coupling

$$C_{zzz} = \frac{90(1-9/5z)}{z^3(1-27z)(1+27z^2)}\,. \tag{5.4.25}$$

For the normalisation, we took the limit $t_i \to t$ in eq. (5.4.17), which yields the asymptotic one-parameter period vector

$$\underline{\Pi}(\underline{t}) \sim \begin{pmatrix} 1 \\ t \\ 15t^2 - 3t - \frac{3}{2} \\ -15t^3 - \frac{9}{2}t + \frac{90\mathrm{i}\zeta_3}{(2\pi\mathrm{i})^3} \end{pmatrix}. \tag{5.4.26}$$

Comparing the cubic term in F_0/X^0 with the appearance of the classical intersection numbers in the prepotential (4.6.45), we find $\kappa_{111} = 90$. In the symmetric limit $t_i \to t$, the prepotential of the three-parameter model becomes

$$\mathcal{F}^{(3)}\big|_{t_i\to t} = \frac{90}{3!}t^3 - \frac{9}{2}t^2 - \frac{3\cdot 36}{24}t - \frac{(-90)\zeta_3}{2(2\pi\mathrm{i})^3} + \mathcal{O}(q)\,. \tag{5.4.27}$$

The asymptotic periods in eq. (5.4.26) can also be described with a prepotential $\mathcal{F}^{(1)} = \mathcal{F}^{(3)}\big|_{t_i\to t}$. However, the double logarithmic period is given by $F^1/X^0 = \frac{1}{3}\partial_t\mathcal{F}$. In the triple-logarithmic period, the normalisation of $\frac{1}{3}$ cancells against the summation over the three Kähler parameter and we have $F_0/X^0 = 2\mathcal{F} - t\partial_t\mathcal{F}$. For such symmetric sub-families, the intersection form is not of the form eq. (5.3.15) but we must account for multiplicities of the intersections

$$\Sigma = \begin{pmatrix} & & 1 \\ & 3 & \\ -3 & & \\ -1 & & \end{pmatrix}. \tag{5.4.28}$$

An intuitive explanation for this matrix comes from the expression $\underline{\Pi}^\dagger\Sigma\,\underline{\Pi}$ in the Kähler potential K in eq. (4.1.14). For K to be identical to that of the restricted three-parameter model, the intersection form must be of the form eq. (5.4.28). An analytical continuation yields the

monodromy group generated by

$$M_0 = \begin{pmatrix} 1 & 0 & 0 & 0 \\ 1 & 1 & 0 & 0 \\ 12 & 30 & 1 & 0 \\ -24 & -54 & -3 & 1 \end{pmatrix}, \quad M_{\frac{\mathrm{i}}{3\sqrt{3}}} = \begin{pmatrix} 10 & 0 & 3 & 3 \\ 3 & 1 & 1 & 1 \\ 0 & 0 & 1 & 0 \\ -27 & 0 & -9 & -8 \end{pmatrix},$$
$$M_{-\frac{\mathrm{i}}{3\sqrt{3}}} = \begin{pmatrix} -8 & -18 & -3 & 3 \\ 3 & 7 & 1 & -1 \\ -18 & -36 & -5 & 6 \\ -27 & -54 & -9 & 10 \end{pmatrix}, \quad M_{\frac{1}{27}} = \begin{pmatrix} 1 & 0 & 0 & 1 \\ 0 & 1 & 0 & 0 \\ 0 & 0 & 1 & 0 \\ 0 & 0 & 0 & 1 \end{pmatrix}, \tag{5.4.29}$$
$$M_\infty = \begin{pmatrix} -5 & -36 & -3 & -7 \\ -4 & -11 & -2 & -3 \\ 0 & 42 & 1 & 6 \\ 24 & 72 & 12 & 19 \end{pmatrix},$$

which satisfy $M^T \Sigma M = \Sigma$ and $M_{\frac{\mathrm{i}}{3\sqrt{3}}} M_0 M_{-\frac{\mathrm{i}}{3\sqrt{3}}} M_{\frac{1}{27}} M_\infty = \mathbb{1}$. Finally, we give the first couple of instanton numbers of the one-parameter model:

$$n_1 = 108\,, \quad n_2 = 351\,, \quad n_3 = 2124\,, \quad n_4 = 12987\,. \tag{5.4.30}$$

These numbers can also be obtained from the instanton numbers n_{ijk} of the three-parameter model, where the symmetric limit corresponds to $n_i = \sum_{|\underline{m}|=i} n_{\underline{m}}$ with $\underline{m} \in \mathbb{N}_0^3$.

5.4.2 Four-folds

While the special geometry property of the complex-structure moduli space for three-folds is sufficient for the computation of an asymptotic integral period basis, this no longer holds in higher dimensions. When we introduced the formalism to obtain integral period bases for Calabi–Yau n-folds in section 5.3, we explained the restriction of the tuples N_k which results in an integral monodromy using the hypersurfaces $\mathbb{P}_{18,12,3,1^3}[36]$. Here, we will discuss the four-fold structure on the simpler family $\mathbb{P}_{12,8,1^4}[24]$ with toric data in Table 5.2 further and exemplify the decomposition of the four-point couplings into triple couplings.

We again first give the topological data consisting of the intersection ring

$$R = 64J_1^4 + 16J_1^3 J_2 + 4J_1^2 J_2^2 + J_1 J_2^3 \tag{5.4.31}$$

and the integrals of the Chern classes

$$c_2 \cdot J_1^2 = 728\,, \quad c_2 \cdot J_1 J_2 = 182\,, \quad c_2 \cdot J_2^2 = 48\,, \tag{5.4.32}$$
$$c_3 \cdot J_1 = -3860\,, \quad c_3 \cdot J_2 = -960\,, \tag{5.4.33}$$
$$\chi = 23328\,. \tag{5.4.34}$$

At level two, representing the cohomology group $H^{2,2}$, we start with the three tuples

$$\mathcal{N}_2 = ([1,1],[1,2],[2,2])\,, \tag{5.4.35}$$

points						l-vectors	
(1	0	0	0	0	0)	-6	0
(1	1	0	0	0	0)	3	0
(1	0	1	0	0	0)	2	0
(1	0	0	1	0	0)	0	1
(1	0	0	0	1	0)	0	1
(1	0	0	0	0	1)	0	1
(1	-12	-8	-1	-1	-1)	0	1
(1	-3	-2	0	0	0)	1	-4

Table 5.2: Integral points and their scaling relations for the mirror of $\mathbb{P}_{12,8,1^4}[24]$.

corresponding to J_1^1, $J_1 J_2$ and J_2^2. The intersection form follows from eq. (5.4.31)

$$c_2 = \begin{pmatrix} 64 & 16 & 4 \\ 16 & 4 & 1 \\ 4 & 1 & 0 \end{pmatrix} . \tag{5.4.36}$$

The kernel of this matrix is generated by $(1, -4, 0)$. Following section 5.3, we conclude that we should omit $[1, 1]$ in N_2. In general, one can show that the central charge corresponding to the sheaf $\mathcal{O}_i$ under a monodromy around z_r obtains the contribution

$$M_r : \ \Pi_{\mathcal{O}_{D_i}} \longmapsto \Pi_{\mathcal{O}_i} + \Pi_{\mathcal{O}_{D_i \cap D_r}} + C_{irrj} t^j \, . \tag{5.4.37}$$

We deduce that integrality of the monodromies demands that the central charges of $\mathcal{O}_{D_i \cap D_r}$ must be obtained by integral combinations of the basis elements at this level. The set N_2 then consists only of the single element $\underline{s}_2 = (2, 3)$ and we have for the 2×2-block in the intersection form $\hat{\Sigma}$ (5.3.14)

$$\hat{\sigma} = \begin{pmatrix} 0 & 1 \\ 1 & 4 \end{pmatrix} . \tag{5.4.38}$$

Note that we sort the generalised B-periods in reverse order, causing the reversed orientation compared to eq. (5.4.36). At level three, we have

$$\mathcal{N}_3 = ([1, 1, 1], [1, 1, 2], [1, 2, 2], [2, 2, 2]) \, , \tag{5.4.39}$$

where the first one is not horizontal to $\underline{s}_2$. There are two possibilities $N_3 = (\{2, 4\}, \{3, 4\})$; here, we choose $\underline{s}_3 = (3, 4) = ([1, 2, 2], [2, 2, 2])$. At level four, there are two horizontal non-vanishing choices $N_4 = (\{[1, 1, 2, 2]\}, \{[1, 2, 2, 2]\})$; we pick the first one $s_4^1 = [1, 1, 2, 2]$. Starting from the back, we immediately find

$$\mathfrak{c}_4^{1122} = \frac{1}{4} \tag{5.4.40}$$

and thus

$$\widetilde{\mathcal{O}}_{n,1} = \frac{1}{4} \mathcal{O}_{D_1 \cap D_1 \cap D_2 \cap D_2} \, . \tag{5.4.41}$$

At level three, we have the intersection form

$$c^3_{i,l} = \begin{pmatrix} c^3_{1221} & c^3_{1222} \\ c^3_{2221} & c^3_{2222} \end{pmatrix} = \begin{pmatrix} 4 & 1 \\ 1 & 0 \end{pmatrix}, \tag{5.4.42}$$

where the row index i is in N_3 and l is in N_1. This implies that the inverse couplings read

$$\mathfrak{c}_3^{l,j} = \begin{pmatrix} \mathfrak{c}_3^{1122} & \mathfrak{c}_3^{1222} \\ \mathfrak{c}_3^{2122} & \mathfrak{c}_3^{2222} \end{pmatrix} = \begin{pmatrix} 4 & 1 \\ 1 & 0 \end{pmatrix}^{-1} = \begin{pmatrix} 0 & 1 \\ 1 & -4 \end{pmatrix}. \tag{5.4.43}$$

These give the basis of sheaves at this level via

$$\underline{\widetilde{\mathcal{O}}}_3 = \begin{pmatrix} 0 & 1 \\ 1 & -4 \end{pmatrix} \begin{pmatrix} \mathcal{O}_{D_1\cap D_2\cap D_2} \\ \mathcal{O}_{D_2\cap D_2\cap D_2} \end{pmatrix}. \tag{5.4.44}$$

Recall that the B-periods, corresponding to the levels $k \leq 2$, are obtained directly from the tuples and no contraction with inverse couplings takes place, cf. eq. (5.3.10). For this model, the two basis changes taking $\underline{\widetilde{\mathcal{O}}}$ to a block-anti-diagonal intersection form via eq. (5.3.13) are given by

$$R_1 = \begin{pmatrix} 1 & 0 & 0 & 0 & 0 & 0 & 0 & 0 \\ 0 & 1 & 0 & 0 & 0 & 0 & 0 & 0 \\ 3 & 0 & 1 & 0 & 0 & 0 & 0 & 0 \\ -4 & 0 & 0 & 1 & 0 & 0 & 0 & 0 \\ -19 & 0 & 0 & 0 & 1 & 0 & 0 & 0 \\ -2 & 0 & 0 & 0 & 0 & 1 & 0 & 0 \\ -33 & 0 & 0 & 0 & 0 & 0 & 1 & 0 \\ -1 & 0 & 0 & 0 & 0 & 0 & 0 & 1 \end{pmatrix}, \; R_2 = \begin{pmatrix} 1 & 0 & 0 & 0 & 0 & 0 & 0 & 0 \\ 0 & 1 & 0 & 0 & 0 & 0 & 0 & 0 \\ 0 & 0 & 1 & 0 & 0 & 0 & 0 & 0 \\ 0 & -1 & 0 & 1 & 0 & 0 & 0 & 0 \\ 0 & 2 & 2 & 0 & 1 & 0 & 0 & 0 \\ 0 & 17 & 2 & 0 & 0 & 1 & 0 & 0 \\ 0 & 33 & 0 & 0 & 0 & 0 & 1 & 0 \\ 0 & 0 & 0 & 0 & 0 & 0 & 0 & 1 \end{pmatrix}. \tag{5.4.45}$$

We use the map eq. (5.2.1) to assign Chern characters to these sheaves and compute their central charges with eq. (5.2.5). The result is the asymptotic period vector

$$\underline{\Pi}(\underline{t}) \sim \begin{pmatrix} 1 \\ t_1 \\ t_2 \\ 2t_1^2 + t_1t_2 - 2t_1 - 2 \\ 8t_1^2 + 4t_1t_2 + \frac{t_2^2}{2} - 8t_1 - \frac{t_2}{2} - \frac{91}{12} \\ -\frac{1}{3}8t_1^3 - 2t_1^2t_2 - \frac{1}{2}t_1t_2^2 + t_1^2 + \frac{t_1t_2}{2} + \frac{37t_1}{4} - 1 + \frac{120\mathrm{i}\zeta_3}{\pi^3} \\ -\frac{1}{3}32t_1^3 - 8t_1^2t_2 - 2t_1t_2^2 - \frac{t_2^3}{6} + 16t_1^2 + 8t_1t_2 + t_2^2 - 8t_1 - \frac{41t_2}{4} - \frac{91}{6} + \frac{965\mathrm{i}\zeta_3}{2\pi^3} \\ \frac{8t_1^4}{3} + \frac{8}{3}t_1^3t_2 + t_1^2t_2^2 + \frac{1}{6}t_1t_2^3 + \frac{91t_1^2}{6} + \frac{91t_1t_2}{12} + t_2^2 - \frac{5\mathrm{i}(193t_1+48t_2)\zeta_3}{2\pi^3} - \frac{43}{6} \end{pmatrix}. \tag{5.4.46}$$

For a detailed analysis of the complex-structure moduli space and the monodromies around the singular loci, see [1]. For the instanton-corrected discussion in the following, we match the solutions of the Picard–Fuchs operator with eq. (5.4.46) to obtain the integral period vector.

For a two-parameter four-fold family with Hodge structure $(1, 2, 2, 2, 1)$, we expect one second and one fourth order differential operator, see Table 5.3. Let us note here that this counting of generic solutions must take into account relations among the z-constant terms of the differential operators. For example, for three-parameter models with Hodge structure $(1, 3, 4, 3, 1)$, one typically finds two second-order and one third-order operator. Counting solutions as in Table 5.3, one must subtract one restriction at logarithmic order five, stemming from a relation among the two operators $\underline{\partial}^2\mathcal{L}_i^{(2)}$. For the model at hand, we find from the l-vectors

$$l^{(1)} = (-6; 3, 2, 1, 0, 0, 0, 0), \quad l^{(2)} = (0; 0, 0, -4, 1, 1, 1, 1) \tag{5.4.47}$$

logarithmic order	0	1	2	3	4	5
n.o. solution	1	2	3	4	5	6
$\mathcal{L}^{(2)}$	–	–	-1	-2	-3	-4
$\mathcal{L}^{(4)}$	–	–	–	–	-1	-2
Hodge numbers	1	2	2	2	1	0

Table 5.3: Estimate for the PFDI of a two-parameter four-fold family. Such families typically have one second-order together and one fourth-order operator spanning the differential ideal.

the generators of the Picard–Fuchs system

$$\mathcal{L}^{(2)} = \theta_1 \left(\theta_1 - 4\theta_2\right) - 12 z_1 \left(6\theta_1 + 1\right)\left(6\theta_1 + 5\right), \tag{5.4.48}$$

$$\mathcal{L}^{(4)} = \theta_2^4 - z_2 \left(\theta_1 - 4\theta_2 - 3\right)\left(\theta_1 - 4\theta_2 - 2\right)\left(\theta_1 - 4\theta_2 - 1\right)\left(\theta_1 - 4\theta_2\right). \tag{5.4.49}$$

The four-point couplings are obtained by solving the system of eqs. (4.5.12) and (4.5.22). As for the previous models, we normalise them such that the constant terms in C_{ijkl} are given by the classical intersection numbers[3]

$$\begin{aligned}
C_{z_1z_1z_1z_1} &= \frac{64}{z_1^4\Delta_1}\,, & C_{z_1z_1z_1z_2} &= \frac{16(1-432z_1)}{z_1^3 z_2\Delta_1}\,,\\
C_{z_1z_1z_2z_2} &= \frac{4(1-432z_1)^2}{z_1^2 z_2^2\Delta_1}\,, & C_{z_1z_2z_2z_2} &= \frac{(1-432z_1)^3}{z_1 z_2^3\Delta_1}\,,\\
C_{z_2z_2z_2z_2} &= \frac{64\left(864z_1-1\right)\left(1-864z_1\left(1-432z_1\right)\right)}{z_2^3\Delta_1\Delta_2}\,,
\end{aligned} \tag{5.4.50}$$

where we denoted the discriminant factors by $\Delta_1 = \left(1-432z_1\right)^4 - 8916100448256 z_1^4 z_2$ and $\Delta_2 = 1 - 256 z_2$. These can either be read-off from the couplings or computed by toric methods as discussed at the end of section 2.2. The q-expansions $C_{ijkl}(\underline{t})$ of the couplings can be obtained from eq. (4.5.17). We mentioned before that all $(p > 3)$-point couplings can be written in terms of three-point couplings. To see how this works for four-folds, we turn to the Griffiths transversality conditions (4.2.15). Working in t coordinates, we expand the holomorphic $(4,0)$-form in terms of the periods in eq. (5.4.46)

$$\Omega_0 = \alpha_0 + t^i\alpha_i + H^\alpha\gamma_\alpha + F_i\beta^i + F_0\beta^0\,. \tag{5.4.51}$$

The homology basis $(\alpha_I, \gamma_\alpha, \beta^I)$ was introduced in section 4.1. For better readability, we write the contraction with the respective block in Σ as "$\cdot$" and abbreviate the derivative as $\partial_{t^i} \equiv \partial_i$. Then, the relations from Griffiths transversality read [112]

$$0 = 2X\cdot F + H\cdot H\,, \tag{5.4.52}$$

$$0 = \partial_i F_0 - t^j\partial_i F_j + H\cdot\partial_i H - F_i\,, \tag{5.4.53}$$

$$0 = \partial_i\partial_j F_0 - t^k\partial_i\partial_j F_k + H\cdot\partial_i\partial_j H\,, \tag{5.4.54}$$

$$0 = \partial_i\partial_j\partial_k F_0 - t^l\partial_i\partial_j\partial_k F_l + H\cdot\partial_i\partial_j\partial_k H\,, \tag{5.4.55}$$

$$C_{ijkl} = \partial_i\partial_j\partial_k\partial_l F_0 - t^m\partial_i\partial_j\partial_k\partial_l F_m + H\cdot\partial_i\partial_j\partial_k\partial_l H\,. \tag{5.4.56}$$

[3]These couplings were obtained with a Mathematica code written by Albrecht Klemm.

We differentiate eqs. (5.4.54) and (5.4.55) and obtain the relations

$$\begin{aligned} 0 &= \partial_i\partial_j\partial_k F_0 - t^l\partial_i\partial_j\partial_k F_l - \partial_i\partial_j F_k + \partial_k H\cdot\partial_i\partial_j H + H\cdot\partial_i\partial_j\partial_k H \\ &\overset{(5.4.55)}{=} -\partial_i\partial_j F_k + \partial_k H\cdot\partial_i\partial_j H\,, \end{aligned} \tag{5.4.57}$$

$$\begin{aligned} 0 &= \partial_i\partial_j\partial_k\partial_l F_0 - t^m\partial_i\partial_j\partial_k\partial_l F_m - \partial_i\partial_j\partial_k F_l + \partial_l H\cdot\partial_i\partial_j\partial_k H + H\cdot\partial_i\partial_j\partial_k\partial_l H \\ &\overset{(5.4.56)}{=} C_{ijkl} - \partial_i\partial_j\partial_k F_l + \partial_l H\cdot\partial_i\partial_j\partial_k H\,. \end{aligned} \tag{5.4.58}$$

Finally, we consider the derivative of eq. (5.4.57) and compare it to eq. (5.4.57), yielding the decomposition

$$C_{ijkl} = \partial_i\partial_j H\cdot\partial_k\partial_l H = \sigma_{\alpha\beta}C_{ij}{}^{\alpha}C_{kl}{}^{\beta}\,. \tag{5.4.59}$$

Recall that σ is given by the inverse of $\hat{\sigma}$ in eq. (5.4.38). The functions $C_{ij}^{\alpha} = \partial_i\partial_j H^{\alpha}$ are the three-point functions. Their q-expansions are readily computed to be

$$\begin{aligned} C_{11}{}^{1} &= 4 + \mathcal{O}\big(q^2\big)\,, & C_{11}{}^{2} &= 16 + 960q_1 + \mathcal{O}\big(q^2\big)\,, \\ C_{12}{}^{1} &= 1 + \mathcal{O}\big(q^2\big)\,, & C_{12}{}^{2} &= 4 + \mathcal{O}\big(q^2\big)\,, \\ C_{22}{}^{1} &= -20q_2 + \mathcal{O}\big(q^2\big)\,, & C_{22}{}^{2} &= 1 + \mathcal{O}\big(q^2\big)\,. \end{aligned} \tag{5.4.60}$$

Note that the constant terms follow directly from the asymptotic form of $\underline{\Pi}$ in eq. (5.4.46) while the instanton corrections stem from the solutions to the Picard–Fuchs equation and the mirror map $z(q)$.

In section 4.6, we reviewed the description of the one-parameter K3 period geometry as a symmetric square of a second order Calabi–Yau operator. Similarly, the periods of a one-parameter four-fold family can be described by the anti-symmetric square of a Calabi–Yau three-fold operator. We will discuss this in more detail in section 6.4, where we will study the relation between three- and four-fold operators in the context of type IIB and M-theory flux vacua.

5.5 Higher-dimensional Calabi–Yau families

The description of an integral period basis proposed in section 5.3 is especially interesting for dimensions $n > 4$. Special geometry yields an integral basis for three-folds via a prepotential, cf. section 4.6. In the language of sheaves, the A-periods (holomorphic and single-logarithmic) correspond to the skyscraper sheaf (5.2.7) and twisted structure sheaves on curves dual to Kähler divisors (5.2.6). The B-periods are, as in our formalism, described by structure sheaves on the entire manifold and on divisors. For four-folds, this basis is extended by structure sheaves on independent intersections of divisors. The double-logarithmic A-periods appearing at $n = 5$ require us to describe them as linear combinations of structure sheaves on triple intersections of divisors, where integrality of the monodromies and an intersection of canonical form follow after contraction with the inverse couplings as in eq. (5.3.10).

In this subsection, we supplement the proposed formalism with data for several Calabi–Yau families. We begin with an analytical continuation of the five-fold family $\mathbb{P}_{15,10,1^5}[30]$ to a conifold singularity and the orbifold point. We identify the vanishing conifold cycle and the splitting of Hodge structure at infinity. This model is an elliptic fibration over $\mathbb{P}^4$ and the five-fold relative of the well-known three- and four-fold models $\mathbb{P}_{9,6,1^3}[18]$ and $\mathbb{P}_{12,8,1^4}[24]$. Afterwards, we

points							l-vectors	
(1	0	0	0	0	0	0)	0	−6
(1	1	0	0	0	0	0)	0	3
(1	0	1	0	0	0	0)	0	2
(1	0	0	1	0	0	0)	1	0
(1	0	0	0	1	0	0)	1	0
(1	0	0	0	0	1	0)	1	0
(1	0	0	0	0	0	1)	1	0
(1	-15	-10	-1	-1	-1	-1)	1	0
(1	-3	-2	0	0	0	0)	-5	1

Table 5.4: Integral points and their scaling relations of the polytope describing the mirror of $\mathbb{P}_{15,10,1^5}[36]$. The origin is parametrised by the modulus ψ and the last entry by ϕ.

discuss the global monodromy groups of the hypersurfaces in $\mathbb{P}^{n+1}$ for $5 \leq n \leq 9$. Finally, we list the first genus-zero invariants of the aforementioned five-fold together with one six- and one seven-dimensional two-parameter CICY in appendix B. For these two-parameter models, we verified integrality of the invariants up to degree ten.

5.5.1 Elliptically fibred five-fold

The family in $\mathbb{P}_{15,10,1^5}$ is given by the vanishing locus of the defining polynomial

$$P_{\mathcal{X}_{30}} = x_1^2 + x_2^3 + \sum_{i=3}^{7} x_i^{30} + \psi \prod_{i=1}^{7} x_i + \phi \prod_{i=3}^{6} x_i^6 \,. \tag{5.5.1}$$

The classical intersections of the two Kähler classes J_1 and J_2 corresponding to the fibre and the base, respectively, are given by

$$R = 625J_1^5 + 125J_1^4J_2 + 25J_1^3J_2^2 + 5J_1^2J_2^3 + J_1J_2^4 \,. \tag{5.5.2}$$

The Chern classes integrate to

$$c_2 \cdot J_1^3 = 7125\,, \quad c_2 \cdot J_1^2J_2 = 1425\,, \quad c_2 \cdot J_1J_2^2 = 285\,, \quad c_2 \cdot J_2^3 = 60\,, \tag{5.5.3}$$

$$c_3 \cdot J_1^2 = -37700\,, \quad c_3 \cdot J_1J_2 = -7540\,, \quad c_3 \cdot J_2^2 = -1500\,, \tag{5.5.4}$$

$$c_4 \cdot J_1 = 227955\,, \quad c_4 \cdot J_2 = 45600\,, \tag{5.5.5}$$

$$\chi = -1367400\,. \tag{5.5.6}$$

We collect the toric data together with the generators of the Mori cone in Table 5.4. The Picard–Fuchs ideal is generated by

$$\mathcal{L}^{(2)} = \theta_1\left(\theta_1 - 5\theta_2\right) - 12\left(36\theta_1^2 + 36\theta_1 + 5\right)z_1\,, \tag{5.5.7}$$

$$\begin{aligned}\mathcal{L}^{(5)} = \theta_2^5 + z_2\big[&- \theta_1^5 + 5\theta_1^4\left(5\theta_2 + 2\right) - 5\theta_1^3\left(50\theta_2^2 + 40\theta_2 + 7\right) \\ &+ 25\theta_1^2\left(50\theta_2^3 + 60\theta_2^2 + 21\theta_2 + 2\right) \\ &- \theta_1\left(3125\theta_2^4 + 5000\theta_2^3 + 2625\theta_2^2 + 500\theta_2 + 24\right) \\ &+ 5\theta_2\left(625\theta_2^4 + 1250\theta_2^3 + 875\theta_2^2 + 250\theta_2 + 24\right)\big]\,.\end{aligned} \tag{5.5.8}$$

We note that a similar analysis as for the four-fold in Table 5.3 shows that these are again the operators one would expect generically.

Here, we will shorten the discussion of the integral period basis construction and refer to the three- and four-fold cases above for elaborate examples. We supplement $\underline{s}_0 = ()$ and $\underline{s}_1 = ([1],[2])$ to an index basis with

$$\begin{aligned} \underline{s}_2 &= ([1,2],[2,2])\,, & \underline{s}_3 &= ([1,2,2],[2,2,2])\,, \\ \underline{s}_4 &= ([1,2,2,2],[2,2,2,2])\,, & \underline{s}_5 &= ([1,1,2,2,2])\,. \end{aligned} \tag{5.5.9}$$

This yields the asymptotic period basis

$$\underline{\Pi}(\underline{t}) \sim \begin{pmatrix} 1 \\ t_1 \\ t_2 \\ \frac{1}{2}t_1\left(5t_1+2t_2\right)-\frac{5}{2}t_1-\frac{5}{2} \\ \frac{t_2^2}{2}-\frac{t_2}{2}+\frac{5}{8} \\ -\frac{1}{6}t_1\left(25t_1^2+15t_2t_1+3t_2^2\right)+\frac{3}{2}t_1\left(5t_1+2t_2\right)+\frac{5}{24}\left(41t_1+12t_2\right)-\frac{15}{2}+\frac{375i\zeta(3)}{2\pi^3} \\ -\frac{1}{6}\left(5t_1+t_2\right)^3+\frac{3}{2}\left(5t_1+t_2\right)^2+\frac{1}{24}\left(1025t_1+253t_2\right)-\frac{285}{8}+\frac{1885i\zeta(3)}{2\pi^3} \\ \frac{1}{24}t_1\left(5t_1+2t_2\right)\left(25t_1^2+10t_2t_1+2t_2^2\right)-\frac{1}{12}t_1\left(25t_1^2+15t_2t_1+3t_2^2\right) \\ \ldots+\frac{1}{48}\left(1445t_1^2+578t_2t_1+60t_2^2\right)-\frac{5}{48}\left(\frac{24i(377t_1+75t_2)\zeta(3)}{\pi^3}+547t_1+12t_2\right)-\frac{265}{16}+\frac{375i\zeta(3)}{4\pi^3} \\ \frac{1}{24}\left(5t_1+t_2\right)^4-\frac{5}{12}\left(5t_1+t_2\right)^3+\frac{385}{48}\left(5t_1+t_2\right)^2-\frac{5(5t_1+t_2)\left(335\pi^3+9048i\zeta(3)\right)}{48\pi^3} \\ \ldots-\frac{50267}{384}+\frac{9425i\zeta(3)}{4\pi^3} \\ -\frac{1}{24}t_1\left(125t_1^4+125t_2t_1^3+50t_2^2t_1^2+10t_2^3t_1+t_2^4\right)-\frac{5}{48}\left(475t_1^3+285t_2t_1^2+57t_2^2t_1+4t_2^3\right) \\ \ldots+\frac{5i\left(1885t_1^2+754t_2t_1+75t_2^2\right)\zeta(3)}{4\pi^3}+\frac{1}{384}\left(22883t_1+4600t_2\right)+\frac{35825i\zeta(3)}{16\pi^3}-\frac{234375i\zeta(5)}{8\pi^5} \end{pmatrix}. \tag{5.5.10}$$

Note that the last three periods extend over two lines each. The three basis changes (5.3.13) bringing Σ into canonical form (5.3.15) are integral. The monodromies M_i around the loci $z_i = 0$ are given by

$$M_1 = \begin{pmatrix} 1 & 0 & 0 & 0 & 0 & 0 & 0 & 0 & 0 & 0 \\ 1 & 1 & 0 & 0 & 0 & 0 & 0 & 0 & 0 & 0 \\ 0 & 0 & 1 & 0 & 0 & 0 & 0 & 0 & 0 & 0 \\ 0 & 5 & 1 & 1 & 0 & 0 & 0 & 0 & 0 & 0 \\ 0 & 0 & 0 & 0 & 1 & 0 & 0 & 0 & 0 & 0 \\ 0 & -10 & 0 & -5 & -1 & 1 & 0 & 0 & 0 & 0 \\ 0 & -50 & 0 & -25 & -5 & 0 & 1 & 0 & 0 & 0 \\ 0 & 180 & 28 & 25 & 5 & 0 & -1 & 1 & 0 & 0 \\ 0 & 750 & 130 & 75 & 15 & 0 & -5 & 0 & 1 & 0 \\ -126 & -750 & -130 & -75 & -15 & 0 & 5 & 0 & -1 & 1 \end{pmatrix}, \tag{5.5.11}$$

$$M_2 = \begin{pmatrix} 1 & 0 & 0 & 0 & 0 & 0 & 0 & 0 & 0 & 0 \\ 0 & 1 & 0 & 0 & 0 & 0 & 0 & 0 & 0 & 0 \\ 1 & 0 & 1 & 0 & 0 & 0 & 0 & 0 & 0 & 0 \\ 0 & 1 & 0 & 1 & 0 & 0 & 0 & 0 & 0 & 0 \\ 0 & 0 & 1 & 0 & 1 & 0 & 0 & 0 & 0 & 0 \\ 0 & 0 & 0 & -1 & 0 & 1 & 0 & 0 & 0 & 0 \\ 0 & 0 & 2 & -5 & -1 & 0 & 1 & 0 & 0 & 0 \\ 0 & 28 & 5 & 3 & 0 & -1 & 0 & 1 & 0 & 0 \\ -51 & 130 & 26 & 5 & 1 & 0 & -1 & 0 & 1 & 0 \\ -5 & -79 & -5 & -3 & 0 & 1 & 0 & -1 & 0 & 1 \end{pmatrix}. \tag{5.5.12}$$

We match the leading order in $\underline{\Pi}(\underline{t})$ with the solutions of the Picard–Fuchs system to obtain the integral period vector $\underline{\Pi}(\underline{z})$. The discriminant of the polytope of Table 5.4 has two components

given by the vanishing locus of

$$\Delta_1 = (1 - 432 z_1)^5 - 2^{20} 3^{15} 5^5 z_1^5 z_2 \,, \tag{5.5.13}$$

$$\Delta_2 = 1 - 5^5 z_2 \,. \tag{5.5.14}$$

We perform an analytical continuation to the neighbourhood of $(z_1 = 0, \Delta_2 = 0)$ to verify integrality of the monodromy representation of a path encircling the discriminant component $\Delta_2 = 0$

$$M_{\Delta_2} = \begin{pmatrix} 1 & 0 & 0 & 0 & 0 & 0 & 0 & 0 & 0 & 0 \\ 0 & 1 & 51 & 10 & 3 & 0 & -2 & -5 & 1 & 0 \\ 0 & 0 & -254 & -50 & -15 & 0 & 10 & 25 & -5 & 0 \\ 0 & 0 & -102 & -19 & -6 & 0 & 4 & 10 & -2 & 0 \\ 0 & 0 & 0 & 0 & 1 & 0 & 0 & 0 & 0 & 0 \\ 0 & 0 & -153 & -30 & -9 & 1 & 6 & 15 & -3 & 0 \\ 0 & 0 & -510 & -100 & -30 & 0 & 21 & 50 & -10 & 0 \\ 0 & 0 & -2601 & -510 & -153 & 0 & 102 & 256 & -51 & 0 \\ 0 & 0 & 0 & 0 & 0 & 0 & 0 & 0 & 1 & 0 \\ 0 & 0 & 0 & 0 & 0 & 0 & 0 & 0 & 0 & 1 \end{pmatrix} . \tag{5.5.15}$$

Furthermore, we find that the vanishing cycle is expressed in the homology basis $\{\gamma_i\}_i$ (cf. section 4.1) by

$$g^T \Sigma = (0, 0, -102, -20, -6, 0, 4, 10, -2, 0) \,, \tag{5.5.16}$$

with $g^T \Sigma \Pi(z_1, \Delta_2 = 0) = 0$. This vanishing cycle is the analogue of the supersymmetric four-fold vacuum discussed in [1]. Its origin will be discussed further in section 7.2, where we will give an instruction on how to find such vanishing cycles from the toric data alone.

As further support for the integrality claim, we want to discuss another integral property of the family. In short, the Hodge structure splits at the point $\psi = \phi = 0$, which we verify explicitly below. Assuming familiarity with section 6.1, one concludes this as follows. In the language of section 2.3, the mirror family has the residual symmetry $\mathbb{Z}_{30} : (0, 0, 0, 0, 0, 0, 1)$ acting as $(\psi, \phi) \mapsto (\alpha\psi, \alpha^6\phi)$. Furthermore, the cohomology has the $\mathbb{Z}_{30}$-weights

$$\{1, \mathbf{5}, 7, 11, 13, 17, 19, 23, \mathbf{25}, 29\} \,,$$

where we emboldened the unfaithful eigenvalues [113]. These values $\mathbf{5}$ and $\mathbf{25}$ correspond to ψ^5 and $\overline{\psi}^5$ parametrising the deformations $x_2 x_3^4 x_4^4 x_5^4 x_6^4 x_7^4$ and its conjugate. Here, we used the Jacobian ideal[4] to remove all appearances of x_i with exponent larger or equal to $w_i - 1$. Note that the $\mathbb{Z}_{30}$-weights of the forms obtain one unit from Ω. At $\phi = 0$ (and only there[5]), ϕ is subject to a cyclic symmetry of order six, which implies a Hodge splitting at $\psi = \phi = 0$.

To perform an analytical continuation to the neighbourhood of $\psi = \phi = 0$, we follow the analysis of the moduli space of the four-fold analogue $\mathbb{P}_{12,8,1^4}[24]$ in [1]. In fact, the moduli spaces of the elliptic fibrations over $\mathbb{P}^3$ and $\mathbb{P}^4$ are natural generalisation of those of the fibration over

[4] The usage of the Jacobian ideal to reduce the exponents of the deformations can be simplified by including the points in faces of codimension one, here $(-1, 0, 0, 0, 0, 0)$, $(-1, -1, 0, 0, 0, 0)$ and $(-2, -1, 0, 0, 0, 0)$ and using eq. (2.2.36) to express them in homogeneous coordinates as $x_2^2 x_3^2 x_4^2 x_5^2 x_6^2$, $x_1 x_3^3 x_4^3 x_5^3 x_6^3$ and $x_2 x_3^4 x_4^4 x_5^4 x_6^4$.

[5] Putting it in terms used in [113], the periodicity condition is not satisfied due to $D \nmid N$, where $D = 5$ is the order in $\mathbb{Z}_{30}$ of ϕ and $N = 6$ the order of the deformation decoupling.

$\mathbb{P}^2$. The limited region of convergence at the MUM point requires us to take several intermediate points[6], where we obtained the monodromy representations

$$M_{D_1'} = \begin{pmatrix} 1 & -1 & 0 & 0 & 0 & 0 & 0 & 0 & 0 & 0 \\ 0 & 1 & 0 & 0 & 0 & 0 & 0 & 0 & 0 & 0 \\ 0 & -5 & 1 & -1 & 0 & 0 & 0 & 0 & 0 & 0 \\ 0 & 5 & 0 & 1 & 0 & 0 & 0 & 0 & 0 & 0 \\ 0 & -35 & 0 & -5 & 1 & 1 & 0 & 0 & 0 & 0 \\ 0 & -10 & 0 & -5 & 0 & 1 & 0 & 0 & 0 & 0 \\ 0 & -10 & 0 & -28 & -5 & 0 & 1 & 1 & 0 & 0 \\ 0 & 5 & 0 & 0 & 0 & 0 & 0 & 1 & 0 & 0 \\ 0 & 126 & 5 & 0 & 15 & 25 & -5 & 0 & 1 & 1 \\ 0 & 0 & 0 & 0 & 0 & 0 & 0 & 0 & 0 & 1 \end{pmatrix}, \tag{5.5.17}$$

$$M_{\Delta_0} = \begin{pmatrix} 0 & 1 & 0 & 0 & 0 & 0 & 0 & 0 & 0 & 0 \\ -1 & 1 & 0 & 0 & 0 & 0 & 0 & 0 & 0 & 0 \\ 5 & 0 & 0 & 1 & 0 & 0 & 0 & 0 & 0 & 0 \\ 5 & -5 & -1 & 1 & 0 & 0 & 0 & 0 & 0 & 0 \\ -15 & 25 & 5 & 0 & 0 & -1 & 0 & 0 & 0 & 0 \\ 15 & -15 & -5 & 5 & 1 & 1 & 0 & 0 & 0 & 0 \\ 10 & 0 & 0 & 28 & 5 & 0 & 0 & -1 & 0 & 0 \\ 55 & -5 & -3 & 0 & -5 & -5 & 1 & 1 & 0 & 0 \\ 0 & -126 & -5 & 0 & -15 & -25 & 5 & 0 & 0 & -1 \\ 1 & 0 & 55 & 10 & 15 & 15 & -5 & -5 & 1 & 1 \end{pmatrix}, \tag{5.5.18}$$

$$M_{E_0} = \begin{pmatrix} 1 & 1 & 55 & 10 & 15 & 15 & -5 & -5 & 1 & 1 \\ 0 & 1 & 55 & 10 & 15 & 15 & -5 & -5 & 1 & 0 \\ 0 & 0 & -275 & -49 & -75 & -75 & 25 & 25 & -5 & 0 \\ 0 & -5 & -276 & -49 & -75 & -75 & 25 & 25 & -5 & 0 \\ 0 & 25 & 830 & 150 & 225 & 224 & -75 & -75 & 15 & 0 \\ 0 & -15 & -830 & -145 & -224 & -224 & 75 & 75 & -15 & 0 \\ 0 & 0 & -550 & -72 & -145 & -150 & 50 & 49 & -10 & 0 \\ 0 & -5 & -3028 & -550 & -830 & -830 & 276 & 276 & -55 & 0 \\ 0 & -126 & -5 & 0 & -15 & -25 & 5 & 0 & 0 & -1 \\ 0 & 0 & 0 & 0 & 0 & 0 & 0 & 0 & 0 & 1 \end{pmatrix}, \tag{5.5.19}$$

$$M_{S_0} = \begin{pmatrix} 0 & 0 & -55 & -10 & -15 & -15 & 5 & 5 & -1 & -1 \\ -1 & 1 & -55 & -10 & -15 & -15 & 5 & 5 & -1 & 0 \\ 5 & 0 & 331 & 60 & 90 & 90 & -30 & -30 & 6 & 1 \\ 6 & -1 & 330 & 61 & 90 & 90 & -30 & -30 & 6 & 0 \\ -20 & 0 & -1156 & -210 & -314 & -315 & 105 & 105 & -21 & -1 \\ 21 & -1 & 1155 & 211 & 315 & 316 & -105 & -105 & 21 & 0 \\ 10 & -5 & 382 & 75 & 106 & 105 & -34 & -35 & 7 & -3 \\ 61 & -26 & 3075 & 558 & 840 & 841 & -280 & -279 & 56 & -5 \\ 0 & -130 & -4373 & -790 & -1185 & -1185 & 396 & 395 & -78 & -79 \\ 5 & 51 & 0 & 0 & 0 & 0 & 0 & 1 & 0 & -4 \end{pmatrix}, \tag{5.5.20}$$

whose labels correspond to those used in Fig. 1 of [1]. The point $\psi = \phi = 0$ lies at the intersection $S_0 \cap \Delta_0$. We verified that all monodromies leave the pairing Σ invariant. Note that, as expected, $M_{S_0}^5 = M_{\Delta_0}$. Following section 6.1, we rotate the Frobenius basis of the PF ideal into a basis

[6] I thank Janis Dücker for explaining the geometry of the resolved moduli space to me.

with monodromy representation in block diagonal form

$$m_{S_0} = \begin{pmatrix} 1 & -1 & 0 & 0 & 0 & 0 & 0 & 0 & 0 & 0 \\ 1 & 0 & 0 & 0 & 0 & 0 & 0 & 0 & 0 & 0 \\ 0 & 0 & 0 & 1 & 0 & 0 & 0 & 0 & 0 & 0 \\ 0 & 0 & 0 & 0 & 1 & 0 & 0 & 0 & 0 & 0 \\ 0 & 0 & 0 & 0 & 0 & 1 & 0 & 0 & 0 & 0 \\ 0 & 0 & 0 & 0 & 0 & 0 & 1 & 0 & 0 & 0 \\ 0 & 0 & 0 & 0 & 0 & 0 & 0 & 1 & 0 & 0 \\ 0 & 0 & 0 & 0 & 0 & 0 & 0 & 0 & 1 & 0 \\ 0 & 0 & 0 & 0 & 0 & 0 & 0 & 0 & 0 & 1 \\ 0 & 0 & -1 & -1 & 0 & 1 & 1 & 1 & 0 & -1 \end{pmatrix}, \tag{5.5.21}$$

where the first block is the $\mathbb{Z}_6$-representation corresponding to $\{\psi^5, \overline{\psi}^5\}$ and the second one the remaining irreducible $\mathbb{Z}_{30}$ representation. The conjugation matrix to the representation on the integral basis is given by

$$A^{-1} = \begin{pmatrix} -1 & -49 & 52 & 11 & 14 & 15 & -5 & -6 & 1 & 1 \\ 0 & -76 & 52 & 8 & 20 & 21 & -6 & -6 & 1 & 0 \\ 1 & 20 & 3 & 32 & 10 & 4 & -1 & -1 & 0 & 0 \\ 0 & 15 & 1 & 33 & 9 & 3 & -1 & -1 & 0 & 0 \\ 0 & 10 & 0 & 33 & 8 & 2 & -1 & -1 & 0 & 0 \\ -1 & 6 & -55 & 22 & -8 & -14 & 4 & 4 & -1 & 0 \\ 1 & 4 & 59 & 40 & 26 & 20 & -7 & -6 & 1 & 1 \\ 0 & 56 & 1 & 27 & 4 & -1 & -1 & 0 & 0 & 0 \\ 0 & 35 & 0 & 21 & 3 & -1 & -1 & 0 & 0 & 0 \\ 0 & 20 & 0 & 15 & 2 & -1 & -1 & 0 & 0 & 0 \end{pmatrix} \tag{5.5.22}$$

with $Am_{S_0}A^{-1} = M_{S_0}$. We furthermore verified numerically that the transition matrix T can be written as $T = AC$ with C a block matrix that commutes with m_{S_0} (cf. section 6.1). We identify the first two rows in the matrix A^{-1} as the fluxes contained in the decoupled $\mathbb{Z}_6$ representation and contained in the orthogonal complement of $H^{5,0} \oplus H^{0,5}$

$$f_1^T \Sigma = (-1, -49, 52, 11, 14, 15, -5, -6, 1, 1)\,, \tag{5.5.23}$$

$$f_2^T \Sigma = (0, -76, 52, 8, 20, 21, -6, -6, 1, 0)\,, \tag{5.5.24}$$

where $f_i^T \Sigma \underline{\Pi}(\psi = \phi = 0) = 0$. These two fluxes have the symplectic pairing $f_1^T \Sigma f_2 = 5$. In analogy to the splitting of the local ζ-function of lower dimensional Calabi–Yau manifolds, here, we expect that the decomposition of the representation is accompanied again by a factorisation of the ζ-function of this fibre.

We list the first genus-zero invariants for this model in appendix B.1, following the expansions of the triple couplings according to eqs. (5.1.8) and (5.1.9). Additionally, in appendices B.2 and B.3, we list the genus-zero invariants of two-parameter six- and seven-fold respectively and verify integrality up to degree ten.

5.5.2 Hypersurfaces in $\mathbb{P}^{n+1}$

In this section, we want to give further motivation for the formalism introduced in section 5.3 by performing a global analysis of the mirror complex-structure moduli spaces of degree-$(n+2)$

hypersurfaces in $\mathbb{P}^{n+1}$ for $5 \leq n \leq 8$. Their defining polynomials are given by

$$P_n = \sum_{i=1}^{n+2} x_i^{n+2} - n\psi \prod_{i=1}^{n+2} x_i \,. \tag{5.5.25}$$

Their classical intersection ring is $R = nJ^n$ with J the single Kähler form of the original hypersurface. We list the topological invariants in Table 5.5. The generators of the Mori cones read

$$l = (-n-2; \underbrace{1, \ldots, 1}_{n}) \,, \tag{5.5.26}$$

which give fundamental periods annihilated by the operators

$$\mathcal{L}^{(n+1)}(z) = \theta^{n+1} - (n+2)z \prod_{i=1}^{n+1} ((n+2)\theta + i) \,. \tag{5.5.27}$$

Depending on whether n is even or odd, the Riemann symbols of these operators are of the forms

$$\mathcal{P}_{\mathcal{L}^{(n+1)}_{\text{odd}}} \left\{ \begin{array}{ccc} 0 & z_{\text{con}} & \infty \\ \hline 0 & 0 & \frac{1}{n+2} \\ \vdots & 1 & \frac{2}{n+2} \\ \vdots & \vdots & \vdots \\ \vdots & \frac{n-1}{2} & \vdots \\ \vdots & \frac{n-1}{2} & \vdots \\ \vdots & \vdots & \vdots \\ 0 & n-1 & \frac{n+1}{n+2} \end{array} , \; z \right\}, \quad \mathcal{P}_{\mathcal{L}^{(n+1)}_{\text{even}}} \left\{ \begin{array}{ccc} 0 & z_{\text{con}} & \infty \\ \hline 0 & 0 & \frac{1}{n+2} \\ \vdots & 1 & \frac{2}{n+2} \\ \vdots & \vdots & \vdots \\ \vdots & \frac{n}{2}-1 & \vdots \\ \vdots & \frac{n-1}{2} & \vdots \\ \vdots & \frac{n}{2}+1 & \vdots \\ \vdots & \vdots & \vdots \\ 0 & n-1 & \frac{n+1}{n+2} \end{array} , \; z \right\} \tag{5.5.28}$$

n	$c_2 \cdot J^{n-2}$	$c_3 \cdot J^{n-3}$	$c_4 \cdot J^{n-4}$	$c_5 \cdot J^{n-5}$	$c_6 \cdot J^{n-6}$	$c_7 \cdot J^{n-7}$	$c_8 \cdot J^{n-8}$
5	147	-784	5733	-39984	–	–	–
6	224	-1344	11312	-90048	720608	–	–
7	324	-2160	20574	-184032	1657044	-14913072	–
8	450	-3300	35100	-348480	3486900	-34867800	348678450

Table 5.5: Integrals of Chern classes for hypersurfaces in $\mathbb{P}^{n+1}$. The Euler number is given by $c_n \cdot J^0$.

with $z_{\text{con}} = (n+2)^{-(n+2)}$. Using the asymptotic basis following section 5.3, we find the following monodromies $M^{(n)}$ around the MUM points $z = 0$:

$$M_0^{(5)} = \begin{pmatrix} 1 & 0 & 0 & 0 & 0 & 0 \\ 1 & 1 & 0 & 0 & 0 & 0 \\ 0 & 1 & 1 & 0 & 0 & 0 \\ 0 & 0 & -7 & 1 & 0 & 0 \\ 0 & 14 & 7 & -1 & 1 & 0 \\ -7 & -14 & -7 & 1 & -1 & 1 \end{pmatrix}, \; M_0^{(8)} = \begin{pmatrix} 1 & 0 & 0 & 0 & 0 & 0 & 0 & 0 & 0 \\ 1 & 1 & 0 & 0 & 0 & 0 & 0 & 0 & 0 \\ 0 & 1 & 1 & 0 & 0 & 0 & 0 & 0 & 0 \\ 0 & 0 & 1 & 1 & 0 & 0 & 0 & 0 & 0 \\ 0 & 0 & 0 & 10 & 1 & 0 & 0 & 0 & 0 \\ 0 & 0 & -20 & -5 & -1 & 1 & 0 & 0 & 0 \\ 0 & 21 & 20 & 25 & 1 & -1 & 1 & 0 & 0 \\ -8 & -21 & -41 & -25 & -1 & 1 & -1 & 1 & 0 \\ 8 & 29 & 41 & 25 & 1 & -1 & 1 & -1 & 1 \end{pmatrix},$$
$$M_0^{(6)} = \begin{pmatrix} 1 & 0 & 0 & 0 & 0 & 0 & 0 \\ 1 & 1 & 0 & 0 & 0 & 0 & 0 \\ 0 & 1 & 1 & 0 & 0 & 0 & 0 \\ 0 & 0 & -4 & 1 & 0 & 0 & 0 \\ 0 & 10 & 4 & -2 & 1 & 0 & 0 \\ -6 & -10 & -14 & 2 & -1 & 1 & 0 \\ 6 & 16 & 14 & -2 & 1 & -1 & 1 \end{pmatrix}, \; M_0^{(7)} = \begin{pmatrix} 1 & 0 & 0 & 0 & 0 & 0 & 0 & 0 \\ 1 & 1 & 0 & 0 & 0 & 0 & 0 & 0 \\ 0 & 1 & 1 & 0 & 0 & 0 & 0 & 0 \\ 0 & 0 & 1 & 1 & 0 & 0 & 0 & 0 \\ 0 & 0 & 0 & 9 & 1 & 0 & 0 & 0 \\ 0 & 0 & -30 & -9 & -1 & 1 & 0 & 0 \\ 0 & 27 & 30 & 9 & 1 & -1 & 1 & 0 \\ -9 & -27 & -30 & -9 & -1 & 1 & -1 & 1 \end{pmatrix}. \tag{5.5.29}$$

As expected due to the Seidel–Thomas twist discussed in [114], the conifold monodromies act only on the periods X^0 and F_0. The projected action is given by

$$M_{z_{\text{con}}}^{\text{even}} = \begin{pmatrix} 0 & -1 \\ -1 & 0 \end{pmatrix} \quad \text{and} \quad M_{z_{\text{con}}}^{\text{odd}} = \begin{pmatrix} 1 & 1 \\ 0 & 1 \end{pmatrix}. \tag{5.5.30}$$

We verified in all cases that the orbifold monodromy is given by $(M_0 \cdot M_{z_{\text{con}}})^{-1}$, which is again integral due to unimodularity of the other two monodromies. All these monodromies leave the intersection form in eq. (5.3.15) invariant. We end this subsection with Table 5.6 containing the first genus-zero invariants for these hypersurfaces. We verified integrality of these corrections up to degree $d = 20$.

coupling	$d=1$	2	3	4
$C^{(113)}$	144256	17462826584	4361238820782872	1482599929913698021888
$C^{(122)}$	-1707797	-510787745643	-222548537108926490	-113635631482486991647224
$C^{(114)}$	1998080	4174644963328	1926128175594267724 8	125084361408234016487458816
$C^{(123)}$	-18751488	-112170352078848	-100037520509367069 0816	-10561059503662331728690397184
$C^{(115)}$	28165644	1084202037851040	997289615808402599300 04	134393273131308624778784312465 28
$C^{(124)}$	84883788	104196994587416 16	198598872923004015513 5220	457418815196953955416250051679264
$C^{(133)}$	1069047153	156037426159482684	338159358062682534335 49768	863874408462709911053866270681280 4
$C^{(116)}$	412077600	315199135892955600	629888601165740265138213600	192972802228254104320965666788460 0000
$C^{(125)}$	1527495200	4034229838611922400	174824389112955477418055016 00	942582519217090098297647141658559040000
$C^{(134)}$	27768048000	100290980400305376000	546627811934015785499223984000	353853193281555680732516761759709280 0000

Table 5.6: Genus-zero invariants of hypersurfaces in $\mathbb{P}^{n+1}$. The entries are the corrections n_d^1 or $n_{d,1}{}^1$ to the triple couplings given by eqs. (5.1.8) and (5.1.9).

5.6 Unipotent period matrix

So far, we have focused exclusively on the periods of the holomorphic $(n, 0)$-form Ω. However, in certain cases—such as the computation of maximal cuts of Feynman integrals given by Calabi–Yau periods—the whole period matrix, that is, all pairings between the middle cohomology and homology, becomes relevant. While the topological homology basis $\{\Gamma_i\}_i$ we introduced in sections 4.1 and 5.3, is standard in the literature, depending on individual preferences and specifics

of the problem, different bases for the middle cohomology are used. In practise, the choice of a basis is determined by which combinations of the periods of Ω and its derivatives make up the period matrix. In the past, many works dealt with one-parameter families whose period matrix can be given as the Wronskian of the n periods of Ω, so $\underline{\Pi}$ together with its $n-1$ derivatives. For $n=3$, this was generalised to families with $m>1$ complex-structure moduli in [115]. besides the zeroth- and m first-order derivatives, one requires independent linear combinations for the orders two and three. The authors used the inverse classical couplings $\mathfrak{c}$ (cf. section 5.3) to contract the $\binom{m+1}{2}$ second-order and $\binom{m+2}{3}$ third-order derivatives to obtain such $m+1$ derivatives of $\underline{\Pi}$ that complete the period matrix.

In [1], we constructed a basis for the middle cohomology that brings the Gauss–Manin connection into its arguably simplest form. Before reviewing the specifics of these bases for different dimensions further below, we note that inverse couplings naturally arise $\underline{q}$-corrected. This is the reason why the discussion of [1] starts with a period matrix where the derivatives are contracted with the full inverse couplings $\mathfrak{C}$ instead of their classical parts $\mathfrak{c}$. Clearly, this is just a matter of convention and—as we explained in [1]—the $\underline{q}$-corrections in the inverse couplings do not affect a p-adic analysis. Whichever period matrix one obtains, one can decompose it into the product of *a semisimple and a unipotent* matrix. This is also known as a Jordan–Chevalley decomposition [116]. Here, we will leave the semisimple matrix implicit and focus on the unipotent period matrix. As we will see below, the latter corresponds to a basis choice in cohomology which furthermore simplifies the Gauss–Manin connection drastically and brings it into a canonical form, revealing much of the Frobenius algebra's rich structure.

As of the time of this writing, the most prominent use-case for this decomposition appears in the computation of Feynman integrals. In multi-loop calculations, these integrals are sometimes given by periods of Calabi–Yau manifolds, whose complex-structure parameters correspond to physical quantities such as masses or momenta of the involved particles. One can reduce the set of possible integrals to a finite set of so-called master integrals with integration-by-parts identities (IBPs) [117]. The vector of master integrals satisfies a first order differential equation [118], which depends on the dimensional regularisation parameter ϵ

$$\nabla \underline{I}(\underline{z},\epsilon) := (d_{\underline{z}} - \mathbf{B}(\underline{z},\epsilon))\underline{I}(\underline{z},\epsilon) = 0\,. \tag{5.6.1}$$

Solving this system of differential equations simplifies, if one finds a rotation $\mathbf{R}(\underline{z},\epsilon)$ with $\underline{J}=\mathbf{R}\underline{I}$ that brings it into ϵ-factorised form [119], see also [120, 121],

$$\nabla \underline{J}(\underline{z},\epsilon) := (d_{\underline{z}} - \epsilon\mathbf{A}(\underline{z}))\underline{J}(\underline{z},\epsilon) = 0\,. \tag{5.6.2}$$

Finding such a rotation matrix $\mathbf{R}$ is non-trivial and in general a challenging task. In the factorisation procedure proposed in [120], one essential step consists in the splitting of the period matrix into a semisimple and a unipotent part. The solutions of the ϵ-factorised differential equation (5.6.2) are then given by iterated integrals

$$\begin{aligned} J(\underline{z},\epsilon) &= \mathbb{P}\exp\left[\epsilon\int_{\underline{z}_0}^{\underline{z}}\underline{\mathbf{A}}(\underline{z})dz\right]J(\underline{z}_0,0) \\ &= \left[\mathbf{1}+\epsilon\int_{\underline{z}_0}^{\underline{z}}\underline{\mathbf{A}}(\underline{z}')dz' + \epsilon^2\int_{\underline{z}_0}^{\underline{z}}\int_{\underline{z}_0}^{\underline{z}'}\underline{\mathbf{A}}(\underline{z}')dz'\underline{\mathbf{A}}(\underline{z}'')dz'' + \mathcal{O}\left(\epsilon^3\right)\right]J(\underline{z}_0,0)\,. \end{aligned} \tag{5.6.3}$$

We will review the discussion for dimensions $1 \leq n \leq 5$ and address the higher-dimensional cases only qualitatively. For explicit results in the case $n = 6$ and for the semisimple parts bringing it into the form discussed above, we refer the reader to [1].

5.6.1 General idea

The focal object of the unipotent period matrix and thus the decomposition is given by a basis in cohomology corresponding to pure elements in the Frobenius algebra. Recall that an element is called pure, if it is contained in one of the graded pieces $\mathcal{A}^{(i)}$ of the vector space $\mathcal{A} = \bigoplus_{p=1}^{n} \mathcal{A}^{(p)}$. The action of the derivative ∂_{t^i} on the elements in the middle cohomology is represented in $\mathcal{A}$ by multiplication with $e_i^{(1)} \in \mathcal{A}^{(1)}$. The fusion rule

$$e_i^{(a)} \cdot e_j^{(b)} = C_{ijk}^{(a,b)} \sigma_{(n-a-b)}^{kl} e_l^{(a+b)} \qquad \text{((v))}$$

then implies that the derivatives of basis elements $e_j^{(p)} \in \mathcal{A}^{(p)} = H^{n-p,p}$ are given by

$$\partial_i e_j^{(p)} = C_{ij}^{(1,p),k} e_k^{(p+1)}\,, \tag{5.6.4}$$

with $\partial_i = \partial_{t^i}$. Note that the covariant derivative D_i in the mirror coordinates reduces to the ordinary derivative ∂_i [104]. As a consequence, the Gauss–Manin connection in a basis for the middle cohomology consisting of pure elements is a block matrix with non-zero entries only on the secondary diagonal[7]. In this section, we will be concerned only with the unipotent period matrix, which comes from pairing this basis with the topological homology basis $\{\Gamma_i\}_i$ (cf. section 4.1) as we will show in the following. We mentioned above that any linearly independent combination of the derivatives of $\underline{\Pi}$ can be used for the period matrix, which can then be decomposed into the unipotent part discussed in the following and a semisimple rotation matrix defined implicitly.

The first row of the period matrix is given by the expansion of Ω in terms of the cohomology basis $\{\gamma^i\}_i$ dual to the basis $\{\Gamma_i\}_i$. We will work in the mirror coordinates $\underline{t}$ (4.3.8) and normalise $\Omega \equiv \Omega_0$ such that the torus period, i.e. the coefficient of the differential form γ^0 dual to the torus T^n, is one. The expansion thus takes the form[8]

$$\Omega_0 = \gamma_0 + t^i \gamma_i + \dots\,. \tag{5.6.5}$$

In the following, we will use different Greek letters α, β,... to denote the cohomology elements γ_i depending on the specific Dolbeault class. As we want to be left with a period matrix of the unipotent form

$$\mathbf{\Pi} = \begin{pmatrix} 1 & * & \cdots & * \\ 0 & \ddots & \ddots & \vdots \\ \vdots & \ddots & \ddots & * \\ 0 & \cdots & 0 & 1 \end{pmatrix}, \tag{5.6.6}$$

[7] The results for $1 \leq n \leq 5$ are given below in eqs. (5.6.9), (5.6.13), (5.6.17), (5.6.18) and (5.6.32) for $n = 1, \dots, 5$.

[8] We move the indices of the forms γ_i following the convention that the mirror coordinates carry a contravariant index.

we can use the t^i-derivatives of Ω for the elements in $\mathcal{A}^{(1)}$

$$\chi_i = \partial_i \Omega_0 \,. \tag{5.6.7}$$

As the next term in eq. (5.6.5) is generally not simply a quadratic term in $\underline{t}$, further elements in the cohomology involve more complicated expressions. Regardless of the dimension, however, eq. (5.6.6) implies that the last form is given by the form symplectically paired with γ_0. In the next subsection, we will see how the triple couplings necessarily appear for unipotency of $\mathbf{\Pi}$ in dimensions $n \geq 3$. Equation (5.6.7) should be seen as the $p = 0$ case of eq. (5.6.4), where $C_{i*}^{(1,0),k} = \delta_i^k$ following from item (iii) in section 5.1 and the canonical intersection form (5.3.15).

5.6.2 Examples

Elliptic curves The holomorphic $(1,0)$-form has the expansion $\Omega_0 = \alpha + t\beta$. As mentioned above, we set $\Omega^0 \coloneqq \beta$. Here, this coincides with $\chi_1 = \partial_t \Omega_0$ and completes the cohomology basis yielding the unipotent period matrix

$$\mathbf{\Pi}_{n=1} = \begin{pmatrix} 1 & t \\ 0 & 1 \end{pmatrix} . \tag{5.6.8}$$

The Gauss–Manin connection takes the form

$$\partial_t \begin{pmatrix} \Omega_0 \\ \Omega^0 \end{pmatrix} = \begin{pmatrix} 0 & 1 \\ 0 & 0 \end{pmatrix} \begin{pmatrix} \Omega_0 \\ \Omega^0 \end{pmatrix} . \tag{5.6.9}$$

K3 surfaces At $n = 2$, things become slightly more interesting. There, the expansion of Ω and its derivatives read

$$\Omega_0 = \alpha + t^i \gamma_i + \frac{1}{2} c_{ij} t^i t^j \beta \,, \tag{5.6.10}$$

$$\chi_i = \partial_i \Omega_0 = \gamma_i + c_{ij} t^j \beta \,, \tag{5.6.11}$$

with c_{ij} being the classical intersections of the Picard lattice, see section 4.6. Translating the above into the period matrix yields

$$\mathbf{\Pi}_{n=2} = \begin{pmatrix} 1 & \underline{t}^T & \frac{1}{2}\underline{t}^T \mathbf{c}\, \underline{t} \\ 0 & \mathbb{1} & \mathbf{c}\, \underline{t} \\ 0 & 0 & 1 \end{pmatrix} . \tag{5.6.12}$$

The Gauss–Manin connection for this cohomology basis reads

$$\partial_i \begin{pmatrix} \Omega_0 \\ \chi_j \\ \Omega^0 \end{pmatrix} = \begin{pmatrix} 0 & \delta_i^k & 0 \\ 0 & 0 & c_{ij} \\ 0 & 0 & 0 \end{pmatrix} \begin{pmatrix} \Omega_0 \\ \chi_k \\ \Omega^0 \end{pmatrix} . \tag{5.6.13}$$

So far, the connection matrix contained only constants. At dimensions three and higher, the connection will contain $\underline{q}$-corrected triple couplings. The matrix c_{ij} in eq. (5.6.13) can be interpreted as the couplings $C_{ij*}^{(1,1,0)}$ (cf. section 5.1) or its inverses, depending on the placement of the indices. The same is true for the Kronecker-δ in eq. (5.6.13), where the only difference to the entry c_{ij} is the index placement.

Three-folds In higher dimensions, this structure of the couplings naturally extends, where now triple couplings appear that are generally $\underline{q}$-corrected. For three-folds, we follow section 4.6 in expanding the $(3,0)$-form in terms of the prepotential (cf. eq. (4.6.40)) and define χ_i as above

$$\begin{aligned}\Omega_0 &= \alpha_0 + t^i\alpha_i + \partial_i\mathcal{F}\beta^i + (2\mathcal{F} - t^i\partial_i\mathcal{F})\beta^0\,,\\ \chi_i &= \partial_i\Omega_0 = \alpha_i + \partial_i\partial_j\mathcal{F}\beta^j + (\partial_i\mathcal{F} - t^j\partial_i\partial_j\mathcal{F})\beta^0\,.\end{aligned}$$

Now, the next forms contracted with the triple couplings should return the derivatives of χ_i. A suitable extension of the above to a basis for the middle cohomology is given by [122]

$$\chi^i = \beta^i - t^i\beta^0\,, \tag{5.6.14}$$

$$\Omega^0 = \beta^0\,. \tag{5.6.15}$$

With $\partial_i\partial_j\partial_k\mathcal{F} = C_{ijk}$ (4.6.48), we find immediately

$$\partial_i\chi_j = C_{ijk}(\beta^k - t^k\beta^0) = C_{ijk}\chi^k\,. \tag{5.6.16}$$

In the above basis, the Gauss–Manin connection then takes the form

$$\partial_i\begin{pmatrix}\Omega_0\\ \chi_j\\ \chi^j\\ \Omega^0\end{pmatrix} = \begin{pmatrix}0 & \delta_i^k & 0 & 0\\ 0 & 0 & C_{ijk} & 0\\ 0 & 0 & 0 & -\delta_i^j\\ 0 & 0 & 0 & 0\end{pmatrix}\begin{pmatrix}\Omega_0\\ \chi_k\\ \chi^k\\ \Omega^0\end{pmatrix}. \tag{5.6.17}$$

Four-folds We recall the results of subsection 5.4.2. Expanding the holomorphic form as

$$\Omega_0 = \alpha_0 + t^i\alpha_i + H^\alpha\gamma_\alpha + F_i\beta^i + F_0\beta^0\,, \tag{5.4.51}$$

one obtains a splitting of the four-point coupling (defined as the pairing of Ω_0 with its fourth derivative)

$$C_{ijkl} = \partial_i\partial_j H\cdot\partial_k\partial_l H = \sigma_{\alpha\beta}C_{ij}{}^\alpha C_{kl}{}^\beta\,, \tag{5.4.59}$$

giving an implicit definition of the triple couplings $C_{ij}{}^\alpha = \partial_i\partial_j H^\alpha$. We will construct the cohomology basis that is subject to the connection

$$\partial_i\begin{pmatrix}\Omega_0\\ \chi_j\\ h_\alpha\\ \chi^j\\ \Omega^0\end{pmatrix} = \begin{pmatrix}0 & \delta_i^k & 0 & 0 & 0\\ 0 & 0 & C_{ij}{}^\beta & 0 & 0\\ 0 & 0 & 0 & C_{ik\gamma} & 0\\ 0 & 0 & 0 & 0 & \delta_i^j\\ 0 & 0 & 0 & 0 & 0\end{pmatrix}\begin{pmatrix}\Omega_0\\ \chi_k\\ h_\beta\\ \chi^k\\ \Omega^0\end{pmatrix}. \tag{5.6.18}$$

As before, we must set $\chi_i \coloneqq \partial_i\Omega_0$. The remaining generators are defined as

$$h_\alpha = \gamma_\alpha + \partial_i H_\alpha\beta^i - (H_\alpha - t^i\partial_i H_\alpha)\beta^0, \tag{5.6.19}$$

$$\chi^i = \beta^i + t^i\beta^0, \tag{5.6.20}$$

$$\Omega^0 = \beta^0\,. \tag{5.6.21}$$

To verify eq. (5.6.18), we calculate

$$\begin{aligned}\partial_i\chi_j &= \partial_i\partial_j H^\beta\gamma_\beta + \partial_i\partial_j F_k\beta^k + \partial_i\partial_j F_0\beta^0\\ &= C_{ij}{}^\beta\gamma_\beta + C_{ij}{}^\beta\partial_k H_\beta\beta^k - C_{ij}{}^\beta(H_\beta - t^i\partial_i H_\beta)\beta^0\\ &= C_{ij}{}^\beta h_\beta\,,\end{aligned} \tag{5.6.22}$$

where, in the second equality, the coefficients of β^0 and β^k follow with eqs. (5.4.54) and (5.4.57). The remaining relations of eq. (5.6.18) follow directly from the definition of the triple coupling.

Five-folds In dimensions $n \geq 5$, one needs to define inverses of the triple couplings to define the pure cohomology bases. We will review the results for $n = 5$, which, together with $n = 6$, where first found by J. Dücker in [1]. As for the case $n = 4$, one requires identities originating in Griffiths transversality. We expand the holomorphic $(5, 0)$-form as

$$\Omega_0 = \alpha_0 + t^i \alpha_i + H^\alpha \gamma_\alpha + K_\alpha \delta^\alpha + F_i \beta^i + F_0 \beta^0 \tag{5.6.23}$$

and enumerate the relations with the Roman numeral representation of k, where

$$(k): \quad 0 = \partial_{\underline{I}} \underline{\Pi}^T \Sigma \underline{\Pi}\,, \quad |\underline{I}| = k\,. \tag{5.6.24}$$

Then, we obtain the following identities used below

$$\begin{aligned}
& 0 = \partial_i\partial_j H^\alpha K_\alpha - \partial_i\partial_j K_\alpha H^\alpha - t^k \partial_i\partial_j F_k - \partial_i\partial_j F_0\,, && \text{(II)}\\
\partial(\text{II}) - (\text{III}): \quad & 0 = \partial_i\partial_j H^\alpha \partial_k K_\alpha - \partial_i\partial_j K_\alpha \partial_k H^\alpha - \partial_i\partial_j F_k\,, && (\Delta\text{III})\\
\partial(\text{III}) - (\text{IV}): \quad & 0 = \partial_i\partial_j\partial_k H^\alpha \partial_l K_\alpha - \partial_i\partial_j\partial_k K_\alpha \partial_l H^\alpha - \partial_i\partial_j\partial_k F_l\,, && (\Delta\text{IV})\\
\partial(\Delta\text{III}) - (\Delta\text{IV}): \quad & 0 = \partial_i\partial_j H^\alpha \partial_k\partial_l K_\alpha - \partial_i\partial_j K_\alpha \partial_k\partial_l H^\alpha\,. && (\Delta^2\text{IV})
\end{aligned}$$

It follows from eq. (5.6.4) that the two triple-couplings are given by

$$C^{(1,1,3)}_{ij\alpha} = \partial_i\partial_j H_\alpha\,, \tag{5.6.25}$$

$$C^{(1,2,2)}_{i\alpha\beta} = \partial_i \left(\mathfrak{C}^{jk}{}_\alpha \partial_j\partial_k K_\beta \right), \tag{5.6.26}$$

where we defined the inverse of $C^{(1,1,3)}$ by demanding

$$C^{(1,1,3)}_{ij\alpha} \mathfrak{C}^{ij\beta} = \delta^\beta_\alpha \tag{5.6.27}$$

with Einstein summation convention. To improve readability, we omit the superscripts indicating the indices' weights. The coupling $C^{(1,1,3)}$ always has one Greek index while $C^{(1,2,2)}$ has two. Besides $\chi_i = \partial_i \Omega_0$, the proposed basis is given by

$$\begin{aligned}
h_\alpha = {} & \gamma_\alpha + \mathfrak{C}^{ij}{}_\beta \partial_i\partial_j K_\alpha \delta^\beta + \left(\partial_k K_\alpha - \mathfrak{C}^{lm}{}_\alpha \partial_l\partial_m K_\beta \partial_k H^\beta \right) \beta^k \\
& + \left(K_\alpha - \mathfrak{C}^{lm}{}_\alpha \partial_l\partial_m K_\beta H^\beta - t^k \left[\partial_k K_\alpha - \mathfrak{C}^{lm}{}_\alpha \partial_l\partial_m K_\beta \partial_k H^\beta \right] \right) \beta^0\,,
\end{aligned} \tag{5.6.28}$$

$$k^\alpha = \delta^\alpha - \partial_k H^\alpha \beta^k + \left(-H^\alpha + t^k \partial_k H^\alpha \right) \beta^0\,, \tag{5.6.29}$$

$$\chi^i = \beta^i - t^i \beta^0\,, \tag{5.6.30}$$

$$\Omega^0 = \beta^0\,. \tag{5.6.31}$$

The claim is that, in this basis, the Gauss–Manin connection is given by

$$\partial_i \begin{pmatrix} \Omega_0 \\ \chi_j \\ h_\alpha \\ k^\alpha \\ \chi^j \\ \Omega^0 \end{pmatrix} = \begin{pmatrix} 0 & \delta^k_i & 0 & 0 & 0 & 0 \\ 0 & 0 & C_{ij}{}^\beta & 0 & 0 & 0 \\ 0 & 0 & 0 & C_{i\alpha\beta} & 0 & 0 \\ 0 & 0 & 0 & 0 & -C_{ik}{}^\alpha & 0 \\ 0 & 0 & 0 & 0 & 0 & -\delta^j_i \\ 0 & 0 & 0 & 0 & 0 & 0 \end{pmatrix} \begin{pmatrix} \Omega_0 \\ \chi_k \\ h_\beta \\ k^\beta \\ \chi^k \\ \Omega^0 \end{pmatrix}. \tag{5.6.32}$$

To verify eq. (5.6.32), we calculate

$$\partial_i\chi_j = C_{ij}{}^{\alpha}\gamma_\alpha + \partial_i\partial_j K_\alpha\delta^\alpha + \partial_i\partial_j F_i\beta^i + \partial_i\partial_j F_0\beta^0\,. \tag{5.6.33}$$

To split off the coupling $C_{ij}{}^{\alpha}$, we insert a $\delta^\beta_\alpha = C_{kl}{}^{\alpha}\mathfrak{C}^{kl}{}_{\beta}$ in the δ^α-component and use (ΔIII) and (II) for the components of β^k and β^0, respectively. This leaves us with

$$\begin{aligned}\partial_i\chi_j = C_{ij}{}^{\alpha}\gamma_\alpha + C_{kl}{}^{\alpha}\mathfrak{C}^{kl}{}_{\beta}\partial_i\partial_j K_\beta\delta^\alpha + \left(C_{ij}{}^{\alpha}\partial_k K_\alpha - \partial_i\partial_j K_\alpha\partial_k H^\alpha\right)\beta^k \\ + \left(\partial_i\partial_j H^\alpha K_\alpha - \partial_i\partial_j K_\alpha H^\alpha - t^k\left[C_{ij}{}^{\alpha}\partial_k K_\alpha - \partial_i\partial_j K_\alpha\partial_k H^\alpha\right]\right)\beta^0\,.\end{aligned} \tag{5.6.34}$$

Using (Δ^2IV) to exchange the indices (kl) and (ij) in the δ^α-component and using the same trick to split off the couplings in the β^k and β^0 parts, one derives the second entry of eq. (5.6.32). To verify the third entry, we compute

$$\partial_i h_\alpha = C_{i\alpha\beta}\delta^\beta + \left(\partial_i\partial_k K_\alpha - \partial_i\partial_k H^\beta\mathfrak{C}^{lm}{}_{\alpha}\partial_l\partial_m K_\beta - \partial_k H^\beta C_{i\alpha\beta}\right)\beta^k + (\ldots)\beta^0\,, \tag{5.6.35}$$

where we used the definition of $C_{i\alpha\beta}$ (5.6.26). The first two terms in the β^k-term cancel each other due to (Δ^2IV). Applying the same methods to the component of β^0 shows the identity. The rest of eq. (5.6.32) follows directly from the definition of $C_{ij}{}^{\alpha}$ in eq. (5.6.25).

Higher dimensions In general, the triple-couplings can be obtained from the period vector $\underline{\Pi}$ for a homology basis with block-anti-diagonal intersection form as follows: The first coupling appearing when taking derivatives of Ω_0 is $C^{(1,1)}$ and is given by the second derivatives of the double-logarithmic periods. The following couplings can be defined iteratively by using eq. (5.6.4) and demanding unipotency of the period matrix. For the triple-coupling $C^{(1,r)}$ with $1 \leq r \leq \lfloor\frac{n-1}{2}\rfloor$, one considers the periods $\underline{\Pi}^{(r+1)}$ with logarithmic order $r+1$ and takes derivatives while removing any lower couplings $C^{(1,s)}$, $s < r$, by contracting with its inverses. Unipotency of the period matrix and general form of the Gauss–Manin connection discussed above implies that one ends up with the coupling $C^{(1,r)}$ after taking $r+1$ derivatives. Independent of the dimension, the first couplings are given by

$$C^{(1,1)}_{ij\alpha} = \partial_i\partial_j\underline{\Pi}^{(2)}_\alpha\,, \tag{5.6.36}$$

$$C^{(1,2)}_{i\alpha A} = \partial_i\left(\mathfrak{C}^{jk}_{(1,1),\alpha}\partial_j\partial_k\underline{\Pi}^{(3)}_A\right)\,, \tag{5.6.37}$$

$$C^{(1,3)}_{iAa} = \partial_i\left(\mathfrak{C}^{j\alpha}_{(1,2),A}\partial_j\left(\mathfrak{C}^{kl}_{(1,1),\alpha}\partial_k\partial_l\underline{\Pi}^{(4)}_a\right)\right)\,, \tag{5.6.38}$$

$$\vdots$$

For a purely horizontal middle cohomology (i.e. with non-degenerate Frobenius algebra), the computation of the inverse couplings can be reduced to a simple matrix inversion. There, we define the functions

$$\tilde{\mathfrak{C}}_{(p,n-p)}:\ \mathcal{A}^{(p)}\times\mathcal{A}^{(n-p)}\to\mathbb{C}\,, \tag{5.6.39}$$

$$\tilde{\mathfrak{C}}^{\alpha A}_{(p,n-p)} = \left(\left(C^{(1,p-1,n-p)}_{\alpha_1,\alpha^*,A}\right)_{\alpha A}\right)^{-1}\,, \tag{5.6.40}$$

where the index $\alpha = (\alpha_1,\alpha^*)$ was split using horizontality into indices in $\mathcal{A}^{(1)}$ and $\mathcal{A}^{(p-1)}$. Instead of the two-fold sums over the first two indices of $\mathfrak{C}$, it suffices to sum over independent elements

in the K-theory group. This simplification is captured in the functions $\tilde{\mathfrak{C}}$ and we can write the above triple-functions as derivatives of matrix multiplications

$$C^{(1,2)}_{i\alpha A} = \partial_i \left(\left(\mathfrak{C}_{(2,n-2)}\right)^{\ \beta}_{\alpha} \partial_{\beta_1}\partial_{\beta_2}\underline{\Pi}^{(3)}_A \right), \tag{5.6.41}$$

$$C^{(1,3)}_{iAa} = \partial_i \left(\left(\mathfrak{C}_{(3,n-3)}\right)^{\ B}_{A} \partial_{B_1} \left(\left(\mathfrak{C}_{(2,n-2)}\right)^{\ \beta}_{B^*} \partial_{\beta_1}\partial_{\beta_2}\underline{\Pi}^{(4)}_a \right) \right). \tag{5.6.42}$$

Together with the integral basis construction in section 5.3, this form is particularly useful for computing triple-couplings with computer algebra systems.

Chapter 6

Symmetric moduli spaces and flux vacua

Until now, the discussion has been restricted to the study of specific Calabi–Yau families over their moduli spaces. Relations among different families and transitions into each other are mathematically rich and physically significant as they offer deep insights into their underlying structure and play an important role in string theory. Mathematically, such relations typically correspond to a splitting of Hodge structure of pure or mixed motives, depending on whether the fibre is smooth or singular. As reviewed in chapter 3, these transitions from one family to another are known to be related to two phenomena in string theory: On the one hand, non-zero background values for the field strengths F_3 and H_3 generically break supersymmetry completely. It turns out that, if a fibre allows for such background values while protecting supersymmetry, its Hodge structure splits. Sometimes, one part of this splitting corresponds to another Calabi–Yau family of the same dimension whose complex-structure moduli space can thus be embedded into the original moduli space. While this happens over generically smooth loci, the second phenomenon—black hole condensation—arises along conifold singularities. The latter will be the topic of chapter 7.

Another realisation of Hodge splitting is that of cyclic quotient families introduced in section 2.3. The middle cohomology splits into irreducible representations of the symmetry group and one can identify the one containing Ω again with the middle cohomology of a family with less complex-structure deformations. We will consider some explicit constructions in section 6.1. These will make a reappearance in section 6.2, where we will analyse flux vacua in several families. We will show how the order of a cyclic symmetry impacts the existence of flux vacua along the fixed-point locus and discuss the compatibility of multiple simultaneous flux configurations. Lastly, we discuss briefly flux vacua in compactifications of M/F-theory on Calabi–Yau four-folds. The vacuum at hand was found in [1] and uses a vanishing cycle given by a shrinking S^4 at the conifold locus. The toric description of the conifold locus will serve as a bridge to the next section, where these loci signal transitions to different Calabi–Yau families.

6.1 Symmetry quotients and their splitting of Hodge structure

Quotients of families made a prominent appearance in the mirror construction in [22]. As we have reviewed in section 2.3, taking the quotient of a hypersurface family w.r.t. the mirror group $\hat{H}$ yields the defining polynomial of the mirror. However, any subgroup $\hat{S} \subset \hat{H}$ can be used to construct a family of Calabi–Yau manifolds. In [1], we showed that the rational cohomology splits into irreducible monodromy representation associated with the symmetry group $\hat{G}/\hat{Q}$, where the quantum symmetry $\hat{Q}$ reflecting the ambient scaling acts trivially. It follows that, on a locus in

points					l-vectors		
(1	0	0	0	0)	0	0	-3
(1	1	0	0	0)	0	0	1
(1	0	1	0	0)	0	1	0
(1	0	0	1	0)	1	0	0
(1	0	0	1	2)	1	0	0
(1	-2	-1	-2	-2)	0	1	0
(1	0	0	1	1)	-2	0	1
(1	-1	0	-1	-1)	0	-2	1

Table 6.1: Integral points and their scaling relations for the defining polynomial of $\mathcal{X}_6^{(3)}$.

the moduli space where all deformation parameters a_i with $\hat{S}a_i \neq a_i$ are zero, the cohomology and thus the Hodge structure splits *over the rationals*. Rationality is important for the quantisation condition in the context of flux configurations. First, we will introduce the three-parameter quotient $\mathcal{X}_6^{(3)}$ used in [1] that serves as an example not only for the quotient construction but also for the compatibility of flux vacua in section 6.2 and strong coupling transitions in section 7.1. Later in this subsection, we then review briefly the argument we gave in [1] for a splitting of Hodge structure on fixed-point loci, which was based on and inspired by [123, 113]

We begin with the degree-six hypersurfaces in $\mathbb{P}_{2,1,1,1,1}$ and consider the quotient by the group $\hat{S}$ generated by

$$g_1 = \mathbb{Z}_3 : (1,0,0,0,2)\,,\ g_2 = \mathbb{Z}_3 : (1,1,1,0,0)\,,\ g_3 = \mathbb{Z}_6 : (2,1,0,0,3)\,. \tag{6.1.1}$$

The elements are expressed in the convention used in section 2.3. The deformations invariant under the action of $\hat{S}$ are collected in the defining polynomial of the quotient family

$$P_{\mathcal{X}_6^{(3)}} = x_1^3 + x_2^6 + x_3^6 + x_4^6 + x_5^6 - a_0 \prod_{i=1}^{5} x_i - a_6 x_2^3 x_5^3 - a_7 x_3^3 x_4^3\,, \tag{6.1.2}$$

To find the anti-canonical bundle of which $P_{\mathcal{X}_6^{(3)}}$ is a section, we must find a reflexive polytope whose points map linearly to the Newton polytope of eq. (6.1.2). In practise, one searches in the database of reflexive four-dimensional polytopes [124] for one with at least $5+3+1=9$ integral points, $h^{2,1} \geq 3$ and whose points map linearly to the Newton polytope. Note that the quotient family can have non-polynomial deformations and thus $h^{2,1} > 3$ and further points inside co-dimension one faces. The polytope reflecting the defining polynomial of $\mathcal{X}_6^{(3)}$ together with its Mori cone generators is given in Table 6.1. For the Mori cone generators, we used SAGEMATH to obtain the unique fine star triangulation of this polytope. Furthermore, we find the following topological data

$$R = 3J_1J_2J_3 + 6J_1J_3^2 + 6J_2J_3^2 + 12J_3^3\,, \tag{6.1.3}$$

$$c_2 \cdot J_1 = 24\,,\ c_2 \cdot J_2 = 24\,,\ c_2 \cdot J_3 = 60\,,\ \chi = -120\,. \tag{6.1.4}$$

The Picard–Fuchs ideal is generated by the operators

$$\mathcal{L}_1^{(2)}(\underline{z}) = \theta_1^2 - z_1(2\theta_1 - \theta_3 + 1)(2\theta_1 - \theta_3)\,, \tag{6.1.5}$$

$$\mathcal{L}_2^{(2)}(\underline{z}) = \theta_2^2 - z_2(2\theta_2 - \theta_3 + 1)(2\theta_2 - \theta_3)\,, \tag{6.1.6}$$

$$\mathcal{L}_3^{(2)}(\underline{z}) = \theta_3\left(\theta_3 - 2\theta_1 - 2\theta_2\right) + 4\theta_1\theta_2 - z_3\left(27\theta_3(\theta_3+1) + 6\right) \tag{6.1.7}$$

with $\underline{z}$ the Batyrev coordinates (4.4.8) of the l-vectors in Table 6.1. This model can also be written as a complete intersection in products of projective spaces

$$\mathcal{X}_6^{(3)} = \left(\begin{array}{c|ccc} \mathbb{P}^1 & 0 & 2 & 0 \\ \mathbb{P}^1 & 0 & 0 & 2 \\ \mathbb{P}^4 & 3 & 1 & 1 \end{array}\right)^{3,63}_{-120}\,, \tag{6.1.8}$$

where we added (h^{21}, h^{11}) and the Euler number as the super- and subscript, respectively. Then, its Mori cone generators are given by (2.2.50)

$$\begin{aligned} l_1 &= (0,-2,0;1,1,0,0,0,0,0,0,0)\,, \\ l_2 &= (0,0,-2;0,0,1,1,0,0,0,0,0)\,, \\ l_3 &= (-3,-1,-1;0,0,0,0,1,1,1,1,1)\,. \end{aligned} \tag{6.1.9}$$

The intersection ring, the remaining topological data and the instanton numbers are identical to that of the hypersurface. The holomorphic periods of the two models obey the relation

$$\varpi_{0,\text{CICY}}(z_1,z_2,z_3) = \frac{1}{\sqrt{(1-4z_1)(1-4z_2)}}\,\varpi_{0,\text{HS}}\left(z_1, z_2, \frac{z_3}{(1-4z_1)(1-4z_2)}\right). \tag{6.1.10}$$

We obtained the description as a CICY while studying the conifold transition of this model to the hypergeometric family $\mathcal{X}_{3,2,2}$, see section 7.2. For the explicit analytical continuation to various neighbourhoods of the moduli space, we refer the reader to [1].

These quotients are sub-families of the original manifold in the sense that their moduli space is embedded in the original complex-structure moduli space. Being a sub-family means that the linear dependent periods over the quotient's moduli space are again solutions to a Picard–Fuchs differential ideal. In the context of flux compactifications, it is crucial that the linear dependencies are rational to guarantee that flux vacua of a theory compactified on a quotient are present in a compactification on the original family. In the following, we will repeat the argument we gave in [1], which verifies the statement under a single assumption that holds in all cases we considered.

The automorphisms of the ambient space are encoded in both the points of the toric polytope inside faces of codimension one and the Jacobian ideal. While in most cases one typically removes redundancies of these reparametrisations by ignoring these points in the polytope, this conceals a beautiful group-theoretic structure of the middle cohomology. For this subsection, we will instead us the relations of the Jacobian ideal

$$0 \equiv \partial_{x_i} P = w_i x_i^{d/w_i - 1} - \ldots \tag{6.1.11}$$

to remove all appearances of x_i with exponents larger or equal to $d/w_i - 1$ in the deformation monomials. For example, for the octic hypersurfaces in $\mathbb{P}_{4,1^4}$ (cf. eq. (2.3.16)), one would remove

x_1 in the single deformation $\psi \prod_{i=1}^{5} x_i$ to get $\psi^2 \prod_{i=2}^{5} x_i^2$. Note that this deformation corresponds to the point $(-1,0,0,0)$ contained in a codimension one face of the underlying polytope. We denote the moduli parametrising these deformations by a_i. In the example above, we thus have $a_0 = \psi^2$.

Following section 4.2, we choose as a basis for the middle cohomology

$$H^3(X,\mathbb{C}) = \text{span}_{\mathbb{C}}\left(\{\Omega\} \cup \left\{\partial_{a_i}\Omega \;\middle|\; i \in \{0,\dots,h^{2,1}-1\}\right\} \cup \text{ c.c.}\right) \tag{6.1.12}$$

with $\Omega = \text{Res}\left(\frac{\mu}{P}\right)$. The properties of the covariant derivative (4.2.18) imply

$$-\text{Res}\left(\frac{\text{def}_i\,\mu}{P^2}\right) = \partial_{a_i}\Omega = \underbrace{D_{a_i}\Omega}_{\in H^{2,1}} - \underbrace{(\partial_{a_i}K)\,\Omega}_{\in H^{3,0}}. \tag{6.1.13}$$

Along loci in the moduli space where the Kähler potential is flat in a certain direction a_i, the form $\partial_{a_i}\Omega$ is contained in $H^{2,1}$. The residual symmetry group $\hat{H}$ leaves Ω invariant, which implies that the Kähler potential (4.1.14) is flat at fixed-point loci $a_i = 0$ of transforming moduli a_i in these directions. Thus, if $\hat{S} \subset \hat{H}$ with $\text{Inv}_{\hat{S}} = \{a_i = 0\}$, we have

$$\partial_{a_i}K\Big|_{\text{Inv}_{\hat{S}}} = 0 \quad \text{and} \quad \partial_{a_i}\Omega\Big|_{\text{Inv}_{\hat{S}}} \in H^{2,1}\,. \tag{6.1.14}$$

By itself, this statement is not particularly interesting. However, if the group $\hat{S}$ is of a suitable order, these forms span a subspace in the rational cohomology $H^3(X,\mathbb{Q})$ as we will show in the following. First, we consider a single modulus that is subject to a symmetry $a_i \mapsto e^{2\pi\mathrm{i}/n}a_i$ where the remaining moduli are invariant. We generalise this to multiple moduli and comment on the rational splitting for a quotient by $\hat{S} \subset \hat{H}$. Finally, we discuss the connection to the Gepner-point/orbifold vacua found in [123, 113] and explain the extension to higher dimensions.

Assume that a family has the symmetry $\sigma:\ a_i \mapsto e^{2\pi\mathrm{i}/k}a_i$ for some i under which the rest of the moduli are invariant. In the fundamental domain of the moduli space, one identifies $a_i \equiv e^{2\pi\mathrm{i}/k}a_i$ and the σ describes a closed path in it and thus induces a monodromy transformation. The action on the cohomology basis in eq. (6.1.12) is of the form

$$\begin{pmatrix} \mathbb{1} & 0 & 0 \\ 0 & e^{2\pi\mathrm{i}/k} & 0 \\ 0 & 0 & e^{-2\pi\mathrm{i}/k} \end{pmatrix}. \tag{6.1.15}$$

For $k \in \{2,3,4,6\}$, we can rotate the basis to one with integral representation

$$N_i = \begin{pmatrix} \mathbb{1} & 0 \\ 0 & n \end{pmatrix}, \tag{6.1.16}$$

where the 2×2 matrix n is given by

$$n_2 = \begin{pmatrix} 1 & 1 \\ e^{2\pi\mathrm{i}/k} & e^{-2\pi\mathrm{i}/k} \end{pmatrix} \begin{pmatrix} e^{2\pi\mathrm{i}/k} & 0 \\ 0 & e^{-2\pi\mathrm{i}/k} \end{pmatrix} \begin{pmatrix} 1 & 1 \\ e^{2\pi\mathrm{i}/k} & e^{-2\pi\mathrm{i}/k} \end{pmatrix}^{-1} \in M_{2\times 2}(\mathbb{Z})\,. \tag{6.1.17}$$

The monodromy transformation of the integral basis[1] $\underline{\Pi}$, denoted by M_i, is—just as N_i—a rational matrix of finite order k. Such matrices are rationally similar [125], i.e. there exists a rational matrix A with

$$M_i = AN_iA^{-1}. \tag{6.1.18}$$

It follows that the transition matrix rotating a local period basis $\underline{\varpi}$ with monodromy N_i into $\underline{\Pi} = T_{\underline{\varpi}\underline{\varpi}}$ is of the form

$$T_{\underline{\varpi}} = AC \tag{6.1.19}$$

with C a matrix commuting with N_i that is generally complex. Expressing C in block form, we have

$$0 = N_i \begin{pmatrix} C_{11} & C_{12} \\ C_{21} & C_{22} \end{pmatrix} - \begin{pmatrix} C_{11} & C_{12} \\ C_{21} & C_{22} \end{pmatrix} N_i = \begin{pmatrix} \mathbb{1}C_{11} - C_{11}\mathbb{1} & \mathbb{1}C_{12} - C_{12}n_2 \\ n_2C_{21} - C_{21}\mathbb{1} & n_2C_{22} - C_{22}n_2 \end{pmatrix}. \tag{6.1.20}$$

Since all eigenvalues of n_2 are unequal to one, the off-diagonal Sylvester equations [126] imply that $C_{12} = C_{21} = 0$ and that the matrix C preserves the rational splitting into the two sub-representations of the monodromy. Families with such a symmetry of order $k \in \{2, 3, 4, 6\}$ have a period vector that can be split *rationally* into an invariant and transforming part

$$A^{-1}\,\underline{\Pi} = \begin{pmatrix} \underline{\Pi}_{\text{inv}} \\ \underline{\Pi}_{\text{n-inv}} \end{pmatrix}, \quad A \in M_{b_3\times b_3}(\mathbb{Q})\,, \tag{6.1.21}$$

where $\underline{\Pi}_{\text{n-inv}}$ is of length two and vanishes at the fixed point. In the context of flux vacua, the last two rows of A^{-1} thus correspond to fluxes, which, together with a suitable value of the axio-dilaton, yield a supersymmetric flux vacuum. At the same time, invariance of $\underline{\Pi}_{\text{inv}}$ renders its derivative w.r.t. a_i zero. Together with the flat Kähler potential (6.1.14), the F-term equations in eq. (3.4.3) for a_i are satisfied automatically on $a_i = 0$ for fluxes formed out of the first $b_3 - 2$ rows of A^{-1}.

We now want to discuss the rational splitting of the cohomology in the mirror construction, i.e. we will argue that the integral middle cohomology of the mirror quotient forms a sublattice inside that of the original family under one condition which we observe to be true in all cases considered. That is, the representation of $\hat{G}$ on the middle cohomology must decompose into at least two sub-representations, one of which is the cohomology group of the mirror. This is indeed the case when choosing the representatives in the quotient ring as explained above. We will review the construction of these sub-representations of $\hat{G}$ together with their integral representation at the end of the subsection. For now, let us assume that the condition holds. Then, the monodromies of $\mathcal{X}$ around the divisors $a_i = 0$ have four independent representations M_i corresponding to the four generators of $\hat{G}/\hat{Q}$. We can express these again in terms of the block matrix of the integral sub-representations

$$M_i = AN_iA^{-1}, \tag{6.1.22}$$

where $T = AC$ is the transition matrix from the local integral basis to that of $\underline{\Pi}$ with C a (complex) matrix commuting now with all four N_i. For all sub-representations except the mirror

[1] By Poincaré duality, each basis in cohomology has a period basis with equivalent monodromy transformation properties. The statements in cohomology therefore translate into homology and Ω-period bases.

cohomology, there exists an N_i belonging to a generator of $\hat{H}$ under which it does not have an eigenvalue one. Otherwise, it would be part of the mirror cohomology. By the same argument as above for Sylvester equations, commutativity with N_i implies that C does not mix the mirror cohomology with the rest. We deduce that the splitting of the cohomology is rational and that it is viable to restrict to the mirror locus when studying flux vacua on the original family.

The decomposition into sub-representations corresponds to a partition of the set $\mathcal{S}$ of generators of $H^3(X,\mathbb{C})$

$$\mathcal{S} = \bigcup_i s_i\,, \quad s_i \cap s_j = \emptyset\,,\ i \neq j\,, \tag{6.1.23}$$

such that for each $s_i = (m_1, \ldots, m_{n_i})$ there exist integers $l(k)$ such that the phase m_k obtains under N_j is given by a power of that of m_1 as

$$N_j\big|_{m_k} = N_j^{l(k)}\big|_{m_1}. \tag{6.1.24}$$

Furthermore, these sets s_i are chosen such that the image of l are the coprime numbers in $\frac{d}{\delta}(1,\ldots,\delta-1)$ for δ a divisor of the hypersurface of degree d. This property implies that we can choose linear combinations of the elements in s_i such that they transform integrally under all N_j. This new basis is defined in terms of a d-th primitive root of unity β

$$\begin{aligned}
\mu_1 &= m_1 + \ldots + m_{n_i}\,,\\
\mu_2 &= \beta^{l(1)} m_1 + \ldots + \beta^{l(n_i)} m_{n_i}\,,\\
&\vdots\\
\mu_{n_i} &= \beta^{l(1)\,(n_i-1)} m_1 + \ldots + \beta^{l(n_i)\,(n_i-1)} m_{n_i}\,.
\end{aligned} \tag{6.1.25}$$

As an example, let us consider the sextic hypersurfaces in $\mathbb{P}_{2,1^4}$. All representations are either one- or two-dimensional with the image of l being $\frac{6}{6}\{1,5\}$, $\frac{6}{3}\{1,2\}$ or $\frac{6}{2}\{1\}$. The possible bases are given by

$$\mu_1^{(1)} = m_1 + m_2\,, \quad \mu_2^{(1)} = \beta m_1 + \beta^5 m_2\,, \tag{6.1.26}$$

$$\mu_1^{(2)} = m_1 + m_2\,, \quad \mu_2^{(2)} = \beta^2 m_1 + \beta^4 m_2\,, \tag{6.1.27}$$

$$\mu_1^{(3)} = m_1 + m_2\,. \tag{6.1.28}$$

The corresponding blocks in N_i are given by

$$n^{(1)} = \begin{pmatrix} 0 & 1 \\ -1 & 1 \end{pmatrix}, \quad n^{(2)} = \begin{pmatrix} 0 & 1 \\ -1 & -1 \end{pmatrix}, \quad n^{(3)} = \begin{pmatrix} -1 \end{pmatrix}. \tag{6.1.29}$$

For this specific model, we find a decomposition into 99 representations $n^{(1)}$ and 5 of $n^{(2)}$. Note that this agrees with $b_3 = 2(h^{2,1}+1) = 208 = 2(99+5)$. The rank-four mirror cohomology itself splits into a sum of $n^{(1)}$ and $n^{(2)}$, which can be seen in form of an attractor point at $\psi = 0$ [74].

For more examples in this formalism we refer to [1]. The above discussion can be generalised to higher-dimensional families, where one needs to pay some more attention to the monomials yielding the generators. For three-folds, we assemble this set from the deformation monomials alone (6.1.12), which is insufficient for $n > 3$. In general, we must consider monomials of order $d \cdot k$, where $1 \leq k \leq \lfloor \frac{n}{2} \rfloor$. Modulo the Jacobian ideal, these generate the primitive middle cohomology according to section 4.2.

A simple four-fold family exemplifying this structure is given by the degree eight hypersurfaces in $\mathbb{P}_{2^2,1^4}$. The deformations parametrising $H^{4,0} \oplus H^{3,1}$ are

$$1 \quad \text{and} \quad \prod_{i=1}^{6} x_i \,. \tag{6.1.30}$$

As a one-parameter model, the horizontal cohomology includes one further element in $H^{2,2}$ corresponding to $\prod_{i=1}^{6} x_i^2$. However, in the primitive cohomology, there exists one further deformation in $H^{2,2}$ given by $\prod_{i=3}^{6} x_i^4$ and its Frobenius algebra is therefore degenerate (cf. section 5.1). This element is crucial for the completion of the sub-representations of M around $\psi = 0$, which are given by[2]

$$\mathbb{Z}_8 : \qquad \left\langle 1,\, \prod_{i=1}^{6} x_i^2,\, \prod_{i=3}^{6} x_i^4, \overline{1} \right\rangle \quad \text{with } \mathbb{Z}_8\text{-weights } \{1,3,5,7\}\,, \tag{6.1.31}$$

$$\mathbb{Z}_4 : \qquad \left\langle \prod_{i=1}^{6} x_i,\, \overline{\prod_{i=1}^{6} x_i} \right\rangle \quad \text{with } \mathbb{Z}_4\text{-weights } \{1,3\}\,. \tag{6.1.32}$$

Note that the deformations for $H^{2,2}$ do not appear complex conjugated.

In subsection 5.5.1, we identified a splitting of Hodge structure on the five-fold family given by the degree 30 hypersurfaces in $\mathbb{P}_{15,10,1^5}$. With the deformation monomials

$$k = 1 : \quad \chi_1 = x_2 \prod_{i=3}^{7} x_i^4 \,,\; \chi_2 = \prod_{i=3}^{7} x_i^6 \,, \tag{6.1.33}$$

$$k = 2 : \quad \chi_1\chi_2 \,,\; \chi_2^2 \,, \tag{6.1.34}$$

and their complex conjugates, we find the following decomposition into irreducible representations of $\mathbb{Z}_{30}$

$$\mathbb{Z}_{30} : \quad \left\langle 1,\, \chi_2,\, \chi_1\chi_2, \chi_2^2 \right\rangle \cup \text{ c.c. with } \mathbb{Z}_{30}\text{-weights } \{1,7,11,13,17,19,23,29\}\,, \tag{6.1.35}$$

$$\mathbb{Z}_6 : \quad \langle \chi_1,\, \overline{\chi_1} \rangle \qquad\qquad \text{with } \mathbb{Z}_6\text{-weights } \{1,5\}\,. \tag{6.1.36}$$

It is important to note that M_ψ^6 is not a symmetry of the family since the modulus parametrising χ_2 is not invariant under it. This violated periodicity condition [113] restricts the splitting to $\psi = \phi = 0$, which we verified explicitly in subsection 5.5.1.

We finish this subsection by giving the rational splitting into mirror periods and orthogonal parametrisations for the sextic quotient introduced in the beginning. The origin of the splitting is the existence of two $\mathbb{Z}_2$ symmetries in the ambient space

$$\sigma_\pm : \quad \begin{matrix} x_2 \leftrightarrow x_3 \\ \pm x_4 \leftrightarrow x_5 \end{matrix} \,, \tag{6.1.37}$$

whose induced maps on the moduli space $\hat{\sigma}_\pm$ have the fixed-point loci $a_\pm = 0$ (cf. eq. (6.1.2)), respectively, where

$$a_\pm := a_6 \pm a_7 \,. \tag{6.1.38}$$

[2]The weights of the monodromy can also be read-off from the indicials at infinity of the model's Picard–Fuchs operator $\mathcal{L}^{(6)}(z) = (1-2\theta)\,\theta^5 + 32z\,(4\theta+1)\,(4\theta+3)\,(8\theta+1)\,(8\theta+3)\,(8\theta+5)\,(8\theta+7)\,.$

The decomposition of $\underline{\Pi}$ into invariant and non-invariant periods in eq. (6.1.21) takes the form

$$\begin{pmatrix} \underline{\Pi}_{\text{inv}} \\ \underline{\Pi}_{+} \\ \underline{\Pi}_{-} \end{pmatrix}(\underline{a}) = \begin{pmatrix} 0 & 0 & 0 & -3 & 1 & -1 & -1 & 2 \\ 1 & 1 & 1 & -1 & 1 & 0 & 0 & 0 \\ 1 & 1 & 1 & 11 & -3 & 0 & 0 & 0 \\ 1 & 0 & 0 & 0 & 0 & 0 & 0 & 0 \\ 1 & 1 & 1 & 3 & -1 & 1 & 1 & 0 \\ 1 & 1 & 1 & 0 & 0 & 0 & 0 & 0 \\ 0 & 1 & -1 & 0 & 0 & 0 & 0 & 0 \\ 0 & 1 & -1 & 0 & 0 & 1 & -1 & 0 \end{pmatrix} \underline{\Pi}(\underline{a})\,, \tag{6.1.39}$$

where $\underline{\Pi}_{\pm}$ changes sign under $a_{\pm} \mapsto -a_{\pm}$ while the other components are invariant. In [1], we performed the above analysis also for the two other three-parameter quotients $\mathcal{X}_8^{(3)}$ and $\mathcal{X}_{10}^{(3)}$ with a similar splitting. In section 6.2, we will see that the two rows of above matrix yielding $\underline{\Pi}_{\pm}$ are fluxes for a supersymmetric vacuum along the locus $a_{\pm} = 0$. We verified that the Kähler potential at $a_{\pm} = 0$ is flat along $a_{\pm}$ guaranteeing that the F-term equations for $a_{\pm}$ are satisfied on this locus for a supersymmetric vacuum on the mirror locus. It follows that the attractor point at the Fermat point $a_0 = a_+ = a_- = 0$ is a supersymmetric vacuum in a compactification on $\mathcal{X}_6^{(3)}$.

6.2 Type IIB flux vacua

The splittings of Hodge structures discussed before are essential for the study of flux vacua. In section 3.4, we saw that vacua presuppose a rank-two lattice inside

$$H^c(X,\mathbb{Z}) = H^3(X,\mathbb{Z}) \cap (H^{2,1}(X,\mathbb{C}) \oplus H^{1,2}(X,\mathbb{C}))\,, \tag{6.2.1}$$

which generically has rank zero. Points in the moduli space where this lattice has rank one are called rank-one attractor points. For rank two, the integral generators f and h together with a suitable value for the axio-dilaton then give rise to a superpotential which preserves $N = 1$ supersymmetry (cf. section 3.3). The F-term equations restrict the moduli to certain loci in the moduli space. This restriction is known as moduli stabilisation, which plays an important part in string phenomenology. Here, we will analyse flux configurations arising from the symmetry considerations of section 6.1. In many-moduli cases, turning on fluxes of different such rank-two lattices is possible, if the values for the axio-dilaton are compatible. We will show that this compatibility is a non-trivial statement and use the family $\mathcal{X}_6^{(3)}$ as an example where it is violated.

To introduce the concepts, we first consider the attractor point/flux vacuum at the Fermat sextic [74]. At the orbifold, one finds four solutions $\widetilde{\varpi}_i\,,\, i \in \{1,2,4,5\}$, to the Picard–Fuchs operator with indicials $i/6$. As we explained in section 6.1, these solutions form two irreducible representations of the $\mathbb{Z}_6$ symmetry group. As in eqs. (6.1.26) and (6.1.27), these sub-representations have integral generators given by

$$\underline{\varpi} = \frac{3}{32}\begin{pmatrix} \widetilde{\varpi}_1 + \widetilde{\varpi}_4 \\ \beta\,\widetilde{\varpi}_1 + \beta^5\widetilde{\varpi}_4 \\ \widetilde{\varpi}_2 + \widetilde{\varpi}_3 \\ \beta^2\widetilde{\varpi}_2 + \beta^4\widetilde{\varpi}_3 \end{pmatrix}, \tag{6.2.2}$$

in a normalisation such that the transition matrix to the integral symplectic basis with $\underline{\Pi} = T_\psi\, \underline{\varpi}$ is given by

$$T_\psi^{-1} = \begin{pmatrix} -6 & -3 & 6 & 3 \\ -3 & 12 & 3 & -1 \\ -6 & -1 & 2 & 3 \\ 3 & 2 & -1 & -3 \end{pmatrix}. \tag{6.2.3}$$

As the second two periods of $\underline{\varpi}$ correspond to elements in the lattice $H^c(X,\mathbb{Z})$, it is generated by the last two rows of T_ψ^{-1}. We verify the former statement with the behaviour of the integral period vector around $\psi = 0$

$$\frac{\underline{\Pi}}{\psi} \propto \left(1 - i\sqrt{3},\, 2,\, 1 - 3i\sqrt{3},\, 2\right) + \mathcal{O}(\psi)\,, \tag{6.2.4}$$

where we performed a Kähler gauge transformation $\underline{\Pi} \mapsto \underline{\Pi}/\psi$ to preserver regularity of the Kähler potential. The two fluxes

$$f^T\Sigma = (-6,-1,2,3) \quad \text{and} \quad h^T = (3,2,-1,-3) \tag{6.2.5}$$

imply with the F-term equation $D_\psi W = 0$

$$(f - \tau h)^T \Sigma D_\psi\, \underline{\Pi}\big|_{\psi=0} \stackrel{!}{=} 0 \quad \Rightarrow \quad \tau = -\frac{1}{2} - \frac{\mathrm{i}\sqrt{3}}{2}\,. \tag{6.2.6}$$

The axio-dilaton is, due to the choice of fluxes in the rank-two lattice, defined only up to a $\mathrm{GL}(2,\mathbb{Z})$ transformation. For a given tadpole, this freedom is reduced to $\mathrm{SL}(2,\mathbb{Z})$. In a similar manner, one can analyse the orbifold attractor points for the one-parameter hypergeometric models $X_{4,3}$ and $X_{6,2}$.

This procedure to construct flux configurations extends to any such vacua along codimension-one loci in the moduli space. For vacua in higher codimension, the condition $G \in H^{2,1}$ may not be realisable due to conflicting values for the axio-dilaton for the different sets of fluxes. We will now show this incompatibility explicitly for the three-parameter model $\mathcal{X}_6^{(3)}$. At the end of the section, we will consider another example where a symmetry between the flux configurations guarantees agreeing values for the axio-dilaton on the vacuum locus. In the language of section 6.1, we have the differential forms

$$\omega_i = \mathrm{Res}\left(\frac{\mathrm{def}_i \mu}{P^2}\right) \tag{6.2.7}$$

with

$$\mathrm{def}_0 = \prod_{i=1}^{5} x_i\,, \quad \mathrm{def}_6 = x_2^3 x_5^3 \quad \text{and} \quad \mathrm{def}_7 = x_3^3 x_4^3\,. \tag{6.2.8}$$

Then, the middle cohomology decomposes into the four representations generated by

$$H^3(X_{\underline{a}},\mathbb{Z}) = \left\langle \Omega, \overline{\Omega} \right\rangle \oplus \left\langle \omega_0, \overline{\omega_0} \right\rangle \oplus \left\langle \omega_6, \overline{\omega_6} \right\rangle \oplus \left\langle \omega_7, \overline{\omega_7} \right\rangle. \tag{6.2.9}$$

While the integral representations of the first two (corresponding to the mirror cohomology) was given above, for the last two, we find the integral generators

$$\begin{aligned} \alpha_1 &= \omega_6 + \overline{\omega_6}\,, \quad \alpha_2 = \beta^4\,\omega_6 + \beta^2\,\overline{\omega_6}\,, \\ \beta_1 &= \omega_7 + \overline{\omega_7}\,, \quad \beta_2 = \beta\,\omega_7 + \beta^5\,\overline{\omega_7} \end{aligned} \tag{6.2.10}$$

with $M_5\omega_6 = \alpha^4\omega_6$ and $M_5\omega_7 = \alpha\,\omega_7$. This basis $(\alpha_1, \alpha_2, \beta_1, \beta_2)$ transforms under the monodromy M_5 as

$$M_5 = \begin{pmatrix} 0 & 1 & 0 & 0 \\ -1 & -1 & 0 & 0 \\ 0 & 0 & 0 & 1 \\ 0 & 0 & -1 & 1 \end{pmatrix}. \tag{6.2.11}$$

We define the elements $\omega_\pm \coloneqq \omega_6 \pm \omega_7$, which are contained in $H^{2,1} \oplus H^{1,2}$ for fibres over $a_\pm = 0$. The integral generators above can be expressed as

$$\alpha_1 + \beta_1 = \omega_+ + \overline{\omega_+} \tag{6.2.12}$$

$$\text{and } \alpha_2 - \beta_2 = -\alpha\,\omega_+ - \alpha^5\overline{\omega_+}\,, \tag{6.2.13}$$

which shows that, in these special fibres, the elements generate a rank-two lattice denoted by $H^c(X_{a_+=0}, \mathbb{Z})$. A similar basis exists on the locus $a_- = 0$.

The defining polynomial of $\mathcal{X}_6^{(3)}$ in eq. (6.1.2) has a residual symmetry given by $b = \mathbb{Z}_6 : (0,0,0,0,5)$, which acts on the above parameters as

$$b: \quad \begin{matrix} a_0 \mapsto \beta\, a_0 \\ a_- \leftrightarrow a_+ \end{matrix}, \quad \beta^6 = 1\,. \tag{6.2.14}$$

Thus, the following discussion of the vacua along the loci $a_\pm = 0$ are mapped into each other under b, while rotating a_0. The splitting of eq. (6.1.39) implies that the fluxes on $a_- = 0$ lie in the lattice generated by

$$f_-^T\Sigma = (0,1,-1,0,0,0,0,0)\,, \tag{6.2.15}$$

$$h_-^T\Sigma = (0,1,-1,0,0,1,-1,0)\,, \tag{6.2.16}$$

since $g^T\Sigma\cdot\underline{\Pi}\big|_{a_-=0} = 0$ for $g \in \{f_-, h_-\}$. The F-term equation for a_- imply that supersymmetric vacua demand

$$\begin{aligned} \tau_- = -\frac{1}{2} + \frac{\mathrm{i}\sqrt{3}}{2} + a_0 \left(\frac{9\left(\sqrt{3}-i\right)\Gamma\left(\frac{2}{3}\right)^6}{16\,2^{2/3}\pi^3} + \mathcal{O}\left(a_+^2\right) \right) \\ + a_0^2 \left(-\frac{27\left(\left(\sqrt{3}-i\right)\left(3i+\sqrt{3}\right)\Gamma\left(\frac{2}{3}\right)^{12}\right)}{512\cdot 2^{1/3}\pi^6} + \mathcal{O}\left(a_+^2\right) \right) + \mathcal{O}\left(a_0^3\right). \end{aligned} \tag{6.2.17}$$

Note that, up to an $\mathrm{SL}(2,\mathbb{Z})$ transformation, the constant term corresponds to the value at the one-parameter vacuum $a_+ = a_0 = 0$ in eq. (6.2.6). Along $a_+ = 0$, the fluxes of eq. (6.1.39) are given by

$$f_+^T\Sigma = (1,1,1,3,-1,1,1,0)\,, \tag{6.2.18}$$

$$h_+^T\Sigma = (1,1,1,0,0,0,0,0) \tag{6.2.19}$$

with the resulting axio-dilaton value

$$\begin{aligned} \tau_+ = -\frac{1}{2} + \frac{\mathrm{i}\sqrt{3}}{2} + a_0 \left(\frac{9\Gamma\left(\frac{2}{3}\right)^6}{4\,2^{2/3}\left(-i+\sqrt{3}\right)\pi^3} + \mathcal{O}\left(a_-^2\right) \right) \\ + a_0^2 \left(\frac{27\left(3-i\sqrt{3}\right)\Gamma\left(\frac{2}{3}\right)^{12}}{256\sqrt[3]{2}\pi^6} + \mathcal{O}\left(a_-^2\right) \right) + \mathcal{O}\left(a_0^3\right). \end{aligned} \tag{6.2.20}$$

The above mentioned equivalence under b-symmetry is expressed as

$$\tau_-(\alpha\, a_0, a_\mp) = \tau_+(a_0, a_\pm)\,. \tag{6.2.21}$$

Thus, the two sets of vacua intersect on the mirror locus $a_+ = a_- = 0$ but a viable vacuum is present only at $a_0 = 0$.

The axio-dilaton value gives the complex-structure parameter of an elliptic curve associated to a specific vacuum fibre. For continuous vacua, one finds a family of elliptic curves whose periods are given by the numerator and denominator of τ as in eq. (3.4.12). Along $a_{=}0$, the periods

$$\left.\begin{pmatrix} f_+^T \Sigma \partial_{a_+} \underline{\Pi} \\ h_+^T \Sigma \partial_{a_+} \underline{\Pi} \end{pmatrix}\right|_{a_\pm=0} (a_0) \tag{6.2.22}$$

are annihilated by the elliptic operator

$$\mathcal{L}^{(2)}_{\mathrm{el},+}(z) = \theta^2 - 12z(3\theta+1)(3\theta+2)\,, \tag{6.2.23}$$

$$\mathcal{P}_{\mathcal{L}^{(2)}_{\mathrm{el},+}} \left\{ \begin{array}{ccc|c} 0 & \frac{1}{108} & \infty & \\ \hline 0 & 0 & \frac{1}{3} & z \\ 0 & 0 & \frac{2}{3} & \end{array} \right\}. \tag{6.2.24}$$

where $z = 1/a_0^3$ and $\theta = z\partial_z$. This family is given by a hypersurface of degree three in $\mathbb{P}^2$ and the operator corresponds to operator B in Table 7.5. We find an integral symplectic period basis for this operator given by

$$\underline{\Pi}^{\mathrm{el},+}(z) = \begin{pmatrix} 1 & 0 \\ -\frac{\mathrm{i}\log 2}{\pi} & \frac{1}{2\pi\mathrm{i}} \end{pmatrix} \underline{\varpi}^{\mathrm{el},+}(z)\,, \tag{6.2.25}$$

with the Frobenius basis $\underline{\varpi}^{\mathrm{el},+}(z) = (1, \log(z)) + \mathcal{O}(z)$. In the patch $z > 1/108$, the components of τ_+ in eq. (6.2.22) are given by

$$\left.\begin{pmatrix} f_+^T \Sigma \partial_{a_+} \underline{\Pi} \\ h_+^T \Sigma \partial_{a_+} \underline{\Pi} \end{pmatrix}\right|_{a_\pm=0} (a_0) = \frac{1}{\pi} \begin{pmatrix} 1 & 3 \\ 1 & 0 \end{pmatrix} \underline{\Pi}^{\mathrm{el},+}(a_0)\,. \tag{6.2.26}$$

As expected from the b-symmetry (6.2.14), we have $\mathcal{L}^{(2)}_{\mathrm{el},-}(z) = \mathcal{L}^{(2)}_{\mathrm{el},+}(-z)$. An integral basis is, for example, given by

$$\underline{\Pi}^{\mathrm{el},-}(z) = \begin{pmatrix} 1 & 0 \\ \frac{1}{2} - \frac{\mathrm{i}\log 2}{\pi} & \frac{1}{2\pi\mathrm{i}} \end{pmatrix} \underline{\varpi}^{\mathrm{el},-}(z)\,, \tag{6.2.27}$$

which implies

$$\left.\begin{pmatrix} f_-^T \Sigma \partial_{a_-} \underline{\Pi} \\ h_-^T \Sigma \partial_{a_-} \underline{\Pi} \end{pmatrix}\right|_{a_\pm=0} (a_0) = \frac{1}{\pi} \begin{pmatrix} 1 & 0 \\ 4 & -3 \end{pmatrix} \underline{\Pi}^{\mathrm{el},-}(a_0)\,. \tag{6.2.28}$$

Finally, we note that the j-invariant is given by

$$j(\tau^{\mathrm{el},\pm}(z)) = \pm \frac{(1 \pm 864z)^3}{4z(1 \mp 108z)^3}\,. \tag{6.2.29}$$

As a counterexample where two codimension one vacua extend to a vacuum on their intersection, we review briefly the symmetric flux vacuum on the three-parameter mirror family of the CICY

$$\mathcal{X}^{(3)}_{\text{sym}} = \left(\begin{array}{c|ccc} \mathbb{P}^2 & 1 & 1 & 1 \\ \mathbb{P}^2 & 1 & 1 & 1 \\ \mathbb{P}^2 & 1 & 1 & 1 \end{array} \right)^{3,48}_{-90} . \tag{6.2.30}$$

The model is completely symmetric in all three complex-structure moduli z_1, z_2 and z_3. To compare it to the model $\mathcal{X}^{(3)}_6$, we change to the new coordinates $u_1 = z_1$, $u_2 = z_1 - z_2$ and $u_3 = z_1 - z_3$. Note that the divisors $u_2 = 0$ and $u_3 = 0$ are fixed-point loci of the $\mathbb{Z}_2$ symmetries $z_1 \leftrightarrow z_2$ and $z_1 \leftrightarrow z_3$, respectively. There, one finds one set of fluxes each with values for the axio-dilaton that agree on $u_2 = u_3 = 0$

$$\tau(z) = -\frac{3i \log(z)}{\pi} + \frac{45iz^2}{2\pi} - \frac{999iz^4}{4\pi} + \mathcal{O}\left(z^5\right), \tag{6.2.31}$$

where we parametrise the one-parameter locus by $z \equiv z_1 = z_2 = z_3$. The compatibility of the axio-dilaton values follow from a $\mathbb{Z}_2$ symmetry between the symmetries mapping $z_2 \leftrightarrow z_3$. In [1], we showed that the one-parameter model defined over this symmetric locus has an attractor point at $z = -1$ whose flux vacuum yields an axio-dilaton value agreeing with eq. (6.2.21). From the above, one expects to see a factorisation at $z_i = -1$ in the local zeta function of the form $R_3(T) = p_1(T)p_2(T)^3$, where $p_i(T)$ are quadratic polynomials and $p_2(T)$ corresponding to the elliptic curve with complex-structure modulus $\tau(-1)$.

6.3 F-theory flux vacua

Similarly to type IIB theory, the supersymmetry conditions for flux compactifications to four dimensions in M/F-theory imply a splitting of the integral Hodge structure. In the previous subsection, we saw that type IIB on three-folds yield flux vacua along loci with a sub-lattice of Hodge structure (0,1,1,0). As discussed in section 3.4, on four-folds, this lattice is required to be of type (0,0,1,0,0) in the primitive cohomology. In [1], we studied a vacuum locus of the four-fold family $\mathbb{P}_{12,8,1^4}[24]$, see subsection 5.4.2 for a review of the specific family. There, the superpotential is given by the integral of the holomorphic $(4,0)$-form $\Omega(z)$ over an S^4 which vanishes along a conifold locus. The explicit analytical continuation throughout the complex-structure moduli space has been been performed before in [127]. Here, we would like to shed light on this vacuum locus from a different perspective. In chapter 7, we will study strong coupling/conifold transition in type IIB compactified on three-folds. We find that the period structure along this vacuum locus is closely related to the discussion there, which is expected due to the similar origin of a shrinking S^n.

We used the mirror of $\mathbb{P}_{12,8,1^4}[24]$ in subsection 5.4.2 to exemplify the integral period structure of four-fold families. The toric and topological data for this model together with the Picard–Fuchs system can be found there. The Hadamard product of two formal power series given by $F(z) = \sum_{i=0}^{\infty} f_i z^i$ and $G(z) = \sum_{i=0}^{\infty} g_i z^i$ is defined as

$$(F * G)(z) = \sum_{i=0}^{\infty} f_i g_i z^i . \tag{6.3.1}$$

The holomorphic period of the four-fold can then be written as the Hadamard product (in z_2) of the holomorphic solution to the order-two operator D (cf. Table 7.5) corresponding to the elliptic fibre and the period

$$\varpi_0^{(2)}(z_1,z_2) = \frac{1}{(2\pi\mathrm{i})^2}\oint_{|x_i|=1}\frac{1}{1+x_1^4+x_2^4+x_3^4+x_4^4+z_2^{-1/4}x_1x_2x_3x_4} \times\frac{\prod_{i=1}^4\mathrm{d}x_i}{x_1x_2x_3x_4+z_1z_2^{1/4}}\,. \tag{6.3.2}$$

At $z_2^{-1/4}=4$, this function becomes a solution to a self-adjoint third order operator

$$\begin{aligned}\mathcal{L}^{(3)}(z) = {}&\theta^3-4z(2\theta(\theta(2\theta+3)+2)+1)+16z^2(\theta+1)(6\theta(\theta+2)+7)\\ &-128z^3(\theta+1)(\theta+2)(2\theta+3)\end{aligned} \tag{6.3.3}$$

with Riemann symbol

$$\mathcal{P}_{\mathcal{L}^{(3)}}\left\{\begin{array}{ccccc|c} 0 & \frac{1}{8} & \frac{1+\mathrm{i}}{8} & \frac{1-\mathrm{i}}{8} & \infty & \\ \hline 0 & 0 & 0 & 0 & 1 & \\ 0 & \frac{1}{2} & \frac{1}{2} & \frac{1}{2} & \frac{3}{2} & , \ z \\ 0 & 1 & 1 & 1 & 2 & \end{array}\right\}. \tag{6.3.4}$$

We note that the degree three order-two operator whose symmetric square yields $\mathcal{L}^{(3)}$ is again self-adjoint, has integral mirror map and holomorphic solution and a Yukawa coupling that has order-two branch cuts between the four singularities besides the MUM point.

Along the vacuum locus $z_2^{-1/4}=4$, the two-parameter family transitions to a one-parameter model described by a seventh-order operator $\mathcal{L}^{(7)} = \mathcal{L}^{(3)} * \mathcal{L}_D^{(2)}$, which is of z-degree three. Instead of giving its lengthy definition, we show only its Riemann symbol:

$$\mathcal{P}_{\mathcal{L}^{(7)}}\left\{\begin{array}{ccccc|c} 0 & \frac{1}{864} & \frac{1+\mathrm{i}}{864} & \frac{1-\mathrm{i}}{864} & \infty & \\ \hline 0 & 0 & 0 & 0 & \frac{1}{6} & \\ 0 & 1 & 1 & 1 & \frac{5}{6} & \\ 0 & \frac{3}{2} & \frac{3}{2} & \frac{3}{2} & \frac{7}{6} & , \ z_1 \\ 0 & 2 & 2 & 2 & \frac{9}{6} & \\ 0 & 3 & 3 & 3 & \frac{11}{6} & \\ 1 & 4 & 4 & 4 & \frac{13}{6} & \\ 2 & 5 & 5 & 5 & \frac{17}{6} & \end{array}\right\}. \tag{6.3.5}$$

In [1], J. Dücker gave the explicit form of the vanishing flux, verified the tadpole bound and showed that the vacuum extends into the regime $z_1 \to 0$ corresponding to weak coupling as $\mathrm{Im}\, t_E \sim 1/g_s \to \infty$.

6.4 (De-)constructing four-fold flux compactifications

For families with one complex-structure parameter, the discussions of the previous section for three- and four-folds are intimately related. At the end of section 4.6, we reviewed the decomposition of any one-parameter K3 Picard–Fuchs operator into the symmetric square of a second order differential operator. This is possible, because, locally, the monodromy groups of these

operators are isomorphic, cf. eq. (4.6.35). A similar relation holds for the fundamental representation of the monodromy group of four-fold operators

$$\mathrm{SO}_0(3,2) \cong \frac{\mathrm{Sp}(4,\mathbb{R})}{\pm\mathbb{1}}\,. \tag{6.4.1}$$

The antisymmetric representation of $\mathrm{Sp}(4,\mathbb{R})$ decomposes into the sum of the fundamental and the trivial representation of $\mathrm{SO}(3,2)$. The pullback of a fifth-order operator to one of order four is named after Yifan Yang (YY) and was studied in [99, 128]. The fifth-order operators belonging to the 14 hypergeometric three-fold families where given explicitly in [129].

This section repeats our discussion in [1], where we have shown that type IIB flux vacua on a three-fold are equivalent to satisfying the M-theory flux conditions on the geometry described by its YY lift. Vice versa, one can search for M-theory flux vacua on four-folds by analysing its YY pullback with the powerful techniques developed for three-fold operators. To our knowledge, there is little reason to believe that a YY partner to a Picard–Fuchs operator describing the period geometry of a Calabi–Yau family again has a geometric realisation. As for the pullbacks of K3-type operators to order two, for monodromies that are not contained in the identity component of the monodromy group, the monodromies on the pullback generally loose integrality and instead lie in an (imaginary) quadratic field extension.

Given a CY-type operator of order four (possibly describing a three-fold geometry) with solutions $\underline{\varpi}$, we denote the minors of its Wronskian by

$$W^{i,j}_{\underline{\varpi}} = 2\pi\mathrm{i}\,\det\begin{pmatrix}\varpi_i & \varpi_j\\ \theta\varpi_i & \theta\varpi_j\end{pmatrix}, \tag{6.4.2}$$

which are solutions to the fifth-order operator given by the YY lift. Since we are interested in flux vacua, we need to obtain an integral basis $\underline{\Pi}^{(4)}$ for this operator, which can be inferred from the integral basis of the three-fold. We mentioned above that the antisymmetric square yields the sum of the fundamental and trivial representation of $\mathrm{SO}(3,2)$. The latter is identified with the relation from Griffiths transversality (4.2.20)

$$\underline{\Pi}^{(3)\,T}\Sigma\partial_z\underline{\Pi}^{(3)} = 0 \Longrightarrow 0 = W^{1,4}_{\underline{\Pi}^{(3)}} + W^{2,3}_{\underline{\Pi}^{(3)}}\,, \tag{6.4.3}$$

reducing the six minors to five independent solution to the fifth-order operator. In the following we will be ignoring the minor $W^{1,4}_{\underline{\Pi}^{(3)}}$ and denote

$$\underline{\Pi}^{(4)} = \left(W^{1,2}_{\underline{\Pi}^{(3)}},\, W^{1,3}_{\underline{\Pi}^{(3)}},\, W^{2,3}_{\underline{\Pi}^{(3)}},\, W^{2,4}_{\underline{\Pi}^{(3)}},\, W^{3,4}_{\underline{\Pi}^{(3)}}\right). \tag{6.4.4}$$

We recall that for type IIB flux vacua, the superpotential W obeys

$$W = F + \tau H = 0 \quad \text{and} \quad \partial W = \partial F + \tau\partial H = 0\,, \tag{6.4.5}$$

$$F = H = 0\,. \tag{6.4.6}$$

We identify eq. (6.4.5) with the vanishing of the minor

$$G = 2\pi\mathrm{i}\,\det\begin{pmatrix}F & H\\ \theta F & \theta H\end{pmatrix}. \tag{6.4.7}$$

Linearity of the determinant implies that G can be expressed as an integral linear combination of the integral basis $\underline{\Pi}^{(4)}$. The second M-theory flux condition follows from the vanishing of F and H

$$\theta G = 2\pi\mathrm{i}\left(F\theta^2 H - H\theta^2 F\right) = 0\,. \tag{6.4.8}$$

Consider, for example, the bi-cubic in $\mathbb{P}^5$ described by the Picard–Fuchs operator AESZ 1.4 in Table 7.6. This model has an attractor point or flux vacuum at $z = -1/2^3 3^6$ [130] with a flux lattice spanned by

$$f_{3,3}^T\Sigma = (-3,0,0,1)\,, \quad h_{3,3}^T\Sigma = (0,0,1,4)\,. \tag{6.4.9}$$

The integral period basis of the YY lift satisfies the M-theory flux conditions $G = \partial G = 0$ at the same point $z = -1/2^3 3^6$, where the flux is given by

$$\tilde{g} = (0,3,-12,0,1)\,, \tag{6.4.10}$$

with $\tilde{g}\cdot\underline{\Pi}^{(4)}(-1/2^3 3^6) = 0$. We also verified that the attractor points of $X_{6,4}$, X_6 and $X_{4,3}$ yield supersymmetric fluxes for the YY lift. The orbifold of the hypergeometric families X_5, X_8, X_{10} and $X_{2,12}$ have a Hodge splitting over a quadratic field extension, meaning that their fibres satisfy the vacuum condition with flux values in that extension. While these do not correspond to supersymmetric vacua, the irrationality cancels in the antisymmetric product yielding an integral supersymmetric flux for the fibre of the YY lift. More precisely, the fluxes for the three-fold families are given by

$$f^T\Sigma = \left(a,0,-b+\sqrt{c},d\right)\,, \quad h^T\Sigma = \left(0,a,0,-b-\sqrt{c}\right)\,, \tag{6.4.11}$$

for some $a,b,c,d\in\mathbb{N}$. With $F = f^T\Sigma\,\underline{\Pi}^{(3)}$ and $H = h^T\Sigma\,\underline{\Pi}^{(3)}$, we find that the irrational contribution with $\sqrt{c}$ in eq. (6.4.7) is proportional to the vanishing expression of eq. (6.4.3). This recovers integrality of the fluxes on the YY lift and the resulting flux satisfies the vacuum conditions.

The above description of the Picard–Fuchs system of a three-fold in terms of an order five operator of CY-type may serve as a testing ground for four-fold vacua in one-parameter models. But, as we mentioned above, we are unaware of an example where these YY lifts correspond to geometric four-fold families. For the rest of this subsection, we will turn to the possibly more interesting direction of describing four-fold vacua with a CY3-type operator. As examples, we will consider the hypergeometric families $X_6\subset\mathbb{P}^5$ and $X_{10}\subset\mathbb{P}_{5,1^5}$ and the symmetric subfamily of the Hulek–Verrill four-fold. The idea is to make an ansatz for the Frobenius basis for the third-order operator whose antisymmetric square yields the solutions of the four-fold's PF operator. As for the other direction discussed above, the connection between the two operators is not just local but the integrality of the four-fold period basis obtained, for example, from the $\hat{\Gamma}$-class singles out a specific rationality condition for the fourth-order operator. Rationality for a three-fold is expressed through the ratio $c = \chi/c_{111}$ of the Euler number and the triple intersection number and a rational period basis can be obtained from a prepotential (4.6.45) of the form

$$\mathcal{F} = \frac{t^3}{3!} - \frac{c\,\zeta_3}{2(2\pi\mathrm{i})^3} + \mathcal{O}(q)\,. \tag{6.4.12}$$

Let us denote $\underline{\Pi}^{(3)}$ as the basis obtained from matching the local solutions of the YY pullback to the asymptotic basis of this prepotential. In [1], we observed two equivalent ways of determining

c for the YY pullback: (1) the matrix relating the minors $W_{\underline{\Pi}^{(3)}}$ to the four-fold basis $\underline{\Pi}^{(4)}$ becomes rational and (2) the entries of the Frobenius F_p becomes, to any finite p-adic order, an algebraic function. For more information on the arithmetic properties of the pullback, we refer to [1] and the references therein. Here, we will focus on the argument (1) and give the mappings for the three geometries under consideration.

The two hypergeometric families are described by the Picard–Fuchs operators

$$\mathcal{L}^{(5)}_{\mathcal{Y}_6} = \theta^5 - 6z\prod_{i=1}^{5}(6\theta+i)\,, \tag{6.4.13}$$

$$\mathcal{L}^{(5)}_{\mathcal{Y}_{10}} = \theta^5 - 2^5 z(10\theta+1)(10\theta+3)(10\theta+5)(10\theta+7)(10\theta+9) \tag{6.4.14}$$

with Riemann symbols

$$\mathcal{P}_{\mathcal{L}^{(5)}_{\mathcal{Y}_6}}\left\{\begin{array}{cccc} 0 & 1/2^6 3^6 & \infty & \\ \hline 0 & 0 & \frac{1}{6} & \\ 0 & 1 & \frac{1}{3} & , z \\ 0 & \frac{3}{2} & \frac{1}{2} & \\ 0 & 2 & \frac{2}{3} & \\ 0 & 3 & \frac{5}{6} & \end{array}\right\}, \quad \mathcal{P}_{\mathcal{L}^{(5)}_{\mathcal{Y}_{10}}}\left\{\begin{array}{cccc} 0 & 1/2^{10} 5^5 & \infty & \\ \hline 0 & 0 & \frac{1}{10} & \\ 0 & 1 & \frac{3}{10} & , z \\ 0 & \frac{3}{2} & \frac{1}{2} & \\ 0 & 2 & \frac{7}{10} & \\ 0 & 3 & \frac{9}{10} & \end{array}\right\}. \tag{6.4.15}$$

From the indicials, we deduce that the monodromies around the conifold and orbifold points have determinant -1 and we expect that their pullbacks have monodromies in a field extension around these points. The pullbacks of the sextic and decic are given by Kähler-gauge transformed versions of the operators AESZ 2.45 and AESZ 2.40, respectively. Here, they appear as

$$\begin{aligned}\mathcal{L}^{(4)}_{2.45} = {} & \theta^4 + 2^2 3^2 z(217 - 18\theta(3\theta-1)(8\theta(12\theta+7)+23)) \\ & + 2^4 3^8 z^2(144\theta(48\theta(9\theta(2\theta+1)+2)-7)+10633) \\ & - 2^{12} 3^{14} z^3(36\theta(6\theta(24\theta(4\theta+3)+19)+43)-301) \\ & + 2^{22} 3^{22} z^4 \theta(2\theta+1)(3\theta+1)(6\theta+1)\,,\end{aligned} \tag{6.4.16}$$

$$\begin{aligned}\mathcal{L}^{(4)}_{2.40} = {} & \theta^4 - 2^4 5 z(2000\theta(\theta(20\theta(4\theta+1)+3)-7)-7189) \\ & + 2^{15} 5^6 z^2(500\theta(\theta(120\theta(2\theta+1)+23)-5)+10079) \\ & - 2^{25} 5^{11} z^3(250\theta(8\theta(10\theta(4\theta+3)+7)+19)-1121) \\ & + 2^{32} 5^{16} z^4(20\theta-1)(20\theta+3)(20\theta+7)(20\theta+11)\end{aligned} \tag{6.4.17}$$

with Riemann symbols

$$\mathcal{P}_{\mathcal{L}^{(4)}_{2.45}}\left\{\begin{array}{cccc} 0 & 1/2^6 3^6 & \infty & \\ \hline 0 & \frac{1}{4} & 0 & \\ 0 & \frac{3}{4} & \frac{1}{6} & , z \\ 0 & \frac{7}{4} & \frac{1}{3} & \\ 0 & \frac{9}{4} & \frac{1}{2} & \end{array}\right\}, \quad \mathcal{P}_{\mathcal{L}^{(4)}_{2.40}}\left\{\begin{array}{cccc} 0 & 1/2^{10} 5^5 & \infty & \\ \hline 0 & \frac{1}{4} & -\frac{1}{20} & \\ 0 & \frac{3}{4} & \frac{3}{20} & , z \\ 0 & \frac{7}{4} & \frac{7}{20} & \\ 0 & \frac{9}{4} & \frac{11}{20} & \end{array}\right\}. \tag{6.4.18}$$

		$\mathcal{Y}_6$-pullback: AESZ 2.45	$\mathcal{Y}_{10}$-pullback: AESZ 2.40
conifold	M_μ	$\frac{\mathrm{i}\sqrt{3}}{192}\begin{pmatrix} -120 & 0 & -192 & 0 \\ 0 & 120 & 0 & 192 \\ 11 & 0 & 120 & 0 \\ 0 & -11 & 0 & -120 \end{pmatrix}$	$\frac{\mathrm{i}}{576}\begin{pmatrix} -840 & 0 & -576 & 0 \\ 0 & 840 & 0 & 576 \\ 649 & 0 & 840 & 0 \\ 0 & -649 & 0 & -840 \end{pmatrix}$
	f, h	$(11, 0, 8(15-8\sqrt{3}), 0)$, $(0, 11, 0, 8(15+8\sqrt{3}))$	$(59, 0, 24, 0)$, $(0, 11, 0, 24)$
	g	$(1, 0, 0, 0, 1)$	$(1, 0, 0, 0, 1)$
orbifold	M_∞	$\frac{\mathrm{i}\sqrt{3}}{192}\begin{pmatrix} 216 & -192 & 192 & 0 \\ 88 & -24 & -192 & -192 \\ -71 & 120 & -120 & 0 \\ 9 & -49 & 120 & 120 \end{pmatrix}$	$\frac{\mathrm{i}}{576}\begin{pmatrix} 1128 & -576 & 576 & 0 \\ 744 & -552 & -576 & -576 \\ -1069 & 840 & -840 & 0 \\ -509 & 229 & 840 & 840 \end{pmatrix}$
	f, h	$(1, 1, 16, 24)$, $(0, 11, 104, 168)$	$(649, 0, -24\left(6\sqrt{5}-35\right), 288)$, $(0, 649, 792, 24(6\sqrt{5}+35)$
	g	$(4, -8, -1, 2, 4)$	$(4, -6, -1, 2, 4)$

Table 6.2: Yifan-Yang pullbacks of four-fold geometries. We supplemented the data with the four-fold fluxes g at the singularities. All fluxes were obtained after a desingularising Kähler-gauge transformation.

We give the matrices relating the bases as $\underline{\Pi}^{(4)} = T\, W_{\underline{\Pi}^{(3)}}$ as a function of the rationality coefficient c, where we omit the minor $(1,4)$ as in eq. (6.4.4):

$$T_{\mathcal{Y}_6} = \begin{pmatrix} 1 & 0 & 0 & 0 & 0 \\ 0 & 1 & 0 & 0 & 0 \\ -\frac{15}{4} & -3 & 6 & 0 & 0 \\ \frac{3}{8}\left(-5+\frac{i(c+140)\zeta(3)}{\pi^3}\right) & -\frac{3}{4} & 3 & 3 & 0 \\ -\frac{75}{64} & -\frac{3i(c+140)\zeta(3)}{8\pi^3} & \frac{15}{4} & 0 & -3 \end{pmatrix}, \quad T_{\mathcal{Y}_{10}} = \begin{pmatrix} 1 & 0 & 0 & 0 & 0 \\ 0 & 1 & 0 & 0 & 0 \\ -\frac{35}{12} & -1 & 2 & 0 & 0 \\ -\frac{35}{24}+\frac{i(c+580)\zeta(3)}{8\pi^3} & -\frac{1}{4} & 1 & 1 & 0 \\ -\frac{1225}{576} & -\frac{i(c+580)\zeta(3)}{8\pi^3} & \frac{35}{12} & 0 & -1 \end{pmatrix}. \tag{6.4.19}$$

We observe that they become rational for $c = -140$ and $c = -580$, respectively. With these values for c in the prepotential, we perform an analytical continuation around the singularities and list the monodromy representations in Table 6.2. There, we also give fluxes corresponding to vanishing periods at the singularities. We observe that the pullback of a rational four-fold basis has monodromy representations in imaginary quadratic field extensions. In [1], a change of coordinates combined with a Kähler-gauge transformation was found that yields rational monodromies for AESZ 2.45.

As a last example, we consider the symmetric locus of the Hulek–Verril four-fold (HV_4) given by the mirror of the configuration

$$\mathrm{HV}_4 = \left(\begin{array}{c|cc} \mathbb{P}^1 & 1 & 1 \\ \mathbb{P}^1 & 1 & 1 \\ \mathbb{P}^1 & 1 & 1 \\ \mathbb{P}^1 & 1 & 1 \\ \mathbb{P}^1 & 1 & 1 \\ \mathbb{P}^1 & 1 & 1 \end{array}\right). \tag{6.4.20}$$

With the methods of section 5.3, we find an integral period basis for this six-parameter model with Hodge structure $(1, 6, 15, 6, 1)$. Along the symmetric locus $z_i = z$, $1 \le i \le 6$, the periods are described by the PF operator

$$\begin{aligned} \mathcal{L}^{(5)}_{\mathrm{HV}_4} = {} & \theta^5 - 2z(2\theta+1)\left(14\theta(\theta+1)\left(\theta^2+\theta+1\right)+3\right) \\ & + 4z^2(\theta+1)^3(196\theta(\theta+2)+255) - 1152z^3(\theta+1)^2(\theta+2)^2(2\theta+3) \end{aligned} \tag{6.4.21}$$

with Riemann symbol

$$\mathcal{P}_{\mathcal{L}^{(5)}_{\mathrm{HV}_4}}\left\{\begin{array}{ccccc|c} 0 & 1/36 & 1/16 & 1/4 & \infty & \\ \hline 0 & 0 & 0 & 0 & 1 & \\ 0 & 1 & 1 & 1 & 1 & \\ 0 & \frac{3}{2} & \frac{3}{2} & \frac{3}{2} & \frac{3}{2} & , z \\ 0 & 2 & 2 & 2 & 2 & \\ 0 & 3 & 3 & 3 & 2 & \end{array}\right\}. \tag{6.4.22}$$

An asymptotic integral basis can be deduced from that of the six-parameter ambient model. For the following, we choose

$$\underline{\Pi}(t) \sim \left(1, t, 6t^2 - \frac{1}{2}, -20t^3 + \frac{10i\zeta(3)}{\pi^3}, -\frac{5}{8} + 15t\left(2t^3 + t - \frac{4i\zeta(3)}{\pi^3}\right)\right), \tag{6.4.23}$$

which corresponds to the intersection form[3]

$$\Sigma = \begin{pmatrix} 0 & 0 & 0 & 0 & 1 \\ 0 & 0 & 0 & 6 & 0 \\ 0 & 0 & 5 & 0 & 0 \\ 0 & 6 & 0 & 0 & 0 \\ 1 & 0 & 0 & 0 & 0 \end{pmatrix}. \tag{6.4.24}$$

The monodromy representations together with their fluxes at the singularities are given in Table 6.3. For the flux at infinity, a Kähler-gauge transformation $\underline{\Pi}^{(4)} \mapsto \underline{\Pi}^{(4)}/(z\log z)$ was performed to regularise the periods. The YY pullback of the operator $\mathcal{L}^{(5)}_{\mathrm{HV}_4}(z)$ is described by a Kähler-gauged version of AESZ 6.1, which is of degree twelve and has Riemann symbol

$$\mathcal{P}_{\mathcal{L}^{(4)}_{6.1}}\left\{\begin{array}{ccccc|c} 0 & 1/36 & 1/16 & 1/4 & \infty & \\ \hline 0 & \frac{1}{4} & \frac{1}{4} & \frac{1}{4} & \frac{1}{4} & \\ 0 & \frac{3}{4} & \frac{3}{4} & \frac{3}{4} & \frac{3}{4} & , z \\ 0 & \frac{7}{4} & \frac{7}{4} & \frac{7}{4} & \frac{3}{4} & \\ 0 & \frac{9}{4} & \frac{9}{4} & \frac{9}{4} & \frac{5}{4} & \end{array}\right\}. \tag{6.4.25}$$

We refer to [1] for its explicit form. The matrix T relating the four-fold basis and the minors of the $\mathcal{L}^{(4)}_{6.1}$ via $\underline{\Pi}^{(4)} = T\, W_{\underline{\Pi}^{(3)}}$ becomes rational for $c = -4/3$. In this specific basis, we find the monodromies and fluxes at the singularities given in Table 6.3. While all four singularities of the four-fold besides the MUM point are equipped with a flux satisfying the vacua conditions, only for the singularity at infinity, the integrality translates to the YY pullback's flux lattice, where we identify a supersymmetric IIB flux vacuum.

[3] Here, we derived the intersection form from the orthogonality relations of the monodromies.

		HV4	pullback: AESZ 6.1
$z=0$	M_0	$\begin{pmatrix} 1 & 0 & 0 & 0 & 0 \\ 1 & 1 & 0 & 0 & 0 \\ 6 & 12 & 1 & 0 & 0 \\ -25 & -60 & -10 & 1 & 0 \\ 60 & 150 & 30 & -6 & 1 \end{pmatrix}$	$\begin{pmatrix} 1 & 0 & 0 & 0 \\ 1 & 1 & 0 & 0 \\ \frac{1}{2} & 1 & 1 & 0 \\ -\frac{1}{6} & -\frac{1}{2} & -1 & 1 \end{pmatrix}$
$z=\frac{1}{36}$	$M_{\frac{1}{36}}$	$\begin{pmatrix} 0 & 0 & 0 & 0 & -1 \\ 0 & 1 & 0 & 0 & 0 \\ 0 & 0 & 1 & 0 & 0 \\ 0 & 0 & 0 & 1 & 0 \\ -1 & 0 & 0 & 0 & 0 \end{pmatrix}$	$\mathrm{i}\sqrt{5/2}\begin{pmatrix} -40 & 0 & -960 & 0 \\ 0 & 40 & 0 & 960 \\ -1 & 0 & 40 & 0 \\ 0 & 1 & 0 & -40 \end{pmatrix}$
	fluxes	$(1,0,0,0,1)$	$(1,0,16\sqrt{10}-40,0)$, $(0,1,0,-16\sqrt{10}-40)$
$z=\frac{1}{16}$	$M_{\frac{1}{16}}$	$\begin{pmatrix} -5 & 30 & 0 & -6 & -6 \\ -1 & 6 & 0 & -1 & -1 \\ 0 & 0 & 1 & 0 & 0 \\ 5 & -25 & 0 & 6 & 5 \\ -6 & 30 & 0 & -6 & -5 \end{pmatrix}$	$\frac{\mathrm{i}\sqrt{3/5}}{48}\begin{pmatrix} -120 & 480 & -2880 & 0 \\ -40 & 120 & 0 & 2880 \\ -3 & 0 & 120 & 480 \\ 0 & 3 & -40 & -120 \end{pmatrix}$
	fluxes	$(1,-5,0,1,1)$	$(1,0,-40+16\sqrt{5/3},-160)$, $(0,3,-40,-120-48\sqrt{5/3})$
$z=\frac{1}{4}$	$M_{\frac{1}{4}}$	$\begin{pmatrix} -44 & 150 & -30 & -30 & -15 \\ -15 & 51 & -10 & -10 & -5 \\ -18 & 60 & -11 & -12 & -6 \\ 75 & -250 & 50 & 51 & 25 \\ -135 & 450 & -90 & -90 & -44 \end{pmatrix}$	$\frac{\mathrm{i}\sqrt{2/3}}{16}\begin{pmatrix} -216 & 960 & -2880 & 0 \\ -80 & 216 & 0 & 2880 \\ -11 & 0 & 216 & 960 \\ 0 & 11 & -80 & -216 \end{pmatrix}$
	fluxes	$(-3,10,-2,-2,-1)$	$(11,0,-8(27-4\sqrt{3/2}),-960)$, $(0,11,-80,-8(27+4\sqrt{3/2}))$
$z=\infty$	M_∞	$\begin{pmatrix} -99 & 300 & -90 & -36 & -10 \\ -45 & 136 & -40 & -15 & -4 \\ -84 & 252 & -71 & -24 & -6 \\ 245 & -735 & 210 & 76 & 20 \\ -490 & 1470 & -420 & -150 & -39 \end{pmatrix}$	$\frac{\mathrm{i}}{32}\begin{pmatrix} -512 & 2400 & -7680 & -11520 \\ -232 & 992 & -2880 & -3840 \\ -48 & 180 & -448 & -480 \\ 5 & -12 & 8 & -32 \end{pmatrix}$
	fluxes	$(7,-21,6,3,1)$	$(3,0,-40,-160)$, $(0,9,-56,-152)$

Table 6.3: Yifan-Yang pullback of symmetric sub-family of HV_4. All fluxes were obtained in a suitable Kähler gauge.

Chapter 7

Black hole condensation

The following sections 7.1 and 7.2 deal with strong coupling and conifold transitions, respectively. As we have reviewed in section 3.5, these can be seen as two degeneration branches of collapsing two- and three-cycles in the internal Calabi–Yau. The conifold transitions on the type IIB side signal the condensation of massless extremal black holes at the (resolved) singularity [43]. Strong coupling transitions have been studied in the past in the context of type II/heterotic duality and their effect on the period geometry is relatively well-known. To our knowledge, the period geometry arising along conifold singularities has not been studied in the literature and the geometric realisation of an integral period basis for the rank-four motive over the singular locus are the first of its kind. We note that integral bases for such operators were obtained in [131], which are however in general different to the ones obtained from the $\hat{\Gamma}$-class of the geometry. In section 6.3, we caught a glimpse of the fibration structure in its generalisation to four-folds, where the vanishing cycles at conifold singularities give rise to supersymmetric flux vacua.

7.1 Strong coupling transitions

Here, we are concerned with the side of the transition where an S^2 shrinks. Typically, the origin of such S^2 are curve singularities which are resolved by blow-ups introducing exceptional divisors $\mathbb{P}^1 \cong S^2$ and yield additional points on edges of the toric polytope. In type IIA compactifications on such families, this leads to gauge symmetry enhancement, as explain in section 3.5. We describe this phenomenon via mirror symmetry on the mirror family in type IIB. The volume of this S^2 is identified by (the imaginary part of) a complexified Kähler parameter t^1, i.e. a ratio of periods. As $t^1 \to 0$, the mirror pair transitions to another such pair, where we identify the partner in type IIB as a subfamily with one less complex structure parameter. There, the expansion variable $q^1 = \exp 2\pi\mathrm{i}\, t^1$ is one and the instanton corrections to the prepotential become (cf. eq. (4.6.47))

$$(2\pi\mathrm{i})^3 \mathcal{F}_{\text{inst}}(\underline{q}) = \sum_{\underline{l}>0} n_{\underline{l}}\, \mathrm{Li}_3\left(\underline{q}^{\underline{l}}\right) \longrightarrow \zeta_3 \sum_{i>0} n_{i,\underline{0}} + \sum_{\underline{k}>0} \sum_{i>0} n_{i,\underline{k}}\, \mathrm{Li}_3\left(\tilde{\underline{q}}^{\underline{k}}\right), \tag{7.1.1}$$

where we used $\mathrm{Li}_3(1) = \zeta_3$ and denoted $\tilde{\underline{q}} = (q^2, \ldots, q^m)$. Comparing with the general form of the prepotential (4.6.45), it follows that the Euler number and instantons of the $(m-1)$-parameter model are given by

$$\chi_{m-1} = \chi - 2\sum_{i>0} n_{i,\underline{0}}\,, \quad (n_{m-1})_{\underline{k}} = \sum_{i>0} n_{i,\underline{k}}\,. \tag{7.1.2}$$

points					l-vectors	
(1	0	0	0	0)	0	-4
(1	1	0	0	0)	0	1
(1	0	1	0	0)	0	1
(1	0	0	1	0)	0	1
(1	0	0	0	1)	1	0
(1	-2	-2	-2	-1)	1	0
(1	-1	-1	-1	0)	-2	1

Table 7.1: Integral points and their scaling relations for the octic mirror family in $\mathbb{P}_{2,2,2,1,1}$.

First, we will review the well-known transition of the two parameter family of octics in $\mathbb{P}_{2,2,2,1,1}$, which is a K3-fibration over $\mathbb{P}^1$. The points in the toric polytope and the Mori-cone generators for this model are given in Table 7.1. More generally, strong coupling transitions arise in K3-fibrations over rational normal curves of degree k [132]. In this picture, the octic hypersurfaces above are X_4-fibrations over $\mathbb{P}^1$, where X_4 is the quartic in $\mathbb{P}^3$ and $\mathbb{P}^1$ is the rational normal curve of degree one. Before considering this fibration over higher-degree bases, we consider the octic strong coupling transition in detail.

The Kähler cone generators dual to the l-vectors in Table 7.1 yield the following and topological data

$$R = 4J_1^2 J_2 + 8J_2^3\,, \tag{7.1.3}$$

$$c_2 \cdot J_1 = 24\,,\ c_2 \cdot J_2 = 56\,,\ \chi = -168\,. \tag{7.1.4}$$

The Picard–Fuchs ideal is generated by the operators

$$\mathcal{L}^{(2)} = \theta_1^2 - z_1\,(2\theta_1 - \theta_2)\,(2\theta_1 - \theta_2 + 1)\,, \tag{7.1.5}$$

$$\mathcal{L}^{(3)} = (2\theta_1 - \theta_2)\,\theta_2^2 + 8z_2\,(2\theta_2 + 1)\,(4\theta_2 + 1)\,(4\theta_2 + 3)\,. \tag{7.1.6}$$

The integral period basis has the asymptotic form

$$\underline{\Pi} \sim \begin{pmatrix} 1 \\ t_1 \\ t_2 \\ 4t_2\,(t_1 + t_2) - 4t_2 - \frac{7}{3} \\ 2t_2^2 - 1 \\ -\frac{2}{3}t_2^2\,(3t_1 + 2t_2) - t_1 - \frac{7t_2}{3} + \frac{21i\zeta_3}{\pi^3} \end{pmatrix}. \tag{7.1.7}$$

The discriminant locus of the model can be determined by using eq. (2.2.53) and has the two components

$$\Delta_1 = 1 - 4z_1 \quad \text{and} \quad \Delta_2 = 1 - 512z_2\,(1 - 128z_2\,(1 - 4z_1))\,. \tag{7.1.8}$$

The transition happens along the discriminant of the base, which is $\Delta_1 = 0$ or $z_1 = 1/4$. In a neighbourhood of the point $(\Delta_1, z_2) = 0$, we find a local period basis given by

$$\underline{\varpi}_{\text{sc}}(\Delta_1, z_2) = \begin{pmatrix} \varpi_0 \\ \log(z_2)\varpi_0 + \sigma_1 \\ \frac{1}{2}\log(z_2)^2\varpi_0 + \log(z_2)\sigma_1 + \sigma_2 \\ \frac{1}{6}\log^3(z_2)\,\varpi_0 + \frac{1}{2}\log(z_2)^2\sigma_1 + \log(z_2)\,\sigma_2 + \sigma_3 \\ \sqrt{\Delta_1}\,\sigma_4 \\ \sqrt{\Delta_1}\,(\log(\Delta_1) + \log(z_2))\,\sigma_4 + \sqrt{\Delta_1}\,\sigma_5 \end{pmatrix}. \tag{7.1.9}$$

Performing a numerical analytical continuation from the MUM point to this region, we find the transition matrix

$$T = \begin{pmatrix} 1 & 0 & 0 & 0 & 0 & 0 \\ 0 & 0 & 0 & 0 & \frac{2}{\pi} & 0 \\ \frac{i\log(2)}{2\pi} & -\frac{i}{2\pi} & 0 & 0 & -\frac{1}{\pi} & 0 \\ -\frac{7}{3} - \frac{\log^2(2)}{\pi^2} - \frac{2i\log(2)}{\pi} & \frac{\log(4)+2i\pi}{\pi^2} & -\frac{2}{\pi^2} & 0 & \frac{4}{\pi} & 0 \\ \frac{1}{6}\left(-7 - \frac{3\log^2(2)}{\pi^2}\right) & \frac{\log(2)}{\pi^2} & -\frac{1}{\pi^2} & 0 & \frac{2(\pi+i(\log(8)-2))}{\pi^2} & \frac{2i}{\pi^2} \\ -\frac{i\left(-132\zeta_3 - \log^3(2) + 7\pi^2\log(2)\right)}{6\pi^3} & \frac{i\left(7\pi^2 - 3\log^2(2)\right)}{6\pi^3} & \frac{i\log(2)}{\pi^3} & -\frac{i}{\pi^3} & 0 & 0 \end{pmatrix} \tag{7.1.10}$$

with $\underline{\Pi}(\Delta_1, z_2) = T \cdot \underline{\varpi}_{\text{sc}}(\Delta_1, z_2)$. Along the locus $\Delta_1 = 0$, we identify the remaining four periods with an integral basis for the CICY $X_{4,2}$ in $\mathbb{P}_{2,1^5}$ of bi-degree $(4,2)$

$$\underline{\Pi}_{4,2}(z) = \begin{pmatrix} 1 & 0 & 0 & 0 & 0 & 0 \\ 0 & 0 & 1 & 0 & 0 & 0 \\ 0 & 0 & 0 & 1 & 0 & 0 \\ 0 & 0 & 0 & 0 & 0 & 1 \end{pmatrix} \cdot \underline{\Pi}(\Delta_1, z) \tag{7.1.11}$$

annihilated by the operator AESZ 1.6 in Table 7.6. We verify integrality by computing the monodromies along this one-parameter locus, given by

$$M_0^{(4,2)} = \begin{pmatrix} 1 & 0 & 0 & 0 \\ 1 & 1 & 0 & 0 \\ 0 & 8 & 1 & 0 \\ -6 & -8 & -1 & 1 \end{pmatrix},\ M_{\frac{1}{512}}^{(4,2)} = \begin{pmatrix} 1 & 0 & 0 & 1 \\ 0 & 1 & 0 & 0 \\ 0 & 0 & 1 & 0 \\ 0 & 0 & 0 & 1 \end{pmatrix} \tag{7.1.12}$$

and $M_\infty^{(4,2)} = \left(M_0^{(4,2)} \cdot M_{1/512}^{(4,2)}\right)^{-1}$. The identities in eq. (7.1.2) can be easily verified with the topological data for both models. For the explicit numbers, we refer the reader to [81]. We performed the resummation for the three-parameter model $\mathcal{X}_6^{(3)}$ of section 6.1 in [1]. In this work, we want to focus on the period structure of these fibrations and the resulting one-parameter model as a Hadamard product. The base of the fibration is described torically by the diagram

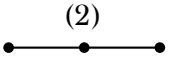

corresponding to a $\mathbb{P}^1$. The node (2) represents the value of the deformation parameter at the transition, see below. The face polynomial is thus of the form $x_1^2 + \phi\, x_1x_2 + x_2^2$, where we used the scaling relations of the ambient space to set the coefficients of x_i^2 to one. The holomorphic period of the three-fold family is now given by a Hadamard product in z_2 between the holomorphic period of the quartic and the expression

$$\varpi_0^{(2)}(z_1, z_2) = \frac{1}{(2\pi\mathrm{i})^2} \oint_{|x_i|=1} \frac{1}{1 + x_1^2 + x_2^2 + \sqrt{z_1}^{-1}x_1x_2} \times \frac{\mathrm{d}x_1\,\mathrm{d}x_2}{x_1x_2 + \sqrt{z_1}z_2}\,, \tag{7.1.13}$$

where we used Batyrev coordinates with $z_1^{-1/2} = \phi$. Strong coupling transitions arise when the face polynomial of the base factorises completely, i.e. can be written as $(x_1 \pm x_2)^{k+1}$. For the case $k = 1$ at hand, this implies $\phi = \pm 2$ or $\Delta_1 = 0$. Here, the second factor in the Hadamard product $\varpi_0^{(2)}$ becomes a solution to the differential operator

$$\mathcal{L}^{(1)}(z) = \theta - 2z\,(2\theta + 1) \tag{7.1.14}$$

corresponding to a zero-dimensional Calabi–Yau family or two points. It follows that the period of this operator has the torus integral representation

$$\begin{aligned}\varpi_0^{(2)}(z) &= \frac{1}{(2\pi\mathrm{i})^2}\oint_{|x_i|=1}\frac{1}{1+x_1^2+x_2^2+2x_1x_2}\times\frac{\mathrm{d}x_1\,\mathrm{d}x_2}{x_1x_2+z}\\ &= \frac{1}{(2\pi\mathrm{i})^2}\oint_{|s|=|t|=1}\frac{1}{1+s(1+t)^2}\times\frac{\mathrm{d}s\,\mathrm{d}t}{s\,t+z} = \sum_{i=0}^{\infty}\binom{2i}{i}z^i\\ &= \frac{1}{\sqrt{1-4z}}\,.\end{aligned} \tag{7.1.15}$$

We included the second line, since these expressions allow for a direct generalisation to higher degree k. The rational normal curve of degree k is given by an embedding

$$\begin{aligned}\nu:\quad &\mathbb{P}^1 \longrightarrow \mathbb{P}^k\,,\\ &(x:y) \longmapsto (X_0:\ldots:X_k) = (x^k : x^{k-1}y : \ldots : y^k)\,.\end{aligned} \tag{7.1.16}$$

In the coordinates $s = x^k$ and $t = x/y$, the polynomial in the denominator of above integrand becomes $s(1+t)^k = (x+y)^k$, which is the face polynomial at the transition. We note that, in the GKZ formula for the periods (4.4.19), the transition embodies the Γ-function identity

$$\sum_{n_1=0}^{\infty}{}'\frac{1}{4^{n_1}\Gamma(n_1+1)^2\Gamma(1-2n_1+n_2)} = \frac{\Gamma(1+2n_2)}{2^{n_2}\Gamma(1+n_2)^3}\,, \tag{7.1.17}$$

where the summmands with $n_1 > \lfloor n_2/2 \rfloor$ vanish due to the second Γ-factor. The r.h.s. allows one to identify the limit with the fundamental period of the CICY $X_{4,2}$.

Let us now consider X_4-fibrations over higher-degree rational normal curves. For $k = 2$, we have the base described torically by

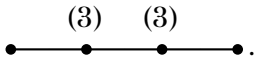

The toric data together with the l-vectors of a three-fold model with this fibration structure is given in Table 7.2. The fact that the l-vector of X_4 is not a generator but lies inside the cone at $l^{(1)} + l^{(3)}$ simply means that the fundamental period remains a formal power series under $z_3 \to \tilde{z}_3 \coloneqq z_1z_3$. The fundamental period of the quartic is given by $\varpi_0(z_1 = z_2 = 0, \tilde{z}_3)$. For the face-polynomial to factor into $(x_1+x_2)^3$, we must set the deformation parameters to the binomial coefficients (3,3). The one-parameter model can then again be written as the Hadamard-product of X_4 together with the period

$$\varpi_0^{(3)}(z) = \frac{1}{(2\pi\mathrm{i})^2}\oint_{|s|=|t|=1}\frac{1}{1+s(1+t)^3}\times\frac{\mathrm{d}s\,\mathrm{d}t}{s\,t+z} = \sum_{i=0}^{\infty}\binom{3i}{i}z^i\,. \tag{7.1.18}$$

points					l-vectors		
(1	0	0	0	0)	0	0	-4
(1	1	0	0	0)	0	0	1
(1	0	1	0	0)	0	0	1
(1	0	0	1	0)	0	0	1
(1	0	0	0	1)	0	1	0
(1	-3	-3	-3	-2)	1	0	-1
(1	-2	-2	-2	-1)	-2	1	2
(1	-1	-1	-1	0)	1	-2	0

Table 7.2: Integral points and their scaling relations for the X_4-fibration over the rational normal curve of degree $k = 2$.

points					l-vectors				
(1	0	0	0	0)	0	0	0	0	-4
(1	1	0	0	0)	0	0	0	0	1
(1	0	1	0	0)	0	0	0	0	1
(1	0	0	1	0)	0	0	0	0	1
(1	0	0	0	1)	0	0	0	1	0
(1	-5	-5	-5	-4)	0	0	1	0	-3
(1	-4	-4	-4	-3)	0	1	-2	0	4
(1	-3	-3	-3	-2)	1	-2	1	0	0
(1	-2	-2	-2	-1)	-2	1	0	1	0
(1	-1	-1	-1	0)	1	0	0	-2	0

Table 7.3: Integral points and their scaling relations for the X_4-fibration over the rational normal curve of degree $k = 4$.

As a last example, we give the fibration over the degree-four rational normal curve, which—as we will show—transitions to the well-known mirror quintic. This model is given by the configuration given in Table 7.3. As before, we must set the deformations of the base to the binomial coefficients according to the nodes in the toric diagram

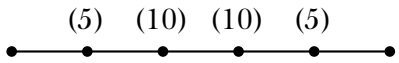

such that the face polynomial becomes $(x+y)^5$. As for the case $k=2$ above, the l-vector of the quartic in the fibre is not a generator of the Mori cone. Instead, it is given by $l^{(1)}+2l^{(2)}+3l^{(3)}+l^{(5)}$, which urges us to define the coordinate $\tilde{z}_5 = z_1 z_2^2 z_3^3 z_5$. The quartic fundamental period is then recovered as $\varpi_0(z_1=z_2=z_3=z_4=0,\tilde{z}_5)$. Then, at the transition, the fundamental period of the five-parameter model becomes the fundamental period of the quintic given by the Hadamard product of the quartic and the $k=5$ generalisation of eqs. (7.1.15) and (7.1.18)

$$\varpi_0^{(5)}(z) = \frac{1}{(2\pi\mathrm{i})^2}\oint_{|s|=|t|=1}\frac{1}{1+s(1+t)^5}\times\frac{\mathrm{d}s\,\mathrm{d}t}{s\,t+z} = \sum_{i=0}^{\infty}\binom{5i}{i}z^i\,. \tag{7.1.19}$$

Expressing hypergeometric function as Hadamard products of lower-dimensional periods has already been discussed in [133]. There, a formulation in terms of iterated integrals was given. We can translate our above analysis into this form by writing the Hadamard product of

$$\varpi_0^{(k)}(z) = \frac{1}{(2\pi\mathrm{i})^2}\oint_{|s|=|t|=1}\frac{1}{1+s(1+t)^k}\times\frac{\mathrm{d}s\,\mathrm{d}t}{s\,t+z} = \sum_{i=0}^{\infty}\binom{k\,i}{i}z^i \tag{7.1.20}$$

with a function $f(z)=\sum_{j=0}^{\infty}c_j z^j$ as the contour integral

$$\varpi_0^{(k)}(z) * f(z) = \frac{1}{2\pi\mathrm{i}}\oint_{|t|=1}\frac{\mathrm{d}t}{t}f\left(\frac{z(1+t)^k}{t}\right). \tag{7.1.21}$$

To verify this, we expand the integrand

$$f\left(\frac{z(1+t)^k}{t}\right) = \sum_{j=0}^{\infty}c_j z^j (1+t)^{k\,j}t^{-j} \tag{7.1.22}$$

and let the contour integral pick out the t-independent term in eq. (7.1.22). This yields the binomial coefficient in eq. (7.1.20) and identifies the integral with the l.h.s. of eq. (7.1.21).

7.2 Conifold transitions

In the previous subsection, we studied strong coupling transitions which arise from curve singularities that are resolved by additional points *on edges* of the toric polytope. Here, we will extend the discussion to conifold transitions, which are point singularities whose regularisations introduce points lying in faces given by reflexive polygons. These models are typically elliptic/genus-one fibrations over two-dimensional bases and we find again Hadamard-product descriptions of the models. The discussion is similar to that of the previous section, where the K3 fibres are replaced by elliptic fibres and the rational normal curves in the base and their zero-dimensional Calabi–Yau periods become two-dimensional bases with elliptic periods in the Hadamard product.

We again begin by studying one simple model in detail. This model is the $\mathbb{P}_{3,2,1}[6]$-fibration over $\mathbb{P}^2$ or, equivalently, the degree-18 hypersurfaces in $\mathbb{P}_{12,8,1^3}$. We perform an analytical continuation to the transition locus and identify the vanishing S^3-cycle. Besides the four one-parameter periods, we find one cycle that breaks open to a chain, which we deduce from an inhomogeneity in the Picard–Fuchs equation. In this way, we obtain an integral basis for a one-parameter model which cannot be described by a prepotential of the form known in the literature (4.6.45). We will discuss more briefly two further examples of genus-one fibrations over different bases. We end the subsection with a local study of all possible bases given by reflexive two-dimensional polytopes and their transitions to one-parameter models given by Hadamard-products.

points					l-vectors	
(1	0	0	0	0)	0	-6
(1	1	0	0	0)	0	3
(1	0	1	0	0)	0	2
(1	0	0	1	0)	1	0
(1	0	0	0	1)	1	0
(1	-9	-6	-1	-1)	1	0
(1	-3	-2	0	0)	-3	1

Table 7.4: Integral points and their scaling relations for the mirror family in $\mathbb{P}_{9,6,1,1,1}$.

The polytope together with the Mori cone generators of $\mathbb{P}_{12,8,1^3}[18]$ are given in Table 7.4. In the dual Kähler generators, the topological data read

$$R = J_1 J_2^2 + 3J_1^2 J_2 + 9J_2^3\,, \tag{7.2.1}$$

$$c_2 \cdot J_1 = 36\,,\ c_2 \cdot J_2 = 102\,,\ \chi = -540\,. \tag{7.2.2}$$

The conifold transition happens along the discriminant locus $0 = \Delta_1 = 1 + 27z_1$, where Δ_1 comes from eq. (2.2.53) for the face containing $(-3,-2,0,0)$. In terms of the deformation parameters a_i of the point i in Table 7.4, this factor vanishes as $a_6 \to -3$, assuming $a_{\text{vertex}} = 1$. Note also that the face polynomial again factorises as for the strong coupling transitions

$$x^3 + y^3 + z^3 + a_6 xyz \xrightarrow{a_6 \to -3} (x+y+z)(x+\alpha\, y+\alpha^2 z)(x+\alpha^2 y+\alpha\, z)\,, \tag{7.2.3}$$

where α is a third root of unity. With the above topological data, we find an asymptotic integral period vector

$$\underline{\Pi} \sim \begin{pmatrix} 1 \\ t_1 \\ t_2 \\ \frac{1}{4}\left(2t_1^2 + 12t_2t_1 + 18t_2^2\right) - \frac{1}{4}\left(2t_1 + 18t_2\right) - \frac{17}{4} \\ \frac{1}{2}t_2\left(2t_1 + 3t_2\right) - \frac{t_2}{2} - \frac{3}{2} \\ \frac{1}{4}\left(-6t_2^3 - 6t_1t_2^2 - 2t_1^2t_2\right) - \frac{1}{4}\left(6t_1 + 17t_2\right) + \frac{135i\zeta_3}{2\pi^3} \end{pmatrix}, \tag{7.2.4}$$

which we match with the solutions to the Picard–Fuchs differential ideal spanned by

$$\mathcal{L}^{(2)}(\underline{z}) = (3\theta_1 - \theta_2)\,\theta_2 + 12 z_2\,(6\theta_2 + 1)\,(6\theta_2 + 5)\ , \tag{7.2.5}$$

$$\mathcal{L}^{(3)}(\underline{z}) = \theta_1^3 + z_1\,(3\theta_1 - \theta_2)\,(3\theta_1 - \theta_2 + 1)\,(3\theta_1 - \theta_2 + 2)\ . \tag{7.2.6}$$

In the neighbourhood of $(\Delta_1 = 0, z_2 = 0)$, we find a local basis given by

$$\varpi(\Delta_1, z_2) = \begin{pmatrix} \sigma_1 \\ \Delta_1\sigma_2 \\ \sigma_1\log(z_2) + \sigma_3 \\ \Delta_1\sigma_2\log(\Delta_1) + \sigma_4 \\ \sigma_1\log(z_2)^2 + 2\,(\sigma_3 - 9\Delta_1\sigma_2)\log(z_2) + \sigma_5 \\ \sigma_1\log(z_2)^3 + 3\,(\sigma_3 - 9\Delta_1\sigma_2)\log(z_2)^2 + 3\sigma_5\log(z_2) - \sigma_6 \end{pmatrix}, \tag{7.2.7}$$

where σ_i are formal power series in the variables Δ_1 and z_2. The transition matrix is obtained numerically and identified with

$$T_{\Delta_1,z_2} = \tag{7.2.8}$$

$$\begin{pmatrix} 1 & 0 & 0 & 0 & 0 & 0 \\ \frac{1}{2} + \frac{27i\sqrt{3}L}{8\pi^2} & \frac{27i\sqrt{3}}{4\pi^2} & 0 & -\frac{27i\sqrt{3}}{4\pi^2} & 0 & 0 \\ \frac{i\left(\pi\log(81) - 9\sqrt{3}L\right)}{8\pi^2} & -\frac{9i\left(\sqrt{3}-2\pi\right)}{4\pi^2} & -\frac{i}{2\pi} & \frac{9i\sqrt{3}}{4\pi^2} & 0 & 0 \\ -\frac{-27i\sqrt{3}L + 35\pi^2 + 9\log^2(3) + 12i\pi\log(3)}{8\pi^2} & \frac{27i\left(\sqrt{3}-2\pi+3i\log(3)\right)}{4\pi^2} & \frac{3(\log(27)+2i\pi)}{4\pi^2} & -\frac{27i\sqrt{3}}{4\pi^2} & -\frac{9}{8\pi^2} & 0 \\ -\frac{35}{24} - \frac{3\log^2(3)}{8\pi^2} & \frac{3\left(2\sqrt{3}\pi - 9\log(3)\right)}{4\pi^2} & \frac{3\log(3)}{4\pi^2} & 0 & -\frac{3}{8\pi^2} & 0 \\ \frac{9i\left(356\zeta_3 + \log^3(3)\right) - 37\pi^3 + 9\pi\log^2(3) - 105i\pi^2\log(3)}{48\pi^3} & \frac{81i\left(\log^2(3) - 3L\right) - 3\pi^2\left(4\sqrt{3} + 105i\right) + 54\pi\log(3)}{16\pi^3} & \frac{i\left(35\pi^2 - 9\log^2(3) + 6i\pi\log(3)\right)}{16\pi^3} & 0 & \frac{3(\pi + 3i\log(3))}{16\pi^3} & -\frac{3i}{16\pi^3} \end{pmatrix}$$

and yields the integral basis as $\underline{\Pi}(\Delta_1, z_1) = T_{\Delta_1,z_2}\underline{\varpi}(\Delta_1, z_1)$. The constant[1] L is the Dirichlet L-function

$$L = \sum_{n=1}^{\infty} \frac{\chi_3(n)}{n^2} = 0.781302412896486\cdots \tag{7.2.9}$$

with the character

$$\chi_3(n) = \begin{cases} 0 & n \equiv 0 \bmod 3 \\ 1 & n \equiv 1 \bmod 3 \\ -1 & n \equiv 2 \bmod 3 \end{cases}. \tag{7.2.10}$$

On the locus $\Delta_1 = 0$, we find one flux

$$f = (0, 3, -1, 3, 0, 0) \tag{7.2.11}$$

with $f^T\Sigma\underline{\Pi}(\Delta_1 = 0, z_2) = 0$ corresponding to the vanishing S^3. Defining the one-parameter coordinate as $z = -3z_2$ together with the mirror map $t = \frac{\log z}{2\pi\mathrm{i}}$, the asymptotic period vector reads

$$\underline{\Pi}(\Delta_1 = 0, z) \sim \begin{pmatrix} 1 \\ \frac{1}{2} + \frac{27i\sqrt{3}L}{8\pi^2} \\ -\frac{9i\sqrt{3}L}{8\pi^2} + t + \frac{1}{2} \\ \frac{1}{8}\left(36t^2 + 12t - 38 + \frac{27i\sqrt{3}L}{\pi^2}\right) \\ \frac{1}{12}\left(18t^2 + 18t - 13\right) \\ \frac{1}{12}\left(-18t^3 - 36t^2 - 75t + \frac{801i\zeta_3}{\pi^3} - 40\right) \end{pmatrix}. \tag{7.2.12}$$

[1] Its decimal expansion is listed in the OEIS as A086724.

new number	AZ label	info	operator
2.1.1	A	$X_{2,2} \subset \mathbb{P}^1 \times \mathbb{P}^1$	$\theta^2 - 4z(2\theta+1)^2$
2.1.2	B	$X_3 \subset \mathbb{P}^2$	$\theta^2 - 3z(3\theta+1)(3\theta+2)$
2.1.3	C	$X_4 \subset \mathbb{P}_{2,1,1}$	$\theta^2 - 4z(4\theta+1)(4\theta+3)$
2.1.4	D	$X_6 \subset \mathbb{P}_{3,2,1}$	$\theta^2 - 12z(6\theta+1)(6\theta+5)$
2.2.1	f	BZ: B	$\theta^2 - 3z\left(3\theta^2+3\theta+1\right) + 27z^2(\theta+1)^2$
2.2.2	b	BZ: D	$\theta^2 - z\left(11\theta^2+11\theta+3\right) - z^2(\theta+1)^2$
2.2.3	d	BZ: E	$\theta^2 - 4z\left(3\theta^2+3\theta+1\right) + 32z^2(\theta+1)^2$
2.2.4	a	BZ: A	$\theta^2 - z\left(7\theta^2+7\theta+2\right) - 8z^2(\theta+1)^2$
2.2.5	c	BZ: C	$\theta^2 - z\left(10\theta^2+10\theta+3\right) + 9z^2(\theta+1)^2$
2.2.6	g	BZ: F	$\theta^2 - z\left(17\theta^2+17\theta+6\right) + 72z^2(\theta+1)^2$
2.2.7	—	—	$(z-1)\left(\theta^2 - z(\theta+1)^2\right)$
2.2.8	e	$\mu(A)$	$\theta^2 - 4z\left(8\theta^2+8\theta+3\right) + 256z^2(\theta+1)^2$
2.2.9	h	$\mu(B)$	$\theta^2 - 3z\left(18\theta^2+18\theta+7\right) + 729z^2(\theta+1)^2$
2.2.10	i	$\mu(C)$	$\theta^2 - 4z\left(32\theta^2+32\theta+13\right) + 4096z^2(\theta+1)^2$
2.2.11	j	$\mu(D)$	$\theta^2 - 12z\left(72\theta^2+72\theta+31\right) + 186624z^2(\theta+1)^2$
2.2.12	k	—	$\theta^2 - 3z(2\theta+1) - 81z^2(\theta+1)^2$
2.2.13	l	—	$\theta^2 - 4z(2\theta+1) - 64z^2(\theta+1)^2$
2.2.14	m	—	$\theta^2 - 24z(2\theta+1) - 1296z^2(\theta+1)^2$

Table 7.5: Elliptic operators of degree one and two [134]. The numbering refers to [135].

The period vector $\underline{\Pi}(\Delta_1 = 0, z)$ satisfies an *inhomogeneous* differential equation

$$\mathcal{L}^{(4)}_{2.23}(z)\underline{\Pi}(\Delta_1 = 0, z) = f\frac{135\mathrm{i}\sqrt{3}z}{\pi^2} \tag{7.2.13}$$

where the operator $\mathcal{L}^{(4)}_{2.23}(z)$ [99] is listed as AESZ 2.23 in [102]. It is given by the Hadamard product $D * f$. The two operators are listed in Table 7.5. One immediately identifies the operator D with that of the fibre of the three-fold. As we will discuss below, the appearance of f is a property of the base $\mathbb{P}^2$. The Riemann symbol reads

$$\mathcal{P}_{\mathcal{L}^{(4)}_{2.23}}\left\{\begin{array}{cccc} 0 & a & \bar{a} & \infty \\ \hline 0 & 0 & 0 & \frac{1}{6} \\ 0 & 1 & 1 & \frac{5}{6} \\ 0 & 1 & 1 & \frac{7}{6} \\ 0 & 2 & 2 & \frac{11}{6} \end{array}\ ,\ z\right\}, \tag{7.2.14}$$

with $a = \frac{-3+i\sqrt{3}}{7776}$ and $\bar{a}$ being the roots of $5038848z^2 + 3888z + 1$. The action of the Picard–Fuchs operator on the holomorphic $(n,0)$-form produces an exact differential whose integrals over cycles vanishes. Let $\mathcal{L}^{(4)}_{2.23}(z)\Omega(z) = \mathrm{d}\beta$, then the inhomogeneity follows with

$$\mathcal{L}^{(4)}_{2.23}(z)\Pi_i = \int_{\Gamma_i}\mathrm{d}\beta = \int_{\partial\Gamma_i}\beta = \underbrace{\langle\Gamma_i,\Phi\rangle}_{f_i}\int_{\partial\Phi}\beta\,, \tag{7.2.15}$$

where Φ is the vanishing cycle dual to the flux f. By comparing eqs. (7.2.14) and (7.2.15), we deduce $\int_{\partial\Phi}\beta = 135\mathrm{i}\sqrt{3}z/\pi^2$. Linearity of the inhomogeneous term implies that all periods are solutions to the fifth-order operator $(\theta-1)\mathcal{L}^{(4)}_{2.23}$.

new number	geometry	operator	Hadamard
1.1	X_5	$\theta^4 - 5z(5\theta+1)(5\theta+2)(5\theta+3)(5\theta+4)$	—
1.2	X_{10}	$\theta^4 - 80z(10\theta+1)(10\theta+3)(10\theta+7)(10\theta+9)$	—
1.3	$X_{2,2,2,2}$	$\theta^4 - 16z(2\theta+1)^4$	A*A
1.4	$X_{3,3}$	$\theta^4 - 9z(3\theta+1)^2(3\theta+2)^2$	B*B
1.5	$X_{3,2,2}$	$\theta^4 - 12z(2\theta+1)^2(3\theta+1)(3\theta+2)$	A*B
1.6	$X_{4,2}$	$\theta^4 - 16z(2\theta+1)^2(4\theta+1)(4\theta+3)$	A*C
1.7	X_8	$\theta^4 - 16(8\theta+1)(8\theta+3)(8\theta+5)(8\theta+7)z$	—
1.8	X_6	$\theta^4 - 36z(3\theta+1)(3\theta+2)(6\theta+1)(6\theta+5)$	B*D
1.8	$X_{12,2}$	$\theta^4 - 144z(12\theta+1)(12\theta+5)(12\theta+7)(12\theta+11)$	—
1.10	$X_{4,4}$	$\theta^4 - 16z(4\theta+1)^2(4\theta+3)^2$	C*C
1.11	$X_{4,3}$	$\theta^4 - 12z(3\theta+1)(3\theta+2)(4\theta+1)(4\theta+3)$	B*C
1.12	$X_{6,4}$	$\theta^4 - 48z(4\theta+1)(4\theta+3)(6\theta+1)(6\theta+5)$	C*D
1.13	$X_{6,6}$	$\theta^4 - 144z(6\theta+1)^2(6\theta+5)^2$	D*D
1.14	$X_{6,2}$	$\theta^4 - 48z(2\theta+1)^2(6\theta+1)(6\theta+5)$	A*D

Table 7.6: Three-fold operator of degree one [136]. The last column refers to the known Hadamard-product descriptions in terms of the elliptic hypergeometric operators in Table 7.5. The numbering refers to [135].

While the appearance of Hadamard products in the process of black hole condensations is interesting in and of itself, it also brings forth an integral period structure for these models that deviates from the classical treatment. We define a one-parameter basis

$$\underline{\Pi}^{(1)}(z) = \begin{pmatrix} 1 & 0 & 0 & 0 \\ -2 & 1 & 0 & 0 \\ 0 & 0 & 1 & 0 \\ 0 & 0 & 2 & 1 \end{pmatrix} \cdot \begin{pmatrix} 1 & 0 & 0 & 0 & 0 & 0 \\ 0 & 1 & 3 & 0 & 0 & 0 \\ 0 & 0 & 0 & 0 & 1 & 0 \\ 0 & 0 & 0 & 0 & 0 & 1 \end{pmatrix} \underline{\Pi}(\Delta_1 = 0, z)\,, \tag{7.2.16}$$

where the 4×6-matrix projects onto an independent set of homogeneous solutions to $\mathcal{L}^{(4)}_{2.23}$, i.e. it omits the vanishing cycle and the degenerating cycle obtaining a boundary. The square matrix allows for a prepotential description as it removes t^2-terms in the last period. The latter is symplectic w.r.t. the standard intersection form in eq. (5.3.15). The period vector $\underline{\Pi}^{(1)}$ has the asymptotic behaviour

$$\underline{\Pi}_1 \sim \left(1, 3t, \frac{1}{3}\partial_t\mathcal{F}, 2\mathcal{F} - t\partial_t\mathcal{F}\right), \tag{7.2.17}$$

where we defined the prepotential as

$$\mathcal{F}(t) = \frac{9}{3!}t^3 + \frac{9/2}{2}t^2 - \frac{78}{24}t - \frac{\left(-534 - \frac{44i\pi^3}{\zeta_3}\right)\zeta_3}{2(2\pi i)^3}\,. \tag{7.2.18}$$

We expressed $\mathcal{F}$ in a way that allows for a comparison to the general form we gave in eq. (4.6.45). Expanding the constant term shows a rational contribution of $-\frac{11}{4}$. This basis then leads to an

integral basis with the following monodromy matrices

$$M_0 = \begin{pmatrix} 1 & 0 & 0 & 0 \\ 3 & 1 & 0 & 0 \\ 3 & 1 & 1 & 0 \\ -8 & 0 & -3 & 1 \end{pmatrix}, \; M_a = \begin{pmatrix} 9 & -1 & 1 & 1 \\ 8 & 0 & 1 & 1 \\ 8 & -1 & 2 & 1 \\ -64 & 8 & -8 & -7 \end{pmatrix}, \tag{7.2.19}$$

$$M_{\bar{a}} = \begin{pmatrix} 4 & 0 & -1 & 1 \\ -3 & 1 & 1 & -1 \\ 0 & 0 & 1 & 0 \\ -9 & 0 & 3 & -2 \end{pmatrix}, \; M_\infty = \begin{pmatrix} 6 & 0 & 0 & 1 \\ 0 & 0 & 1 & 0 \\ 0 & -1 & 1 & 0 \\ -31 & 0 & 0 & -5 \end{pmatrix}. \tag{7.2.20}$$

They are all symplectic w.r.t. the standard intersection form and fulfil the closed contour relation $\mathbb{1} = M_a M_0 M_{\bar{a}} M_\infty$.

The exact same approach for the $\mathbb{P}^2[3]$-fibration over $\mathbb{P}^2$ leads to an integral basis for the operator AESZ 2.21 with Riemann symbol

$$\mathcal{P}_{\mathcal{L}^{(4)}_{2.21}} \left\{ \begin{array}{cccc|c} 0 & b & \bar{b} & \infty & \\ \hline 0 & 0 & 0 & \frac{1}{3} & \\ 0 & 1 & 1 & \frac{2}{3} & , \; z \\ 0 & 1 & 1 & \frac{4}{3} & \\ 0 & 2 & 2 & \frac{5}{3} & \end{array} \right\}, \tag{7.2.21}$$

with $b = -\left(3 + i\sqrt{3}\right)/486$ and $\bar{b}$ roots of $19683 z_1^2 + 243 z_1 + 1$. As expected from the fibration, this one-parameter limit is the Hadamard-product $B * f$.

points					l-vectors	
(1	0	0	0	0)	0	-3
(1	1	0	0	0)	0	1
(1	0	1	0	0)	0	1
(1	0	0	1	0)	1	0
(1	1	2	1	3)	1	0
(1	-4	-5	-2	-3)	1	0
(1	-1	-1	0	0)	-3	1

Table 7.7: Integral points and their scaling relations for the $\mathbb{P}^2[3]$-fibration over $\mathbb{P}^2$.

With the toric data collected in Table 7.7, the topological data are given by

$$R = J_1 J_2^2 + 3 J_1^2 J_2 + 9 J_2^3 \,, \tag{7.2.22}$$

$$c_2 \cdot J_1 = 12 \,, \; c_2 \cdot J_2 = 30 \,, \; \chi = -72 \,. \tag{7.2.23}$$

and, after the same projection as in eq. (7.2.16), we find the one-parameter prepotential

$$\mathcal{F}(t) = \frac{9}{3!} t^3 + \frac{9/2}{2} t^2 - \frac{6}{24} t - \frac{\left(-66 - \frac{12 i \pi^3}{\zeta_3}\right) \zeta_3}{2(2\pi i)^3} \,, \tag{7.2.24}$$

with a rational constant contribution of $-3/4$. This leads to the monodromy group

$$M_0 = \begin{pmatrix} 1 & 0 & 0 & 0 \\ 3 & 1 & 0 & 0 \\ 3 & 1 & 1 & 0 \\ -2 & 0 & -3 & 1 \end{pmatrix}, \; M_b = \begin{pmatrix} 4 & 0 & -3 & 3 \\ -3 & 1 & 3 & -3 \\ 0 & 0 & 1 & 0 \\ -3 & 0 & 3 & -2 \end{pmatrix}, \tag{7.2.25}$$

$$M_{\bar{a}} = \begin{pmatrix} 7 & -3 & 3 & 3 \\ 6 & -2 & 3 & 3 \\ 6 & -3 & 4 & 3 \\ -12 & 6 & -6 & -5 \end{pmatrix}, \; M_\infty = \begin{pmatrix} 4 & 0 & 0 & 3 \\ 0 & -2 & 3 & 0 \\ 0 & -1 & 1 & 0 \\ -7 & 0 & 0 & -5 \end{pmatrix}. \tag{7.2.26}$$

We note that, while the author of [131] generalised the ansatz for a prepotential to obtain integral bases for these Hadamard-products, for the operator describing $B * f$, the values for the topological data disagree with the present realisation via conifold transitions.

Genus-one fibrations over $\mathbb{P}^2$ have holomorphic periods that can be written as a Hadamard product of the fibre (depending on z_2) and

$$\begin{aligned} \varpi_0^{(2)}(z_1, z_2) = \frac{1}{(2\pi\mathrm{i})^3} \oint_{|x_i|=1} & \frac{1}{1 + x_1^3 + x_2^3 + x_3^3 + (z_1)^{-1/3} x_1 x_2 x_3} \\ & \times \frac{\mathrm{d}x_1 \, \mathrm{d}x_2 \, \mathrm{d}x_3}{x_1 x_2 x_3 + z_1^{1/3} z_2}, \end{aligned} \tag{7.2.27}$$

where the modulus parametrising the inner point is given by $\phi = z_1^{-1/3}$. On the locus of the conifold transition, so at $\phi = -3$ or $z_1 = (-3)^{-3}$ and $z_2 = -3z$, this period becomes the holomorphic solution to the operator[2]

$$\mathcal{L}_f^{(2)}(z) = \theta^2 + 3z\left(3\theta^2 + 3\theta + 1\right) + 27z^2(\theta+1)^2 \tag{7.2.28}$$

given by

$$\begin{aligned} \varpi_0(z) &= \frac{1}{(2\pi\mathrm{i})^3} \oint_{|x_i|=1} \frac{1}{1 + x_1^3 + x_2^3 + x_3^3 - 3x_1 x_2 x_3} \times \frac{\mathrm{d}x_1 \, \mathrm{d}x_2 \, \mathrm{d}x_3}{x_1 x_2 x_3 + z} \\ &= 1 - 3z + 9z^2 + \mathcal{O}\left(z^3\right). \end{aligned} \tag{7.2.29}$$

The above motivates us to describe the one-parameter models arising in conifold transitions as Hadamard-products, where the two factors are properties of the fibres and bases, respectively. Before generalising the above to other bases, we want to study two more of them in detail. These are depicted in Figures 7.1b and 7.1c, where Figure 7.1a represents the above case of a $\mathbb{P}^2$-base.

In these polygons, we already indicated the values of the deformation parameters where the transition happens. For both bases (d) and (a), we will give the Hadamard-factor in the holomorphic period and give one example model.

[2] Comparing to the operators in Table 7.5, here, we find it expressed in $-z$.

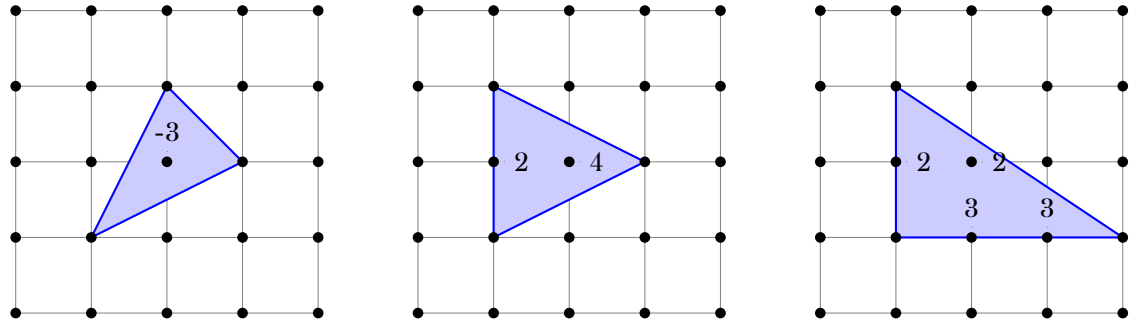

(a) Face of f-transition. (b) Face of d-transition. (c) Face of a-transition.

Figure 7.1: The faces of conifold transitions of type a, d and f. The numbers correspond to the values of the deformation parameters where the transition happens.

Conifold transition d This base is the Hirzebruch surface F_2 which in turn is equivalent to F_0 [137]. We consider the toric description in Figure 7.1b with l-vectors

$$l^{(1)} = (\dots;\dots,1,1,0,-2,0)\,, \tag{7.2.30}$$
$$l^{(2)} = (\dots;\dots,0,0,1,1,-2)\,, \tag{7.2.31}$$

where the last two entries correspond to the points in Figure 7.1b with values two and four, which are parametrised by a_6 and a_7, respectively. We assume that the fibre is parametrised by the coordinate z_3 and that the l-vector looks like $(\dots;\dots,0,0,0,0,1)$. Then, we can again express the holomorphic period as a Hadamard product of the fibre and a period, which now depends on three moduli:

$$\varpi_0^{(3)}(z_1,z_2,z_3) = \frac{1}{(2\pi\mathrm{i})^3}\oint_{|x_i|=1} \frac{1}{1+x_1^2+x_2^4+x_3^4+z_1^{-1/2}x_2^2x_3^2+z_1^{-1/4}z_2^{-1/2}x_1x_2x_3} \times \frac{\mathrm{d}x_1\,\mathrm{d}x_2\,\mathrm{d}x_3}{x_1x_2x_3+z_1^{1/4}z_2^{1/2}z_3}\,, \tag{7.2.32}$$

with $a_6 = z_1^{-1/2}$ and $a_7 = z_1^{-1/4}z_2^{-1/2}$. On the conifold locus $a_6 = 2$ and $a_7 = 4$ parametrised by $z_3 = 4z$, above period is the holomorphic solution at the MUM point of the Picard–Fuchs operator

$$\mathcal{L}_d^{(2)}(z) = \theta^2 - 4z\left(3\theta^2+3\theta+1\right) + 32z^2(\theta+1)^2 \tag{7.2.33}$$

and can be expressed as

$$\begin{aligned}\varpi_0(z) &= \frac{1}{(2\pi\mathrm{i})^3}\oint_{|x_i|=1} \frac{1}{1+x_1^2+x_2^4+x_3^4+2x_2^2x_3^2+4x_1x_2x_3} \times \frac{\mathrm{d}x_1\,\mathrm{d}x_2\,\mathrm{d}x_3}{x_1x_2x_3+z} \\ &= 1+4z+20z^2+\mathcal{O}\left(z^3\right),\end{aligned} \tag{7.2.34}$$

where we again identify the face polynomial at the transition in the denominator of the integrand. A realisation of this fibration is given by the degree-24 hypersurface in $\mathbb{P}_{12,8,2,1^2}$ whose mirror has three complex-structure parameters. The fibre is of type $\mathbb{P}_{3,2,1}[6]$ and the one-parameter model is thus $D*d$.

Conifold transition a Here, the face at the transition is depicted in Figure 7.1c. The l-vectors are given by

$$l^{(1)} = (\dots;\dots,0,0,-1,1,0,1,-1)\,, \tag{7.2.35}$$
$$l^{(2)} = (\dots;\dots,0,0,1,-2,1,0,0)\,, \tag{7.2.36}$$
$$l^{(3)} = (\dots;\dots,0,1,0,1,-2,0,0)\,, \tag{7.2.37}$$
$$l^{(4)} = (\dots;\dots,1,0,1,0,0,-2,0)\,, \tag{7.2.38}$$

where the last four entries, in backwards order, corresponds to the inner point $(0,0)$, $(-1,0)$, $(1,-1)$ and $(0,-1)$ in Figure 7.1c. Here, the holomorphic period is given by a Hadamard product of the fibre and

$$\varpi_0^{(3)}(z_1,z_2,z_3,z_4,z_5) = \frac{1}{(2\pi\mathrm{i})^3}\oint_{|x_i|=1}\frac{\mathrm{d}x_1\,\mathrm{d}x_2\,\mathrm{d}x_3}{x_1x_2x_3+z_1z_2^{2/3}z_3^{1/3}z_4^{1/2}z_5} \tag{7.2.39}$$
$$\times\,\frac{1}{1+x_1^2+x_2^6+x_3^3+z_4^{-1/2}x_1x_2^3+z_1^{-1}z_2^{-2/3}z_3^{-1/3}z_4^{-1/2}x_1x_2x_3+z_2^{-2/3}z_3^{-1/3}x_2^4x_3+z_2^{-1/3}z_3^{-2/3}x_2^2x_3^2}\,,$$

with the deformation parameters set to $a_6 = z_2^{-2/3}z_3^{-1/3}$, $a_7 = z_2^{-1/3}z_3^{-2/3}$, $a_8 = z_4^{-1/2}$ and $a_9 = z_1^{-1}z_2^{-2/3}z_3^{-1/3}z_4^{-1/2}$. On the conifold locus at $a_6 = a_7 = 3$ and $a_8 = a_9 = 2$ implying $z_5 = 2z$, above period is the holomorphic solution at the MUM point of the Picard–Fuchs operator

$$\mathcal{L}_a^{(2)}(z) = \theta^2 - z\left(7\theta^2+7\theta+2\right) - 8z^2(\theta+1)^2\,, \tag{7.2.40}$$

which can thus be written as

$$\begin{aligned}\varpi_0(z) =& \frac{1}{(2\pi\mathrm{i})^3}\oint_{|x_i|=1}\frac{\mathrm{d}x_1\,\mathrm{d}x_2\,\mathrm{d}x_3}{x_1x_2x_3+z}\\ &\times\frac{1}{1+x_1^2+x_2^6+x_3^3+2x_1x_2^3+2x_1x_2x_3+3x_2^4x_3+3x_2^2x_3^2}\,.\end{aligned} \tag{7.2.41}$$

A realisation is given by the degree-36 hypersurface in $\mathbb{P}_{18,12,3,2,1}$. The fibre is again given by $\mathbb{P}_{3,2,1}[6]$ and the transition results therefore in $D * a$.

For the rest of the subsection, we will consider one-parameter fibrations with l-vector of the form

$$l^{(h^{2,1})} = (\dots;\underbrace{*,\dots,*}_{\text{vertices}},0,\dots,0,1) \tag{7.2.42}$$

over different bases. Given a triangulation of a toric three-fold, it is sufficient for this vector to lie in the Mori cone, i.e. that it is given by a *positive* linear combination of the l-vectors. From the point of view of the holomorphic period, restricting to a sub-cone of the Mori cone yields monomials in the Batyrev coordinates with non-minimal exponents in the sense that a coordinate transformation exists that reduces the monomials' degrees while preserving holomorphicity. Extending the Mori cone, however, would introduce fractions of the Batyrev coordinates which can introduce terms in the holomorphic period that are absent for a model with such l-vectors, since the Γ-functions in the denominator would diverge, cf. eq. (4.4.19).

The bases we consider are described torically by reflexive two-dimensional polytopes classified in [138]. All 16 of them can be embedded in either the bi-quadratic in $\mathbb{P}^1 \times \mathbb{P}^1$ (Figure 7.2a), the quartic in $\mathbb{P}_{2,1,1}$ (Figure 7.3a) or the cubic in $\mathbb{P}^2$ (Figure 7.4a). By tuning the deformation parameters, one obtains the different bases depicted in Figures 7.2b, 7.3b and 7.4b, where those corresponding to the vertices (filled circles) are set to one while the inner points (hollow circles) are free moduli. The embedding allows us to obtain the Hadamard factor of the base in terms of contour integrals

$$\varpi_0^{(2,2)}(z) = \frac{1}{(2\pi\mathrm{i})^4} \oint_{\mathcal{C}} \frac{1}{1+P(s,t,v,w)} \frac{\mathrm{d}s\,\mathrm{d}t\,\mathrm{d}v\,\mathrm{d}w}{stvw+z}\,, \tag{7.2.43}$$

$$\varpi_0^{(4)}(z) = \frac{1}{(2\pi\mathrm{i})^3} \oint_{\mathcal{C}} \frac{1}{1+P(p,q,r)} \frac{\mathrm{d}p\,\mathrm{d}q\,\mathrm{d}r}{pqr+z}\,, \tag{7.2.44}$$

$$\varpi_0^{(3)}(\tilde{z}) = \frac{1}{(2\pi\mathrm{i})^3} \oint_{\mathcal{C}} \frac{1}{1+P(x,y,z)} \frac{\mathrm{d}x\,\mathrm{d}y\,\mathrm{d}z}{xyz+\tilde{z}}\,, \tag{7.2.45}$$

where the contours $\mathcal{C}$ are defined by the absolute values of all integration variables to be one. The notation $\tilde{z}$ in $\varpi_0^{(3)}$ is due to the clashing of conventions in [139] with the Batyrev coordinates z and has no further meaning. We summarise our findings for the three embeddings in Tables 7.8 to 7.10, respectively. There, the a_i correspond to the values of the free moduli of the base at the transition, where bold entries indicate that the point is either a vertex (1) or outside the diagram (0). With the Weierstraß-form of these embeddings[3] given in [139], we obtain the coefficients g_2 and g_3 as functions of the deformation parameters a_i. Setting the edge deformations to the values of the transition and leaving a_0 untouched for now, we give the j-invariant for the embeddings. Following the Kodaira classification of singular fibres [140], we identify the singular fibres with the Picard–Fuchs operators of elliptic families [134, 101] (cf. Table 7.5). For the bases (4) and (10), we instead obtain an essentially self-adjoint operator of degree four in z given by[4]

$$\begin{aligned}\mathcal{L}_{5a}^{(2)}(z) = {} & 7\theta^2 - z\left(4\theta^2+24\theta+7\right) - z^2\left(139\theta^2+238\theta+105\right) \\ & - 5z^3\left(69\theta^2+139\theta+72\right) - 250z^4(\theta+1)^2\end{aligned} \tag{7.2.46}$$

with Riemann symbol

$$\mathcal{P}_{\mathcal{L}_{5a}^{(2)}} \left\{ \begin{array}{cccc|c} -7/10 & 0 & \Delta=0 & \infty & \\ \hline 0 & 0 & 0 & 1 & z \\ 2 & 0 & 0 & 1 & \end{array} \right\}. \tag{7.2.47}$$

Here $\Delta = 1 - 2z - 17z^2 - 25z^3$ and $\Delta = 0$ represents its three roots. Note that $z = -7/10$ is an apparent singularity and not one of the five singular fibres. We observe that the two hypergeometric families A and B (bi-quadratic and cubic) appear together with their μ-transformed [101] operators (e and h) and that the classification respects the fact that operators a, c and g all belong to the same Beauville family IV [141], see also [134]. Even when taking into account the equivalence of the families a, c and g, we still find four bases ((1), (7), (13) and (15)) that allow for transitions with different elliptic fibres and thus serve as connections between one-parameter three-fold families.

[3] I thank Albrecht Klemm for providing me with the MATHEMATICA implementation.

[4] The index 5 refers to the number of singular fibres. We obtain two such operators that we index by a and b. There is no connection between them and the second-order operators a and b.

We note that we restricted the search summarised in Tables 7.8 to 7.10 to non-zero deformation values. Leaving the edge-deformations a_i, $i > 0$ fixed as in the tables, we observe further rational zeros of the discriminant at $a_0 = 0$. For example, transitions that would yield the operator d at finite a_0-values give transitions at $a_0 = 0$ described by $\mathcal{L}_A^{(2)}(z^2)$. Similarly, those listed as f transition at $a_0 = 0$ to $\mathcal{L}_B^{(2)}(z^3)$. Edge-deformations giving B (or $\mu(B) = h$) result in a reparametrised operator B. Lastly, polygon number 16 has a transition at $a_0 = 0$, where the base-factor of the Hadamard product is annihilated by the operator

$$\begin{aligned}\mathcal{L}_{5b}^{(2)}(z) = 8\theta^2 + z\,\theta\,(17\theta - 1) - z^2\left(55\theta^2 + 128\theta + 64\right) - 12z^3\left(30\theta^2 + 78\theta + 47\right)\\ - 4z^4\left(103\theta^2 + 250\theta + 147\right) - 99z^5\left(\theta^2 + 3\theta + 2\right)\end{aligned} \tag{7.2.48}$$

with Riemann symbol

$$\mathcal{P}_{\mathcal{L}_{5b}^{(2)}}\left\{\begin{array}{cccc} -8/9 & 0 & \Delta = 0 & \infty \\ \hline 0 & 0 & 0 & 1 \\ 2 & 0 & 0 & 2 \end{array}\;,\; z\right\} \tag{7.2.49}$$

with now $\Delta = 1 + z - 8z^2 - 36z^3 - 11z^4$ of degree four while infinity is a regular point.

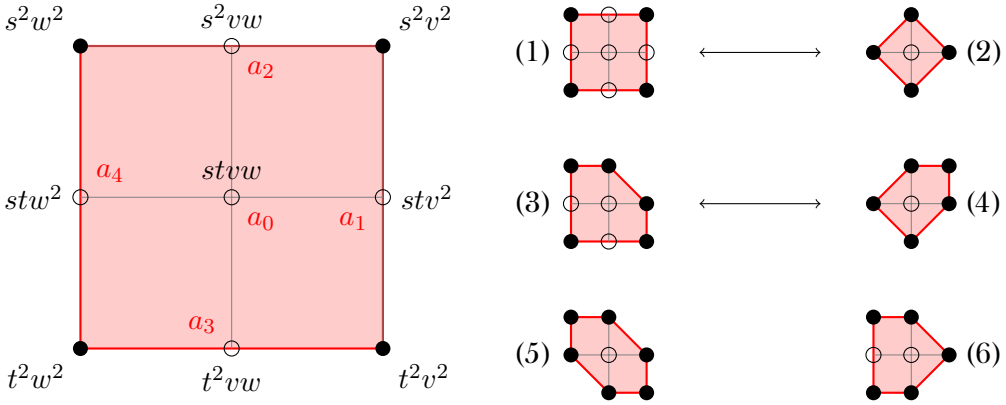

(a) Deformations in bi-quadratic. (b) Sub-polytopes of Figure 7.2a.

Figure 7.2: Elliptic families embedded in the bi-quadratic in $\mathbb{P}^1 \times \mathbb{P}^1$. Polytopes (1,2) and (3,4) form reflexive pairs while 5 and 6 are self-dual. Polytopes (2,4,6) can also be embedded in the quartic family in Figure 7.3 and (2-6) in the cubic family of Figure 7.4.

no.	deformations				$j(a_0)$	transition		
	a_1	a_2	a_3	a_4		a_0	$\mathcal{L}^{(2)}$	sing. fibres
1	2			2	$\frac{(a_0^2+8a_0-32)^3}{1728(a_0-4)(a_0+12)}$	4	A	I_1, I_1^*, I_4
						-12	$e=\mu(A)$	
				-2	$\frac{(a_0^4-16a_0^2+256)^3}{1728a_0^4(a_0-4)^2(a_0+4)^2}$	± 4	d	I_2, I_2, I_4, I_4
2	1				$\frac{(a_0^4-16a_0^2+16)^3}{1728a_0^2(a_0+4)(a_0-4)}$	± 4	d	I_1, I_1, I_2, I_8
3	1		2		$-\frac{(a_0^4-40a_0^2+120a_0-80)^3}{1728(a_0-3)^5(a_0^2+5a_0-25)}$	3	b	I_1, I_1, I_5, I_5
4	1				$-\frac{(a_0^4-16a_0^2+24a_0+16)^3}{1728(a_0-1)^2(a_0^3-a_0^2-18a_0+43)}$	1	$\mathcal{L}^{(2)}_{5a}$	I_1, I_1, I_1, I_2, I_7
5	1				$\frac{a_0^3(a_0^3-24a_0+48)^3}{1728(a_0-3)^2(a_0-2)^3(a_0+6)}$	2	a	I_1, I_2, I_3, I_6
						3	c	
						-6	g	
6	1			2	$\frac{a_0^3(a_0^3-24a_0+48)^3}{1728(a_0-3)^2(a_0-2)^3(a_0+6)}$	2	a	I_1, I_2, I_3, I_6
						3	c	
						-6	g	

Table 7.8: Transitions for bi-quadratic bases depicted in Figure 7.2. The singular fibres follow the Kodaira classification and were obtained from the polynomials f and g of the Weierstraß form.

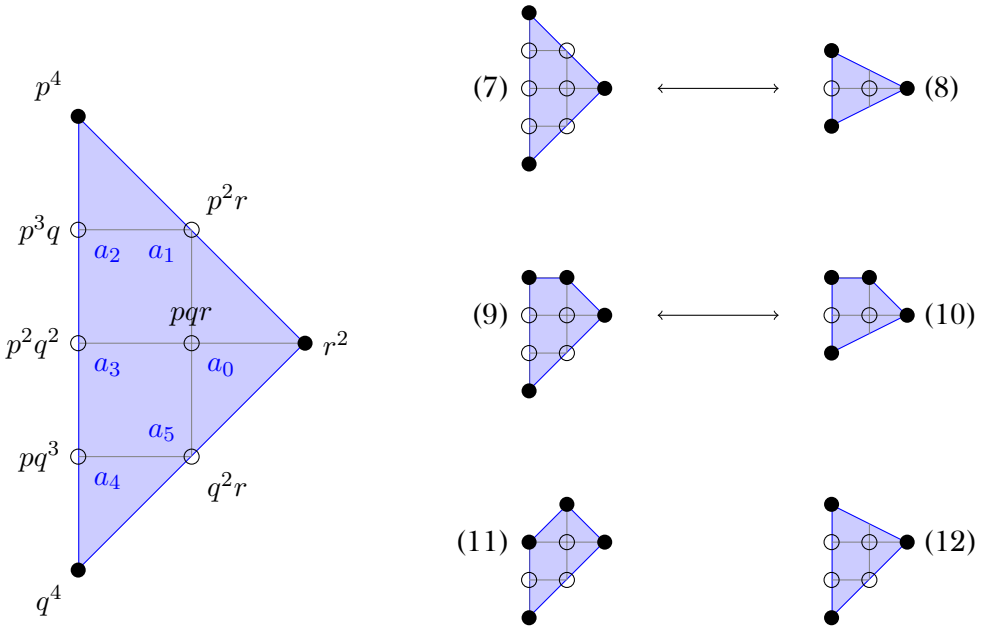

(a) Deformations in quartic. (b) Sub-polytopes of Figure 7.3a.

Figure 7.3: Elliptic families embedded in the quartic in $\mathbb{P}_{2,1,1}$. Polytopes (7,8) and (9,10) form reflexive pairs while 11 and 12 are self-dual, where (8) and (10) can also be embedded in both the bi-quadratic in Figure 7.2 and the cubic in Figure 7.4.

no.	deformations					$j(a_0)$	transition		
	a_1	a_2	a_3	a_4	a_5		a_0	$\mathcal{L}^{(2)}$	sing. fibres
7	2	4	6	4	2	$\frac{(a_0^2+8a_0-32)^3}{1728(a_0-4)(a_0+12)}$	4	A	I_1, I_1^*, I_4
							-12	$e=\mu(A)$	
	-2					$\frac{(a_0^4-16a_0^2+256)^3}{1728a_0^4(a_0^2-16)^2}$	±4	d	I_2, I_2, I_4, I_4
8	**0**	**1**	2	**1**	**0**	$\frac{(a_0^4-16a_0^2+16)^3}{1728a_0^2(a_0^2-16)}$	±4	d	I_2, I_2, I_4, I_4
9	**1**		3	3	2	$\frac{-(a_0^4-40a_0^2+120a_0-80)^3}{1728(a_0-3)^5(a_0^2+5a_0-25)}$	3	b	I_1, I_1, I_5, I_5
10	**1**		2	**1**	**0**	$\frac{-(a_0^4-16a_0^2+24a_0+16)^3}{1728(a_0-1)^2(a_0^3-a_0^2-18a_0+43)}$	1	$\mathcal{L}_{5a}^{(2)}$	I_1, I_1, I_1, I_2, I_7
11	**1**	**0**	**1**	2	2	$\frac{a_0^3(a_0^3-24a_0+48)^3}{1728(a_0-3)^2(a_0-2)^3(a_0+6)}$	2	a	I_1, I_2, I_3, I_6
							3	c	
							-6	g	
12	**0**	**1**	3	3	2	$\frac{a_0^3(a_0^3-24a_0+48)^3}{1728(a_0-3)^2(a_0-2)^3(a_0+6)}$	2	a	I_1, I_2, I_3, I_6
							3	c	
							-6	g	

Table 7.9: Transitions for quartic bases depicted in Figure 7.3. The singular fibres follow the Kodaira classification and were obtained from the polynomials f and g of the Weierstraß form.

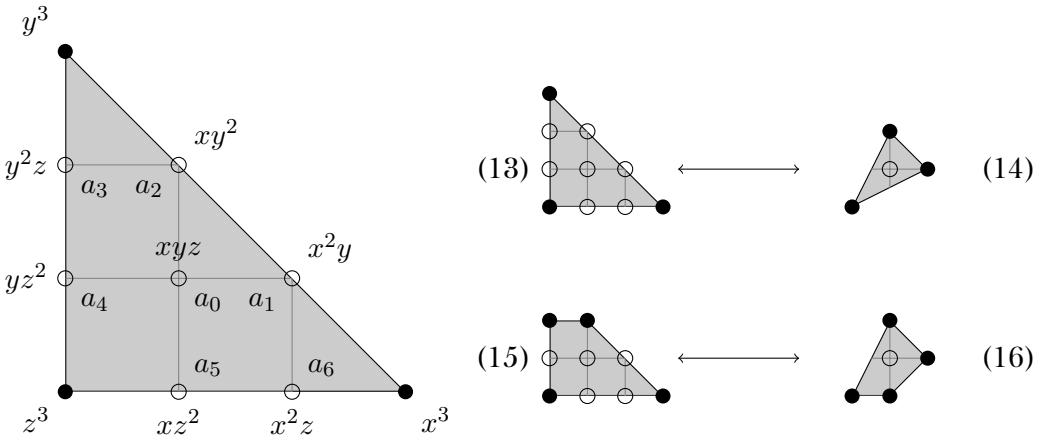

(a) Deformations in quartic. (b) Sub-polytopes of Figure 7.3a.

Figure 7.4: Elliptic families embedded in the cubic in $\mathbb{P}_{3,2,1}$. Polytopes (13,14) and (15,16) form reflexive pairs, where (14) and (16) can also be realised in both the bi-quadratic and the quartic of Figure 7.2 and Figure 7.3, respectively.

no.	deformations						$j(a_0)$	transition		
	a_1	a_2	a_3	a_4	a_5	a_6		a_0	$\mathcal{L}^{(2)}$	sing. fibres
13	3						$-\frac{(a_0-6)(a_0+18)^3}{1728(a_0+21)}$	6	B	I_1, I_3, IV^*
								-21	$h=\mu(B)$	
	-1						$-\frac{\left(\frac{a_0^4}{12}-2a_0^2-16a_0+60\right)^3}{(a_0-3)(a_0-2)^6(a_0+6)^2}$	2	a	I_1, I_2, I_3, I_6
								3	c	
								-6	g	
	0						$-\frac{a_0^3\left(a_0^3-216\right)^3}{1728\left(a_0^3+27\right)^3}$	6	f	I_1, I_1, I_1, I_9
								-3		
14	**1**		**0**				$-\frac{a_0^3\left(a_0^3+24\right)^3}{1728\left(a_0^3+27\right)}$	-3	f	I_1, I_1, I_1, I_9
15	2	**1**		2	3		$\frac{\left(a_0^2+8a_0-32\right)^3}{1728(a_0-4)(a_0+12)}$	4	A	I_1, I_1^*, I_4
								-12	$e=\mu(A)$	
	-2						$\frac{\left(a_0^4-16a_0^2+256\right)^3}{1728a_0^4(a_0-4)^2(a_0+4)^2}$	±4	d	I_2, I_2, I_4, I_4
16	**1**		**0**	**0**	**1**	**0**	$\frac{\left(a_0^4-8a_0^2+24a_0+16\right)^3}{1728\left(a_0^4-a_0^3-8a_0^2+36a_0-11\right)}$	– [5]		I_1, I_1, I_1, I_1, I_8

Table 7.10: Transitions for cubic bases depicted in Figure 7.4. The singular fibres follow the Kodaira classification and were obtained from the polynomials f and g of the Weierstraß form.

[5] As explained in the text, a transition exists at $a_0 = 0$ with base operator $\mathcal{L}^{(2)}_{5b}$.

Chapter 8

Conclusions

Our central question was how string compactifications on different families of Calabi–Yau manifolds are related by physical processes. While the interconnectedness of all families is still out of reach, we extended the web with new methods that fall into two categories.

In Chapter 6, we studied *smooth* fixed-point loci in the moduli space of residual discrete symmetries in the moduli space. For all quotients of hypersurface families we considered, a rational splitting of the period vector into invariant and non-invariant parts was obtained. Both components are given by rational linear combinations of the integral basis obtained from the $\hat{\Gamma}$-class at the MUM point. Even in models with a number of complex-structure moduli large enough to make an explicit analysis of the periods intractable, we can deduce two important results. First, there exist integral fluxes given by the rows of the splitting matrix (cf. eq. (6.1.39)) that drive the moduli towards the fixed-point loci. Importantly, for loci of codimension larger than one, this presumes compatibility of the individual flux configurations. Second, the F-term equations for the non-invariant moduli are satisfied automatically by superpotentials built from linear combinations of the invariant periods. It follows that searches for supersymmetric flux vacua on symmetric loci in moduli spaces of many-parameter families can be reduced to those on the sub-family over that locus. The compatibility of axio-dilaton values τ in consecutive moduli stabilisations is an essential requirement and generically not guaranteed, which we exemplified on the model $\mathcal{X}_6^{(3)}$ with two flux vacua along codimension-one loci with conflicting values for τ on their intersection (cf. eq. (6.2.21)). Only at a specific point $a_0 = 0$ do the values agree and realise a known one-parameter flux vacuum inside the three-parameter model.

We utilised the Yifan-Yang pullback to study pairs of one-parameter Calabi–Yau operators of order four and five to show the equivalence of the supersymmetric flux vacua conditions in type IIB on three-folds and in M-theory on their Yifan-Yang lift. This allows for an application of the tools developed for finding attractor points in three-folds families on four-fold compactifications and may simplify the search for supersymmetric flux vacua in M-theory .

Linking to the second category of transitions arising along singular loci, the conditions for supersymmetric flux vacua in F-theory are satisfied at fibres with a shrunken S^4. In section 6.3, we expressed the periods along a known vacuum of this form as a Hadamard product whose factors depend only on the fibre and base of the fibration, respectively.

We studied *singular* transitions in type IIB compactifications in Chapter 7, where we gave precise descriptions of the period structures in exemplary models arising in strong coupling and conifold transitions. Since the former is conceptually already well understood, we focused on

drawing a connection to flux vacua. To our knowledge, the precise analysis of conifold transitions in genus-one fibrations given in section 7.2 is the first of its kind. It is illuminating to see how the shrinking S^3 breaks open its dual cycle and makes its period a solution to an inhomogeneous Picard–Fuchs equation, cf. eq. (7.2.15). The remaining integrals of $\Omega(z)$ over the cycles are identified with Hadamard products, where one factor belongs to the elliptic fibre and the other depends on the geometry of the two-dimensional base. For all bases described torically by reflexive polygons, we observed at least one transition to a Hadamard product. Four of them have multiple distinct one-parameter models embedded in their moduli space, which serves as new connections in the web of Calabi–Yau families. The realisation of these models inside well-understood geometries provides them with an integral structure in the vector space of periods. The embedding supports a conjectural form of the prepotential, which includes a constant rational term.

The $\hat{\Gamma}$-class formalism necessary for integral bases in four-fold compactifications enabled us to construct a Jordan–Chevalley splitting of period matrices in any dimension into unipotent and semisimple parts in section 5.6. This decomposition has applications in the computation of multi-loop Feynman integrals as it helps to bring the differential equation into an ϵ-factorised form. It furthermore motivated our proposal in section 5.3 for an integral period basis in non-degenerate Calabi–Yau families in any dimension. We supported the claim of integrality by monodromy calculations and genus-zero invariants in several higher-dimensional models.

Outlook. The methods presented here to find and describe strong coupling and conifold transitions can be utilised in the context of compactifications of M- and F-theory. In section 6.3, we touched on the simplest example of an elliptic fibration over $\mathbb{P}^3$. The flux dual to the S^4 vanishing for suitable values of the deformation parameters plays the role of the S^3 in conifold transitions in type IIB compactifications. We expect that a classification analogous to that of section 7.2 yields a variety of supersymmetric flux vacua in genus-one fibrations over three-dimensional bases described by three-dimensional reflexive polyhedra. Together with transitions at suitable values of deformations originating from points inside faces of codimension three and four, these will be part of an upcoming article.

Chapter A

Picard–Fuchs systems over non-simply-connected spaces

The landscape conjectures by Ooguri and Vafa [142] exclude the existence of non-trivial cycles of minimal length. In the future, it might therefore become interesting to search for three-folds over moduli spaces with such cycles. These exist, if the moduli space itself is of higher genus. To our knowledge, three-fold families with this property have not yet been found. In the following two sections, we give examples of how Picard–Fuchs systems defined over higher genus moduli spaces yield the monodromy representations after an identification of the branch cuts. The modular forms, group generators and some code snippets given in footnotes are taken from the LMFDB [143].

A.1 $\mathcal{L}^{(3)}$ over $X_0(11)$

We consider the modular congruence subgroup

$$\Gamma_0(11) = \left\{ \begin{pmatrix} a & b \\ c & d \end{pmatrix} \in \mathrm{SL}(2,\mathbb{Z}) \,\middle|\, c \equiv 0 \bmod 11 \right\}, \tag{A.1.1}$$

generated by[1]

$$\underline{g} = \left\{ \begin{pmatrix} 1 & 1 \\ 0 & 1 \end{pmatrix}, \begin{pmatrix} 7 & -2 \\ 11 & -3 \end{pmatrix}, \begin{pmatrix} 8 & -3 \\ 11 & -4 \end{pmatrix}, \begin{pmatrix} -1 & 0 \\ 0 & -1 \end{pmatrix} \right\}. \tag{A.1.2}$$

The corresponding modular curve $X_0(11) = \Gamma_0(11)\backslash\mathbb{H}$ given by[2]

$$y^2 + y = x^3 - x^2 - 10x - 20 \tag{A.1.3}$$

has genus one and j-invariant $-2^{12}31^3 11^{-5}$. There are two weight-two modular forms of $\Gamma_0(11)$ with q-expansion[3]

$$m_1 = 1 + 12q^2 + 12q^3 + 12q^4 + 12q^5 + \mathcal{O}(q^6)\,, \tag{A.1.4}$$

$$m_2 = q - 2q^2 - q^3 + 2q^4 + q^5 + \mathcal{O}\left(q^6\right). \tag{A.1.5}$$

As an invariant coordinate, we define a ratio of (linear combinations of) these modular forms that is of the form $q + \mathcal{O}(q^2)$

$$\begin{aligned} z(q) &= \frac{m_2}{m_1} \\ &= q - 2q^2 - 13q^3 + 14q^4 + 169q^5 + O\left(q^6\right). \end{aligned} \tag{A.1.6}$$

[1] SAGEMATH: `Gamma0(11).generators()`

[2] `https://www.lmfdb.org/EllipticCurve/Q/11/a/2`

[3] SAGEMATH: `ModularForms(Gamma0(11),2).basis()`

We invert this series and find

$$q(z) = z + 2z^2 + 21z^3 + 156z^4 + 1486z^5 + O\left(z^6\right). \tag{A.1.7}$$

Expressing now the two modular forms m_i in terms of z makes them solutions to differential operators of degree three $\mathcal{L}_i^{(3)} m_i = 0$. The two operators are not independent but are related via

$$\mathcal{L}_2^{(3)} = z\mathcal{L}_1^{(3)} \frac{1}{z} \tag{A.1.8}$$

and we will therefore write $\mathcal{L}^{(3)} \equiv \mathcal{L}_1^{(3)}$ with

$$\begin{aligned}\mathcal{L}^{(3)} = {} & \theta^3 - 2z\,\theta\,(\theta+1)(2\theta+1) - 8z^2(\theta+1)(11\theta\,(\theta+2)+12) \\ & - 150z^3(\theta+1)(\theta+2)(2\theta+3) - 304z^4(\theta+1)(\theta+2)(\theta+3)\,.\end{aligned} \tag{A.1.9}$$

The Riemann $\mathcal{P}$-symbol of $\mathcal{L}^{(3)}$ is given by

$$\mathcal{P}_{\mathcal{L}^{(3)}}\left\{\begin{array}{cccccc} a & \bar{a} & -\frac{1}{4} & 0 & b & \infty \\ \hline 0 & 0 & 0 & 0 & 0 & 0 \\ \frac{1}{2} & \frac{1}{2} & \frac{1}{2} & 0 & \frac{1}{2} & 1 \\ 1 & 1 & 1 & 0 & 1 & 2 \end{array}, z\right\}, \tag{A.1.10}$$

where

$$\begin{aligned} a = {} & \frac{1}{228}\left(-\sqrt[3]{627\sqrt{33}+6947} - \sqrt[3]{6947-627\sqrt{33}} - 56\right) \\ & + \frac{\mathrm{i}}{76\sqrt{3}}\left(\sqrt[3]{6947-627\sqrt{33}} - \sqrt[3]{627\sqrt{33}+6947}\right) \approx -0.407 - 0.053\mathrm{i}\,, \end{aligned} \tag{A.1.11}$$

$$b = \frac{1}{228}\left(2\sqrt[3]{627\sqrt{33}+6947} + \sqrt[3]{55576-5016\sqrt{33}} - 56\right) \approx 0.078 \tag{A.1.12}$$

and a, $\bar{a}$ and b are the three roots of the polynomial $\Delta_c \coloneqq 76z^3 + 56z^2 + 8z - 1$. This operator is essentially self-adjoint with Yukawa coupling

$$C_{11}(z) \propto \frac{1}{z^2(1+4z)\Delta_c}. \tag{A.1.13}$$

To verify that this moduli space is indeed given by $X_0(11)$, we consider the elliptic curve family whose symmetric square makes up the K3 family under consideration. This will allow us to identify the monodromy group with the generators of $\Gamma_0(11)$. Performing this analysis for the K3, we would obtain the symmetric representation of the modular group. The Picard–Fuchs operator for the elliptic family is the one that annihilates $\sqrt{m_1(z)}$:

$$\begin{aligned}\mathcal{L}^{(2)} = {} & \theta^2 - 2z\,\theta\,(2\theta+1) - 8z^2(11\theta\,(\theta+1)+3) - 150z^3(\theta+1)(2\theta+1) \\ & - 76z^4(4\theta\,(\theta+2)+3)\,.\end{aligned} \tag{A.1.14}$$

Its Riemann $\mathcal{P}$-symbol reads

$$\mathcal{P}_{\mathcal{L}^{(2)}}\left\{\begin{array}{cccccc} a & \bar{a} & -\frac{1}{4} & 0 & b & \infty \\ \hline 0 & 0 & 0 & 0 & 0 & \frac{1}{2} \\ \frac{1}{2} & \frac{1}{2} & \frac{1}{2} & 0 & \frac{1}{2} & \frac{3}{2} \end{array}, z\right\} \tag{A.1.15}$$

$$M_a = \tfrac{1}{\mathrm{i}\sqrt{11}}\begin{pmatrix} 11 & -4 \\ 33 & -11 \end{pmatrix} \qquad M_{\bar{a}} = \tfrac{1}{\mathrm{i}\sqrt{11}}\begin{pmatrix} 22 & -15 \\ 33 & -22 \end{pmatrix}$$
$$M_{-\frac{1}{4}} = \tfrac{1}{\mathrm{i}\sqrt{11}}\begin{pmatrix} 11 & -6 \\ 22 & -11 \end{pmatrix} \qquad M_0 = \begin{pmatrix} 1 & 1 \\ 0 & 1 \end{pmatrix}$$
$$M_b = \tfrac{1}{\mathrm{i}\sqrt{11}}\begin{pmatrix} 0 & -1 \\ 11 & 0 \end{pmatrix} \qquad M_\infty = \begin{pmatrix} -1 & 0 \\ 0 & -1 \end{pmatrix}$$

Table A.1: Monodromy representation on solutions $\underline{\Pi}$ of $\mathcal{L}^{(2)}$ defined on $X_0(11)$.

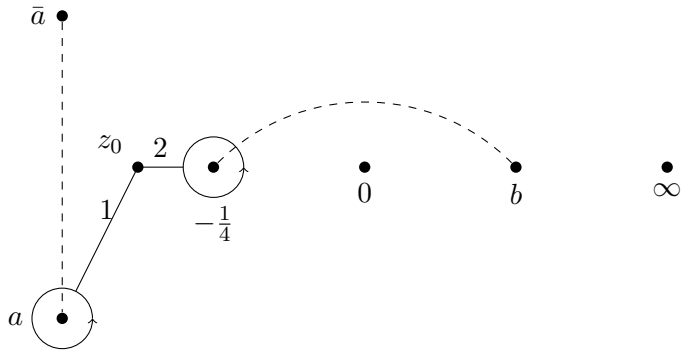

Figure A.1: A-cycle: Starting at a point z_0, the period vector is transported counterclockwise around a and then $-\frac{1}{4}$. The monodromy representation is given by g_2.

and the operator is essentially self-adjoint Yukawa coupling

$$C_1(z) \propto \sqrt{C_{11}(z)} \propto \frac{1}{z\sqrt{(1+4z)\Delta_c}}\,. \tag{A.1.16}$$

For $C_1(z)$ to be well-defined, its domain of definition must be a double cover of $\mathbb{P}^1$ where the four roots of $(1+4z)\Delta_c$ are connected to branch cuts. There are several choices of inserting these and we will show below that closed cycles on this space give rise to integral monodromy transformations. It would be naïve to expect a basis of periods where the monodromies around *all* singularities become integral, since, due to the double-cover-property of the domain of definition, the cycles around some singularities cannot correspond to closed contours.

Choosing the basis of solutions of $\mathcal{L}^{(2)}$ around $z=0$ given by

$$\underline{\Pi}(z) = \begin{pmatrix} \frac{\log(z)}{2\pi\mathrm{i}} \\ 1 \end{pmatrix} + \mathcal{O}(z)\,, \tag{A.1.17}$$

we find the monodromy representation collected in Table A.1. The monodromies around singularities connected to a branch cut are not integral but square to the identity. Only when going around these points twice, one returns to the same point. Therefore, these points are not typical singularities of the family.

We identify the generators $g_1 = M_0$ and $g_4 = M_\infty$. The remaining two generators correspond to the transport around closed loops sketched in Figures A.1 and A.2. They are given in

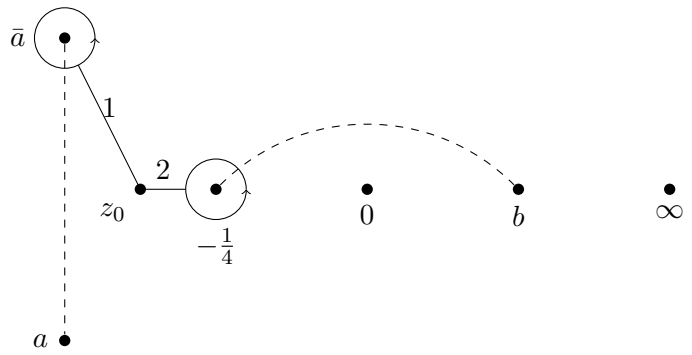

Figure A.2: B-cycle: Starting at a point z_0, the period vector is transported counterclockwise around $\bar{a}$ and then $-\frac{1}{4}$. The monodromy representation is given by g_3.

terms of the monodromy matrices listed in Table A.1

$$g_2 = M_{-\frac{1}{4}} \cdot M_a \,, \tag{A.1.18}$$

$$g_3 = M_{\bar{a}} \cdot M_{-\frac{1}{4}} \,. \tag{A.1.19}$$

Encircling the singularities in opposite order reverses the direction of the path. This is reflected in the matrix representation in the sense that $g_2^{-1} = M_a \cdot M_{-\frac{1}{4}}$ and $g_3^{-1} = M_{-\frac{1}{4}} \cdot M_{\bar{a}}$.

Another verification of the differential system to be defined over $X_0(11)$ is the computation of the j-invariant. We may map the singularities to that of the Legendre curve given by

$$y^2 = x(x-1)(x-\lambda), \quad \lambda \notin \{0,1\}$$

via a Möbius transformation over $\mathrm{SL}(2,\mathbb{C})$. We place the branch cuts of the Legendre curve along $[\infty, 0]$ and $[1, \lambda]$. The Möbius transformation is then determined by the mapping of the three points

$$\{b, a, -\frac{1}{4}\} \mapsto \{0, 1, \infty\} \,,$$

implying $\bar{a} \mapsto \lambda \approx 0.908125 + \mathrm{i}\, 0.418699$. This allows us to recover the j-invariant of $X_0(11)$ via the formula

$$j(\lambda) = 256 \frac{\left(\lambda^2 - \lambda + 1\right)^3}{\lambda^2 (\lambda - 1)^2} = -\frac{2^{12} 31^3}{11^5} \,.$$

Finally, we may compute the mirror map of the operator $\mathcal{L}^{(2)}$ given by

$$t(z) = \frac{\Pi_1}{\Pi_2} \,,$$

which satisfies the relation

$$e^{2\pi \mathrm{i}\, t(z)} = q(z) \,,$$

with $q(z)$ as in eq. (A.1.7). This is a direct consequence of $\mathcal{L}^{(3)}$ being the symmetric square of $\mathcal{L}^{(2)}$.

A.2 $\mathcal{L}^{(4)}$ over $X_{\chi_{15}}(15)$

Similarly to the proceedings of appendix A.1, we can obtain an fourth-order operator given by the symmetric cube of a second-order one. The group we consider is defined by

$$\Gamma_{\chi_{15}}(15) = \left\{ \begin{pmatrix} a & b \\ c & d \end{pmatrix} \in \mathrm{SL}(2,\mathbb{Z}) \,\middle|\, c \equiv 0 \bmod 15 \text{ and } \chi_{15}(a) = 1 \right\} \tag{A.2.1}$$

with the quadratic Dirichlet character given by $\chi_{15}(n) = \chi_3(n)\chi_5(n)$ and for a prime p

$$\chi_p(n) = \begin{cases} 1 & \exists\, r \in \mathbb{N} :\ n \equiv r^2 \bmod p\,, \\ 0 & p|n\,, \\ -1 & \text{else.} \end{cases} \tag{A.2.2}$$

In other words, the entry a is restricted to $\{1,2,4,8\}$. The lowest weight of modular forms is three. Their q-expansions read[4]

$$m_1 = q - q^2 + 3q^3 - 3q^4 - 5q^5 + \mathcal{O}\big(q^6\big)\,, \tag{A.2.3}$$
$$m_2 = q^2 - 3q^3 + 5q^5 + \mathcal{O}\big(q^6\big)\,. \tag{A.2.4}$$

We obtain the Batyrev coordinate again as $z = m_2/m_1$, whose inversion yields the mirror map

$$q(z) = z + 2z^2 + 13z^3 + 81z^4 + 588z^5 + \mathcal{O}\big(z^6\big)\,. \tag{A.2.5}$$

The degree-four operator annihilating the normalised modular form m_1/z as a function of z is of z-degree twelve and can be written as $\mathcal{L}^{(4)} = \mathrm{Sym}^3\big(\mathcal{L}^{(2)}\big)$ with the essentially self-adjoint second-order operator

$$\begin{aligned} \mathcal{L}^{(2)}(z) = {} & 9\theta^2 - 3z(2\theta+1)(6\theta+1) - z^2(432\theta^2 + 402\theta + 119) \\ & - 3z^3\left(366\theta^2 + 463\theta + 165\right) - 2z^4(6\theta+5)(99\theta+76) \\ & - 6z^5(3\theta+2)(32\theta+41) - 11z^6(3\theta+2)(3\theta+5) \end{aligned} \tag{A.2.6}$$

with Riemann symbol

$$\mathcal{P}_{\mathcal{L}^{(2)}}\left\{ \begin{array}{ccccccc} a & -1 & b & \bar{a} & 0 & \bar{b} & \infty \\ \hline 0 & \frac{1}{3} & 0 & 0 & 0 & 0 & \frac{2}{3} \\ \frac{1}{2} & \frac{1}{3} & \frac{1}{2} & \frac{1}{2} & 0 & \frac{1}{2} & \frac{5}{3} \end{array}, z \right\}. \tag{A.2.7}$$

Here, we denoted the singularities by $a = -(3+\sqrt{5})/2$ and $b = -(9+5\sqrt{5})/22$, where barred means $\sqrt{5} \mapsto -\sqrt{5}$. With an asymptotic period basis as in eq. (A.1.17), one obtains the monodromies listed in Table A.2 together with $M_\infty = e^{-2\pi\mathrm{i}/3}\mathbb{1}$. We note that the proportionality to a root of unity of M_{-1} and M_∞ can be resolved by a Kähler-gauge transformation $\underline{\Pi} \mapsto (1+z)^{-1/3}\underline{\Pi}$ and that all monodromies around points with indials $(0,1/2)$ square to unity. Furthermore, we verified that the product of monodromy transformations in the order in the

[4] SAGEMATH:

```
from sage.modular.dirichlet import DirichletCharacter
H = DirichletGroup(15, base_ ring=CyclotomicField(2))
chi = DirichletCharacter(H, H._module([1, 1]))
Newforms(chi, 3)
```

$$M_a = \tfrac{1}{\mathrm{i}\sqrt{15}}\begin{pmatrix} 15 & -4 \\ 60 & -15 \end{pmatrix} \qquad M_{\bar{a}} = \tfrac{1}{\mathrm{i}\sqrt{15}}\begin{pmatrix} 15 & -8 \\ 30 & -15 \end{pmatrix}$$
$$M_b = \tfrac{1}{\mathrm{i}\sqrt{15}}\begin{pmatrix} 45 & -17 \\ 120 & -45 \end{pmatrix} \qquad M_{\bar{b}} = \tfrac{1}{\mathrm{i}\sqrt{15}}\begin{pmatrix} 0 & -1 \\ 15 & 0 \end{pmatrix}$$
$$M_{-1} = e^{2\pi\mathrm{i}/3}\begin{pmatrix} -14 & 5 \\ -45 & 16 \end{pmatrix} \qquad M_0 = \begin{pmatrix} 1 & 1 \\ 0 & 1 \end{pmatrix}$$

Table A.2: Monodromy representation on solutions $\underline{\Pi}$ of $\mathcal{L}^{(2)}$ defined on $X_{\chi_{15}}(15)$.

Riemann symbol is trivial. With branch cuts between (a, b) and $(\bar{a}, \bar{b})$, we identify four generators of the rank-five group $\Gamma_{\chi_{15}}(15)$

$$\begin{aligned} M_0 &= \begin{pmatrix} 1 & 1 \\ 0 & 1 \end{pmatrix}, & M_A &\coloneqq M_a \cdot M_b = \begin{pmatrix} -13 & 5 \\ -60 & 23 \end{pmatrix}, \\ M_B &\coloneqq M_b \cdot M_{\bar{a}} = \begin{pmatrix} -11 & 7 \\ -30 & 19 \end{pmatrix}, & M_C &\coloneqq M_{-1} \cdot M_\infty = \begin{pmatrix} -14 & 5 \\ -45 & 16 \end{pmatrix}. \end{aligned} \tag{A.2.8}$$

The monodromy representation on the order-four operator is given by the symmetric cube of the above. We note that, there, infinity becomes a regular point and that the monodromy around $z = -1$ is integral by itself. All instanton corrections to the triple coupling vanish, which is expected for symmetric cubes of second-order operators.

Chapter B

Genus-zero invariants of higher-dimensional two-parameter families

This appendix lists the first genus-zero invariants for two-parameter five-, six- and seven-folds computed with the formalism of section 5.3.

B.1 Five-fold $\mathbb{P}_{15,10,1^5}[30]$

Tables B.1 and B.2 contain the genus-zero invariants for the degree-30 hypersurface in $\mathbb{P}_{15,10,1^5}$. This model was discussed in more detail in subsection 5.5.1.

${n_{d_1 d_2}}^1$	$d_2 = 0$	1	2	3	4
$d_1 = 0$	–	130	-58345	55837430	-73589158000
1	0	-55500	41337000	-56023509000	95692879557000
2	0	14314500	-15970505250	29728628829000	-64866615149502000
3	0	-3190201000	4521652482000	-11158432052002500	30609325097795488000
4	0	575513349750	-1032624284555250	3310653667485273000	-1128084768290565790200 0
${n_{d_1 d_2}}^2$	$d_2 = 0$	1	2	3	4
$d_1 = 0$	–	-650	291725	-279187150	367945790000
1	1500	241500	-193563000	268338729000	-463423560804000
2	3000	-58234500	71165528250	-137352543993000	305433626311098000
3	4500	12717419000	-19432506624000	50037802437232500	-140631707204082788000
4	6000	-2098887405750	4300685843195250	-14467844481295497000	5071103575769584200 6000

Table B.1: Corrections to the components ${C_{ij}}^{\alpha}$ of the triple couplings $C^{(1,1,3)}$ belonging to the five-fold $\mathbb{P}_{15,10,1^5}[30]$.

B.2 Complete intersection six-fold

As a second example, we consider the six-fold complete intersection given by the configuration (cf. section 2.2)

$$\left(\begin{array}{c|cc} \mathbb{P}^1 & 0 & 2 \\ \mathbb{P}^7 & 7 & 1 \end{array}\right) \tag{B.2.1}$$

with Hodge structure $(1, 2, 2, 2, 2, 2, 1)$ and intersection ring given by

$$R = 7J_1 J_2^5 + 14J_2^6 \,. \tag{B.2.2}$$

$n_{d_1d_2,1}{}^1$	$d_2=0$	1	2	3	4
$d_1=0$	–	0	0	0	0
1	0	87000	-88053000	145836336000	-289794139173000
2	0	-41953500	66078582000	-151975940112000	387743791488726000
3	0	11247432000	-26385247644000	82815777839355000	-268662318135628656000
4	0	-2316774073500	7492529798596500	-31499193318974785500	12862162303886640674700 0
$n_{d_1d_2,1}{}^2$	$d_2=0$	1	2	3	4
$d_1=0$	–	0	0	0	0
1	-1500	36000	-13122000	11778816000	-15040836981000
2	-6000	-42426000	34892496000	-53271434304000	101028526771824000
3	-13500	19481508000	-23788181358000	50776237757340000	-124611083496124956000
4	-24000	-5451403122000	9260364467574000	-27004642733470722000	844535466747414065160 00
$n_{d_1d_2,2}{}^1$	$d_2=0$	1	2	3	4
$d_1=0$	–	-245	289035	-499858460	1013558891950
1	0	106500	-207544500	506590888500	-1328646245206500
2	0	-28622250	81762541500	-272311461024750	909393935613849000
3	0	5861483000	-23291351752000	103190445948877500	-432819166908356696000
4	0	-960037032375	5283232845747750	-30757856154831156375	160526772200304513189000

Table B.2: Corrections to the components $C_{i\alpha}{}^{\beta}$ of the triple couplings $C^{(1,2,2)}$ belonging to the five-fold $\mathbb{P}_{15,10,1^5}[30]$. Due to the symmetry in the couplings, we have $n_{d_1d_2,2}{}^2 = n_{d_1d_2,1}{}^1$.

The non-vanishing integrals of Chern classes yield

$$c_2 \cdot J_1 J_2^3 = 147\,, \quad c_2 \cdot J_2^4 = 308\,, \tag{B.2.3}$$

$$c_3 \cdot J_1 J_2^2 = -784\,, \quad c_3 \cdot J_2^3 = -1582\,, \tag{B.2.4}$$

$$c_4 \cdot J_1 J_2 = 5733\,, \quad c_4 \cdot J_2^2 = 11774\,, \tag{B.2.5}$$

$$c_5 \cdot J_1 = -39984\,, \quad c_5 \cdot J_2 = -81844\,, \tag{B.2.6}$$

$$\chi = 573216\,. \tag{B.2.7}$$

Here, we are interested only in the genus-zero invariants coming from the triple couplings. These are listed in Tables B.3 and B.6. Considering a similar transformation of variables as in eq. (6.1.10) for describing the three-parameter three-fold hypersurface $\mathcal{X}_6$ as a CICY

$$\widetilde{\varpi}_0(z_1, z_2) = \sqrt{1-4z_1}\varpi_0\left(z_1, z_2(1-4z_1)\right), \tag{B.2.8}$$

we find that this two-parameter six-fold period becomes one of a six-fold one-parameter model as $z_1 \to 1/4$. We did not verify whether this is a transition of the entire integral structure of the middle (co-)homology. The one-parameter model is—up to a rescaling of the complex-structure modulus—the mirror family of degree-eight hypersurfaces in $\mathbb{P}^7$. This model together with its invariants was discussed briefly in subsection 5.5.2.

B.3 Complete intersection seven-fold

As a last example, we compute the genus-zero invariants for the seven-fold complete intersection with configuration matrix (cf. section 2.2)

$$\left(\begin{array}{c|cc} \mathbb{P}^2 & 0 & 3 \\ \mathbb{P}^7 & 6 & 2 \end{array}\right) \tag{B.3.1}$$

with Hodge structure $(1,2,3,3,3,3,2,1)$ and intersection ring given by

$$R = 18J_1^6 J_2 + 12J_1^5 J_2^2\,. \tag{B.3.2}$$

$n_{d_1d_2}{}^1$	$d_2=0$	1	2	3	4
$d_1=0$	–	102312	16517690280	4769975120009400	1783670482131896286936
1	-2	-102312	0	13884917535601728	13878201868881305449536
2	0	0	-16517690280	-13884917535601728	0
3	0	0	0	-4769975120009400	-13878201868881305449536
4	0	0	0	0	-1783670482131896286936
$n_{d_1d_2}{}^2$	$d_2=0$	1	2	3	4
$d_1=0$	–	144256	17462826584	4361238820782872	1482599929913698021888
1	1	246568	111214311768	60280546074034888	35582521273000808347024
2	0	0	33980516864	74165463609636616	98957248755268188958344
3	0	0	0	9131213940792272	4946072314188211379656 0
4	0	0	0	0	3266270412045594308824

Table B.3: Corrections to the components $C_{ij}{}^{\alpha}$ of the triple couplings $C^{(1,1,4)}$ belonging to the six-fold CICY with configuration (B.2.1).

$n_{d_1d_2}{}^1$	$d_2=0$	1	2	3
$d_1=0$	–	24	60	72
1	31248	1884672	29312352	246666816
2	864771840	251330413248	13448862258048	325897035614208
3	48806303416560	37587089999646720	4729909879978778880	244361471415416879616
$n_{d_1d_2}{}^2$	$d_2=0$	1	2	3
$d_1=0$	–	6	-6	0
1	52056	1131840	9926496	57490560
2	1751053248	237515715504	8141727014784	143263083868560
3	110451495327912	44325978297836544	3809259647533642752	148534191907426263744
$n_{d_1d_2}{}^3$	$d_2=0$	1	2	3
$d_1=0$	–	-9	9	0
1	6480	-6480	-6480	19440
2	468555840	22534293960	331045477200	2684891924280
3	36098796486960	6996784294736640	340157317297898880	7975643229362097360

Table B.4: Corrections to the components $C_{ij}{}^{\alpha}$ of the triple couplings $C^{(1,1,5)}$ belonging to the seven-fold CICY with configuration (B.3.1).

The non-vanishing integrals of Chern classes are

$$c_2\cdot J_1^5=144\,,\quad c_2\cdot J_1^4J_2=360\,,\quad c_2\cdot J_1^3J_2^2=192\,, \tag{B.3.3}$$

$$c_3\cdot J_1^4=-432\,,\quad c_3\cdot J_1^3J_2=-1440\,,\quad c_3\cdot J_1^2J_2^2=-864\,, \tag{B.3.4}$$

$$c_4\cdot J_1^3=3600\,,\quad c_4\cdot J_1^2J_2=9612\,,\quad c_4\cdot J_1J_2^2=5448\,, \tag{B.3.5}$$

$$c_5\cdot J_1^2=-20736\,,\quad c_5\cdot J_1J_2=-56880\,,\quad c_5\cdot J_2^2=-32544\,, \tag{B.3.6}$$

$$c_6\cdot J_1=125856\,,\quad c_6\cdot J_2=341784\,, \tag{B.3.7}$$

$$\chi=-756000\,. \tag{B.3.8}$$

We computed the corrections to all three kinds of triple couplings $C^{(1,1,5)}$, $C^{(1,2,4)}$ and $C^{(1,3,3)}$ and verified integrality for all invariants up to degree ten. Tables B.4, B.5 and B.7 contain only those up to degree six.

$n_{d_1d_2,1}{}^1$	$d_2=0$	1	2	3
$d_1=0$	–	0	0	0
1	51408	4646592	81078192	713536128
2	3480188544	1638018262080	102614475965760	2700408095048448
3	340699613797008	443580519776385024	66746494882328109696	3808839040148938175424
$n_{d_1d_2,1}{}^2$	$d_2=0$	1	2	3
$d_1=0$	–	0	0	0
1	159408	3977424	34708176	200819088
2	15354551808	2508720993072	91410103984032	1649786984060112
3	1842317884132848	910220645248233984	84987202697514235008	3461752753566352373520
$n_{d_1d_2,1}{}^3$	$d_2=0$	1	2	3
$d_1=0$	–	0	0	0
1	56376	-56376	-56376	169128
2	12662640576	638518427064	9498379105008	77441416430472
3	1970806334319000	406698336573147648	20299181309916803712	482482007499962659176
$n_{d_1d_2,2}{}^1$	$d_2=0$	1	2	3
$d_1=0$	–	24	120	216
1	0	4063104	145475424	1974341952
2	0	792196666560	97547371167744	3853185239923200
3	0	152646749932087296	44146180958592215808	3731345234028755383680
$n_{d_1d_2,2}{}^2$	$d_2=0$	1	2	3
$d_1=0$	–	6	-12	0
1	31248	5120352	84729744	716072832
2	1729543680	1585305899856	106161995483136	2798799527906640
3	146418910249680	395034539070915072	66069779379280490880	388932023296893539606 4
$n_{d_1d_2,2}{}^3$	$d_2=0$	1	2	3
$d_1=0$	–	-9	18	0
1	52056	496800	1045656	-1191024
2	3502106496	652736337624	17968769365824	221288575643352
3	331354485983736	239740983855804672	20862042260120541504	717208482226285343520
$n_{d_1d_2,3}{}^1$	$d_2=0$	1	2	3
$d_1=0$	–	8	80	144
1	0	944640	59846976	983387520
2	0	138464375616	29778304538880	1496493979157952
3	0	21496923053051904	10982311619619110400	1205419021134994635264
$n_{d_1d_2,3}{}^2$	$d_2=0$	1	2	3
$d_1=0$	–	12	0	0
1	0	1859904	44129088	409701888
2	0	378437228064	38168465855616	1219320016231968
3	0	72969792055197696	18870292826536596480	13859852124477895655 04
$n_{d_1d_2,3}{}^3$	$d_2=0$	1	2	3
$d_1=0$	–	-18	0	0
1	0	-30240	-3945888	-33032448
2	0	145115226000	5493651469056	62807354169552
3	0	45222971429730816	5970377187935352576	247238235764772444000

Table B.5: Corrections to the components $C_{i\alpha}{}^A$ of the triple couplings $C^{(1,2,4)}$ belonging to the seven-fold CICY with configuration (B.3.1).

$n_{d_1d_2,1}{}^1$	$d_2=0$	1	2	3	4
$d_1=0$	–	-1009792	-244479572176	-91586015236440312	-415127980375835446128 64
1	0	-5141570	-4965596259918	-4246906117760960430	-34776256500927618779457 74
2	0	0	-2020568042990	-7244630844138458820	-13706392224511660576981848
3	0	0	0	-1031787508592869476	-82176109590887458285031 62
4	0	0	0	0	-588297859142101773554288
$n_{d_1d_2,1}{}^2$	$d_2=0$	1	2	3	4
$d_1=0$	–	0	0	0	0
1	-1	-490539	-317309353165	-218775592666383389	-154971594113590251424 69
2	0	0	-215682899621	-580781296121491794	-92296384192723717316 3492
3	0	0	0	-115605567354848998	-73108975218923633098 7719
4	0	0	0	0	-678088896656592545581 52
$n_{d_1d_2,2}{}^1$	$d_2=0$	1	2	3	4
$d_1=0$	–	-6151362	-2265047615166	-1123373523829309788	-62981065717968531816 7152
1	0	-6151362	-9931192519836	-11491536961899419250	-11695236609181507706448936
2	0	0	-2265047615166	-11491536961899419250	-27412784449023321153963696
3	0	0	0	-1123373523829309788	-11695236609181507706448936
4	0	0	0	0	-62981065717968531816 7152
$n_{d_1d_2,2}{}^1$	$d_2=0$	1	2	3	4
$d_1=0$	–	-243971	-72969677949	-31792648158418070	-16233661640355284521032
1	0	-634795	-709370894274	-672941559993242855	-59782626465108638394 0916
2	0	0	-250608552789	-968706577420959895	-19580560320730943681402 64
3	0	0	0	-128689283817197614	-10729218223748432884089 32
4	0	0	0	0	-73739289385314046645704

Table B.6: Corrections to the components $C_{i\alpha}{}^A$ of the triple couplings $C^{(1,2,3)}$ belonging to the six-fold CICY with configuration (B.2.1).

$n_{d_1d_2,1}{}^1$	$d_2=0$	1	2	3
$d_1=0$	–	0	0	0
1	374976	62532864	1227921984	11154848256
2	20754524160	21822618405888	1623748819567104	46091237254566912
3	1757026922996160	5828568982666831872	1077438759065501501952	6791709649523263561958 4
$n_{d_1d_2,1}{}^2$	$d_2=0$	1	2	3
$d_1=0$	–	0	0	0
1	2838240	164026944	2450707488	20250336960
2	246898015488	79412370217920	4275629866493568	103344246119419200
3	28240407657940320	26313513524024813568	3440966909368285285632	1801949671527549049065 60
$n_{d_1d_2,1}{}^3$	$d_2=0$	1	2	3
$d_1=0$	–	0	0	0
1	5178816	103576320	911471616	5282392320
2	749905433856	92800356120576	3102643862205696	54113192709493248
3	110786116630769856	42255450273862849536	3553111889756245744128	1371205388956755710983 68
$n_{d_1d_2,2}{}^1$	$d_2=0$	1	2	3
$d_1=0$	–	288	1440	2592
1	0	58095360	2268711936	31837743360
2	0	12491635511808	1698454087681536	70419524279687424
3	0	2561907357813841920	827653058905474031616	7407918243727729701350 4
$n_{d_1d_2,2}{}^2$	$d_2=0$	1	2	3
$d_1=0$	–	504	2016	3888
1	616896	184996224	5012601408	61286979456
2	41762262528	53731276319808	4922479282576896	168736438415077056
3	4088395365564096	13562068585975289856	2892594017628967444992	2096301107745383120075 52
$n_{d_1d_2,3}{}^1$	$d_2=0$	1	2	3
$d_1=0$	–	96	960	1728
1	0	14335488	952971264	16081473024
2	0	2347865222400	542565640203264	28210866264168192
3	0	391264002124849152	218865069056061554688	2503342606868314112563 2

Table B.7: Corrections to the components $C_{ia}{}^b$ of the triple couplings $C^{(1,3,3)}$ belonging to the seven-fold CICY with configuration (B.3.1). The remaining invariants follow from the symmetry of the couplings in the last two indices.

Bibliography

[1] J. Dücker, A. Klemm and J. F. Piribauer. "Calabi–Yau Period Geometry and Restricted Moduli in Type II Compactifications". In: *JHEP* 07 (2025), p. 225. DOI: 10.1007/JHEP07(2025)225. arXiv: 2503.00272 [hep-th].

[2] P. Blesse, J. Dücker, A. Klemm and J. F. Piribauer. "Geometry and Arithmetic of Transitions in Type II String Theory". *In preparation*.

[3] P. Candelas. *Lectures on Complex Manifolds*. World Scientific., 1987, p. 1–88.

[4] P. Candelas, X. C. De La Ossa, P. S. Green and L. Parkes. "A Pair of Calabi–Yau Manifolds as an Exactly Soluble Superconformal Theory". In: *Nucl. Phys. B* 359 (1991). Ed. by S.-T. Yau, pp. 21–74. DOI: 10.1016/0550-3213(91)90292-6.

[5] A. Klemm. "The B-Model Approach to Topological String Theory on Calabi–Yau n-folds". In: *B-Model Gromov–Witten Theory*. Springer, 2019, pp. 79–397.

[6] E. Calabi. "On Kähler Manifolds with Vanishing Canonical Class, Algebraic Geometry and Topology". In: *A Sympodium in Honor of S. Lefschetz* (1957), pp. 78–89.

[7] S.-T. Yau. "On the Ricci Curvature of a Compact Kähler Manifold and the Complex Monge–Ampère Equation, I". In: *Commun. Pure Appl. Math.* 31.3 (1978), pp. 339–411. DOI: 10.1002/cpa.3160310304.

[8] P. Candelas, G. T. Horowitz, A. Strominger and E. Witten. "Vacuum Configurations for Superstrings". In: *Nucl. Phys. B* 258 (1985), pp. 46–74. DOI: 10.1016/0550-3213(85)90602-9.

[9] K. Kodaira and D. C. Spencer. "On Deformations of Complex Analytic Structures, I". In: *Annals of Mathematics* 67.2 (1958), pp. 328–401.

[10] G. Tian. "Smoothness of the Universal Deformation Space of Compact Calabi–Yau Manifolds and its Peterson–Weil Metric". In: *Mathematical Aspects of String Theory*. World Scientific, 1987, pp. 629–646.

[11] A. N. Todorov. "The Weil–Petersson Geometry of the Moduli Space of SU($n \geq 3$) (Calabi–Yau) manifolds I". In: *Communications in Mathematical Physics* 126 (1989), pp. 325–346.

[12] V. V. Batyrev. "Dual Polyhedra and Mirror Symmetry for Calabi–Yau Hypersurfaces in Toric Varieties". In: *J. Alg. Geom.* 3 (1994), pp. 493–545. arXiv: alg-geom/9310003.

[13] L. Borisov. "Towards the Mirror Symmetry for Calabi–Yau Complete Intersections in Gorenstein Toric Fano Varieties". In: *arXiv preprint alg-geom/9310001* (1993).

[14] V. V. Batyrev and L. A. Borisov. "On Calabi-Yau Complete Intersections in Toric Varieties". In: (Dec. 1994). arXiv: alg-geom/9412017.

[15] T. Oda and H. S. Park. "Linear Gale Transforms and Gelfand–Kapranov–Zelevinskij Decompositions". In: *Tohoku Mathematical Journal, Second Series* 43.3 (1991), pp. 375–399.

[16] S. Hosono, A. Klemm, S. Theisen and S.-T. Yau. "Mirror Symmetry, Mirror map and applications to Calabi-Yau hypersurfaces". In: *Commun. Math. Phys.* 167 (1995), pp. 301–350. DOI: 10.1007/BF02100589. arXiv: hep-th/9308122.

[17] P. Candelas et al. "Mirror Symmetry for Two Parameter Models. 1." In: *Nucl. Phys. B* 416 (1994). Ed. by B. Greene and S.-T. Yau, pp. 481–538. DOI: 10.1016/0550-3213(94)90322-0. arXiv: hep-th/9308083.

[18] D. A. Cox, J. B. Little and H. K. Schenck. *Toric Varieties*. Vol. 124. American Mathematical Society, 2024.

[19] D. A. Cox. "Mirror Symmetry and Polar Duality of Polytopes". In: *Symmetry* 7.3 (2015), pp. 1633–1645. ISSN: 2073-8994. DOI: 10.3390/sym7031633. URL: https://www.mdpi.com/2073-8994/7/3/1633.

[20] I. M. Gelfand, M. M. Kapranov and A. V. Zelevinsky. *A-Discriminants*. Springer, 1994.

[21] P. S. Aspinwall, M. R. Plesser and K. Wang. "Mirror Symmetry and Discriminants". In: *arXiv preprint arXiv:1702.04661* (2017).

[22] B. Greene and M. Plesser. "Duality in Calabi–Yau Moduli Space". In: *Nuclear Physics B* 338.1 (1990), pp. 15–37. ISSN: 0550-3213. DOI: https://doi.org/10.1016/0550-3213(90)90622-K.

[23] D. A. Cox and S. Katz. *Mirror Symmetry and Algebraic Geometry*. 2000.

[24] G. Veneziano. "Construction of a Crossing-Symmetric, Regge-Behaved Amplitude for Linearly Rising Trajectories". In: *Il Nuovo Cimento A (1965-1970)* 57.1 (1968), pp. 190–197.

[25] M. A. Virasoro. "Alternative Constructions of Crossing-Symmetric Amplitudes with Regge Behavior". In: *Phys. Rev.* 177 (5 Jan. 1969), pp. 2309–2311. DOI: 10.1103/PhysRev.177.2309. URL: https://link.aps.org/doi/10.1103/PhysRev.177.2309.

[26] J. A. Shapiro. "Narrow-Resonance Model with Regge Behavior for $\pi\pi$ Scattering". In: *Phys. Rev.* 179 (5 Mar. 1969), pp. 1345–1353. DOI: 10.1103/PhysRev.179.1345. URL: https://link.aps.org/doi/10.1103/PhysRev.179.1345.

[27] Y. Nambu. "Quark Model and the Factorization of the Veneziano Amplitude". In: *Broken Symmetry*, pp. 258–267. DOI: 10.1142/9789812795823_0024.

[28] L. Susskind. "Dual Symmetric Theory of Hadrons. 1." In: *Nuovo Cim. A* 69 (1970), pp. 457–496. DOI: 10.1007/BF02726485.

[29] H. Nielsen. "An Almost Physical Interpretation of the Dual N Point Function". In: *Nordita Report, unpublished* (1969).

[30] P. Goddard, J. Goldstone, C. Rebbi and C. B. Thorn. "Quantum Dynamics of a Massless Relativistic String". In: *Nucl. Phys. B* 56 (1973), pp. 109–135. DOI: 10.1016/0550-3213(73)90223-X.

[31] P. Ramond. "Dual Theory for Free Fermions". In: *Phys. Rev. D* 3 (1971), pp. 2415–2418. DOI: 10.1103/PhysRevD.3.2415.

[32] A. Neveu and J. H. Schwarz. "Factorizable Dual Model of Pions". In: *Nucl. Phys. B* 31 (1971), pp. 86–112. DOI: 10.1016/0550-3213(71)90448-2.

[33] F. Gliozzi, J. Scherk and D. I. Olive. "Supersymmetry, Supergravity Theories and the Dual Spinor Model". In: *Nucl. Phys. B* 122 (1977), pp. 253–290. DOI: 10.1016/0550-3213(77)90206-1.

[34] J. Scherk and J. H. Schwarz. "Dual Models for Nonhadrons". In: *Nucl. Phys. B* 81 (1974), pp. 118–144. DOI: 10.1016/0550-3213(74)90010-8.

[35] M. B. Green and J. H. Schwarz. "Anomaly Cancellation in Supersymmetric D=10 Gauge Theory and Superstring Theory". In: *Phys. Lett. B* 149 (1984), pp. 117–122. DOI: 10.1016/0370-2693(84)91565-X.

[36] D. J. Gross, J. A. Harvey, E. J. Martinec and R. Rohm. "The Heterotic String". In: *Phys. Rev. Lett.* 54 (1985), pp. 502–505. DOI: 10.1103/PhysRevLett.54.502.

[37] C. M. Hull and P. K. Townsend. "Unity of Superstring Dualities". In: *Nucl. Phys. B* 438 (1995), pp. 109–137. DOI: 10.1201/9781482268737-24. arXiv: hep-th/9410167.

[38] E. Witten. "String Theory Dynamics in Various Dimensions". In: *Nucl. Phys. B* 443 (1995), pp. 85–126. DOI: 10.1201/9781482268737-32. arXiv: hep-th/9503124.

[39] P. K. Townsend. "The Eleven-Dimensional Supermembrane Revisited". In: *Phys. Lett. B* 350 (1995), pp. 184–187. DOI: 10.1201/9781482268737-25. arXiv: hep-th/9501068.

[40] J. Polchinski. "Dirichlet Branes and Ramond-Ramond Charges". In: *Phys. Rev. Lett.* 75 (1995), pp. 4724–4727. DOI: 10.1103/PhysRevLett.75.4724. arXiv: hep-th/9510017.

[41] P. Horava and E. Witten. "Heterotic and Type I String Dynamics from Eleven Dimensions". In: *Nucl. Phys. B* 460 (1996), pp. 506–524. DOI: 10.1201/9781482268737-35. arXiv: hep-th/9510209.

[42] C. Vafa. "Evidence for F-Theory". In: *Nucl. Phys. B* 469 (1996), pp. 403–418. DOI: 10.1016/0550-3213(96)00172-1. arXiv: hep-th/9602022.

[43] B. R. Greene, D. R. Morrison and A. Strominger. "Black Hole Condensation and the Unification of String Vacua". In: *Nucl. Phys. B* 451 (1995), pp. 109–120. DOI: 10.1016/0550-3213(95)00371-X. arXiv: hep-th/9504145.

[44] R. Blumenhagen, D. Lüst and S. Theisen. *Basic concepts of string theory*. Theoretical and Mathematical Physics. Heidelberg, Germany: Springer, 2013. ISBN: 978-3-642-29496-9. DOI: 10.1007/978-3-642-29497-6.

[45] F. Gliozzi, J. Scherk and D. I. Olive. "Supergravity and the Spinor Dual Model". In: *Phys. Lett. B* 65 (1976), pp. 282–286. DOI: 10.1016/0370-2693(76)90183-0.

[46] A. Dabholkar. "Ten-Dimensional Heterotic String as a Soliton". In: *Phys. Lett. B* 357 (1995), pp. 307–312. DOI: 10.1016/0370-2693(95)00949-L. arXiv: hep-th/9506160.

[47] C. M. Hull. "String-String Duality in Ten-Dimensions". In: *Phys. Lett. B* 357 (1995), pp. 545–551. DOI: 10.1016/0370-2693(95)01000-G. arXiv: hep-th/9506194.

[48] J. Polchinski and E. Witten. "Evidence for Heterotic - Type I String Duality". In: *Nucl. Phys. B* 460 (1996), pp. 525–540. DOI: 10.1016/0550-3213(95)00614-1. arXiv: hep-th/9510169.

[49] J. H. Schwarz. "An SL(2, $\mathbb{Z}$) Multiplet of Type IIB Superstrings". In: *Phys. Lett. B* 360 (1995). [Erratum: Phys.Lett.B 364, 252 (1995)], pp. 13–18. DOI: 10.1016/0370-2693(95)01405-5. arXiv: hep-th/9508143.

[50] S. Kachru and C. Vafa. "Exact Results for $N = 2$ Compactifications of Heterotic Strings". In: *Nucl. Phys. B* 450 (1995), pp. 69–89. DOI: 10.1016/0550-3213(95)00307-E. arXiv: hep-th/9505105.

[51] A. Klemm, W. Lerche and P. Mayr. "K3 Fibrations and Heterotic Type II String Duality". In: *Phys. Lett. B* 357 (1995), pp. 313–322. DOI: 10.1016/0370-2693(95)00937-G. arXiv: hep-th/9506112.

[52] K. Narain, M. Sarmadi and E. Witten. "A Note on Toroidal Compactification of Heterotic String Theory". In: *Nuclear Physics B* 279.3 (1987), pp. 369–379. ISSN: 0550-3213. DOI: https://doi.org/10.1016/0550-3213(87)90001-0.

[53] T. Buscher. "Path-Integral Derivation of Quantum Duality in Nonlinear Sigma-Models". In: *Physics Letters B* 201.4 (1988), pp. 466–472. ISSN: 0370-2693. DOI: https://doi.org/10.1016/0370-2693(88)90602-8.

[54] S. Weinberg. "Photons and Gravitons in S-Matrix Theory: Derivation of Charge Conservation and Equality of Gravitational and Inertial Mass". In: *Phys. Rev.* 135 (4B Aug. 1964), B1049–B1056. DOI: 10.1103/PhysRev.135.B1049.

[55] W. Nahm. "Supersymmetries and Their Representations". In: *Nuclear Physics B* 135.1 (1978), pp. 149–166. ISSN: 0550-3213. DOI: https://doi.org/10.1016/0550-3213(78)90218-3.

[56] T. Weigand. "F-Theory". In: *PoS* TASI2017 (2018), p. 016. arXiv: 1806.01854 [hep-th].

[57] A. Sen. "F-Theory and Orientifolds". In: *Nucl. Phys. B* 475 (1996), pp. 562–578. DOI: 10.1016/0550-3213(96)00347-1. arXiv: hep-th/9605150.

[58] A. Sen. "Orientifold Limit of F-Theory Vacua". In: *Phys. Rev. D* 55 (1997), R7345–R7349. DOI: 10.1103/PhysRevD.55.R7345. arXiv: hep-th/9702165.

[59] J. Halverson, C. Long and B. Sung. "On the Scarcity of Weak Coupling in the String Landscape". In: *JHEP* 02 (2018), p. 113. DOI: 10.1007/JHEP02(2018)113. arXiv: 1710.09374 [hep-th].

[60] A. Collinucci. "New F-Theory Lifts". In: *JHEP* 08 (2009), p. 076. DOI: 10.1088/1126-6708/2009/08/076. arXiv: 0812.0175 [hep-th].

[61] A. Collinucci. "New F-Theory Lifts. II. Permutation Orientifolds and Enhanced Singularities". In: *JHEP* 04 (2010), p. 076. DOI: 10.1007/JHEP04(2010)076. arXiv: 0906.0003 [hep-th].

[62] V. V. Batyrev and L. A. Borisov. "Mirror Duality and String Theoretic Hodge Numbers". In: *Invent. Math.* 126 (1996), p. 183. DOI: 10.1007/s002220050093. arXiv: alg-geom/9509009.

[63] J. Polchinski and A. Strominger. "New Vacua for Type II String Theory". In: *Phys. Lett. B* 388 (1996), pp. 736–742. DOI: 10.1016/S0370-2693(96)01219-1. arXiv: hep-th/9510227.

[64] S. Gukov, C. Vafa and E. Witten. "CFT's from Calabi–Yau four-folds". In: *Nucl. Phys. B* 584 (2000). [Erratum: Nucl.Phys.B 608, 477–478 (2001)], pp. 69–108. DOI: 10.1016/S0550-3213(00)00373-4. arXiv: hep-th/9906070.

[65] T. R. Taylor and C. Vafa. "RR Flux on Calabi–Yau and Partial Supersymmetry Breaking". In: *Phys. Lett. B* 474 (2000), pp. 130–137. DOI: 10.1016/S0370-2693(00)00005-8. arXiv: hep-th/9912152.

[66] G. Curio, A. Klemm, D. Lust and S. Theisen. "On the Vacuum Structure of Type II String Compactifications on Calabi–Yau Spaces with H Fluxes". In: *Nucl. Phys. B* 609 (2001), pp. 3–45. DOI: 10.1016/S0550-3213(01)00285-1. arXiv: hep-th/0012213.

[67] B. S. Acharya, M. Aganagic, K. Hori and C. Vafa. "Orientifolds, Mirror Symmetry and Superpotentials". In: (Feb. 2002). arXiv: hep-th/0202208.

[68] S. B. Giddings, S. Kachru and J. Polchinski. "Hierarchies from Fluxes in String Compactifications". In: *Phys. Rev. D* 66 (2002), p. 106006. DOI: 10.1103/PhysRevD.66.106006. arXiv: hep-th/0105097.

[69] D. Z. Freedman and A. Van Proeyen. *Supergravity*. Cambridge, UK: Cambridge Univ. Press, May 2012. ISBN: 978-1-139-36806-3. DOI: 10.1017/CBO9781139026833.

[70] S. Deser and B. Zumino. "Broken Supersymmetry and Supergravity". In: *Phys. Rev. Lett.* 38 (25 June 1977), pp. 1433–1436. DOI: 10.1103/PhysRevLett.38.1433.

[71] S. Kachru, R. Kallosh, A. D. Linde and S. P. Trivedi. "De Sitter Vacua in String Theory". In: *Phys. Rev. D* 68 (2003), p. 046005. DOI: 10.1103/PhysRevD.68.046005. arXiv: hep-th/0301240.

[72] D. Zwanziger. "Quantum Field Theory of Particles with Both Electric and Magnetic Charges". In: *Phys. Rev.* 176 (1968), pp. 1489–1495. DOI: 10.1103/PhysRev.176.1489.

[73] E. Witten. "On Flux Quantization in M-Theory and the Effective Action". In: *J. Geom. Phys.* 22 (1997), pp. 1–13. DOI: 10.1016/S0393-0440(96)00042-3. arXiv: hep-th/9609122.

[74] G. Moore. "Arithmetic and Attractors". In: *arXiv preprint hep-th/9807087* (1998).

[75] C. Clemens. "Double Solids". In: *Advances in Mathematics* 47.2 (1983), pp. 107–230. ISSN: 0001-8708. DOI: https://doi.org/10.1016/0001-8708(83)90025-7.

[76] R. Friedman. "Simultaneous Resolution of Threefold Double Points". In: *Mathematische Annalen* 274.4 (1986), pp. 671–689.

[77] M. Reid. "The Moduli Space of 3-folds with $K = 0$ May Nevertheless Be Irreducible". In: *Mathematische Annalen* 278.1 (1987), pp. 329–334.

[78] P. S. Green and T. Hubsch. "Connecting Moduli Spaces of Calabi–Yau Threefolds". In: *Commun. Math. Phys.* 119 (1988), pp. 431–441. DOI: 10.1007/BF01218081.

[79] P. Candelas and X. C. de la Ossa. "Comments on Conifolds". In: *Nucl. Phys. B* 342 (1990), pp. 246–268. DOI: 10.1016/0550-3213(90)90577-Z.

[80] A. Strominger. "Massless Black Holes and Conifolds in String Theory". In: *Nucl. Phys. B* 451 (1995), pp. 96–108. DOI: 10.1016/0550-3213(95)00287-3. arXiv: hep-th/9504090.

[81] A. Klemm and P. Mayr. "Strong Coupling Singularities and Non-Abelian Gauge Symmetries in $N = 2$ String Theory". In: *Nucl. Phys. B* 469 (1996), pp. 37–50. DOI: 10.1016/0550-3213(96)00108-3. arXiv: hep-th/9601014.

[82] S. H. Katz, D. R. Morrison and M. R. Plesser. "Enhanced Gauge Symmetry in Type II String Theory". In: *Nucl. Phys. B* 477 (1996), pp. 105–140. DOI: 10.1016/0550-3213(96)00331-8. arXiv: hep-th/9601108.

[83] M. Bershadsky et al. "Geometric Singularities and Enhanced Gauge Symmetries". In: *Nucl. Phys. B* 481 (1996), pp. 215–252. DOI: 10.1016/S0550-3213(96)90131-5. arXiv: hep-th/9605200.

[84] S. H. Katz, A. Klemm and C. Vafa. "Geometric Engineering of Quantum Field Theories". In: *Nucl. Phys. B* 497 (1997), pp. 173–195. DOI: 10.1016/S0550-3213(97)00282-4. arXiv: hep-th/9609239.

[85] S. H. Katz and C. Vafa. "Matter from Geometry". In: *Nucl. Phys. B* 497 (1997), pp. 146–154. DOI: 10.1016/S0550-3213(97)00280-0. arXiv: hep-th/9606086.

[86] C. A. Peters and J. H. Steenbrink. *Mixed Hodge Structures*. Springer, 2008.

[87] P. Deligne. "Local Behavior of Hodge Structures at Infinity". In: *Mirror symmetry, II* 1 (1997), pp. 683–699.

[88] P. A. Griffiths. "On the Periods of Certain Rational Integrals: I". In: *Annals of Mathematics* 90.3 (1969), pp. 460–495. ISSN: 0003486X.

[89] M. Asakura and S. Saito. "Generalized Jacobian Rings for Open Complete Intersections". In: *Mathematische Nachrichten* 279.1-2 (2006), pp. 5–37.

[90] B. H. Lian and S.-T. Yau. "Period Integrals of CY and General Type Complete Intersections". In: *Inventiones mathematicae* 191.1 (Mar. 2012), pp. 35–89. ISSN: 1432-1297. DOI: 10.1007/s00222-012-0391-6.

[91] C. Doran, B. Greene and S. Judes. "Families of Quintic Calabi–Yau 3-folds with Discrete Symmetries". In: *Commun. Math. Phys.* 280 (2008), pp. 675–725. DOI: 10.1007/s00220-008-0473-x. arXiv: hep-th/0701206.

[92] C. Voisin. *Hodge Theory and Complex Algebraic Geometry I*. Ed. by L. Schneps. Cambridge Studies in Advanced Mathematics. Cambridge University Press, 2002.

[93] J. Polchinski. *String Theory. Vol. 2: Superstring Theory and Beyond*. Cambridge Monographs on Mathematical Physics. Cambridge University Press, Dec. 2007. ISBN: 978-0-521-63304-8. DOI: 10.1017/CBO9780511618123.

[94] I. M. Gel'fand, A. V. Zelevinskii and M. M. Kapranov. "Hypergeometric Functions and Toral Manifolds". In: *Functional Analysis and its Applications* 23.2 (1989), pp. 94–106.

[95] P. Candelas, A. Font, S. H. Katz and D. R. Morrison. "Mirror Symmetry for Two Parameter Models. 2." In: *Nucl. Phys. B* 429 (1994), pp. 626–674. DOI: 10.1016/0550-3213(94)90155-4. arXiv: hep-th/9403187.

[96] A. Gerhardus and H. Jockers. "Quantum Periods of Calabi–Yau Fourfolds". In: *Nucl. Phys. B* 913 (2016), pp. 425–474. DOI: 10.1016/j.nuclphysb.2016.09.021. arXiv: 1604.05325 [hep-th].

[97] D. van Straten. "Calabi–Yau Operators". In: *arXiv preprint arXiv:1704.00164* (2017).

[98] J. J. Gray. "Fuchs and the Theory of Differential Equations". In: *Bulletin of the American Mathematical Society* 10.1 (1984), pp. 1–26.

[99] G. Almkvist and W. Zudilin. "Differential Equations, Mirror Maps and Zeta Values". In: *arXiv preprint math/0402386* (2004).

[100] G. Almkvist, C. van Enckevort, D. van Straten and W. Zudilin. "Tables of Calabi–Yau Equations". In: *arXiv preprint math/0507430* (2005).

[101] G. Almkvist and D. van Straten. "Calabi–Yau Operators of Degree Two". In: *Journal of Algebraic Combinatorics* 58.4 (2023), pp. 1203–1259.

[102] *CYCluster: AESZ*. https://cycluster.mpim-bonn.mpg.de. [Online; accessed 31 July 2025].

[103] P. S. Aspinwall and D. R. Morrison. "Topological Field Theory and Rational Curves". In: *Commun. Math. Phys.* 151 (1993), pp. 245–262. DOI: 10.1007/BF02096768. arXiv: hep-th/9110048.

[104] B. R. Greene, D. R. Morrison and M. R. Plesser. "Mirror Manifolds in Higher Dimension". In: *Commun. Math. Phys.* 173 (1995). Ed. by B. Greene and S.-T. Yau, pp. 559–598. DOI: 10.1007/BF02101657. arXiv: hep-th/9402119.

[105] W. Fulton and J. Harris. *Representation Theory*. Graduate Texts in Mathematics. New York: Springer, 2004. ISBN: 978-1-4612-0979-9. DOI: 10.1007/978-1-4612-0979-9.

[106] C. Curtis and I. Reiner. *Representation Theory of Finite Groups and Associative Algebras*. A Wiley-interscience publication. Interscience Publishers, 1962. ISBN: 9780470189757.

[107] A. Klemm, B. Lian, S. S. Roan and S.-T. Yau. "Calabi–Yau Fourfolds for M-Theory and F-Theory Compactifications". In: *Nucl. Phys. B* 518 (1998), pp. 515–574. DOI: 10.1016/S0550-3213(97)00798-0. arXiv: hep-th/9701023.

[108] D. R. Morrison. "Mathematical Aspects of Mirror Symmetry". In: *Complex Algebraic Geometry* 3 (1997), pp. 265–340.

[109] H. Iritani. "An Integral Structure in Quantum Cohomology and Mirror Symmetry for Toric Orbifolds". In: *Advances in Mathematics* 222.3 (2009), pp. 1016–1079.

[110] M. Kontsevich. "Homological Algebra of Mirror Symmetry". In: *Proceedings of the International Congress of Mathematicians: August 3–11, 1994 Zürich, Switzerland*. Springer. 1995, pp. 120–139.

[111] H. Iritani. "Ruan's Conjecture and Integral Structures in Quantum Cohomology". In: *New Developments in Algebraic Geometry, Integrable Systems and Mirror Symmetry (RIMS, Kyoto, 2008)*. Vol. 59. Adv. Stud. Pure Math. Math. Soc. Japan, Tokyo, 2010, pp. 111–166. ISBN: 978-4-931469-62-4. DOI: 10.2969/aspm/05910111.

[112] P. Mayr. "Mirror Symmetry, $N = 1$ Superpotentials and Tensionless Strings on Calabi–Yau Four-Folds". In: *Nucl. Phys. B* 494 (1997), pp. 489–545. DOI: 10.1016/S0550-3213(97)00196-X. arXiv: hep-th/9610162.

[113] O. DeWolfe. "Enhanced Symmetries in Multiparameter Flux Vacua". In: *JHEP* 10 (2005), p. 066. DOI: 10.1088/1126-6708/2005/10/066. arXiv: hep-th/0506245.

[114] N. C. Bizet, A. Klemm and D. V. Lopes. "Landscaping with Fluxes and the E8 Yukawa Point in F-Theory". In: *arXiv preprint arXiv:1404.7645* (2014).

[115] P. Candelas, X. de la Ossa and P. Kuusela. "Local Zeta Functions of Multiparameter Calabi–Yau Threefolds from the Picard–Fuchs Equations". In: (May 2024). arXiv: 2405.08067 [hep-th].

[116] C. Chevalley. *Théorie des groupes de Lie, Tome II: groupes algébriques*. Vol. 1303. Hermann & Cie, 1951.

[117] K. G. Chetyrkin and F. V. Tkachov. "Integration by Parts: The Algorithm to Calculate β-Functions in 4 Loops". In: *Nucl. Phys. B* 192 (1981), pp. 159–204. DOI: 10.1016/0550-3213(81)90199-1.

[118] S. Laporta. "High-Precision Calculation of Multiloop Feynman Integrals by Difference Equations". In: *International Journal of Modern Physics A* 15.32 (2000), pp. 5087–5159.

[119] J. M. Henn. "Multiloop Integrals in Dimensional Regularization Made Simple". In: *Phys. Rev. Lett.* 110 (2013), p. 251601. DOI: 10.1103/PhysRevLett.110.251601. arXiv: 1304.1806 [hep-th].

[120] L. Görges, C. Nega, L. Tancredi and F. J. Wagner. "On a Procedure to Derive ϵ-Factorised Differential Equations beyond Polylogarithms". In: *JHEP* 07 (2023), p. 206. DOI: 10.1007/JHEP07(2023)206. arXiv: 2305.14090 [hep-th].

[121] C. Duhr et al. "Aspects of Canonical Differential Equations for Calabi–Yau Geometries and Beyond". In: (Mar. 2025). arXiv: 2503.20655 [hep-th].

[122] A. Klemm. "The B-model approach to topological string theory on Calabi-Yau n-folds". In: *B-model Gromov-Witten theory* (2018), pp. 79–397.

[123] O. DeWolfe, A. Giryavets, S. Kachru and W. Taylor. "Enumerating Flux Vacua with Enhanced Symmetries". In: *JHEP* 02 (2005), p. 037. DOI: 10.1088/1126-6708/2005/02/037. arXiv: hep-th/0411061.

[124] M. Kreuzer and H. Skarke. *Calabi–Yau Data*. http://hep.itp.tuwien.ac.at/~kreuzer/CY/. [Online; accessed 20 June 2025].

[125] R. Koo. "A Classification of Matrices of Finite Order over $\mathbb{C}$, $\mathbb{R}$ and $\mathbb{Q}$". In: *Mathematics Magazine* 76.2 (2003), pp. 143–148. ISSN: 0025570X, 19300980.

[126] J. J. Sylvester. "Sur l'équation en matrices $p\,x = x\,q$". In: *CR Acad. Sci. Paris* 99.2 (1884), pp. 67–71.

[127] C. F. Cota, A. Klemm and T. Schimannek. "Modular Amplitudes and Flux-Superpotentials on Elliptic Calabi–Yau Fourfolds". In: *Journal of High Energy Physics* 2018.1 (2018), pp. 1–55.

[128] G. Almkvist. "Calabi–Yau Differential Equations of Degree 2 and 3 and Yifan Yang's Pullback". In: *arXiv preprint math/0612215* (2006).

[129] J. Gu, A.-K. Kashani-Poor, A. Klemm and M. Marino. "Non-Perturbative Topological String Theory on Compact Calabi–Yau 3-Folds". In: *SciPost Phys.* 16.3 (2024), p. 079. DOI: 10.21468/SciPostPhys.16.3.079. arXiv: 2305.19916 [hep-th].

[130] K. Bönisch, M. Elmi, A.-K. Kashani-Poor and A. Klemm. "Time Reversal and CP Invariance in Calabi–Yau Compactifications". In: *JHEP* 09 (2022), p. 019. DOI: 10.1007/JHEP09(2022)019. arXiv: 2204.06506 [hep-th].

[131] E. Pichon-Pharabod. "Periods of Fibre Products of Elliptic Surfaces and the Gamma Conjecture". In: *arXiv preprint arXiv:2505.07685* (2025).

[132] J. Harris. *Algebraic Geometry: A First Course*. Vol. 133. Springer Science & Business Media, 2013.

[133] C. F. Doran and A. Malmendier. "Calabi–Yau manifolds Realizing Symplectically Rigid Monodromy Tuples". In: *Adv. Theor. Math. Phys.* 23.5 (2019), pp. 1271–1359. DOI: 10.4310/ATMP.2019.v23.n5.a3. arXiv: 1503.07500 [math.AG].

[134] D. Zagier. "Integral Solutions of Apéry-Like Recurrence Equations". In: *Groups and Symmetries* 47 (2009), pp. 349–366.

[135] D. van Straten and P. Metelitsyn. *Calabi–Yau Differential Operator Database V.3*. https://cydb.mathematik.uni-mainz.de. [Online; accessed 04 September 2025].

[136] C. F. Doran and J. W. Morgan. "Mirror Symmetry and Integral Variations of Hodge Structure Underlying One Parameter Families of Calabi–Yau Threefolds". In: *Workshop on Calabi-Yau Varieties and Mirror Symmetry*. May 2005, pp. 517–537. arXiv: math/0505272.

[137] D. R. Morrison and C. Vafa. "Compactifications of F-Theory on Calabi–Yau Threefolds. 1". In: *Nucl. Phys. B* 473 (1996), pp. 74–92. DOI: 10.1016/0550-3213(96)00242-8. arXiv: hep-th/9602114.

[138] V. V. Batyrev. "Higher-Dimensional Toric Varieties with Ample Anticanonical Class". PhD thesis. Moscow State University, 1985, Text in Russian, 1984.

[139] M.-X. Huang, A. Klemm and M. Poretschkin. "Refined Stable Pair Invariants for E-, M- and $[p, q]$-Strings". In: *JHEP* 11 (2013), p. 112. DOI: 10.1007/JHEP11(2013)112. arXiv: 1308.0619 [hep-th].

[140] K. Kodaira. "On Compact Analytic Surfaces II". In: *Annals of Mathematics* 77.3 (1963), pp. 563–626. DOI: 10.2307/1970180.

[141] A. Beauville. "Les familles stables de courbes elliptiques sur $\mathbb{P}^1$ admettant quatre fibres singulières". In: *CR Acad. Sci. Paris Sér. I Math* 294.19 (1982), pp. 657–660.

[142] H. Ooguri and C. Vafa. "On the Geometry of the String Landscape and the Swampland". In: *Nucl. Phys. B* 766 (2007), pp. 21–33. DOI: 10.1016/j.nuclphysb.2006.10.033. arXiv: hep-th/0605264.

[143] The LMFDB Collaboration. *The L-Functions and Modular Forms Database*. https://www.lmfdb.org. [Online; accessed 27 August 2025]. 2025.